



**Dimorphic fruits, seeds, and seedlings in
Aethionema arabicum as adaptation
mechanisms to abiotic stress in
unpredictable environments**

Waheed Arshad

Thesis submitted for the degree of
Doctor of Philosophy in Biological Sciences

Royal Holloway University of London
School of Biological Sciences

September 2019

“

Every one is familiar with the difference between the ray and central florets of, for instance, the daisy, [...] in some of these plants, the seeds also differ in shape and sculpture. [...] But with respect to the seeds, it seems impossible that their differences in shape, which are not always correlated with any difference in the corolla, can be in any way beneficial [...] Hence modifications of structure, viewed by systematists as of high value, may be wholly due to the laws of variation and correlation, without being, as far as we can judge, of the slightest service to the species.

”

~ On the Origin of Species by Means of Natural Selection (Darwin, 1859)

I. Declaration of Authorship

I, Waheed Arshad, hereby declare that this thesis and the work presented in it is entirely my own.

Where I have consulted the work of others, this is always clearly stated.

Where any collaboration has taken place with other researchers, I have clearly stated my personal contributions in the investigation.

Signed:

Date: 27th September, 2019

II. Acknowledgments

I must firstly thank both the Natural Environment Research Council and the London Doctoral Training Partnership, for making the past four years a truly unforgettable experience.

I thank my supervisor, Prof. Gerhard Leubner, who deserves my utmost gratitude for the support, development, and guidance throughout my PhD project. Thank you for providing the chance to study such a fascinating natural history phenomenon, work from which opened up numerous opportunities across the world I could only have dreamt about.

I would also like to thank my other supervisors – Dr Wolfgang Stuppy and Prof. Margaret Collinson – for many thought-provoking discussions, project and personal development. Thank you also to Prof. Vincent Jansen for providing valuable input, and to Dr Anne Visscher for support towards the latter half of the project.

I wish to acknowledge all members of the ERA-CAPS SeedAdapt consortium, in particular Prof. Klaus Mummenhoff. I have thoroughly enjoyed being part of a diverse team of researchers, and am truly grateful for having the opportunity to contribute to several aspects in the field.

Particular thanks are due to past and present members of the Leubner laboratory — Dr Kai Graeber, for introducing me to *Aethionema*; to Dr-Ing Tina Steinbrecher, for helping me answer questions in cross-disciplinary ways; to Dr Marta Pérez-Suárez, for curing my molecular biology woes; and to Dr Jake Chandler, for keeping me sane (home and away) and for enriching this thesis through *endless* discussions.

Last, but definitely not least, my deep and sincere gratitude to Lara Nouri for all her love, unparalleled patience, and wholehearted support – and also to my family for their ongoing encouragement throughout this academic journey.

Thank you.

III. Abstract

Diaspores – here, fruits and seeds – function as higher plant dispersal units, eminently adapted to a highly varied and changeable environment. While most plant species commit to a monomorphic propagation strategy, diaspores may exhibit heteromorphism, where two or more different types of fruits or seeds are produced by a single individual plant. One species exhibiting this intriguing phenomenon is *Aethionema arabicum*, an annual belonging to the earliest diverging lineage of the Brassicaceae family, which exhibits true diaspore dimorphism with no intermediate morphs. It has the remarkable ability to produce two morphologically distinct fruit (dehiscent and indehiscent) and seed (mucilaginous and non-mucilaginous) morphs on the same inflorescence.

This thesis elucidates the eco-physiological, biomechanical, and molecular mechanisms of dimorphic fruits, seeds, and seedlings. A biophysical trait-based approach reveals contrasting syndromes associated with the promotion and prevention of diaspore dispersal. Together with fracturing biomechanics, these constitute important attributes leading to fruit dehiscence and abscission. Comparative imaging and transcriptome analyses during reproductive development provides an insight into the distinct mechanisms underpinning the transition from an unfertilised ovule to a dispersed seed propagule, namely in the development of seed coat mucilage. A large-scale screening of tissue-specific traits, under a range of abiotic stresses, reveals

resilience of the derived seedlings and a time-course for transcriptional “resetting” during seed germination and early seedling growth. This results in plants developing from the two different seed morphs that are indistinguishable upon maturity.

The independent PhD work builds on resources and knowledge from the ERA-CAPS SeedAdapt project, establishing how seed and fruit heteromorphism functions as a “bet-hedging” strategy in variable and unpredictable environments. The presented findings make *Ae. arabicum* an attractive model species for continuing and future research on diaspora dimorphism.

Contents

I.	Declaration of Authorship	i
II.	Acknowledgments	ii
III.	Abstract	iii
IV.	List of Figures	ix
V.	List of Tables	xi
VI.	List of Abbreviations	xii
1.	General Introduction	1
1.1	Thesis structure.....	1
1.2	Diaspore monomorphism and heteromorphism.....	2
1.3	Taxonomic distributions of seed heteromorphism.....	3
1.3.1	<i>Notable examples within the Brassicaceae</i>	8
1.4	<i>Aethionema arabicum</i> – a new model for diaspore dimorphism.....	10
1.4.1	<i>Dehiscent and indehiscent fruit morphs</i>	14
1.4.2	<i>Carpic dominance underpinning fruit morph production</i>	16
1.4.3	<i>Seed coat dimorphism and mucilage production</i>	18
1.4.4	<i>Effects of seed heteromorphism on seedling growth and establishment</i>	25
1.5	Overall project aims and rationale.....	27
1.6	References.....	29
2.	Materials and methods	35
2.1	Methods employed in Chapter 3.....	35
2.1.1	<i>Seed collection and plant growth</i>	35
2.1.2	<i>Diaspore biometrics and aerodynamic properties</i>	35
2.1.3	<i>Measurement of abscisic acid (ABA) concentration</i>	36
2.1.4	<i>Quantification of fruit valve dehiscence</i>	36
2.1.5	<i>Fruit, fruit valve, and seed resistance to raindrop impact</i>	37
2.1.6	<i>Dispersal ability in still air</i>	37
2.1.7	<i>Dispersal ability in flowing air</i>	38
2.1.8	<i>Effect of diaspore on substrate attachment</i>	38
2.1.9	<i>Diaspore displacement mediated by surface water run-off</i>	39
2.1.10	<i>Diaspore buoyancy properties</i>	39

2.1.11	<i>Statistical analyses</i>	39
2.2	Methods employed in Chapter 4	41
2.2.1	<i>Fruit valve tensile testing and energy absorption relations</i>	41
2.2.2	<i>Scanning Electron Microscopy (SEM) analysis of fractured fruit valve surfaces</i>	41
2.2.3	<i>Synchrotron-based Radiation X-ray Tomographic Microscopy (SRXTM) of fracture zones</i>	42
2.3	Methods employed in Chapter 5	44
2.3.1	<i>Plant material and experimental growth conditions</i>	44
2.3.2	<i>Synchrotron-based Radiation X-ray Tomographic Microscopy (SRXTM) of reproductive development</i>	44
2.3.3	<i>Whole seed staining for mucilage</i>	44
2.3.4	<i>Histological analysis of seed coat differentiation during development</i>	44
2.3.5	<i>RNA extraction for RNA-seq</i>	46
2.3.6	<i>RNA-seq, data trimming, filtering, and analysis</i>	46
2.3.7	<i>Gene Ontology (GO) term and promoter motif analyses</i>	47
2.3.8	<i>Identification of gene orthologs</i>	48
2.3.9	<i>Gene expression analysis via quantitative RT-PCR</i>	49
2.3.10	<i>Primers used for qRT-PCR</i>	50
2.4	Methods employed in Chapter 6	52
2.4.1	<i>Temperature profiling for optimal germination</i>	52
2.4.2	<i>Seed sterilisation and germination</i>	52
2.4.3	<i>Preparation of plant growth medium</i>	52
2.4.4	<i>Basal thermotolerance assay</i>	53
2.4.5	<i>Time-course characterisation of chlorophyll content</i>	54
2.4.6	<i>Seedling sample selection and RNA extraction</i>	55
2.4.7	<i>Assessment of RNA quantity and quality</i>	56
2.4.8	<i>RNA-seq, data processing and differentially expressed gene (DEG) detection</i>	57
2.4.9	<i>Statistical analyses</i>	57
2.5	References	58
3.	Dispersal biophysics and adaptive significance of dimorphic diaspores	61
3.1	Paper as published in <i>New Phytologist</i>	61
3.2	Author contributions.....	62

4.	Dimorphic fruit fracture biomechanics	63
4.1	Paper as published in <i>Botany</i>	63
4.2	Author contributions	64
5.	Molecular regulation of dimorphic seed coat development.....	65
5.1	Manuscript in advanced stages for intended submission to <i>Plant Cell</i>	65
5.2	Author contributions	66
6.	Effect of seed dimorphism on seedling physiology and abiotic stress tolerance	67
6.1	Introduction.....	67
6.1.1	<i>Dimorphic post-germination seedling growth</i>	67
6.2	Aims and objectives	70
6.3	Results.....	71
6.3.1	<i>Germination optima based on temperature profiling</i>	71
6.3.2	<i>Growth responses under water deficit (osmotic stress) conditions</i>	73
6.3.3	<i>Growth responses under thermal stress conditions</i>	76
6.3.4	<i>Basal thermotolerance of seedlings</i>	79
6.3.5	<i>Time-course characterisation of chlorophyll content</i>	81
6.3.6	<i>Growth responses under salinity stress</i>	82
6.3.7	<i>Selection for RNA-sequencing</i>	86
6.3.8	<i>Sample clustering and Principal Components Analysis</i>	87
6.3.9	<i>Differentially expressed gene detection and analysis</i>	90
6.4	Discussion and conclusions	93
6.5	References	98
7.	Discussion and critical evaluation	101
7.1	Summary of findings	101
7.2	Critical evaluation	103
7.2.1	<i>Dispersal ecology and the need for field-based validations</i>	103
7.2.2	<i>Imaging datasets as complementation to transcriptome studies</i>	105
7.2.3	<i>Ecologically-relevant seedling comparisons</i>	107
7.2.4	<i>Requirements of a transgenic approach for functional genomics</i>	109
7.3	Directions for future work	111

7.3.1	<i>Compositional and functional analyses of seed coat mucilage</i>	111
7.3.2	<i>Morph longevity and soil seed bank dynamics</i>	113
7.3.3	<i>Biophysical and material properties of the IND pericarp</i>	114
7.3.4	<i>Integrative analysis of seedling transcriptomes with hormonomes</i>	114
7.4	References	116
8.	Conclusions	120
9.	Appendices	122
9.1	Reference-free (<i>de novo</i> assembly) versus reference-dependent (genome-based) approaches for differential expression analysis	122
9.2	The light control of seed germination: accessions with natural variation between light-sensitive and light-neutral responses	124
9.3	Successful proposal to conduct Synchrotron-based X-ray Tomographic Microscopy (SRXTM).....	125

IV. List of Figures

Figure 1-1: Regions rich in diaspore-heteromorphic species, where research efforts have been focussed.....	6
Figure 1-2: Schematic drawings of the dimorphic syndrome in <i>Cakile</i> spp. (Brassicaceae) fruits and seeds.....	9
Figure 1-3: Seed and fruit heteromorphism in <i>Diptychocarpus strictus</i> (Brassicaceae), showing morphology of the two types of siliques and seeds.....	10
Figure 1-4: Isoflor map of the frequency and distribution of <i>Aethionema</i> spp. across the Irano-Turanian region.....	12
Figure 1-5: Cladogram of maximum likelihood analyses with <i>Aethionema</i> traits, revealing three major clades within the genus.....	13
Figure 1-6: Mature <i>Ae. arabicum</i> infructescence from a plant with supported growth, with schematic drawings of the multiple-seeded dehiscent (DEH) and single-seeded indehiscent (IND) fruit morphs.	14
Figure 1-7: Lignification, dehiscence zone, and valve anatomy in <i>Ae. arabicum</i> fruit morphs.....	16
Figure 1-8: Morphological comparison of dimorphic <i>Ae. arabicum</i> seeds. ...	19
Figure 1-9: Toluidine blue (cell wall) stained cross-sections of outer integument cells of <i>Arabidopsis thaliana</i> , showing stages of differentiation, with labelled schematic and associated embryo stage.....	22
Figure 1-10: Germination and water uptake patterns of <i>Ae. arabicum</i> diaspores at 14°C in continuous light.	24
Figure 6-1: Schematic summary of proposed seedling work, investigating the effect of seed dimorphism on seedling physiology and abiotic stress tolerance during establishment.	70
Figure 6-2: Temperature profile for freshly-harvested M ⁺ seed, M ⁻ seed, and IND fruit germination.....	72
Figure 6-3: <i>Ae. arabicum</i> seedling growth responses to increasing concentrations of polyethylene glycol (PEG).	74

Figure 6-4: Mean fresh weights of separated root and shoot tissue from 31 day-old seedlings grown under different osmotic stress conditions using 0, 10, 20 and 30 mM polyethylene glycol (PEG).....	75
Figure 6-5: <i>Ae. arabicum</i> seedling growth responses to a range of constant growth temperatures.....	77
Figure 6-6: M ⁺ and M ⁻ seedling weights after 10 days of growth under temperatures representative of thermal stress.....	78
Figure 6-7: Basal thermotolerance assay for <i>Ae. arabicum</i> seedlings grown from M ⁺ and M ⁻ seeds.	80
Figure 6-8: Time-course characterisation of chlorophyll <i>a</i> and <i>b</i> content during seedling growth of <i>Ae. arabicum</i> morphs.....	81
Figure 6-9: Representative growth plates of M ⁺ and M ⁻ seedlings grown under (a) control, (b) 50 mM, (c) 100 mM, and (d) 150 mM NaCl conditions...	82
Figure 6-10: <i>Ae. arabicum</i> seedling growth responses to increasing concentrations of sodium chloride (NaCl).....	84
Figure 6-11: Comparisons of mean seedling length after 10 days of growth under different salt controls, which comprised sodium chloride (NaCl), mannitol, and lithium chloride (LiCl).....	85
Figure 6-12: Seedling sample selection for RNA-seq.....	86
Figure 6-13: Overall experimental design for comparative RNA-seq analysis of seed germination and seedling establishment.....	87
Figure 6-14: Principal Components (PC) analysis of RNA-seq samples obtained during M ⁺ seed, M ⁻ seed, and IND fruit germination and seedling establishment.....	88
Figure 6-15: Principal Components (PC) analysis of RNA-seq samples obtained during M ⁺ seed, M ⁻ seed, and IND fruit germination (a) and seedling establishment (b and c).	89
Figure 6-16: Total number of Differentially Expressed Genes (DEGs) detected during the developmental transition from germination to seedling establishment.....	91
Figure 7-1: Summary of <i>Ae. arabicum</i> life-history stages elucidated in this thesis.	101

V. List of Tables

Table 1-1: List of angiosperm families with heteromorphic species (data from Imbert, 2002).	4
Table 2-1: List of primers used for quantitative RT-PCR analysis.	51
Table 2-2: Classification of seedlings in tests of basal thermotolerance.	54

VI. List of Abbreviations

Abbreviation	Definition within this thesis
ABA	Abscisic acid
Ae.	<i>Aethionema</i>
ANOVA	Analysis of variance
APG	Angiosperm Phylogeny Group
CPD	Critical point drying
DAP	Days after pollination
DEG	Differentially expressed gene
DEH	Dehiscent
DOI	Digital object identifier
ERA-CAPS	European research area network for coordinating action in plant sciences
EtOH	Ethanol
FDR	False discovery rate
F_{max}	Maximum force
FW	Fresh weight
GA	Gibberellins
G_{max}	Maximum germination
GO	Gene ontology
GR_g	Germination rate for a given seed fraction (g)
hat	Hours after transfer
HDi	High dispersal ability
HDo	High dormancy
HSD	Honest significant difference
IAA	Indole-3-acetic acid
IND	Indehiscent
ISTA	International Seed Testing Association
LDi	Low dispersal ability

LDo	Low dormancy
LiCl	Lithium chloride
LOD	Limit of detection
M⁻	Non-mucilaginous
M⁺	Mucilaginous
MEE	Maternal effect embryo arrest
mRNA	Messenger ribonucleic acid
MS	Murashige and Skoog
NaCl	Sodium chloride
∅	Diameter
PC	Principal component
PCA	Principal component analysis
PEG	Polyethylene glycol
RH	Relative humidity
RIL	Recombinant inbred lines
RNA-seq	RNA-sequencing
RT-qPCR	Reverse transcription quantitative polymerase chain reaction
SeedAdapt	ERA-CAPS consortium project
SEM	Depending on context: scanning electron microscope, or standard error of the mean
SLS	Swiss Light Source
sp.	Species (singular)
spp.	Species (plural)
SRXTM	Synchrotron-based X-ray tomographic microscopy
TOMCAT	TOMographic Microscopy and Coherent rAdiology experimentS
T_{opt}	Optimum temperature
VST	Variance stabilising transformation

1. General Introduction

1.1 Thesis structure

Chapter 1 provides a critical evaluation of key literature relevant to the research, identifying gaps in the current knowledge that this thesis aims to address. Chapter 2 describes the methods employed during the research, making reference to the main thesis content derived from those methods. Chapter 3 describes the adaptive significance of dimorphic diaspores in relation to their biophysical and ecophysiological properties, and is presented as a first-author paper published in *New Phytologist* (2019). Chapter 4 evaluates the biomechanics underlying dimorphic fruit opening mechanisms, and is presented as a first-author paper published in *Botany* (2020). Chapter 5 explores the molecular mechanisms underpinning dimorphic reproduction in the context of seed coat development, and is presented as a first-author manuscript in advanced stages for intended submission to *Plant Cell* (2020). Chapter 6 (monograph-style) characterises abiotic stress physiology and tissue-specific transcriptomes during early seedling growth. Finally, Chapter 7 critically evaluates the project's main findings in relation to current literature, provides an outline for future direction, and concludes this work (Chapter 8). In the Appendices (Chapter 9) are highlighted co-author contributions made to other published works distinct from, but related to, this thesis.

1.2 Diaspore monomorphism and heteromorphism

Diaspores function in plant dispersal, and may be formed of a seed, fruit, or infructescence as the unit of dispersal of the plant. Fruits and seeds may vary continuously in size, mass, shape, colour *etc.* within populations, individual plants, or even individual inflorescences (Baskin & Baskin, 2014). While most diaspores exhibit one unimodal peak with normal or skewed distribution for a given trait (monomorphism), seeds and fruits that are heteromorphic will exhibit discontinuous variation (two or more peaks). The production of two or more distinctly different diaspores, sometimes with accessory parts, is a term equivalent to what Harper *et al.* (1970) termed “somatic polymorphism”. Diaspore heteromorphism occurs as a result of extreme environmental differences, where intermediate adaptations have low fitness, to cope with the spatial and temporal variation in environmental suitability (Venable, 1985). The risk posed by uncertain conditions is therefore spread across different phenotypes adapted to different environments. Consequently, diaspores from heteromorphic plants may differ in a number of morpho-physiological traits, such as size/mass of the embryo, thickness of pericarp, level and degree of dormancy, dispersal ability, and persistence in the soil seed bank. Differences across the autoecological, population, genetic, and molecular levels thus provide powerful comparisons, between and among diaspores, for use in biological models to test theoretical predictions of bet-hedging (Venable, 1985; Jiang *et al.*, 2019).

1.3 Taxonomic distributions of seed heteromorphism

Seed heteromorphism has been described in 18 of the 413 angiosperm families (Table 1-1) (Imbert, 2002; Bremer *et al.*, 2009), with 63% of the recorded species being in the Asteraceae, 8% in the Amaranthaceae, and 5% in the Brassicaceae. Some families with similarly high species diversity of the Asteraceae (*e.g.* Fabaceae), do not exhibit the same degree of seed heteromorphism, suggesting these families do not have “morphological characteristics favouring the appearance of seed heteromorphism and ecological features that maintain it” (Imbert, 2002).

Table 1-1: List of angiosperm families with heteromorphic species (data from Imbert, 2002). Number of species and genera per family are from Kadereit *et al.* (2003) and Mabberley (2008). This list is not exhaustive and is ordered alphabetically, by family.

Family	Seed heteromorphic species		Total diversity	
	No.	No.	No.	No.
	species	genera	species	genera
Amaranthaceae	18	10	2500	180
Apiaceae	3	3	3500	428
Asteraceae	138	52	23600	1590
Brassicaceae	12	8	3400	321
Caryophyllaceae	11	2	2630	85
Cistaceae	4	1	170	9
Commelinaceae	1	1	600	40
Euphorbiaceae	1	1	6500	229
Fabaceae	5	5	19500	720
Fumariaceae	1	1	530	17
Nyctaginaceae	9	1	350	27
Papaveraceae	2	2	230	23
Plantaginaceae	1	1	275	3
Poaceae	7	7	10550	715
Polygonaceae	1	1	1200	46
Rubiaceae	1	1	10900	563
Thymelaeaceae	1	1	850	45
Valerianaceae	2	1	300	10
Total	218	99	–	–

In many species of Asteraceae, heteromorphic differentiation mainly occurs positionally, among the achenes in the disc (central, tubular) and ray (peripheral, ligulate) florets of the capitulum. Such achenes differ in their level of dormancy, size, dispersal structures (e.g. presence or absence of pappi or trichomes), colour, and shape (Baskin & Baskin, 2014). In the genus *Picris* for example, central pappose achenes are wind-dispersed singly, while larger and heavier epappose marginal achenes are retained aloft on the skeleton of the mother plant. Small barbs present on involucre bracts may also become attached to passing animals (Ellner & Shmida, 1984). While in *Picris* spp. peripheral achenes are typically heavier than central ones, for a few species, it is the opposite. In *Carduus pycnocephalus* and *C. tenuiflorus*, central achenes are heavier than peripheral ones due to differences in embryo size (Olivieri & Berger, 1985). Though differentiation in this family mainly occurs among the peripheral and central achenes (and thus seed dimorphism), for several species intermediate achenes can also be found (e.g. the three or four achene morphs of *Calendula*) (Heyn *et al.*, 1974). A major point about heteromorphic systems in Asteraceae is that there is a developmental constraint, namely that positional effects in the flower determine the morph of diaspore produced.

Nowhere on Earth is the phenomenon of diaspore heteromorphism known to be more prevalent than in the cold deserts of the northern Xinjiang Province of Central Asia (Figure 1-1a), where at least 20 species are heterodiasporic (dimorphic, trimorphic, or polymorphic) annuals; 14 of these belong to the Amaranthaceae, formerly assigned to Chenopodiaceae *sensu* Angiosperm

Phylogeny Group (APG) II classification for the orders and families of flowering plants (Bremer *et al.*, 2009). Substantial research has been conducted on heterodiasporic plants native to these deserts, more so than in any other biogeoclimatic zone on earth. A study by Ellner and Shmida (1981) is the only other paper collating information for a relatively large number of heteromorphic species from a single region (Baskin *et al.*, 2014). Within the Flora of Israel (Figure 1-1b), heteromorphic traits were more frequent in desert habitats (1.3% of 604 species) than in Mediterranean/semi-desert habitats (0.7% of 1560 species), functioning in various ecological roles in seed protection, regulation of germination timing, and seasonal staggering of dispersal (Ellner & Shmida, 1981). Thus, the potential benefits of diaspore heteromorphism are diverse, and, together with a combination of their life history traits, could potentially contribute to the naturalisation success of species exhibiting this phenomenon (Fenesi *et al.*, 2019).

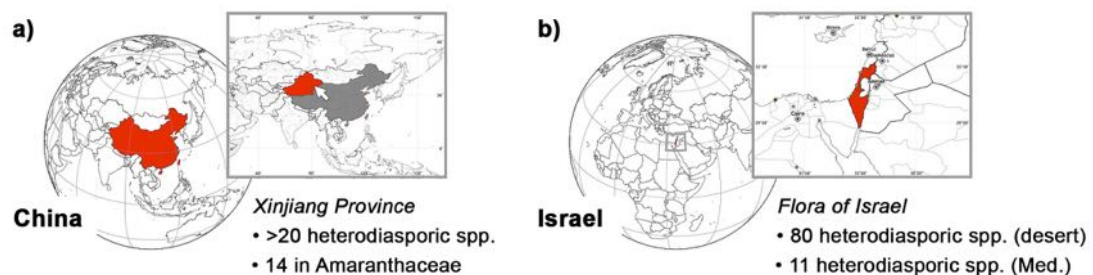


Figure 1-1: Regions rich in diaspore-heteromorphic species, where research efforts have been focussed. (a) Xinjiang Province of north-west China (inset, indicated by the white arrow); (b) Desert and Mediterranean (Med.) environments of Israel.

The habitat types in which heteromorphic species are found and the selection pressures acting upon them, provides the opportunity to study conspecific

seed dormancy and dormancy-breaking mechanisms. Appropriate germination timing is influenced by the well-known phytohormones abscisic acid (ABA) and gibberellins (GAs). While ABA inhibits seed germination, GAs promote this process (Koorneef *et al.*, 2002; Finch-Savage & Leubner-Metzger, 2006). The small black seeds and large brown seeds of desert annual halophytes in the genus *Suaeda* (Amaranthaceae) are a good case study (Ding *et al.*, 2010; Wang *et al.*, 2012). Brown seeds were found to be non-dormant, reaching high germination percentages across a wide range of temperatures in light and in darkness. In contrast, black seeds had physiological dormancy [for an in-depth review of seed dormancy types, see Baskin and Baskin (2004)], reaching low germination percentages under all germination test conditions. While cold stratification did not break this dormancy, the application of GAs promoted germination in darkness (Wang *et al.*, 2012).

Interestingly, dry seed ABA contents were 2.5-fold higher in non-dormant brown than in dormant black seeds. However, brown seeds showed a higher germination percentage and faster germination rate than black seeds, thought to be attributed to their insensitivity to ABA (Li *et al.*, 2016). In addition to phytohormone responses, transcriptional profiling revealed differentially expressed genes associated with embryo development, fatty acid, and osmotic regulation substances in brown and black seeds (Xu *et al.*, 2017). Thus, multiple adaptive strategies through diverse seed dormancy mechanisms, differential germination, and gene expression under salinity stress are thought to contribute to successful survival of heteromorphic

Suaeda spp. in inland salt deserts (Wang *et al.*, 2012; Gul *et al.*, 2013; Li *et al.*, 2016).

1.3.1 Notable examples within the Brassicaceae

The Brassicaceae, an important family at both the agronomic and scientific levels, includes several model species such as *Brassica* spp., *Lepidium* spp. and *Arabidopsis thaliana* (Couvreur *et al.*, 2009). Though the sequencing of *A. thaliana* was a major landmark in plant biology (Arabidopsis Genome Initiative, 2000), recent advances in high-throughput technology has led to the extension of whole-genome sequencing projects to non-model organisms, with now over ten species' genomes sequenced in the Brassicaceae (Schranz *et al.*, 2006; Sharma *et al.*, 2014).

In this large family, diaspore heteromorphism has been studied most extensively in the genus *Cakile*, due to the range of adaptive advantages that are conferred on its species (Maun & Maun, 2009). The dimorphism in *Cakile* spp. consists of morphologically distinct upper and lower fruit segments (Figure 1-2), which exhibit high phenotypic plasticity in response to environmental variability (Cordazzo, 2006). The upper segments abscise, thought to allow the colonisation of new areas, whereas lower segments remain attached to the plant, thereby remaining in the proven habitat of the maternal parent (Maun & Payne, 1989). The two seed morphs have been shown to contribute to plant fitness through differences in dispersal (Cordazzo, 2006), germination behaviour (Zhang, 1993), seedling emergence and survival rates (Zhang, 1993; Zhang, 1995).

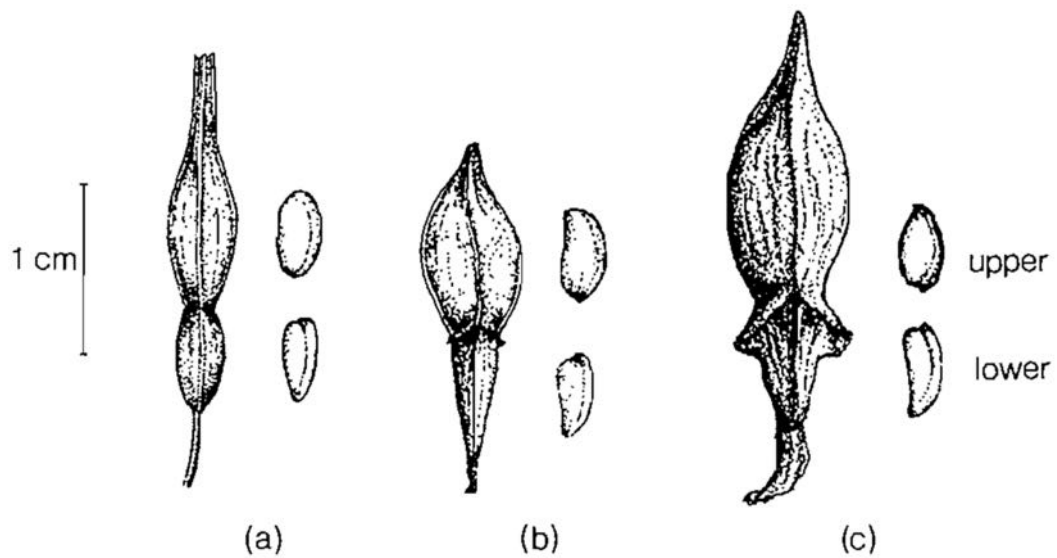


Figure 1-2: Schematic drawings of the dimorphic syndrome in *Cakile* spp. (Brassicaceae) fruits and seeds. (a) *Cakile edentula* var. *lacustris*; (b) *Cakile edentula* var. *edentula*; and (c) *Cakile maritima*. Figure from Maun and Payne (1989).

Another heteromorphic Brassicaceae species on which recent research has been focussed is *Diptychocarpus strictus*, an annual native to Middle Asia, Iran, Turkey, Caucasia and China. Owing to its annual, ephemeral life-history and occurrence in cold desert habitats, this single species in the genus has provoked questions on survivability by mechanisms of escaping in space and time (Lu *et al.*, 2010). Two distinct types of fruits (upper and lower) are produced, each with varying seed morphologies (Figure 1-3). Wind or rain permits the rapid dispersal of siliques and/or seeds within a few days after maturity. Pericarps of upper siliques dehisce first, containing winged seeds. However, lower siliques do not dehisce (presence of lignified pericarp), and disperse in their entirety near the mother plant. Thus, seeds represent the dispersal units of upper siliques, and intact siliques represent the dispersal

units of lower siliques (Lu *et al.*, 2010). This complex fruit and seed heteromorphism plays a significant role in post-release fates, such that the dispersal ability of seeds from upper siliques is much greater than seeds inside the intact lower siliques, and that lower siliques may form a persistent seed bank to enhance survival in their arid zone habitats (Lu *et al.*, 2010; Lu *et al.*, 2015).

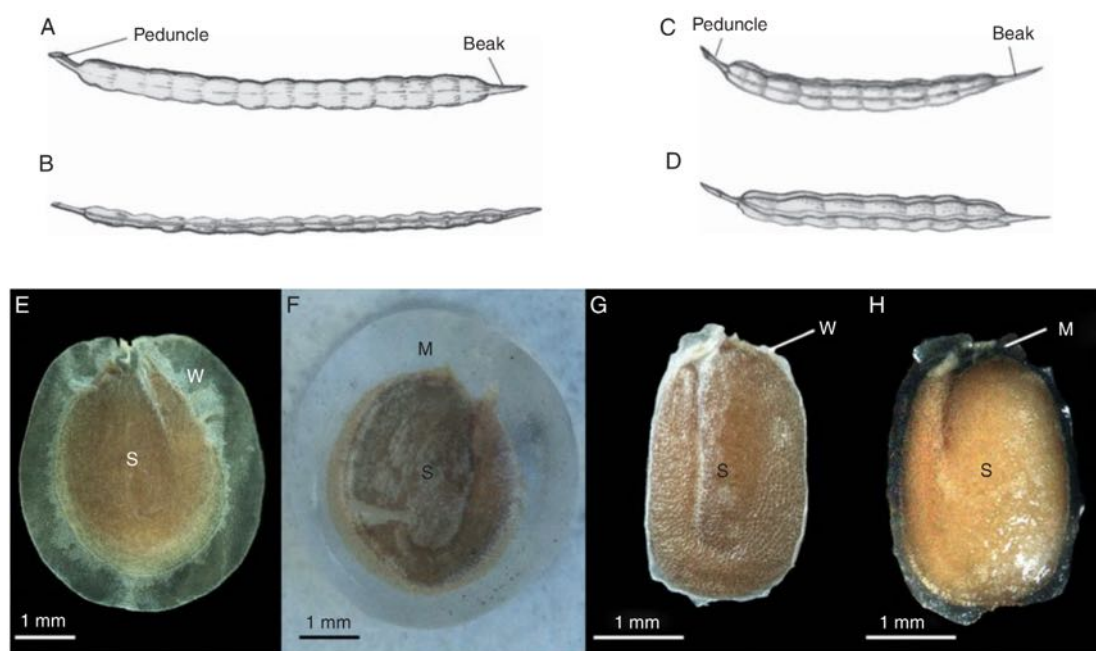


Figure 1-3: Seed and fruit heteromorphism in *Diptychocarpus strictus* (Brassicaceae), showing morphology of the two types of siliques and seeds. Ventral (A) and lateral (B) side of the upper silique. Ventral (C) and lateral (D) side of the lower silique. Dry (E) and (F) imbibed seed from upper siliques. Dry (G) and imbibed (H) seed from lower siliques. Abbreviations: **M** = mucilage; **S** = seed; **W** = wing. Figure from Lu *et al.* (2010).

1.4 *Aethionema arabicum* – a new model for diaspore dimorphism

Aethionema arabicum (L.) Andr. ex DC. is an annual species belonging to the Aethionemeae, the earliest diverging, sister tribe within the Brassicaceae

family. The genus comprises approximately 56 species and, although it has not been monographed and many taxonomic issues are still not resolved, a basal split between this lineage and the rest of the family has been confirmed in various studies using different chloroplast and nuclear markers (e.g. Al-Shehbaz *et al.*, 2006; Beilstein *et al.*, 2006; Warwick *et al.*, 2010; Franzke *et al.*, 2011). This early branching lineage (tribe Aethionemeae vs. core Brassicaceae) has led to suggestions that the Brassicaceae is thought to have originated in the ecologically, altitudinally and geologically diverse Irano-Turanian region. Here, high species diversity is found (Figure 1-4), and also where *Aethionema* is most diversified (Hedge, 1976; Al-Shehbaz *et al.*, 2006; Mohammadin *et al.*, 2017).

The high species diversity can be correlated with past tectonic events (e.g. formation of the Alborz, Zagros, and Kopeh-Dagh mountain ranges in Iran, and the Taurus and Pontic mountain ranges in Turkey), causing aridification of the Irano-Turanian region (Mohammadin *et al.*, 2017). Nearly all recent Aethionemeae species are found in Turkey, with much fewer species extending eastward into Turkmenistan and westward into Spain and Morocco (Al-Shehbaz *et al.*, 2007; Franzke *et al.*, 2009). Connecting the eastern and western floras of the Holarctic Kingdom, this continental climate region represents a biodiversity hotspot. However, the lack of local floristic and environmental knowledge makes the Irano-Turanian region especially challenging to study (Manafzadeh *et al.*, 2017).

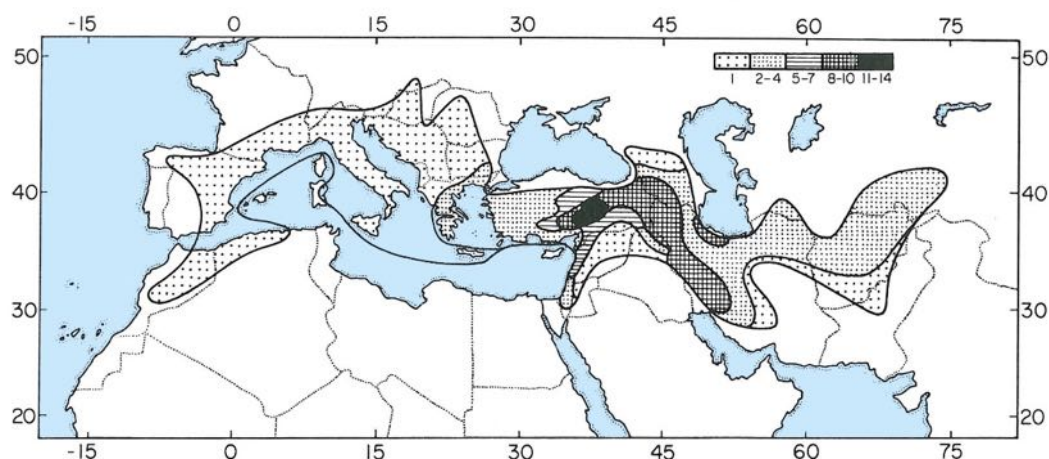


Figure 1-4: Isoflor map of the frequency and distribution of *Aethionema* spp. across the Irano-Turanian region. Away from central eastern Anatolia, the number of species decreases rapidly. Distribution patterns correspond to the number of species found in that area. Axes represent longitude (x) and latitude (y), expressed in degrees. Figure adapted from Hedge (1976).

Heteromorphy in the Aethionemeae has been reported in a number of species. Initial phylogenetic analyses of 38 sampled *Aethionema* species showed that five heteromorphic species (*Ae. arabicum*, *Ae. carneum*, *Ae. syriacum*, *Ae. froedinii* and *Ae. heterocarpum*) form a monophyletic group, all of an annual life history. The sixth heteromorphic species, *Ae. saxatile*, clustered in a separate clade, suggesting an independent origin of its heteromorphism (Lenser *et al.*, 2016). Though this phylogeny had a resolved backbone discerning three clades, the poorly-resolved relationships within these clades were more comprehensively investigated using whole plastome and nuclear ribosomal DNA sequences (Mohammadin *et al.*, 2017). Since annual life form and the presence of a heterocarpic infructescence independently evolved two or three times (Clade A, Figure 1-5), it is therefore thought that perenniality and the presence of only dehiscent fruits are the ancestral traits for the genus *Aethionema*.

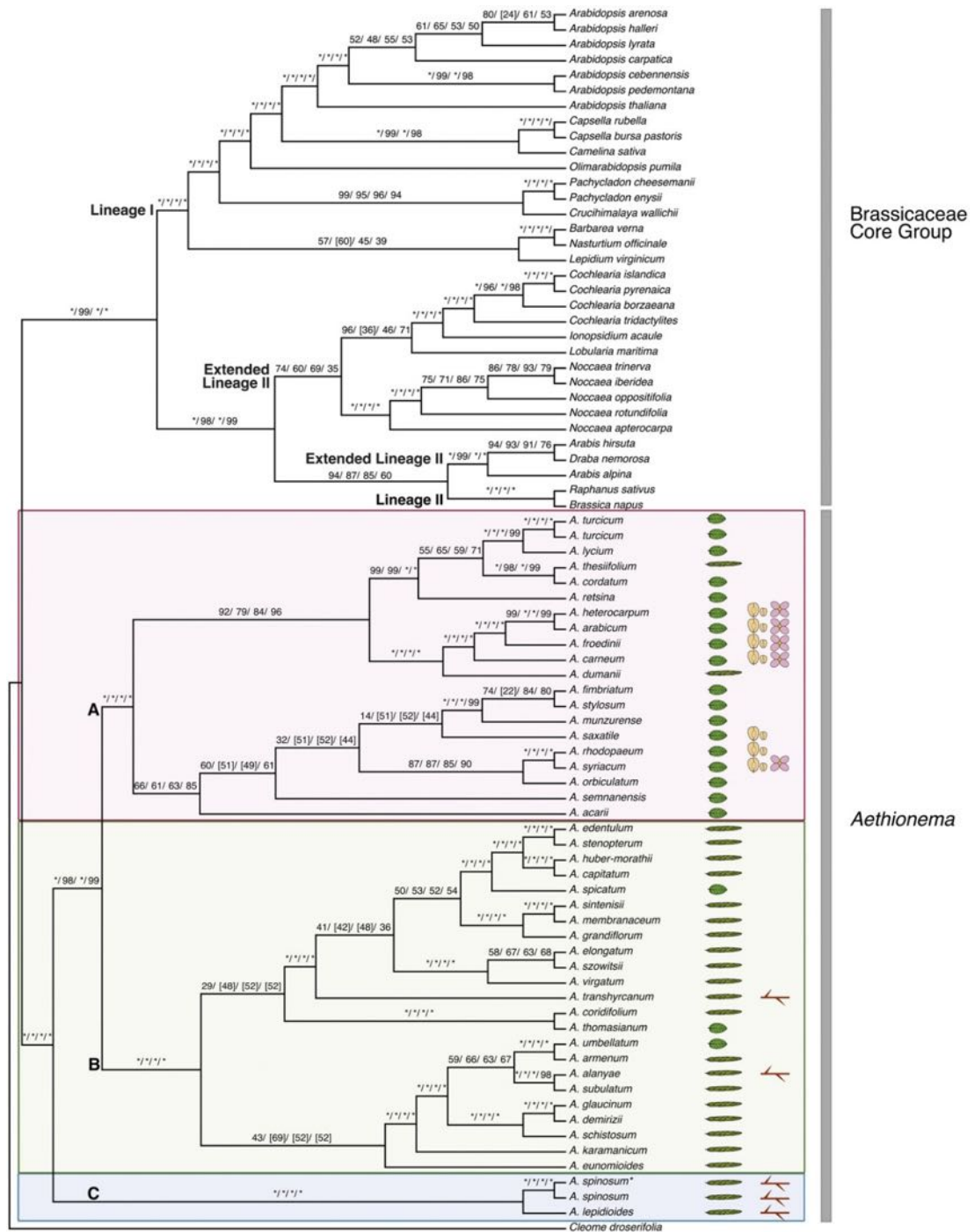


Figure 1-5: Cladogram of maximum likelihood analyses with *Aethionema* traits, revealing three major clades within the genus. Clade **A** comprises seven heteromorphic species in separate lineages. Icons show leaf shape (linear/ovate), heterocarpic species (two differently sized fruits), annual species (pink flowers), and species with spines (spiny branch). Figure and caption from Mohammadin *et al.* (2017).

1.4.1 Dehiscent and indehiscent fruit morphs

An important advantage of this model is that *Ae. arabicum* exhibits true diaspore dimorphism with no intermediate morphs (Figure 1-6), together with high phenotypic plasticity in morph ratio formation in response to temperature (Lenser *et al.*, 2016), branch removal (Zohary & Fahn, 1950; Lenser *et al.*, 2018), mechanical damage, and herbivory (Bhattacharya *et al.*, 2018). This is different to many other systems (*e.g.* Asteraceae), where developmental constraint only allows the alteration of morphs together, but not individually. On the same *Ae. arabicum* infructescence, two fruit morphs are produced: dehiscent (DEH) fruits with multiple mucilaginous (M^+) seeds, and indehiscent (IND) fruits each with a single non-mucilaginous (M^-) seed.

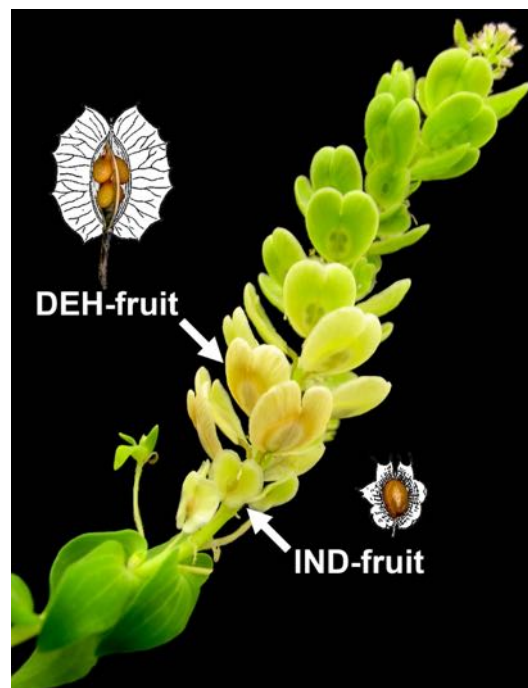


Figure 1-6: Mature *Ae. arabicum* infructescence from a plant with supported growth, with schematic drawings of the multiple-seeded dehiscent (**DEH**) and single-seeded indehiscent (**IND**) fruit morphs. Depicted is the main branch on which the production of DEH fruits is favoured, while IND fruits are produced in greater number on secondary branches. See Lenser *et al.* (2016) for details on fruit proportions.

Fruit morphs differ markedly in size, seed-number and septum formation (Lenser *et al.*, 2016). DEH fruits contain a dehiscence zone, separating lignified cells of the replum (partition between fruit locules) from those of the endocarp layer on the inside of the fruit valves. No such structure is found in the fruits of the IND morph (Figure 1-7). A putative abscission zone at the fruit-pedicel junction in IND fruits separates the lignified cells at the fruit-base from those of the pedicel, whereas a bridge of lignified cells is tightly connected with the pedicel in the DEH fruit morph (Lenser *et al.*, 2016). It is thought that these distinct anatomical differences confer specific physical and mechanical properties, which have consequences for fruit opening during dispersal.

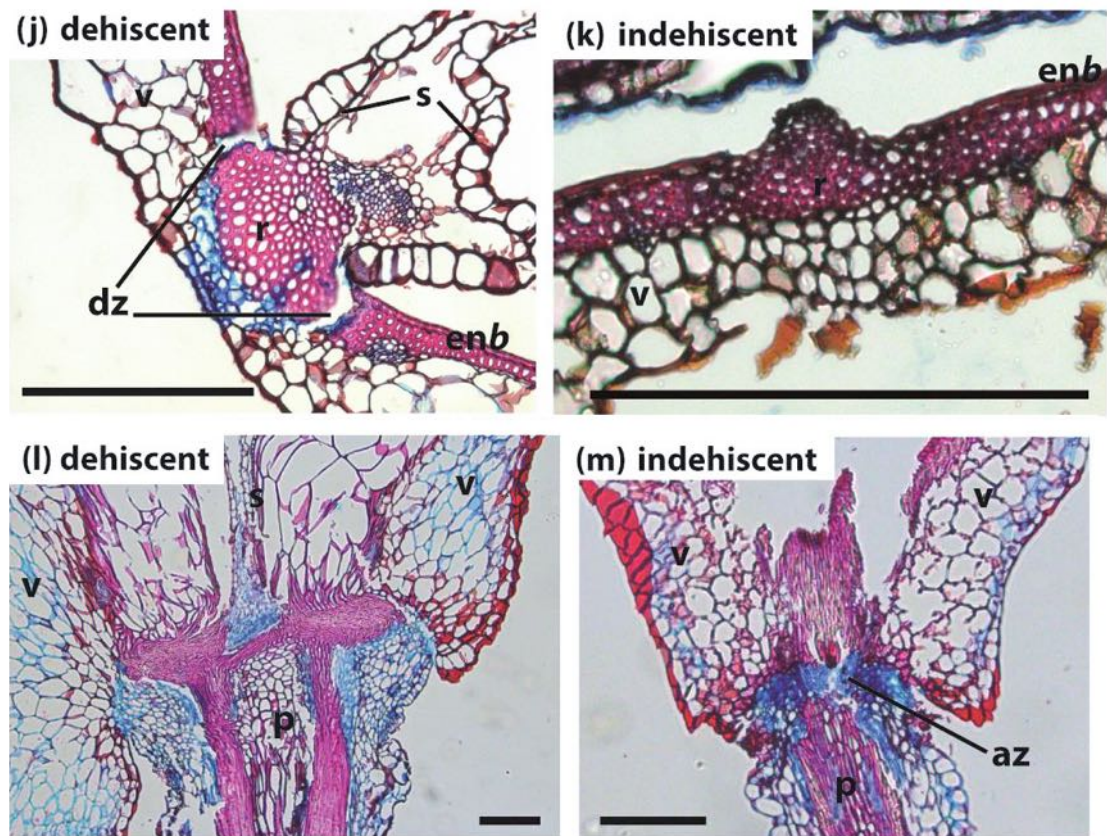


Figure 1-7: Lignification, dehiscence zone, and valve anatomy in *Ae. arabicum* fruit morphs. Thin sections stained with safranin (lignified tissues) and astrablue (non-lignified tissues) show the *Ae. arabicum* dehiscent fruit morph (j) with a dehiscence zone (dz) present, separating lignified (red) cells of the replum (r) from those of the endocarp layer (enb) on the inside of the fruit valves (v). The enb is directly fused to the lignified cells of the replum in the indehiscent morph (k). A solid bridge of lignified cells connect fruit base and pedicel in the dehiscent fruit morph (l), whereas an abscission zone (az) separates the fruit base from the lignified cells of the pedicel in the indehiscent fruits (m). Scale bars = 200 μm . Figure and caption adapted from Lenser *et al.* (2016).

1.4.2 Carpic dominance underpinning fruit morph production

Fruit morphs are not evenly distributed throughout the *Ae. arabicum* plants (Lenser *et al.*, 2016; Lenser *et al.*, 2018). The large, many-seeded, DEH morph is preferentially produced on the main infructescence (flowering branch), while an increasing preference for the small, single-seeded, IND morph has been

observed on higher-order side branches. The ratio of fruit morph production also shows a plastic response to various environmental parameters, and there is a further shift towards an increased production of the DEH morph in response to the removal of shoot branches (Zohary & Fahn, 1950; Lenser *et al.*, 2016). Both these observations indicate a possible connection between fruit morph determination and correlative dominance relationships, whereby hormonal signals transferring dominance effects control the growth of one shoot organ versus another (Bangerth, 1989). One such example of “primigenic dominance”, in which the earlier developed sink inhibits later developed organs, is in the development of fruits where early developing fruits suppress the growth of later developing pollinated ovaries (Smith & Samach, 2013). Among the main signals mediating dominance relationships is the export of auxins (Domagalska & Leyser, 2011; Smith & Samach, 2013), and thus much research has been directed at understanding the mechanism by which auxin regulates shoot branching.

While the exact mechanism in *Ae. arabicum* still remains unclear, hormone and gene expression analyses have shown that the regulatory network determining fruit morph determination may be a modified version of that which usually controls carpic dominance (Lenser *et al.*, 2018). Dehiscent fruits develop preferentially under growth-promoting conditions, and indehiscent fruits are primarily produced under growth-inhibitory conditions. Expression of *BRANCHED1* (*BRC1*), encoding a transcription factor known for its conserved function as a branching repressor, together with an accumulation balance of auxin and cytokinin in flowers, appears to be a key factor in generating the

indehiscent fruits of *Ae. arabicum*. Thus, it is thought that indehiscent fruits are produced via a precise and highly-specific, derived developmental program (Lenser *et al.*, 2016; Lenser *et al.*, 2018).

1.4.3 Seed coat dimorphism and mucilage production

Seeds developing within the dimorphic fruits also exhibit remarkable morphophysiological differences, unambiguously connected with the two fruit morphs. Upon imbibition, M⁺ seeds from DEH fruits produce mucilage from the outer cell walls of the seed coat epidermal cells. This water-containing, gel-like pectinaceous layer surrounds seeds, with a surface covered in dome-like structures and crinkles around their base (Figure 1-8). Each of these corresponds to a mucilage-producing epidermal cell that forms conical masses. Upon imbibition, *Ae. arabicum* papillae swell and expand up to 200 µm with a globe-like tip, later drying to form knob-shaped tips. In contrast, M⁻ seeds show a uniform, slightly grooved surface structure, lacking mucilage upon imbibition (Figure 1-8) (Lenser *et al.*, 2016). The final products of the dimorphic syndrome, namely the mature M⁺ and M⁻ seeds and their fruits, have therefore been characterised, but the development which brings about this seed coat dimorphism is completely unknown. As the dehiscent fruit containing mucilaginous seeds is representative of the “default” trait for the Brassicaceae (Mühlhausen *et al.*, 2013), it is speculated that M⁻ seeds deviate from this pathway during early development.

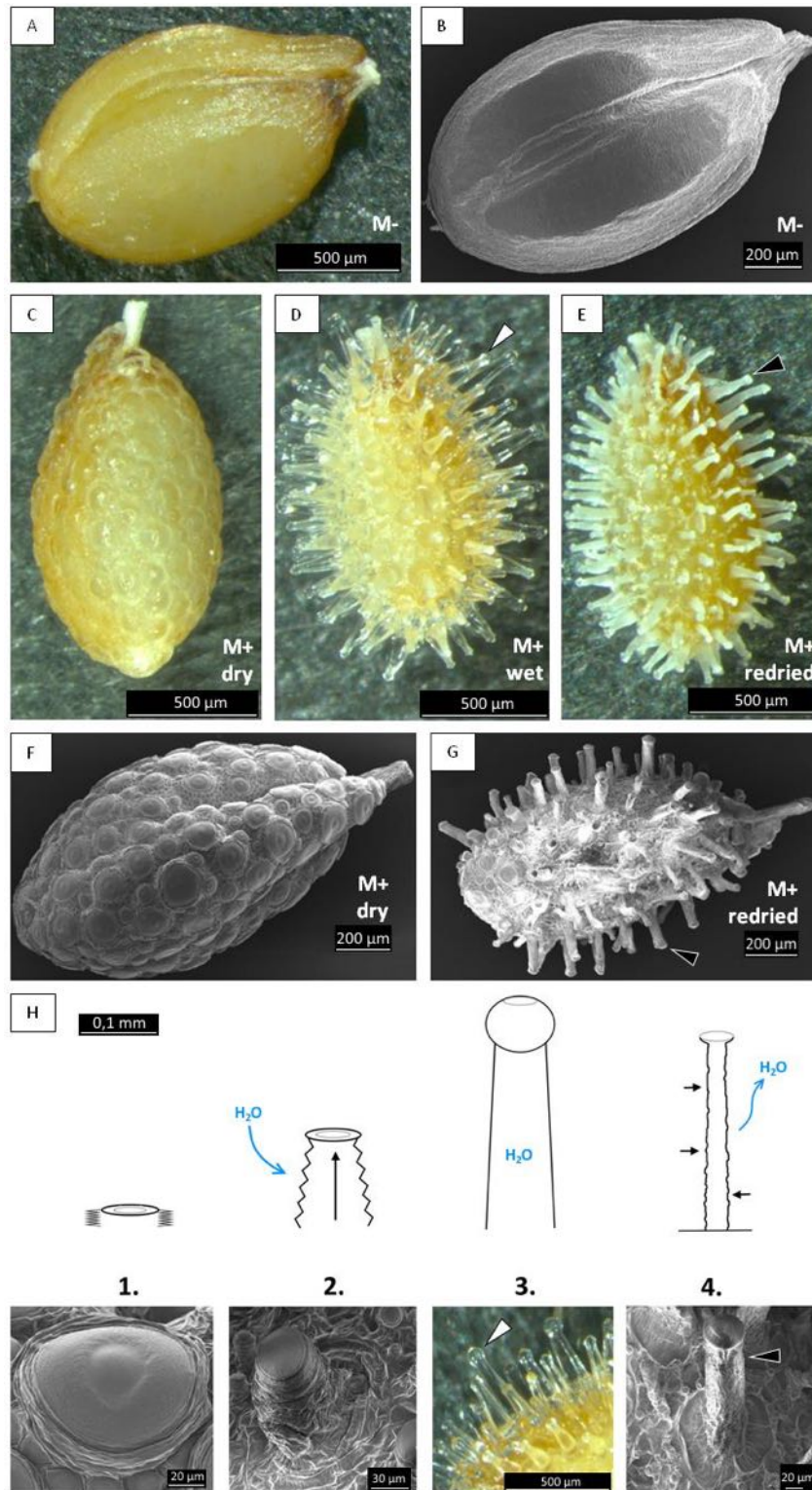


Figure 1-8: Morphological comparison of dimorphic *Ae. arabicum* seeds. Seeds from indehiscent fruits (M⁻; **A, B**) possess a smooth surface and do not produce mucilage upon imbibition. Seeds from dehiscent fruits (M⁺; **C–G**) are densely covered in dome-like structures that form papillae (**D, H**) with globe-shaped tips (white arrow) upon imbibition. When re-dried, papillae shrink and form dried, knob-shaped tips (**E, G, H, black arrow**). Figure from Lenser *et al.* (2016).

This remarkable phenomenon of mucilage production, known as myxospermy, is reported in diaspores of species from 37 orders, 110 families and at least 230 genera of angiosperms (Yang *et al.*, 2012; Phan & Burton, 2018). The main ecological adaptation of seed mucilage may be in the facilitation for imbibition and maintenance of moisture for growth in water-deficient environments (Huang *et al.*, 2000). Seed coat mucilage may also slow germination rates by impeding the diffusion of oxygen (Witztum *et al.*, 1969), as well as impact fruit and seed dispersal (Lobova *et al.*, 2003). Often referred to as “slime”, mucilage is a general term for polysaccharides or proteoglycans secreted during development, usually characterised by the presence of the pectin rhamnogalacturonan (RG) I and hemicelluloses such as arabinoxylan (Lerouxel *et al.*, 2006; Western, 2012). In addition to composition, seed coat mucilages are also classified by the presence or absence of dispersed cellulose microfibrils, which can be detected through histochemical staining, polarised light microscopy, and electron microscopy (*e.g.* Willats *et al.*, 2001; Kreitschitz & Vallès, 2007; Western, 2012).

In *Ae. arabicum*, light microscope analysis of stained longitudinal and transversal cross-sections has highlighted varying cellular differences between the two seed morph outermost seed coat layers (Lenser *et al.*, 2016). The outermost epidermal layer forms large mucilage papillae in M⁺ seeds, whereas on a very thin film of mucilage is formed from the epidermal layer in M⁻ seeds. Adjacent to this is a single layer of palisade cells, followed by multiple crushed palisade cells. These layers consist of dead cells and form the seed coat. Between this and the embryo is a thin layer of endosperm cells

(multi-layered and thicker around the radicle tip), a layer which plays an important role for the temperature- and gibberellin-dependent regulation of seed dormancy and germination in many Brassicaceae species (Müller *et al.*, 2006; Graeber *et al.*, 2012; Graeber *et al.*, 2014).

Although a rich literature exists on the presence and distribution of seed coat and pericarp mucilage, it has received less attention in recent decades. The epidermal cells of the *Arabidopsis thaliana* seed coat act as an interesting model because of their easily-accessible pectin, and many mutants affecting mucilage production and mucilage secretory cell differentiation have been since isolated (Western, 2012). In *Arabidopsis*, mucilage synthesis occurs within the developing seed and is deposited in the outer cell layer of the seed coat. This two-cell layered outer integument undergoes a dramatic differentiation process from the octant embryo stage to the mature seed (Figure 1-9). A ring of mucilage is secreted between the plasma membrane and the outer cell wall, forcing the cytoplasm into a columnar shape in the centre of the cell. The production and degradation of starch granules is integral to this process; a highly-reinforced wall surrounding the columnar protoplast and radial walls results in a cell containing large amounts of mucilage. Dehydration of the mucilage causes the columella and radial walls to persist as an epidermal layer comprising visible reticulations on the mature seed (Western *et al.*, 2000; Windsor *et al.*, 2000). It is completely unknown whether the development in *Ae. arabicum* seed morphs follows this pattern.

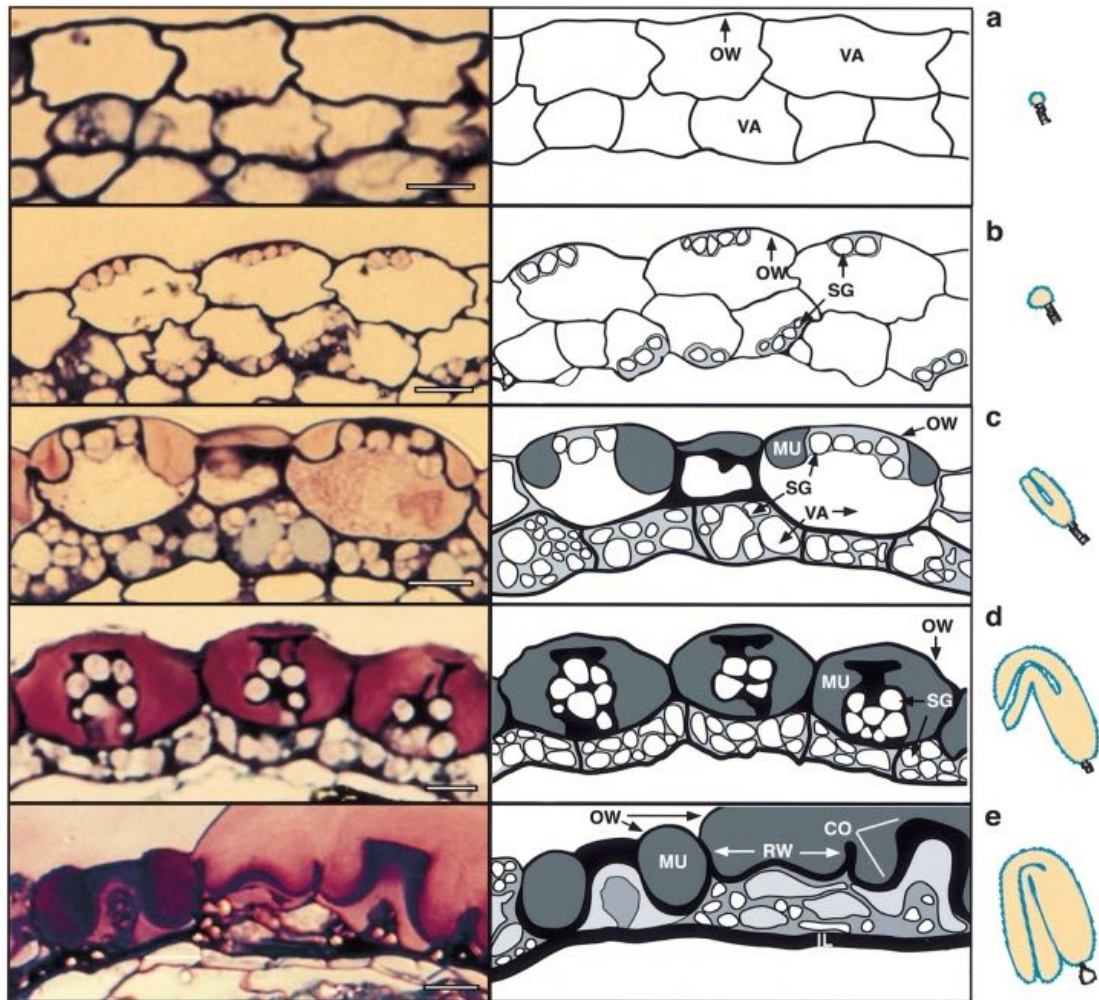


Figure 1-9: Toluidine blue (cell wall) stained cross-sections of outer integument cells of *Arabidopsis thaliana*, showing stages of differentiation, with labelled schematic and associated embryo stage. (a) Outer and inner integuments comprise cells with a large single vacuole and compressed cytoplasm, with no starch granules or mucilage visible. (b) Starch granule production occurs in both outer and inner cell layers. (c) Mucilage is secreted by the outer cells between the outer primary wall and the protoplast, forcing the protoplast to assume the columella shape while starch granules continue to enlarge. (d) The completion of mucilage production forces the protoplast to form a column, and starch granules begin to degrade. (e) A reinforced secondary wall is deposited adjacent to the column-shaped protoplast, the basal area of the cell, and the radial walls between cells. Mucilage hydration causes the outer wall to break free from its connections to the top of the columella and radial walls. Abbreviations: **OW** = outer wall of the outer cell; **VA** = vacuole; **SG** = starch granules; **MU** = mucilage; **CO** = columella; **IL** = inner cell layer of the outer integument; **RW** = radial wall. Scale bars = 10 mm. Figure and caption from Windsor *et al.* (2000).

A resurgence of interest in seed coat mucilages has taken place due to the recent availability of seed coat mutants in *A. thaliana*, where at least 44 genes have been identified with roles in mucilage production or mucilage secretory cell differentiation (Haughn & Chaudhury, 2005; Western, 2012). Defects in differentiation of the outer integument during seed development have been correlated with the lack of mucilage synthesis. *A. thaliana apetala2 (ap2)* single- and *nac regulated seed morphology1 (nars1)* and *nars2* double-mutants lack differentiation of their mucilage secretory cells and subtending palisade cells, as well as exhibiting morphological defects (Western *et al.*, 2001; Kunieda *et al.*, 2008). All three genes encode transcription factors involved in the seed development pathway. As seed coats in the *nars1/nars2* double mutant are similar to the shrivelled appearance of *Ae. arabicum* M⁻ seed surface, conserved developmental regulators may be differentially employed in M⁺ and M⁻ seeds (Lenser *et al.*, 2016), and therefore require further investigation.

The dimorphic syndrome in *Ae. arabicum* has consequences for seed germination. Following fruit maturation, IND fruits abscise from the mother plant and M⁻ seeds remain in the soil seed bank due to pericarp-induced dormancy. Here, the whole IND fruit represents the dispersal unit, and seeds need to germinate within the fruit under natural conditions, unless the fruit coat is removed by unknown external means. M⁻ seeds within IND fruits germinate slowly, but faster and more efficient germination is attained when seeds were isolated from IND fruits, indicating a germination inhibiting role of the pericarp. In comparison, M⁺ seeds are released following fruit dehiscence and

germinate readily within three days (Figure 1-10a). When tested for their water uptake patterns, M^+ seeds show a classical tri-phasic response (Figure 1-10b). Isolated M^- seeds also show a tri-phasic water uptake pattern, but overall moisture content during imbibition remains lower, and phase II is prolonged in comparison to M^+ seeds. The IND fruit appears to take up similar amounts of water to M^+ seeds during phase I, indicating that IND fruit coats may aid in water absorption (Lenser *et al.*, 2016). How the processes of dispersal, germination, and water uptake kinetics in *Ae. arabicum* morphs relate to survivability in semi-arid environments remains unknown.

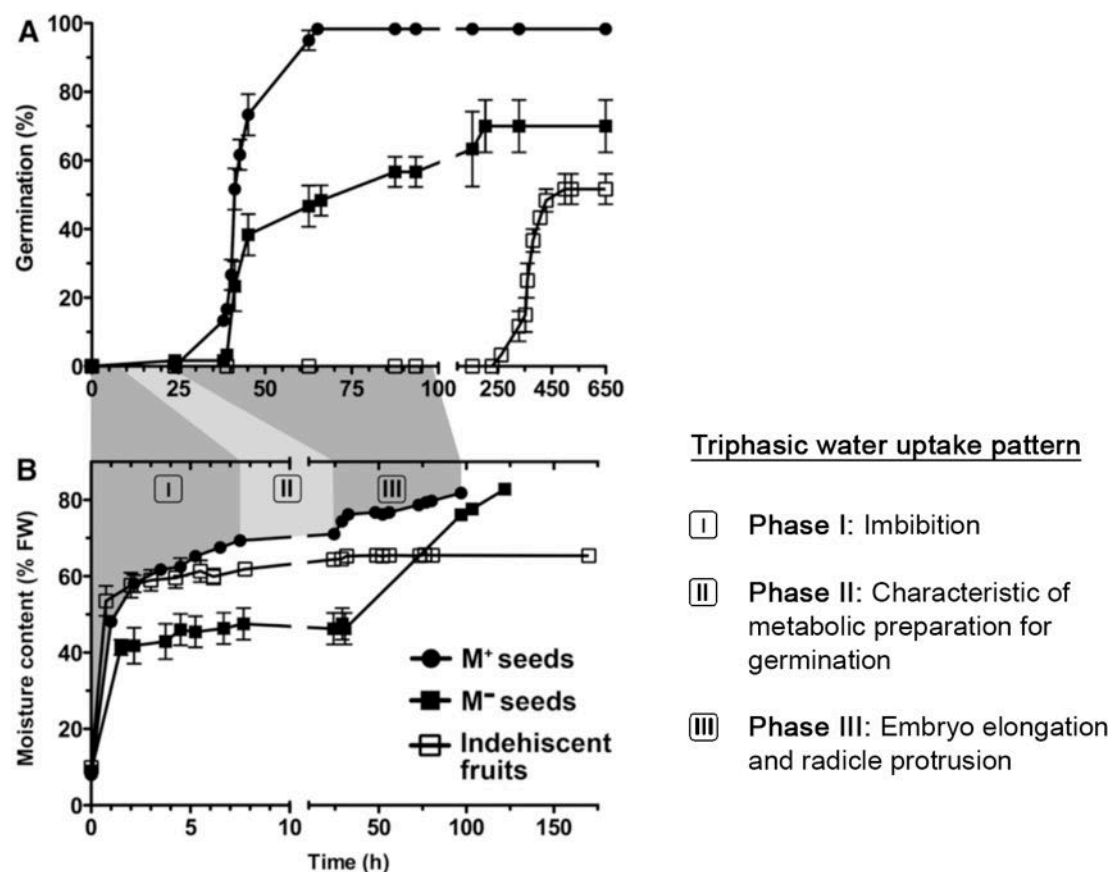


Figure 1-10: Germination and water uptake patterns of *Ae. arabicum* diaspores at 14°C in continuous light. Germination (A) is shown in relation to water uptake kinetics (B), expressed as the percentage moisture content of fresh weight (FW). Figure and caption adapted from Lenser *et al.* (2016).

1.4.4 Effects of seed heteromorphism on seedling growth and establishment

Seedlings – young spermatophyte plants following the completion of germination – face the unpredictability of biotic and abiotic factors affecting their growth and establishment. The morphological and physiological diversity among seedlings, as with seeds, often reflects adaptations to ensure success in heterogeneous habitats (Leck *et al.*, 2008). This critical stage of a plant's life cycle, especially for an annual plant, is therefore a bottleneck where selection pressures are assumed to be high (Harper, 1977). Not only is seed heteromorphism thought to be a form of maternal “bet-hedging”, post-germination effects on seedlings may confer different degrees of survivability, thus protecting against total offspring mortality in heterogeneous or unpredictable environments (Venable, 1985; Lundgren & Sultan, 2005).

Seedlings may exhibit little (*e.g.* agricultural crops) or considerable within-species variability, depending on the constraints imposed by genetic and environmental factors. For example, in *Heterosperma pinnatum* (Asteraceae), central florets typically produce fruits with a long, awned beak, while peripheral achenes are usually wider and lack awns. However, unlike other seed heteromorphic Asteraceae which are typically developmentally-constrained, all *H. pinnatum* florets can produce either awned or unawned fruits. This conspicuous heteromorphism was not associated with ecologically relevant differences in seedlings grown from disk, ray, and intermediate achenes with regards to their size, growth, or competitive ability (Venable *et al.*, 1987; Venable *et al.*, 1995). By contrast, in *Calendula micrantha* (Asteraceae), where multiple ornamented and non-ornamented fruit types all originate from ray

flowers, embryo size is positively correlated with fruit size. This heteromorphism also influenced later life-history parameters with regards to growth, size, and competitive ability of the resulting seedlings (Gardocki *et al.*, 2000).

Differences among heteromorphic diaspores are often associated with differences in embryo size, and thus a difference in seedling growth response may be expected (Imbert, 2002). In the few studies available, seedlings from heavier seeds were more vigorous (*e.g.* Ellison, 1987; Imbert *et al.*, 1996) or had higher reproductive output as adults (Cheplick & Quinn, 1982). However, it is clear that distinct gaps in our knowledge remain with regards to differences in life-history stages of plants grown from different seed morphs. More recent studies in heteromorphic taxa have focused mainly on germinability, dispersibility, and competitive ability, but the manifestation of seed heteromorphism on seedling growth and establishment is poorly understood (Mandák & Pyšek, 2005).

Since the *Ae. arabicum* dimorphism is strongly observed in its fruits and seeds, but not in adult plants (Lenser *et al.*, 2016), the system presents a valuable framework with which to study post-germination behaviours. While most seedlings may face temporarily dry conditions, the effects of drought are heightened in the semi-arid desert environments in which *Ae. arabicum* grows. Thus, seedling establishment of desert annuals requires adaptations and plasticity to allow timing of critical life-history stages with episodic events of favourable environmental conditions. How the seed dimorphism in

Ae. arabicum may confer on seedlings to cope with stressors representative of temporally- and spatially-heterogeneous environments, remains completely unknown.

1.5 Overall project aims and rationale

The overarching aim of this project was to elucidate morpho-physiological, developmental, and underlying molecular mechanisms of fruit, seed, and seedling traits that evolved as adaptations to unpredictable environments. Although these traits are cornerstones for food quality and safety, as well as for the fate of ecosystems, the molecular and developmental biodiversity of mechanisms underlying adaptations to abiotic stresses are only poorly understood. To provide novel insight into heteromorphism as an important bet-hedging strategy, this interdisciplinary project utilised the distinct dimorphic diaspores that develop on the same plant of the annual *Ae. arabicum* (Brassicaceae).

The specific aims of the project were as follows:

- *Chapter 3: Diaspore biophysics and dispersal mechanisms*
 - Determine biomechanical, developmental, and ecophysiological properties influencing the dispersal of M⁺ seeds and IND fruits;
 - Compare the interdependence of dormancy and dispersal for diaspore antitelechory and telechory.
- *Chapter 4: Dimorphic fruit fracturing biomechanics influencing dispersal*
 - Obtain detailed biomaterial profiles for DEH and IND fruits during valve separation;

- Link structure and function of internal and external fruit-related traits during dispersal-mediated fracture.
- *Chapter 5: Comparative development of seed coat mucilage*
 - Determine molecular framework and key transcription factors underpinning morph-specific seed coat development;
 - Conduct high-resolution three-dimensional volumetric investigations during reproductive development, to contextualise with transcriptome analyses.
- *Chapter 6: Seedling physiology, abiotic stress tolerance, and transcriptional “resetting”*
 - Compare development of M⁺ and M⁻ seedling growth in response to abiotic stress factors affecting establishment;
 - Investigate seed, shoot, and root tissue transcriptional profiles for differentially expressed gene expression.

The objectives of my independent research were achieved in collaboration with consortium partner laboratories with distinct expertise. Investigating the regulatory and developmental basis of fruit, seed, and seedling trait diversity is ideal for integrating new technologies and complementary expertise, in order to study a field with utmost importance in ecology, evolution, seed industry and crop breeding.

1.6 References

- Al-Shehbaz IA, Beilstein MA, Kellogg EA. 2006.** Systematics and phylogeny of the Brassicaceae (Cruciferae): an overview. *Plant Systematics and Evolution* **259**(2-4): 89-120.
- Al-Shehbaz IA, Mutlu B, Dönmez AA. 2007.** The Brassicaceae (Cruciferae) of Turkey, updated. *Turkish Journal of Botany* **31**: 327–336.
- Arabidopsis Genome Initiative. 2000.** Analysis of the genome sequence of the flowering plant *Arabidopsis thaliana*. *Nature* **408**(6814): 796.
- Bangerth F. 1989.** Dominance among fruits/sinks and the search for a correlative signal. *Physiologia Plantarum* **76**(4): 608–614.
- Baskin CC, Baskin JM. 2014.** *Seeds: Ecology, Biogeography, and Evolution of Dormancy and Germination*: Elsevier.
- Baskin JM, Baskin CC. 2004.** A classification system for seed dormancy. *Seed Science Research* **14**(1): 1–16.
- Baskin JM, Lu JJ, Baskin CC, Tan DY, Wang L. 2014.** Diaspore dispersal ability and degree of dormancy in heteromorphic species of cold deserts of northwest China: A review. *Perspectives in Plant Ecology, Evolution and Systematics* **16**(2): 93–99.
- Beilstein MA, Al-Shehbaz IA, Kellogg EA. 2006.** Brassicaceae phylogeny and trichome evolution. *American Journal of Botany* **93**(4): 607–619.
- Bhattacharya S, Mayland-Quellhorst S, Müller C, Mummenhoff K. 2018.** Two-tier morpho-chemical defence tactic in *Aethionema* via fruit morph plasticity and glucosinolates allocation in diaspores. *Plant, Cell & Environment* **42**(4): 1381–1392.
- Bremer B, Bremer K, Chase M, Fay M, Reveal J, Soltis D, Soltis P, Stevens P. 2009.** An update of the Angiosperm Phylogeny Group classification for the orders and families of flowering plants: APG III. *Botanical Journal of the Linnean Society* **161**: 105–121.
- Cheplick G, Quinn J. 1982.** *Amphicarpum purshii* and the “pessimistic strategy” in amphicarpic annuals with subterranean fruit. *Oecologia* **52**(3): 327–332.
- Cordazzo CV. 2006.** Seed characteristics and dispersal of dimorphic fruit segments of *Cakile maritima* Scopoli (Brassicaceae) population of southern Brazilian coastal dunes. *Brazilian Journal of Botany* **29**(2): 259–265.
- Couvreur TLP, Franzke A, Al-Shehbaz IA, Bakker FT, Koch MA, Mummenhoff K. 2009.** Molecular phylogenetics, temporal diversification and principles of evolution in the mustard family (Brassicaceae). *Molecular Biology and Evolution* **27**(1): 55–71.
- Ding X, Zhang S, Li Y, Tian C, Feng G. 2010.** Seed polymorphism of an euhalophyte, *Suaeda acuminata* and its adaptation strategy to extremely saline soil. *Acta Botanica Boreali-Occidentalia Sinica* **30**: 2293–2299.
- Domagalska MA, Leyser O. 2011.** Signal integration in the control of shoot branching. *Nature Reviews Molecular Cell Biology* **12**(4): 211–221.

- Ellison AM. 1987.** Effect of seed dimorphism on the density-dependent dynamics of experimental populations of *Atriplex triangularis* (Chenopodiaceae). *American Journal of Botany* **74**(8): 1280–1288.
- Ellner S, Shmida A. 1981.** Why are adaptations for long-range seed dispersal rare in desert plants? *Oecologia* **51**(1): 133–144.
- Ellner SP, Shmida A. 1984.** Seed dispersal in relation to habitat in the genus *Picris* (Compositae) in Mediterranean and arid regions. *Israel Journal of Botany* **33**(1): 25–39.
- Fenesi A, Sándor D, Pyšek P, Dawson W, Ruprecht E, Essl F, Kreft H, Pergl J, Weigelt P, Winter M. 2019.** The role of fruit heteromorphism in the naturalization of Asteraceae. *Annals of Botany* **123**(6): 1043–1052.
- Finch-Savage WE, Leubner-Metzger G. 2006.** Seed dormancy and the control of germination. *New Phytologist* **171**(3): 501–523.
- Franzke A, German D, Al-Shehbaz IA, Mummenhoff K. 2009.** *Arabidopsis* family ties: molecular phylogeny and age estimates in Brassicaceae. *Taxon* **58**(2): 425–437.
- Franzke A, Lysak MA, Al-Shehbaz IA, Koch MA, Mummenhoff K. 2011.** Cabbage family affairs: the evolutionary history of Brassicaceae. *Trends in Plant Science* **16**(2): 108–116.
- Gardocki ME, Zablocki H, El-Keblawy A, Freeman DC. 2000.** Heterocarpy in *Calendula micrantha* (Asteraceae): the effects of competition and availability of water on the performance of offspring from different fruit morphs. *Evolutionary Ecology Research* **2**(6): 701–718.
- Graeber K, Linkies A, Steinbrecher T, Mummenhoff K, Tarkowská D, Turečková V, Ignatz M, Sperber K, Voegelé A, de Jong H, et al. 2014.** DELAY OF GERMINATION 1 mediates a conserved coat-dormancy mechanism for the temperature- and gibberellin-dependent control of seed germination. *Proceedings of the National Academy of Sciences* **111**(34): E3571–E3580.
- Graeber K, Nakabayashi K, Miatton E, Leubner-Metzger G, Soppe WJ. 2012.** Molecular mechanisms of seed dormancy. *Plant, Cell & Environment* **35**(10): 1769–1786.
- Gul B, Ansari R, Flowers TJ, Khan MA. 2013.** Germination strategies of halophyte seeds under salinity. *Environmental and Experimental Botany* **92**: 4–18.
- Harper JL. 1977.** *Population Biology of Plants*. Caldwell, New Jersey: The Blackburn Press.
- Harper JL, Lovell P, Moore K. 1970.** The shapes and sizes of seeds. *Annual Review of Ecology and Systematics* **1**(1): 327–356.
- Haughn G, Chaudhury A. 2005.** Genetic analysis of seed coat development in *Arabidopsis*. *Trends in Plant Science* **10**(10): 472–477.
- Hedge I. 1976.** A systematic and geographical survey of the Old World Cruciferae. In: Vaughan JG, Macleod AJ eds. *The Biology and Chemistry of the Cruciferae*. London: Academic Press.
- Heyn C, Dagan O, Nachman B. 1974.** The annual *Calendula* species, taxonomy and relationships. *Israel Journal of Botany* **23**: 169–201.

- Huang Z, Gutterman Y, Hu Z. 2000.** Structure and function of mucilaginous achenes of *Artemisia monosperma* inhabiting the Negev Desert of Israel. *Israel Journal of Plant Sciences* **48**(4): 255–266.
- Imbert E. 2002.** Ecological consequences and ontogeny of seed heteromorphism. *Perspectives in Plant Ecology, Evolution and Systematics* **5**(1): 13–36.
- Imbert E, Escarre J, Lepart J. 1996.** Achene dimorphism and among-population variation in *Crepis sancta* (Asteraceae). *International Journal of Plant Sciences* **157**(3): 309–315.
- Jiang L, Wang L, Baskin CC, Tian C, Huang Z. 2019.** Maternal effects on seed heteromorphism: a dual dynamic bet hedging strategy. *Seed Science Research* **29**(2): 149–153.
- Kadereit G, Borsch T, Weising K, Freitag H. 2003.** Phylogeny of Amaranthaceae and Chenopodiaceae and the evolution of C₄ photosynthesis. *International Journal of Plant Sciences* **164**(6): 959–986.
- Koornneef M, Bentsink L, Hilhorst H. 2002.** Seed dormancy and germination. *Current Opinion in Plant Biology* **5**(1): 33–36.
- Kreitschitz A, Vallès J. 2007.** Achene morphology and slime structure in some taxa of *Artemisia* L. and *Neopallasia* L. (Asteraceae). *Flora – Morphology, Distribution, Functional Ecology of Plants* **202**(7): 570–580.
- Kunieda T, Mitsuda N, Ohme-Takagi M, Takeda S, Aida M, Tasaka M, Kondo M, Nishimura M, Hara-Nishimura I. 2008.** NAC family proteins NARS1/NAC2 and NARS2/NAM in the outer integument regulate embryogenesis in *Arabidopsis*. *The Plant Cell* **20**(10): 2631–2642.
- Leck MA, Parker VT, Simpson RL. 2008.** *Seedling Ecology and Evolution*. United States of America: Cambridge University Press, New York.
- Lenser T, Graeber K, Cevik ÖS, Adigüzel N, Dönmez AA, Grosche C, Kettermann M, Mayland-Quellhorst S, Mérai Z, Mohammadin S, et al. 2016.** Developmental control and plasticity of fruit and seed dimorphism in *Aethionema arabicum*. *Plant Physiology* **172**(3): 1691–1707.
- Lenser T, Tarkowská D, Novák O, Wilhelmsson P, Bennett T, Rensing SA, Strnad M, Theißen G. 2018.** When the BRANCHED network bears fruit: How carpic dominance causes fruit dimorphism in *Aethionema*. *The Plant Journal* **94**: 352–371.
- Lerouxel O, Cavalier DM, Liepman AH, Keegstra K. 2006.** Biosynthesis of plant cell wall polysaccharides – a complex process. *Current opinion in plant biology* **9**(6): 621–630.
- Li W, Yamaguchi S, Khan AM, An P, Liu X, Tran L-S. 2016.** Roles of gibberellins and abscisic acid in regulating germination of *Suaeda salsa* dimorphic seeds under salt stress. *Frontiers in Plant Science* **6**: 1235.
- Lobova TA, Mori SA, Blanchard F, Peckham H, Charles-Dominique P. 2003.** *Cecropia* as a food resource for bats in French Guiana and the significance of fruit structure in seed dispersal and longevity. *American Journal of Botany* **90**(3): 388–403.
- Lu JJ, Tan DY, Baskin JM, Baskin CC. 2010.** Fruit and seed heteromorphism in the cold desert annual ephemeral *Diptychocarpus strictus*

- (Brassicaceae) and possible adaptive significance. *Annals of Botany* **105**(6): 999–1014.
- Lu JJ, Tan DY, Baskin JM, Baskin CC. 2015.** Post-release fates of seeds in dehiscent and indehiscent siliques of the diaspore heteromorphic species *Diptychocarpus strictus* (Brassicaceae). *Perspectives in Plant Ecology, Evolution and Systematics* **17**(4): 255–262.
- Lundgren MR, Sultan SE. 2005.** Seedling expression of cross-generational plasticity depends on reproductive architecture. *American Journal of Botany* **92**(2): 377–381.
- Mabberley DJ. 2008.** *Mabberley's Plant-book: A Portable Dictionary of Plants, their Classifications, and Uses*: Cambridge University Press.
- Manafzadeh S, Staedler YM, Conti E. 2017.** Visions of the past and dreams of the future in the Orient: the Irano-Turanian region from classical botany to evolutionary studies. *Biological Reviews* **92**(3): 1365–1388.
- Mandák B, Pyšek P. 2005.** How does seed heteromorphism influence the life history stages of *Atriplex sagittata* (Chenopodiaceae)? *Flora – Morphology, Distribution, Functional Ecology of Plants* **200**(6): 516–526.
- Maun A, Maun MA. 2009.** *The Biology of Coastal Sand Sunes*: Oxford University Press.
- Maun M, Payne A. 1989.** Fruit and seed polymorphism and its relation to seedling growth in the genus *Cakile*. *Canadian Journal of Botany* **67**(9): 2743–2750.
- Mohammadin S, Peterse K, van de Kerke SJ, Chatrou LW, Dönmez AA, Mummenhoff K, Pires JC, Edger PP, Al-Shehbaz IA, Schranz ME. 2017.** Anatolian origins and diversification of *Aethionema*, the sister lineage of the core Brassicaceae. *American Journal of Botany* **104**(7): 1042–1054.
- Mühlhausen A, Lenser T, Mummenhoff K, Theißen G. 2013.** Evidence that an evolutionary transition from dehiscent to indehiscent fruits in *Lepidium* (Brassicaceae) was caused by a change in the control of valve margin identity genes. *The Plant Journal* **73**(5): 824–835.
- Müller K, Tintelnot S, Leubner-Metzger G. 2006.** Endosperm-limited Brassicaceae seed germination: abscisic acid inhibits embryo-induced endosperm weakening of *Lepidium sativum* (cress) and endosperm rupture of cress and *Arabidopsis thaliana*. *Plant and Cell Physiology* **47**(7): 864–877.
- Olivieri I, Berger A. 1985.** Seed dimorphism for dispersal: physiological, genetic and demographical aspects. In: Jacquard P, Heim G, Antonovics J eds. *Genetic Differentiation and Dispersal in Plants*: Springer-Verlag Berlin Heidelberg, 413–429.
- Phan JL, Burton RA. 2018.** New insights into the composition and structure of seed mucilage. *Annual Plant Reviews* **1**: 1–41.
- Schranz ME, Lysak MA, Mitchell-Olds T. 2006.** The ABC's of comparative genomics in the Brassicaceae: building blocks of crucifer genomes. *Trends in Plant Science* **11**(11): 535–542.
- Sharma A, Li X, Lim YP. 2014.** Comparative genomics of Brassicaceae crops. *Breeding Science* **64**(1): 3–13.

- Smith HM, Samach A. 2013.** Constraints to obtaining consistent annual yields in perennial tree crops. I: Heavy fruit load dominates over vegetative growth. *Plant Science* **207**: 158–167.
- Venable DL. 1985.** The evolutionary ecology of seed heteromorphism. *The American Naturalist* **126**(5): 577–595.
- Venable DL, Burquez A, Corral G, Morales E, Espinosa F. 1987.** The ecology of seed heteromorphism in *Heterosperma pinnatum* in central Mexico. *Ecology* **68**(1): 65–76.
- Venable DL, Dyreson E, Morales E. 1995.** Population dynamic consequences and evolution of seed traits of *Heterosperma pinnatum* (Asteraceae). *American Journal of Botany*: 410–420.
- Wang H-L, Wang L, Tian C-Y, Huang Z-Y. 2012.** Germination dimorphism in *Suaeda acuminata*: a new combination of dormancy types for heteromorphic seeds. *South African Journal of Botany* **78**: 270–275.
- Warwick SI, Mummenhoff K, Sauder CA, Koch MA, Al-Shehbaz IA. 2010.** Closing the gaps: phylogenetic relationships in the Brassicaceae based on DNA sequence data of nuclear ribosomal ITS region. *Plant Systematics and Evolution* **285**: 209–232.
- Western TL. 2012.** The sticky tale of seed coat mucilages: production, genetics, and role in seed germination and dispersal. *Seed Science Research* **22**: 1–25.
- Western TL, Burn J, Tan WL, Skinner DJ, Martin-McCaffrey L, Moffatt BA, Haughn GW. 2001.** Isolation and characterization of mutants defective in seed coat mucilage secretory cell development in *Arabidopsis*. *Plant Physiology* **127**(3): 998–1011.
- Western TL, Skinner DJ, Haughn GW. 2000.** Differentiation of mucilage secretory cells of the *Arabidopsis* seed coat. *Plant Physiology* **122**(2): 345–356.
- Willats WG, McCartney L, Knox JP. 2001.** *In-situ* analysis of pectic polysaccharides in seed mucilage and at the root surface of *Arabidopsis thaliana*. *Planta* **213**(1): 37–44.
- Windsor JB, Symonds VV, Mendenhall J, Lloyd AM. 2000.** *Arabidopsis* seed coat development: morphological differentiation of the outer integument. *The Plant Journal* **22**(6): 483–493.
- Witztum A, Gutterman Y, Evenari M. 1969.** Integumentary mucilage as an oxygen barrier during germination of *Blepharis persica* (Burm.) Kuntze. *Botanical Gazette* **130**(4): 238–241.
- Xu Y, Zhao Y, Duan H, Sui N, Yuan F, Song J. 2017.** Transcriptomic profiling of genes in matured dimorphic seeds of euhalophyte *Suaeda salsa*. *BMC Genomics* **18**(727): 1–14.
- Yang X, Baskin JM, Baskin CC, Huang Z. 2012.** More than just a coating: Ecological importance, taxonomic occurrence and phylogenetic relationships of seed coat mucilage. *Perspectives in Plant Ecology, Evolution and Systematics* **14**(6): 434–442.
- Zhang J. 1993.** Seed dimorphism in relation to germination and growth of *Cakile edentula*. *Canadian Journal of Botany* **71**(9): 1231–1235.
- Zhang J. 1995.** Differences in phenotypic plasticity between plants from dimorphic seeds of *Cakile edentula*. *Oecologia* **102**(3): 353–360.

Zohary M, Fahn A. 1950. On the heterocarpy of *Aethionema*. *Palestine Journal of Botany: Jerusalem Series* **5**: 28–31.

2. Materials and methods

2.1 Methods employed in Chapter 3

2.1.1 *Seed collection and plant growth*

Mature plants of *Aethionema arabicum* (L.) Andr. ex DC. were grown from accession ES1020 (obtained from Eric Schranz, Wageningen University and Research Centre). This is an accession that was used to generate the reference genome (Haudry *et al.*, 2013), and also used for the first characterisation of its seed and fruit dimorphism (Lenser *et al.*, 2016). Plants were grown in Levington F₂ compost with added horticultural grade sand (F₂ + S), containing Exemptor[®] (10% w/w thiacloprid) at the maximum individual dose of 400 g per cubic metre of compost. Plants were grown under long-day conditions (16 h light/20°C and 8 h dark/18°C) in a greenhouse.

2.1.2 *Diaspore biometrics and aerodynamic properties*

Sixty replicates each of M⁺ seeds, M⁻ seeds extracted from IND fruits, and IND fruits were used to quantify height, width, and depth. A Leica DFC480 digital camera system, Leica Applications Suite (v4.5), and ImageJ (v1.5i) were used to measure distances (in µm) from photographs. The mean mass of single diaspores was determined based on International Seed Testing Association (ISTA) methodology (ISTA, 2015). Diaspore shapes were approximated as triaxial ellipsoids in order to calculate surface area. Time taken (in hours) for cumulative germination to reach 50% of its maximum (T₅₀) was obtained from seed germination experiments with freshly harvested mature fruits and seeds

placed in Petri dishes containing two layers of filter paper, 3 ml of dH₂O, and 0.1% (v/v) Plant Preservative Mixture (Plant Cell Technology). Plates were incubated in an MLR-350 Versatile Environmental Test Chamber (Sanyo-Panasonic) at 14°C, with 100 $\mu\text{mol s}^{-1} \text{m}^{-2}$ constant white light, as described in Lenser *et al.* (2016).

2.1.3 Measurement of abscisic acid (ABA) concentration

Endogenous ABA content was determined using the Phytodetek[®] ABA enzyme immunoassay kit (Agdia Inc., USA) according to the manufacturer's instructions. Five replicates of diaspores (each of 50 mg) were frozen in liquid nitrogen, ground to a fine powder for 30 sec using a Precellys[®]-24 tissue homogeniser (Bertin Instruments, CNIM Group). ABA was extracted with a chilled solution of 80% (v/v) methanol, 100 mg l⁻¹ butylated hydroxytoluene, and 0.5 g l⁻¹ citric acid monohydrate. This test utilised a competitive antibody binding method, whereby ABA-tracer labelled with alkaline phosphatase was added along with the extracts to anti-ABA monoclonal antibody coated microwells. Extract ABA competes with the ABA-tracer for antibody binding sites (competitive binding reaction). After the unbound ABA-tracer is washed away before adding the substrate, the colouration produced is inversely proportional to the amount of ABA in the sample, the intensity of which is related to sample ABA concentration by a standard curve.

2.1.4 Quantification of fruit valve dehiscence

Mature DEH and IND fruits from dry (17% relative humidity [RH]), high-humidity (65% RH) and water-sprayed (100% RH) plants were clamped into

the jaws of a single-column tensile testing machine (Zwick Roell ZwickiLine Z0.5) configured with a 200 N load cell (Zwick Roell Xforce HP). Separation speed (*i.e.* displacement) was set at 1 mm min⁻¹. A transducer connected in series with the specimen holder provides an electronic reading of the load corresponding to the displacement. Force-displacement data were obtained using 30 (17% RH and 65% RH) and 40 (100% RH) replicates from mature main branch infructescences. Maximum force (F_{\max}) and the slope of the linear elastic element were obtained. During low strain of the sample, materials typically obey Hooke's law to a reasonable approximation, such that the stress is proportional to strain. Increasing strain results in deviation from linear proportionality of the sample (stress-induced "plastic" flow in the specimen) (Roylance, 2001). Thus, parameters describing the material properties of a specimen can be obtained from such biomechanical profiles.

2.1.5 Fruit, fruit valve, and seed resistance to raindrop impact

A raindrop test method was applied to mature fruits on dry and wet infructescences. The opening (\varnothing 1.5 mm) of a burette was placed 50 cm above a single fruit or seed. The number of single raindrops (of mean mass 53.55 ± 0.97 mg) directly impacting the fruit/seed were counted until fruit abscission (in DEH and IND fruits) or seed detachment (in M⁺ seeds) occurred. 100 replicates of each diaspore were tested.

2.1.6 Dispersal ability in still air

The time required for 100 diaspores to fall individually from a height of 108 cm in a plastic tube (\varnothing 15 cm) was measured using high-speed (120 frames sec⁻¹)

movies, recorded using a Nikon Coolpix P100 and processed with Windows Movie Maker program (Version 2012). Fall rate (m s^{-1}) was calculated over this height.

2.1.7 Dispersal ability in flowing air

To index dispersal capacity and distribution patterns, the distances travelled by dispersing diaspores were determined following Telenius and Torstensson (1989) and Lu *et al.* (2010). One hundred diaspores were individually exposed for 60 s to a constant stream of air parallel to a flat landing surface. A ventilator (Quigg BF-12A) was used to simulate a wind velocity of 4 m s^{-1} , representative of the environment (Apaydin *et al.*, 2011), in a custom-built wind channel (H: 60 cm, L: 360 cm, W: 48 cm). Diaspores were released from a height of 30 cm, 10 cm from the front of the ventilator, and the total distance travelled was measured to the nearest 0.01 m.

2.1.8 Effect of diaspore on substrate attachment

Adherence potential was tested by placing diaspores on dry and water-saturated sand (< 2 mm grains) in Petri dishes for 10 min. Seeds/fruits were rotated to allow whole-surface contact with the substrate, and subsequently removed. The mass of the dry seeds/fruits, including the soil particles attached to them, was compared with the mass of the same dry seeds or fruits before exposure. Three replicates each of 25 diaspores were tested.

2.1.9 *Diaspore displacement mediated by surface water run-off*

Diaspore displacement by surface water run-off was quantified using a custom-built device consisting of a container with 53 holes (\varnothing 400 μ m) above a 6°-sloped 80 × 30 cm plate, covered with 80-grit sandpaper (modified from García-Fayos *et al.*, 2010). During each simulation, water flow was stopped after 1 l had been discharged from the sprinkling head within 2.5 min. The total distance one hundred replicates of each diaspore had travelled on the plate was measured.

2.1.10 *Diaspore buoyancy properties*

To test the comparative effects of buoyancy on seed and fruit dispersal, three replicates, each of 25 diaspores, were placed on the surface of 150 ml water contained within 250 ml Erlenmeyer flasks. Water movement of flasks was simulated by agitation on an orbital shaker at 100 rpm (Truscott *et al.*, 2006; Sun *et al.*, 2012). The number of floating diaspores were counted over time.

2.1.11 *Statistical analyses*

R was used to assess the distribution of the data and test for normality and homogeneity of variance. Normal and homogeneous data were subjected to one-way analysis of variance (ANOVA), with *post-hoc* comparisons made by a Tukey's honest significant difference (HSD) test. The rejection level for all analyses was $P < 0.05$. Data exhibiting a non-Gaussian distribution or non-homogeneous variances were transformed by a Box-Cox (Box & Cox, 1964) transformation using the MASS package (Venables & Ripley, 2002) in *R*. Analyses of diaspore behaviour on substrata were performed by a three-way

ANOVA (with diaspore morph, imbibition state, and sand state as main factors). Analyses of diaspore buoyancy were performed by a univariate type-III repeated-measures ANOVA (with diaspore morph and time interaction included as fixed effects). All statistical analyses were conducted in *R* (v3.4.2) or GraphPad Prism (v7.0a).

2.2 Methods employed in Chapter 4

2.2.1 *Fruit valve tensile testing and energy absorption relations*

Data from Arshad *et al.* (2019) were re-analysed to obtain the energy absorption of fruit valve separation. As described in 2.1.4, force-displacement data were obtained using 30 replicates from three mature main branch infructescences. All fruits were freshly-harvested from plants grown under long-day conditions (16 h 20°C : 8 h 18°C, light : dark) in a glasshouse, and mechanically tested at room temperature (20°C) and 31% relative humidity. The total area under the resultant force-displacement curve was calculated as the mechanical energy consumed by the pericarp in straining it to its fracture point. Using a digital camera (Canon EOS 5D Mark II, fitted with a EF 100 mm f/2.8 macro lens) and Fiji (Schindelin *et al.*, 2012), the area representing the pericarp fracture zone was determined for 50 manually-separated replicates each of DEH and IND fruits. An unpaired two-samples *t*-test was carried out using *R* version 3.5.1 (R Foundation for Statistical Computing, Vienna, Austria).

2.2.2 *Scanning Electron Microscopy (SEM) analysis of fractured fruit valve surfaces*

Mature, dry fruit pericarps of both *Ae. arabicum* morphs were mounted on 12.5 mm Cambridge aluminium specimen stubs, using conductive putty (Lennox Educational, Ireland) or two-component epoxy (Araldite®, Huntsman Advanced Materials GmbH, Switzerland). Samples were sputter-coated with a 40 nm thickness of gold or gold-palladium using a Polaron SEM Coating Unit E5100 (Bio-Rad Microscience Division, UK) at the Imaging and Microscopy

Centre, University of Southampton. Pericarp fracture surfaces were studied using SEM (Hitachi S-3000N, Japan) at an acceleration voltage of 20 kV, at Royal Holloway University of London. Images were subsequently contrast adjusted in Adobe Photoshop CC.

2.2.3 Synchrotron-based Radiation X-ray Tomographic Microscopy (SRXTM) of fracture zones

Mature, dry fruits were fixed in 3% glutaraldehyde plus 4% formaldehyde in 0.1 M piperazine-*N,N'*-bis(2-ethanesulfonic acid) (PIPES) buffer at pH 7.2, for 3 h. Samples were then rinsed twice for 10 min with 0.1 M PIPES, before dehydration in five changes of ethanol (30%, 50%, 70%, 95%, 100%). Samples were critical point dried (Balzers CPD-030, Bal-Tec, Germany) using ethanol as the intermediate fluid and CO₂ as the transitional fluid. Dehiscent and indehiscent fruit samples were mounted onto 3 mm diameter brass pin stubs using two-component epoxy (Araldite[®], Huntsman Advanced Materials GmbH, Switzerland) and imaged at the TOMographic Microscopy and Coherent rAdiology experimentTs (TOMCAT) beamline of the Swiss Light Source, Paul Scherrer Institute (Stampanoni *et al.*, 2006). Data were acquired using a 10× objective and a sCMOS camera (PCO.edge, PCO, Kelheim, Germany), with an exposure time of 80 ms at 12 keV (isotropic voxel dimensions = 0.65 μm). A total of 1501 projections were acquired equiangularly over 180°, post-processed and reconstructed using a Fourier-based algorithm (Marone & Stampanoni, 2012). For verification, three replicates were examined for each fruit morph. Axial tomographic slice data derived from the scans were analysed and manipulated using Avizo™ 9.5.0

(Thermo Scientific™, Visualization Science Group Inc., Burlington, MA) for Windows 10 Pro 64-bit, and contrast adjusted in Adobe Photoshop CC.

2.3 Methods employed in Chapter 5

2.3.1 *Plant material and experimental growth conditions*

Growth conditions are as described in 2.1.1. The day after pollination (DAP) was defined phenotypically as the time after at which the flowers open (anthesis) and the four long stamens extend over the gynoecium.

2.3.2 *Synchrotron-based Radiation X-ray Tomographic Microscopy (SRXTM) of reproductive development*

SRXTM of buds, flowers, immature (~7–10 DAP) fruits, and mature (~ 30–40 DAP) fruits is as described in 2.2.3.

2.3.3 *Whole seed staining for mucilage*

Whole M⁺ and M⁻ seeds were imbibed in 0.01% (w/v) ruthenium red (Sigma-Aldrich, 11103-72-3) or 0.01% (w/v) methylene blue (VWR, 3470.0025) for two minutes, then visualised under a Leica MZ-125 stereomicroscope.

2.3.4 *Histological analysis of seed coat differentiation during development*

Developing gynoecia from 0 to 7 DAP were harvested and fixed in vacuum-infiltrated FAA fixation solution (2% formaldehyde, 5% glacial acetic acid, 60% EtOH, 0.1% Tween-20) at 4°C for 24 h. Samples were then washed twice for 5 min with 70% EtOH. Subsequent preparation followed Huang *et al.* (2015). *Dehydration*: samples were dehydrated in three changes of ethanol (80%, 95%, 100%) by shaking on ice for 60 minutes each. *Clearing*: dehydrated materials were treated in different concentrations of ethanol in six changes. 100% EtOH (30 mins), 100% EtOH (1 h), 25% HistoClear™ in EtOH (1 h), 50%

HistoClear™ in EtOH (1 h), 75% HistoClear™ in EtOH (1 h), 100% HistoClear™ (4 h). Finally, HistoClear™ and first-grade paraffin were added, and incubated at 42°C. *Paraffin inclusion and embedding*: samples were incubated at 60°C overnight, and transferred into fresh melted paraffin every 3–5 h. Materials were then embedded by pouring the melted paraffin plus samples into Peel-A-Way® disposable embedding moulds. *Sectioning*: 6 µm sections were prepared with a MICROM HM 355 S rotary microtome (Walldorf, Germany) and Leica 819 low-profile disposable blades. *Section mounting*: paraffin sections were retrieved and mounted on glass slides using Mayer's egg albumin solution. Slides were then spread on a hot plate at 42°C. *Deparaffinisation*: slides were successively incubated in two changes of 100% HistoClear™ for 1 h each, seven changes of different concentrations of ethanol as follows: 100%/30 min, 100%/30 min, 95%/30 min, 85%/30 min, 75%/30 min, 50%/30 min, and 30%/30 min, then in 0.85% NaCl for 1 h, and finally 1 × PBS (pH 7.0) for 5 min. *Staining*: for toluidine staining, slides were dipped into 0.05% toluidine blue for 1 min, then gently washed with dH₂O. For safranin and astrablue counterstaining, slides were dipped into 1% safranin for 1 min, gently washed with dH₂O, dipped into 0.5% astrablue for 2 min, and finally washed with dH₂O. *Microscopy examination*: sections were inspected using a Nikon ECLIPSE Ni-E upright motorised microscope and photographs were acquired using Nikon Imaging Software NIS-Elements Basic Research (Version 4.2). Image files were converted to TIFF format, and subsequently enhanced for colour and clarity using Adobe Photoshop Lightroom Classic CC (Version 7.2).

2.3.5 RNA extraction for RNA-seq

Floral buds (0 DAP), flowers at anthesis (1 DAP), and fruits (~30 DAP) at their full length (prior to the onset of yellowing and drying) were harvested from second-order branches of plants that grew undisturbed (IND) or from the main branch of plants where side branches were constantly removed during development (DEH), as previously described (Lenser *et al.*, 2018). Total RNA was isolated from 50 mg of bud, flower, and fruit tissue using QIAzol Lysis Reagent (Qiagen, Hilden, Germany). Genomic DNA was removed by DNaseI (Roche, Mannheim, Germany) digestion in solution, followed by RNA purification using RNeasy Mini spin columns (QIAGEN, Hilden, Germany). RNA quantity and purity were determined using a NanoDrop™ spectrophotometer (ND-1000, ThermoScientific™, Delaware, USA) and Agilent 2100 Bioanalyzer with the RNA 6000 Nano Kit (Agilent Technologies, CA, USA) using the 2100 Expert Software to calculate RNA Integrity Number (RIN) values. Four biological replicate RNA samples were used. Sequencing was performed at the Vienna BioCenter Core Facilities (VBCF) Next Generation Sequencing Unit, Vienna, Austria (www.vbcf.ac.at). Libraries were sequenced in 50-bp single-end mode on Illumina® HiSeq 2000 Analyzers using the manufacturer's standard cluster generation and sequencing protocols.

2.3.6 RNA-seq, data trimming, filtering, and analysis

The cDNA sequence libraries were processed, including data trimming, filtering, read mapping and feature counting, as previously described (Wilhelmsson *et al.*, 2019). Raw RNA-seq reads were quality control checked (FastQC), processed to remove adapters and low-quality bases (Trimmomatic,

PrinSeq), and cleaned reads mapped (GSNAP) to the *Aethionema arabicum* genome version 2.5 (Haudry *et al.*, 2013). After normalisation, genome-mapped reads were compared at each developmental stage using *R* (R Core Team, 2013) and the Bioconductor package DESeq2 (Love *et al.*, 2014; Huber *et al.*, 2015), to identify differentially expressed genes using an adjusted *P*-value (FDR) cut-off for optimising the independent filtering set to 0.05 (= α). The differential expression analysis was based on the Negative Binomial (Gamma-Poisson) distribution model (= DESeqDataSet), and created using an input matrix of non-negative integers (= countdata). The contrasts argument was used to specify the individual comparisons from the DESeqDataSet, in order to build a results table at each developmental time point. Indehiscent samples were compared against dehiscent samples (baseline) in all comparisons.

Principal Component Analyses (PCAs) and clustered heat-maps were created using a custom script, the *pheatmap* (Kolde, 2015) package in *R*, and GraphPad Prism (v.7.0a; San Diego, CA, USA). In summary, the count data were transformed using a variance stabilising transformation (VST), yielding a matrix of approximately homoskedastic values (having constant variance along the range of mean values), and then the top 500 genes (selected by highest row variance) visualised on the first three principal components.

2.3.7 Gene Ontology (GO) term and promoter motif analyses

Transcripts of *Aethionema arabicum* genome (version 2.5) were annotated with GO terms as previously described (Wilhelmsson *et al.*, 2019). GO term

enrichment was analysed with the topGO Bioconductor package using the classic algorithm, where each GO category is tested independently, and the fisher statistic (Huber *et al.*, 2015; Alexa & Rahnenfuhrer, 2016), using a *P* value cut-off at 0.05.

Enriched promoter motifs from the *Arabidopsis* DNA affinity purification motif database (O'Malley *et al.*, 2016) were identified using Analysis of Motif Enrichment (AME) in MEME Suite 5.0.4, with DEG promoter sequences used as the primary sequences and all promoter sequences used as the control sequences (average odds score with fisher's exact test) (Bailey *et al.*, 2009; Buske *et al.*, 2010). Promoter sequences were defined as –1000 and +100 base pairs from the transcription start site based on *Ae. arabicum* genome (version 2.5) mRNA annotation.

2.3.8 Identification of gene orthologs

Orthologs of *Arabidopsis thaliana* genes were identified in *Ae. arabicum* by searching query sequences with BLASTP (Altschul *et al.*, 1990) against a plant-specific protein database. To detect homologous sequences, results were filtered for adequate query coverage and amino acid similarity (Rost, 1999). Sequence data from *Ae. arabicum* are available in the CoGe database (<https://genomevolution.org/coge/>) under the following genome ID: v2.5, id33968.

2.3.9 Gene expression analysis via quantitative RT-PCR

Floral buds (0 DAP), and flowers at 1, 3, and 10 DAP were harvested from second-order branches (indehiscent) or from the main branch (dehiscent) of multiple undisturbed plants. Tissue was frozen in liquid nitrogen, and ground using a Precellys®-24 tissue homogeniser (Bertin Instruments, CNIM Group). RNA was extracted using methods described for RNA-seq. The quantity and purity of RNA was determined using an Agilent 2100 Bioanalyzer with the RNA 6000 Nano Kit (Agilent Technologies, CA, USA), using the 2100 Expert Software to calculate RNA Integrity Number (RIN) values. One µg DNase I-treated RNA was used for cDNA synthesis with random hexamer primers, using the Invitrogen™ SuperScript™ III First-Strand Synthesis System (Thermo Scientific).

qRT-PCR reactions were performed in a CFX96 Touch™ Real-Time PCR Detection System (Bio-Rad), using ABsolute qPCR SYBR Green Mix (Thermo Scientific) and primer pairs listed in 2.3.10, with the following parameters: 95°C for 15 min, 40 cycles with 95°C for 15 sec, and 60°C for 30 sec, and 72°C for 30 sec, then 65°C for 31 sec.

Melt-curve analysis verified the absence of primer-dimer artefacts and amplification of a single product from each qPCR assay. PCR efficiencies and C_q values were calculated using Real-time PCR Miner algorithm (Zhao & Fernald, 2005; Graeber *et al.*, 2011) using raw fluorescence data as input. The geometric mean of *Aethionema* orthologues of ADAPTIN FAMILY PROTEIN (AearAFP, AA44G00404), CALCINEURIN-LIKE METALLO-

PHOSPHOESTERASE SUPERFAMILY PROTEIN (AearCMSP, AA10G00283), and the unknown protein AA19G00315 (AearAA19G00315) was used as reference for normalisation. All qRT-PCR experiments were performed using five independent biological replicates. Statistical analysis was performed using GraphPad Prism (v.7.0a; San Diego, CA, USA), using a two-way ANOVA with a Šídák's *post-hoc* correction for multiple comparisons.

2.3.10 Primers used for qRT-PCR

Primers used for measurement of gene expression were designed in Geneious® (v.8.1.9; Biomatters Ltd.) using Primer3 (Untergasser *et al.*, 2012). Sequences are given in Table 2-1.

Table 2-1: List of primers used for quantitative RT-PCR analysis.

Name	<i>Aethionema arabicum</i> (genome v2.5) ID	Sequence (5' – 3')
AA19G00315_2 - 546 F	AA19G00315	TGGTGCACGTGAGCTCTTAG
AA19G00315_2 - 723 R		ATCTTTGGTGGGAGTGCTGG
AFP_1 - 415 F	AA44G00404	AGAACGGTGGCTGTAACTGG
AFP_1 - 617 R		GATTCCTTTTCCCGGCATGC
CMSP_1 - 239 F	AA10G00283	TTGGTCCGGCTTTGTCTTTG
CMSP_1 - 445 R		CACCAAAGTTATCATGGTTTCCCC
AP2_1 - 271 F	AA30G00232	AAACGGTGAAAGCGGTTGTG
AP2_2 - 399 R		GAGCTCCGTGATCTTGACC
GL2_1 - 377 F	AA89G00009	ATCCGGACGAGAAGCAAAGG
GL2_1 - 511 R		CTTTCAGCAGCGAGTTCTCG
MEEA14_1 - 121 F	AA123G00058	GTGGTTCGGTGTTCAAGCAC
MEEA14_1 - 268 R		AGTCATCACCTTCCAGCGTC
MYB61_1 - 247 F	AA42G00001	GCAGTCCTCGGAAACAGATG
MYB61_1 - 421 R		TTGCAGAAGAAGTTGAAGCAGG
TTG1_1 - 274 F	AA13G00129	CTTCGTCGCTCATCTACCGG
TTG1_1 - 414 R		CAACGGTGCACAGAACTCAC
CESA2_2 - 907 F	AA20G00013	TGTGAGATTTGGTTTGCTGTTTC
CESA2_2 - 1,074 R		TGCTAATCCTGATGGCTTCCC
MUM3/CESA5_2 - 652 F	AA4G00210	CGAATGGAGGAATGGAAGCG
MUM3/CESA5_2 - 783 R		TCGTGATAACGGTTGCCTCC
MUM4/RHM2_1 - 1,469 F	AA15G00120	CAGAGGGGTCAGGGATTGG
MUM4/RHM2_1 - 1,640 R		ATGAAGTTTCGCGGGTTCTC
PMEI6_1 - 180 F	AA21G00495	TTCGCCATTCTCCTCTCTCG
PMEI6_1 - 293 R		CGCCGCGTTTTGAGTAAGAG
MEEA59_2 - 367 F	AA30G00244	GGTGAGGAGAGTGTAACCGC
MEEA59_2 - 454 R		CATTTGTCGCCGGATTTCCC

2.4 Methods employed in Chapter 6

2.4.1 *Temperature profiling for optimal germination*

A temperature gradient ranging from 5 to 29 °C (in 2 or 2.5 °C increments) was established using a previously-equilibrated thermo-gradient table (Model: GRD1, Grant Instruments, Cambridge, UK). Three replicate Petri dishes, each containing approximately 30 freshly harvested mature fruits or seeds, were imbibed on two layers of filter paper with 3 ml of dH₂O and 0.1% (v/v) Plant Preservative Mixture (Plant Cell Technology). Final germination percentage (G_{\max}) and rates for germination to reach 50% of its maximum (GR_{50}) were obtained using automated curve fitting on cumulative germination data, using the Solver add-in in Germinator (El-Kassaby *et al.*, 2008; Joosen *et al.*, 2010).

2.4.2 *Seed sterilisation and germination*

M⁺ and M⁻ seeds were surface-sterilised in 2% (v/v) sodium hypochlorite (NaClO) solution supplemented with 0.02% (v/v) Triton X-100 (112298, Merck), for five minutes and washed four times with sterile dH₂O. After surface sterilisation, seeds were placed in Petri dishes containing two layers of filter paper and 3 ml of sterile dH₂O. Seeds were germinated under dark conditions at 10°C, and selected for transfer to plates containing media based on 1 mm protrusion of the radicle.

2.4.3 *Preparation of plant growth medium*

' $\frac{1}{10}$ MS' was prepared by dissolving 0.44 g Murashige and Skoog (MS) basal medium (M5519, Sigma) per litre of water containing 1% (w/v) agar (P1001.1000, Duchefa Biochemie), and subsequently autoclaved (Murashige

& Skoog, 1962). This recipe was the basis for all vertical seedling growth experiments and adapted for specific stresses.

For growth during osmotic stress, water potentials were lowered by using high-molecular weight polyethylene glycol (PEG₆₀₀₀; 26603.293, VWR) using an overlay method (as described in van der Weele *et al.*, 2000; Verslues & Bray, 2004). For growth responses under salinity stress, $\frac{1}{10}$ MS was prepared containing 0 mM, 20 mM, 40 mM, and 60 mM NaCl (S3014, Sigma-Aldrich), with 80 mM mannitol (M1902, Sigma-Aldrich) and 4 mM lithium chloride (62476, Sigma-Aldrich) prepared as comparative osmotic and the ionic controls, respectively (Tester & Davenport, 2003; Kazachkova *et al.*, 2016).






All plates were grown vertically at a constant temperature of 14°C (osmotic), a range of temperatures between 14°C and 35°C (thermal stress), and at 30°C for salinity stress.

2.4.4 Basal thermotolerance assay

Seeds that had completed germination (1 mm radicle protrusion) under dark conditions at 10°C were transferred to plates containing $\frac{1}{10}$ MS with 0.8% (w/v). Seedlings were grown at 25°C in constant light (170 $\mu\text{mol m}^{-2} \text{s}^{-1}$), before being heat shocked (20 minutes in water bath at specified temperature) at 4 days old. Heat shock temperatures were 25°C (control), 39°C, 42°C, 45°C, 48°C, and 51°C. A photograph was obtained following the heat shock, after which plates were returned to 25°C constant light. Plates were scored multiple

days after heat shock to determine viability and to visually score seedlings based on the following 5-point scale (Table 2-2).

Table 2-2: Classification of seedlings in tests of basal thermotolerance. Seedlings were classified based on the presence or absence of lesions indicating possible necrosis of leaf tissue. Representative photographs are provided (not to scale).

Numerical score	Description of seedling phenotype	Representative photographs
0	Healthy, not affected	
1	Evidence of abnormality / very small heat shock lesion	
2	Moderate damage (< 50% lesions)	
3	Severe damage (> 50% lesions)	
4	Completely dead (100% lesions)	

2.4.5 Time-course characterisation of chlorophyll content

Three replicate plates, each containing 10 M⁺ and M⁻ seedlings transferred to 1/10 MS with 0.8% (w/v), were grown horizontally at 30°C. Chlorophyll content of seedlings was determined after extracting pigments from leaf tissues homogenised in methanol at room temperature for 15 mins while shaking at 1000 rpm on a thermomixer (S8012-0000, Starlab). Extracts were centrifuged for 5 min at 14,000 g. The absorbance of the supernatant was determined at

750 nm, 665 nm and 652 nm using a microplate reader (Spark[®] 10M, Tecan, Switzerland), and subsequently used to calculate chlorophyll concentration using equations given in Porra *et al.* (1989).

2.4.6 Seedling sample selection and RNA extraction

Three replicates, each of 90 individual M⁺ seeds, M⁻ seeds, and IND fruits imbibed on two layers of filter paper with 3 ml of dH₂O and 0.1% (v/v) Plant Preservative Mixture (Plant Cell Technology) under darkness at 9°C, were harvested at T_{1%} and T_{100%}. These samples were prepared as described in 2.4.2, and represented the germination process. Approximately 12 surface-sterilised M⁺ seeds, M⁻ seeds, and IND fruits that had completed germination (1 mm radicle protrusion) were transferred to plates containing 1/10 MS and 1% (w/v) agar, and grown vertically at 30°C. Root and shoot tissue was separated from seedlings that had been grown under constant light (170 μmol m⁻² s⁻¹) for four and 10 days, corresponding to the maximum growth rate and emergence of true leaves respectively.

Tissue was homogenised at 6500 rpm using a Precellys[®]-24 (Bertin Instruments, CNIM Group). Seed and shoot total RNA was isolated using a protocol modified from Chang *et al.* (1993). After the addition of RNA extraction buffer (2% [w/v] hexadecyltrimethylammonium bromide [CTAB], 2% [w/v] polyvinylpolypyrrolidone [PVP], 100 mM Tris-HCl pH 8.0, 25 mM ethylenediaminetetraacetic acid [EDTA], 2 M NaCl, and 2% [v/v] β-mercaptoethanol), samples were incubated at 65°C for 10 mins with intermittent vortexing. Chloroform:isoamylalcohol (24:1) extractions were

repeated three times. After the addition of 10 M LiCl to a final concentration of 2 M, RNA was precipitated overnight at 4°C, and then dissolved in Sodium Chloride-Tris-EDTA (STE) buffer (1 M NaCl, 0.5% [w/v] SDS, 10 mM Tris-HCl pH 8.0, 1 mM EDTA). Three further chloroform:isoamylalcohol (24:1) extractions were then performed, before precipitation in 100% (v/v) ethanol overnight at –80°C. Samples were then centrifuged for 20 min at 4°C. After removal of the aqueous phase, the RNA pellet was washed with 70% (v/v) ethanol. Samples were centrifuged for 20 min, the ethanol was carefully removed, and the RNA subsequently dissolved in RNase-free water. Genomic DNA was removed by DNase-I (QIAGEN) digestion in solution, followed by additional purification using columns (QIAGEN RNeasy Kit). Shoot tissue RNA was isolated using the RNeasy Plant Mini Kit (QIAGEN) and manufacturer's instructions.

2.4.7 Assessment of RNA quantity and quality

RNA quantity and purity were determined using a NanoDrop™ spectrophotometer (ND-1000, ThermoScientific™, Delaware, USA). Only high-quality samples with absorbance ratios of at least 2.0 (260/280 nm) and 1.8 (260/230 nm) were separated electrophoretically on an Agilent 2100 Bioanalyzer with the RNA 6000 Nano Kit (Agilent Technologies, CA, USA) and 2100 Expert Software (Version B.02.08.SI648) to calculate RNA Integrity Number (RIN) values. At least three biological replicate RNA samples were used for sequencing and mRNA library preparation as described in 2.3.5 and 2.3.6.

2.4.8 RNA-seq, data processing and differentially expressed gene (DEG) detection

Processed reads mapped against the *Ae. arabicum* genome (version 2.5) were analysed using the pipeline as described in Wilhelmsson *et al.* (2019). Two parametric methods (EdgeR and DESeq2) and a non-parametric method (NOISeq) were used to normalise read counts and to detect Differentially Expressed Genes (DEGs) in a strict consensus (overlap) approach.

2.4.9 Statistical analyses

Data are expressed as mean \pm 1 standard error. Statistical analysis of experiments was performed using GraphPad Prism (v.7.0a; San Diego, CA, USA), using analysis of variance (ANOVA) procedures. For studies examining abiotic stress effects, data were analysed by two-way ANOVA, with seedling morph and seedling age (time) as between-group factors. Multiple comparisons were performed using Šídák's *post-hoc* correction (Abdi, 2007) in GraphPad Prism. Results were considered statistically significant if the *P* value was less than 0.05.

2.5 References

- Abdi H. 2007.** Bonferroni and Šidák corrections for multiple comparisons. *Encyclopedia of Measurement and Statistics* **3**: 103–107.
- Alexa A, Rahnenfuhrer J. 2016.** topGO: Enrichment Analysis for Gene Ontology. *R package version 2.32.0*.
- Altschul SF, Gish W, Miller W, Myers EW, Lipman DJ. 1990.** Basic local alignment search tool. *Journal of Molecular Biology* **215**(3): 403–410.
- Apaydin H, Anli AS, Ozturk F. 2011.** Evaluation of topographical and geographical effects on some climatic parameters in the Central Anatolia Region of Turkey. *International Journal of Climatology* **31**(9): 1264–1279.
- Arshad W, Sperber K, Steinbrecher T, Nichols B, Jansen V, Leubner-Metzger G, Mummenhoff K. 2019.** Dispersal biophysics and adaptive significance of dimorphic diaspores in the annual *Aethionema arabicum* (Brassicaceae). *New Phytologist* **221**(3): 1434–1446.
- Bailey TL, Boden M, Buske FA, Frith M, Grant CE, Clementi L, Ren J, Li WW, Noble WS. 2009.** MEME SUITE: Tools for motif discovery and searching. *Nucleic Acids Research* **37**: W202–W208.
- Box GE, Cox DR. 1964.** An analysis of transformations. *Journal of the Royal Statistical Society. Series B (Methodological)* **26**(2): 211–252.
- Buske FA, Bodén M, Bauer DC, Bailey TL. 2010.** Assigning roles to DNA regulatory motifs using comparative genomics. *Bioinformatics* **26**(7): 860–866.
- Chang S, Puryear J, Cairney J. 1993.** A simple and efficient method for isolating RNA from pine trees. *Plant Molecular Biology Reporter* **11**(2): 113–116.
- El-Kassaby YA, Moss I, Kolotelo D, Stoehr M. 2008.** Seed germination: mathematical representation and parameters extraction. *Forest Science* **54**(2): 220–227.
- García-Fayos P, Bochet E, Cerdà A. 2010.** Seed removal susceptibility through soil erosion shapes vegetation composition. *Plant and Soil* **334**: 289–297.
- Graeber K, Linkies A, Wood ATA, Leubner-Metzger G. 2011.** A guideline to family-wide comparative state-of-the-art quantitative RT-PCR analysis exemplified with a Brassicaceae cross-species seed germination case study. *The Plant Cell* **23**(6): 2045–2063.
- Haudry A, Platts AE, Vello E, Hoen DR, Leclercq M, Williamson RJ, Forczek E, Joly-Lopez Z, Steffen JG, Hazzouri KM, et al. 2013.** An atlas of over 90,000 conserved noncoding sequences provides insight into crucifer regulatory regions. *Nature Genetics* **45**(8): 891–898.
- Huang D, Wang C, Yuan J, Cao J, Lan H. 2015.** Differentiation of the seed coat and composition of the mucilage of *Lepidium perfoliatum* L.: a desert annual with typical myxospermy. *Acta Biochimica et Biophysica Sinica* **47**(10): 775–787.
- Huber W, Carey VJ, Gentleman R, Anders S, Carlson M, Carvalho BS, Bravo HC, Davis S, Gatto L, Girke T. 2015.** Orchestrating high-

- throughput genomic analysis with Bioconductor. *Nature Methods* **12**(2): 115–121.
- ISTA 2015.** International Rules for Seed Testing. Basserdorf, Switzerland: International Seed Testing Association.
- Joosen RV, Kodde J, Willems LA, Ligterink W, van der Plas LH, Hilhorst HW. 2010.** GERMINATOR: a software package for high-throughput scoring and curve fitting of *Arabidopsis* seed germination. *The Plant Journal* **62**(1): 148–159.
- Kazachkova Y, Khan A, Acuña T, López-Díaz I, Carrera E, Khozin-Goldberg I, Fait A, Barak S. 2016.** Salt induces features of a dormancy-like state in seeds of *Eutrema (Thellungiella) salsugineum*, a halophytic relative of *Arabidopsis*. *Frontiers in Plant Science* **7**(1071): 1–18.
- Kolde R. 2015.** pheatmap: Pretty Heatmaps. *R package version 1.0.12*.
- Lenser T, Graeber K, Cevik ÖS, Adigüzel N, Dönmez AA, Grosche C, Kettermann M, Mayland-Quellhorst S, Mérai Z, Mohammadin S, et al. 2016.** Developmental control and plasticity of fruit and seed dimorphism in *Aethionema arabicum*. *Plant Physiology* **172**(3): 1691–1707.
- Lenser T, Tarkowská D, Novák O, Wilhelmsson P, Bennett T, Rensing SA, Strnad M, Theißen G. 2018.** When the BRANCHED network bears fruit: How carpic dominance causes fruit dimorphism in *Aethionema*. *The Plant Journal* **94**: 352–371.
- Love MI, Huber W, Anders S. 2014.** Moderated estimation of fold change and dispersion for RNA-seq data with DESeq2. *Genome Biology* **15**: 550.
- Lu JJ, Tan DY, Baskin JM, Baskin CC. 2010.** Fruit and seed heteromorphism in the cold desert annual ephemeral *Diptychocarpus strictus* (Brassicaceae) and possible adaptive significance. *Annals of Botany* **105**(6): 999–1014.
- Marone F, Stampanoni M. 2012.** Regridding reconstruction algorithm for real-time tomographic imaging. *Journal of Synchrotron Radiation* **19**(6): 1029–1037.
- Murashige T, Skoog F. 1962.** A revised medium for rapid growth and bio assays with tobacco tissue cultures. *Physiologia Plantarum* **15**(3): 473–497.
- O'Malley RC, Huang S-sC, Song L, Lewsey MG, Bartlett A, Nery JR, Galli M, Gallavotti A, Ecker JR. 2016.** Cistrome and episcistrome features shape the regulatory DNA landscape. *Cell* **165**(5): 1280–1292.
- Porra R, Thompson W, Kriedemann P. 1989.** Determination of accurate extinction coefficients and simultaneous equations for assaying chlorophylls *a* and *b* extracted with four different solvents: verification of the concentration of chlorophyll standards by atomic absorption spectroscopy. *Biochimica et Biophysica Acta (BBA) – Bioenergetics* **975**(3): 384–394.
- R Core Team. 2013.** *R: A language and environment for statistical computing*.
- Rost B. 1999.** Twilight zone of protein sequence alignments. *Protein Engineering* **12**(2): 85–94.
- Roylance D. 2001.** *Stress-strain Curves*. Cambridge, Massachusetts: Massachusetts Institute of Technology.

- Schindelin J, Arganda-Carreras I, Frise E, Kaynig V, Longair M, Pietzsch T, Preibisch S, Rueden C, Saalfeld S, Schmid B, et al. 2012.** Fiji: an open-source platform for biological-image analysis. *Nature Methods* **9**: 676–682.
- Stampanoni M, Groso A, Isenegger A, Mikuljan G, Chen Q, Bertrand A, Henein S, Betemps R, Frommherz U, Böhler P, et al. 2006.** Trends in synchrotron-based tomographic imaging: the SLS experience. *Developments in X-ray Tomography V: International Society for Optics and Photonics*. U199–U212.
- Sun Y, Tan DY, Baskin CC, Baskin JM. 2012.** Role of mucilage in seed dispersal and germination of the annual ephemeral *Alyssum minus* (Brassicaceae). *Australian Journal of Botany* **60**(5): 439–449.
- Telenius A, Torstensson P. 1989.** The seed dimorphism of *Spergularia marina* in relation to dispersal by wind and water. *Oecologia* **80**(2): 206–210.
- Tester M, Davenport R. 2003.** Na⁺ tolerance and Na⁺ transport in higher plants. *Annals of Botany* **91**(5): 503–527.
- Truscott AM, Soulsby C, Palmer SCF, Newell L, Hulme PE. 2006.** The dispersal characteristics of the invasive plant *Mimulus guttatus* and the ecological significance of increased occurrence of high-flow events. *Journal of Ecology* **94**(6): 1080–1091.
- Untergasser A, Cutcutache I, Koressaar T, Ye J, Faircloth BC, Remm M, Rozen SG. 2012.** Primer3—new capabilities and interfaces. *Nucleic Acids Research* **40**(15): e115.
- van der Weele CM, Spollen WG, Sharp RE, Baskin TI. 2000.** Growth of *Arabidopsis thaliana* seedlings under water deficit studied by control of water potential in nutrient-agar media. *Journal of Experimental Botany* **51**(350): 1555–1562.
- Venables WN, Ripley BD. 2002.** *Modern Applied Statistics with S*. New York: Springer.
- Verslues PE, Bray EA. 2004.** *LWR1* and *LWR2* are required for osmoregulation and osmotic adjustment in *Arabidopsis*. *Plant Physiology* **136**(1): 2831–2842.
- Wilhelmsson P, Chandler J, Fernandez-Pozo N, Graeber K, Ullrich K, Arshad W, Khan S, Hofberger J, Buchta K, Edger P, et al. 2019.** Usability of reference-free transcriptome assemblies for detection of differential expression: a case study on *Aethionema arabicum* dimorphic seeds. *BMC Genomics* **20**: 1–25.
- Zhao S, Fernald RD. 2005.** Comprehensive algorithm for quantitative real-time polymerase chain reaction. *Journal of Computational Biology* **12**(8): 1047–1064.

3. Dispersal biophysics and adaptive significance of dimorphic diaspores

3.1 Paper as published in *New Phytologist*

Chapter 3 addresses how distinct biomechanical, developmental and ecophysiological properties of the dimorphic fruits/seeds (diaspores) in *Ae. arabicum* influence their dispersal and ability to persist in high-elevational scree-slope environments. The adaptive significance of dispersal mechanisms is discussed, and how these act in magnifying the options for successful germination/seedling establishment. The comparative approach used to understand the dimorphic diaspore syndrome integrates novel biomechanics, dispersal aerodynamics, and phenotypic plasticity – thereby linking the evolution of distinct diaspore traits to their ecological significance. Two very contrasting dispersal mechanisms of the *Ae. arabicum* diaspores were revealed, preventing (antitelechory) and promoting (telechory) dispersal. Understanding the functional morphology, biophysics, and ecophysiology of species which combine distinct diaspore dispersal/dormancy strategies has far-reaching consequences, particularly for annual plants.

The results of the work were published in *New Phytologist* under the title “Dispersal biophysics and adaptive significance of dimorphic diaspores in the annual *Aethionema arabicum* (Brassicaceae)” (DOI: 10.1111/nph.15490). The paper is presented here in its full form.

3.2 Author contributions

Data gathering and experiments were performed by W Arshad (Figures 1–2, and Table 1). W Arshad derived Figures 3–6 from experiments performed together with K Sperber (University of Osnabrück, Germany). W Arshad analysed all data.

The concepts and narrative of the manuscript were conceived by W Arshad. Project supervision was provided by T Steinbrecher (Royal Holloway University of London, UK), G Leubner-Metzger (Royal Holloway University of London, UK), and K Mummenhoff (University of Osnabrück, Germany). Both B Nichols (Royal Holloway University of London, UK) and VAA Jansen (Royal Holloway University of London, UK) formulated the hypothesis that temperature provides the cue for elevation, leading to the adaptive plasticity of diaspore ratio.

W Arshad was the lead author of this manuscript, prepared all figures, and wrote the majority of the text. W Arshad prepared all manuscript components for submission, wrote the covering letter to *New Phytologist*, and co-ordinated the revision process with all co-authors.

Dispersal biophysics and adaptive significance of dimorphic diaspores in the annual *Aethionema arabicum* (Brassicaceae)

Waheed Arshad^{1*} , Katja Sperber^{2*}, Tina Steinbrecher¹ , Bethany Nichols¹ , Vincent A. A. Jansen¹ ,
Gerhard Leubner-Metzger^{1,3*}  and Klaus Mummenhoff^{2*} 

¹School of Biological Sciences, Royal Holloway University of London, Egham, TW20 0EX, UK; ²Department of Biology, Botany, University of Osnabrück, Barbarastraße 11, D-49076, Osnabrück, Germany; ³Laboratory of Growth Regulators, Centre of the Region Haná for Biotechnological and Agricultural Research, Institute of Experimental Botany, Academy of Sciences of the Czech Republic, Palacký University, 78371 Olomouc, Czech Republic

Summary

- Heteromorphic diaspores (fruits and seeds) are an adaptive bet-hedging strategy to cope with spatiotemporally variable environments, particularly fluctuations in favourable temperatures and unpredictable precipitation regimes in arid climates.
- We conducted comparative analyses of the biophysical and ecophysiological properties of the two distinct diaspores (mucilaginous seed (M⁺) vs indehiscent (IND) fruit) in the dimorphic annual *Aethionema arabicum* (Brassicaceae), linking fruit biomechanics, dispersal aerodynamics, pericarp-imposed dormancy, diaspore abscisic acid (ABA) concentration, and phenotypic plasticity of dimorphic diaspore production to its natural habitat and climate.
- Two very contrasting dispersal mechanisms of the *A. arabicum* dimorphic diaspores were revealed. Dehiscence of large fruits leads to the release of M⁺ seed diaspores, which adhere to substrata via seed coat mucilage, thereby preventing dispersal (antitelechory). IND fruit diaspores (containing nonmucilaginous seeds) disperse by wind or water currents, promoting dispersal (telechory) over a longer range.
- The pericarp properties confer enhanced dispersal ability and degree of dormancy on the IND fruit morph to support telechory, while the M⁺ seed morph supports antitelechory. Combined with the phenotypic plasticity to produce more IND fruit diaspores in colder temperatures, this constitutes a bet-hedging survival strategy to magnify the prevalence in response to selection pressures acting over hilly terrain.

Authors for correspondence:

Klaus Mummenhoff

Tel: +49 541 969 2856

Email: Klaus.Mummenhoff@biologie.uni-osnabrueck.de

Gerhard Leubner-Metzger

Tel: +44 1784 44 3553

Email: Gerhard.Leubner@rhl.ac.uk

Received: 29 March 2018

Accepted: 3 September 2018

New Phytologist (2019) **221**: 1434–1446
doi: 10.1111/nph.15490

Key words: abscisic acid (ABA), *Aethionema arabicum*, bet-hedging, dimorphic diaspores, dispersal by wind and water, environmental adaptations, fruit biomechanics, pericarp-imposed properties.

Introduction

Diaspores – fruits and seeds – with specific dispersal abilities and germinabilities evolved to support the angiosperm life cycle in adaptation to the prevailing environment (Linkies *et al.*, 2010; Baskin *et al.*, 2014; Willis *et al.*, 2014). Climate change can trigger species range shifts and local extinctions, and is a global threat to plant diversity (Thuiller *et al.*, 2005; Walck *et al.*, 2011). Examples of this include the fact that global warming shifts the timing of alpine plant germination to unsuitable seasons (Mondoni *et al.*, 2012), and also that several weeds will exert additional pressure for crop–weed competition and its management (Ramesh *et al.*, 2017). For many plant species, the dispersed seed or fruit is the only phase in its life cycle when it can travel, with the potential to carry the whole plant, population, or indeed the entire species (Kessler & Stuppy, 2012). Diaspore dispersal therefore has far-reaching demographic, ecological and evolutionary consequences (Robledo-Arnuncio *et al.*, 2014; Willis *et al.*,

2014). Knowledge of the ways in which plants disperse – and acquire the characteristics necessary for successful dispersal – has therefore been the subject of much theoretical and empirical research, dating back to observations by Linnaeus (van der Pijl, 1982) and Ridley's (1930) seminal compilation of early dispersal studies. The diversity of morphological and biomechanical shapes and structures inherent in plant seeds and fruits is the result of the pursuit of different strategies for successful dispersal and appropriate germination timing (Baskin *et al.*, 2014; Larson-Johnson, 2016; Sperber *et al.*, 2017; Steinbrecher & Leubner-Metzger, 2017). These early life-history traits are especially important for annual plants, as they can only restart a new cycle via regeneration from the seed.

Most plant species commit themselves to monomorphism (monodiaspory) as their life-history strategy, producing seeds and fruits of a single type that are optimally adapted to the respective habitat (Donohue *et al.*, 2010; Walck *et al.*, 2011; Baskin & Baskin, 2014). Interestingly, many plant species evolved a heteromorphism (heterodiaspory) strategy (Imbert, 2002; Baskin & Baskin, 2014; Baskin *et al.*, 2014), a phenomenon described by

*These authors contributed equally to this work.

1434 *New Phytologist* (2019) **221**: 1434–1446
www.newphytologist.com

© 2018 The Authors
New Phytologist © 2018 New Phytologist Trust
This is an open access article under the terms of the Creative Commons Attribution License, which permits use, distribution and reproduction in any medium, provided the original work is properly cited.

Venable (1985) as 'the production by single individuals of seeds (or sometimes single-seeded fruits) of different form or behaviour'. Diaspore heteromorphism is confined to 18 of 413 angiosperm families, with distinct properties having been observed not only in size, shape, and/or colour, but also in other morphological, biomechanical, and germination characteristics, the degree of dormancy, dispersal ability, mucilage production upon imbibition, and ability to form a persistent seed bank (Sorensen, 1978; Mandák & Pyšek, 2001; Imbert, 2002; Lu *et al.*, 2010; Dubois & Cheptou, 2012; Baskin & Baskin, 2014; Baskin *et al.*, 2014). Heteromorphic diaspore traits may function as a bet-hedging strategy to cope with the spatiotemporal variability of unpredictable habitats (Slatkin, 1974; Venable, 1985). Species with heteromorphic diaspores are most commonly annuals in dry Mediterranean and desert habitats, or in other frequently disturbed and stressful environments (Imbert, 2002). Almost all heteromorphic species of the cold deserts of northwest China are annuals (Baskin *et al.*, 2014). Diaspores that differ in dispersal ability and germinability allow annual species to escape the harshness and unpredictability of their habitat in space (via dispersal) and time (delayed germination via dormancy).

In the Brassicaceae family, diaspore heteromorphism has evolved independently in a few genera (Imbert, 2002; Baskin *et al.*, 2014; Willis *et al.*, 2014; Mohammadin *et al.*, 2017). Distinct types of diaspore heteromorphism evolved in the genus *Cakile* (Cordazzo, 2006; Avino *et al.*, 2012), in the desert annual *Diptychocarpus strictus* (Lu *et al.*, 2010, 2015), and in *Aethionema arabicum* (Mühlhausen *et al.*, 2010; Lenser *et al.*, 2016; Mohammadin *et al.*, 2017). The genus *Aethionema*, the sister lineage of the core Brassicaceae, is thought to have originated and diversified in the ecologically, altitudinally, and geologically diverse Irano-Turanian region (Franzke *et al.*, 2011; Jiménez-Moreno *et al.*, 2015; Mohammadin *et al.*, 2017). The dispersal of *Aethionema* spp. correlates with local events, such as the uplift of the Anatolian and Iranian plateaus, the formation of major mountain ranges, and probably a climatic change in seasonality towards summer aridity. Contemporary phylogenetic and biogeographic analyses identified Anatolia (Turkey) as one of the world's hotspots of biodiversity, which includes *c.* 550 Brassicaceae species (Şekercioğlu *et al.*, 2011; Jiménez-Moreno *et al.*, 2015; Mohammadin *et al.*, 2017). Semiarid steppe (Central Anatolian Plateau) and Mediterranean climates with dry summers (southwest Anatolia) dominate the region. The varied topography creates microclimates by elevation, including in the major mountain belts, e.g. the South Anatolian Taurus, which surround the Central Anatolian steppe. Diaspore heteromorphism evolved at least twice within the genus *Aethionema*, and was associated with a switch to an annual life form (Mohammadin *et al.*, 2017).

Aethionema arabicum is a small, diploid, annual, herbaceous species whose genome sequence is published (Haudry *et al.*, 2013). An advantage of *A. arabicum* as a model system for diaspore heteromorphism is that it exhibits true seed and fruit dimorphism with no intermediate morphs. Two distinct fruit types are produced on the same fruiting inflorescence (infructescence): dehiscent (DEH) fruits with four to six mucilaginous (M^+) seeds, and indehiscent (IND) fruits each containing a single

nonmucilaginous (M^-) seed (Lenser *et al.*, 2016, 2018). Upon maturity, dehiscence of the DEH fruit morph leads to the dispersal of M^+ seeds, while the IND fruit morph is dispersed in its entirety by abscission. Comparative analyses of the anatomy and physiology of M^+ and M^- seeds, and the DEH and IND fruits that contain them, have shown a multitude of differences. These findings suggest different roles and mechanisms of the dimorphic diaspores in the dispersal and germination strategy of *A. arabicum*. While principal agents of diaspore dispersal include transport by wind (anemochory), water (hydrochory), animals (zoochory), and the plant itself (autochory) (Fahn & Werker, 1972), little is known about morph-specific dispersal properties and the adaptive benefits of bet-hedging mechanisms associated with heteromorphic diaspore dispersal. Thus, the structural, functional, and physiological differences in *A. arabicum* diaspores, underpinned by mucilage production (M^+) and fruit coat (pericarp) restraint (IND), remain unknown.

In this study, we used a comparative approach to investigate how distinct biomechanical, hormonal, and ecophysiological properties of the diaspores (M^+ seed vs IND fruit) influence their dispersal and ability to persist in the high-elevational scree-slope environments of Anatolia. By integrating pericarp biomechanics, flight aerodynamics, and phenotypic plasticity, we investigated the suitability of *A. arabicum* diaspores for dispersal by hydrochory and anemochory as two contrasting mechanisms. This is consistent with the distinct ABA content and germinability of the dimorphic diaspores. Elucidating the bet-hedging dispersal strategies in *A. arabicum*, and the plasticity of this dimorphism, allows us to better understand the adaptive significance of dispersal prevention and promotion mechanisms.

Materials and Methods

Seed collection and plant growth

Mature plants of *Aethionema arabicum* (L.) Andr. ex DC. were grown from accession ES1020 (obtained from Eric Schranz, Wageningen University and Research Centre). Plants were grown in Levington F2 compost with added horticultural grade sand (F2 + S), under long-day conditions (16 h 20°C : 8 h 18°C, light : dark) in a glasshouse.

Diaspore biometrics and aerodynamic properties

Sixty replicates each of M^+ seeds, M^- seeds extracted from IND fruits, and IND fruits were used to quantify height, width, and depth. A Leica DFC480 digital camera system, LEICA APPLICATIONS SUITE (v.4.5), and IMAGEJ (v.1.5i) were used to measure distances. The mean mass of single diaspores was determined using eight replicates of 100 individuals. Diaspore shapes were approximated as triaxial ellipsoids (M^+/M^- seeds, prolate spheroids; IND fruits, oblate spheroids), in order to calculate surface area. The time taken (h) for cumulative germination to reach 50% of its maximum (T_{50}) was obtained from seed germination experiments with freshly harvested mature fruits and seeds placed in Petri dishes containing two layers of filter paper, 3 ml of dH₂O, and 0.1% (v/v) Plant Preservative Mixture (Plant Cell

Technology, Washington, DC, USA). Plates were incubated in an MLR-350 Versatile Environmental Test Chamber (Sanyo-Panasonic, Osaka, Japan) at 14°C and 100 $\mu\text{mol s}^{-1} \text{m}^{-2}$ constant white light, as described in Lenser *et al.* (2016).

Measurement of ABA concentration

Endogenous ABA concentration was determined using the Phytodetek[®] ABA enzyme immunoassay kit (Agdia Inc., Elkhart, IN, USA) according to the manufacturer's instructions. Five replicates of diaspores (50 mg) were frozen in liquid nitrogen, and ground to a fine powder for 30 s using a Precellys[®] 24 tissue homogenizer (Bertin Instruments, Montigny-le Bretonneux, France). ABA was extracted with a chilled solution of 80% (v/v) methanol, 100 mg l^{-1} butylated hydroxytoluene, and 0.5 g l^{-1} citric acid monohydrate.

Quantification of fruit valve dehiscence

Mature DEH and IND fruits from dry (17% relative humidity, RH), high-humidity (65% RH) and water-sprayed (100% RH) plants were clamped into the jaws of a single-column tensile testing machine (Zwick Roell ZwickiLine Z0.5, Ulm, Germany) configured with a 200 N load cell. Separation speed was set at 1 mm min^{-1} . Force–displacement data were obtained using 30 (17% RH and 65% RH) and 40 (100% RH) replicates from mature main branch infructescences. Maximum force (F_{max}) and the slope of the linear elastic element were obtained.

Fruit, fruit valve, and seed resistance to raindrop impact

A raindrop test method was applied to mature fruits on dry and wet infructescences. The opening (1.5 mm diameter) of a burette was placed 50 cm above a single fruit or seed. The number of single raindrops (of mean mass 53.55 ± 0.97 mg) directly impacting the fruit/seed were counted until fruit abscission (in DEH and IND fruits) or seed detachment (in M^+ seeds) occurred. One hundred replicates of each diaspore were tested.

Dispersal ability in still air

The time required for 100 diaspores to fall individually from a height of 108 cm in a plastic tube (15 cm diameter) was measured using high-speed (120 frames s^{-1}) videos (Nikon Coolpix P100, Tokyo, Japan). The fall rate (m s^{-1}) was calculated over this height.

Dispersal ability in flowing air

Distances travelled by dispersing diaspores were determined following Lu *et al.* (2010). One hundred diaspores were individually exposed for 60 s to a constant stream of air parallel to a flat landing surface. A ventilator (Quigg BF-12A, Hamburg, Germany) was used to simulate a wind velocity of 4 m s^{-1} in a custom-built wind channel (height 60 cm, length 360 cm, width 48 cm). Diaspores were released from a height of 30 cm, 10 cm from the front of the ventilator, and the total distance travelled was measured to the nearest 0.01 m.

Effect of diaspore on substrate attachment

Adherence potential was tested by placing diaspores on dry and water-saturated sand (grains < 2 mm) in Petri dishes for 10 min. Seeds/fruits were rotated to allow whole-surface contact with the substrate, and subsequently removed. The mass of the dry seeds/fruits, including the soil particles attached to them, was compared with the mass of the same dry seeds or fruits before exposure. Three replicates each of 25 diaspores were tested.

Diaspore displacement mediated by surface water runoff

Diaspore displacement by surface water runoff was quantified using a custom-built device consisting of a container with 53 holes (400 μm diameter) above a 6°-sloped 80 × 30 cm plate, covered with 80-grit sandpaper (modified from García-Fayos *et al.*, 2010). During each simulation, water flow was stopped after 1 l had been discharged from the sprinkling head within 2.5 min. The total distance travelled by 100 replicates of each diaspore on the plate was measured.

Diaspore buoyancy

Three replicates, each of 25 diaspores, were placed on the surface of 150 ml of water contained in 250 ml Erlenmeyer flasks. Water movement in the flasks was simulated by agitation on an orbital shaker at 100 rpm (Truscott *et al.*, 2006; Sun *et al.*, 2012). The number of floating diaspores was counted over time.

Statistical analyses

R was used to assess the distribution of the data and test for normality and homogeneity of variance. Normal and homogeneous data were subjected to one-way ANOVA, with *post hoc* comparisons made by a Tukey's honest significant difference test. The rejection threshold for all analyses was $P < 0.05$. Data exhibiting a non-Gaussian distribution or nonhomogeneous variances were transformed by a Box–Cox (Box & Cox, 1964) transformation using the MASS package (Venables & Ripley, 2002) in R (non-transformed data are shown in all figures and tables). Analyses of diaspore behaviour on substrata were performed with a three-way ANOVA (with diaspore type, imbibition state, and sand state as main factors). Analyses of diaspore buoyancy were performed with a univariate type-III repeated-measures ANOVA (with diaspore type and time interaction included as fixed effects). All statistical analyses were conducted in R (v.3.4.2; R Foundation for Statistical Computing, Vienna, Austria) or Graphpad PRISM (v.7.0a; San Diego, CA, USA).

Results

Aethionema arabicum habitat and dimorphic diaspore properties

The dimorphism of *A. arabicum* is characterized by the M^+ seed diaspores, dispersed by dehiscence, and by the IND fruit

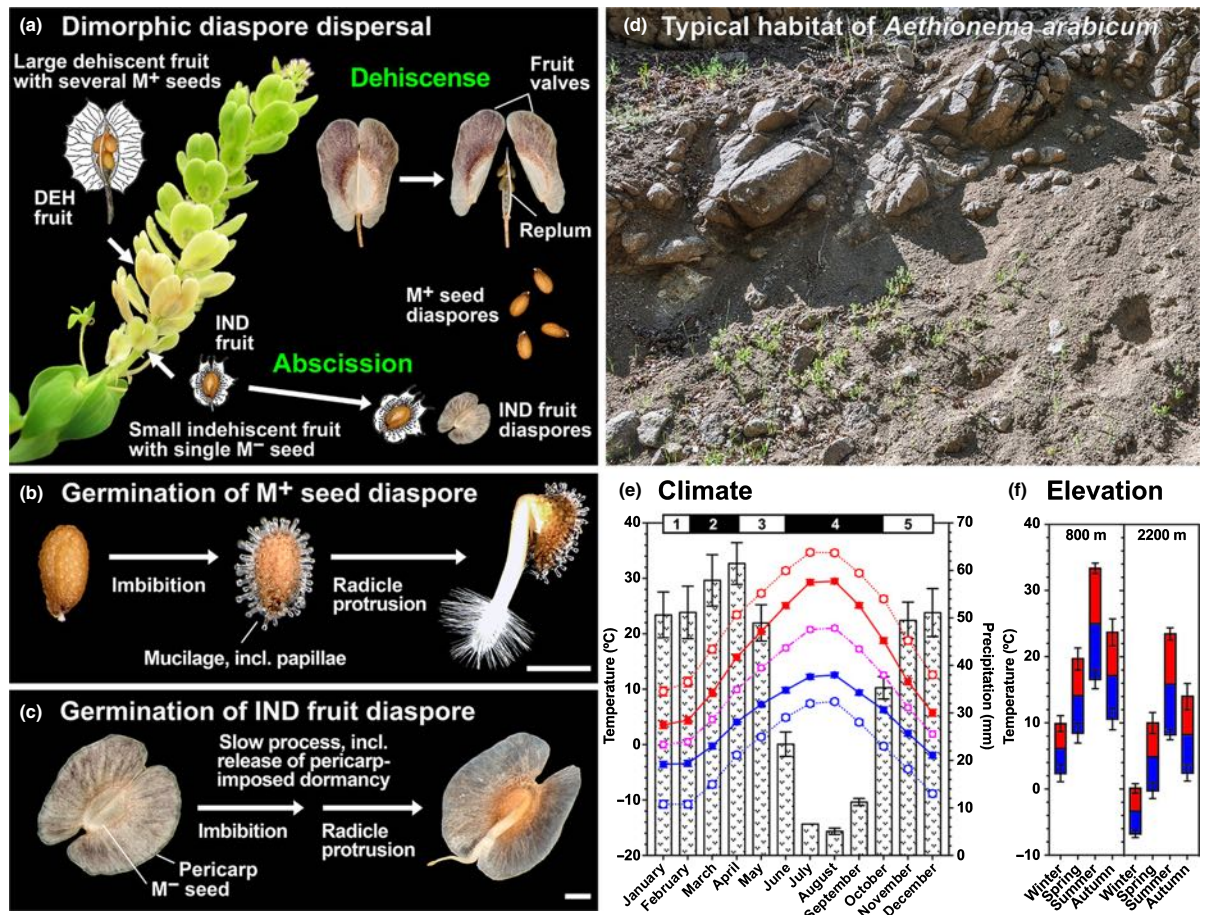


Fig. 1 Dispersal, germination, habitat and climate of the dimorphic fruits and seeds of *Aethionema arabicum*. (a) *Aethionema arabicum* infructescence showing dehiscent (DEH) and indehiscent (IND) fruit morphs. Mature DEH fruits do not abscise from the mature infructescence, but instead disperse multiple mucilaginous (M^+) seed diaspores. Mature IND fruit diaspores, containing a single, nonmucilaginous (M^-) seed, disperse in their entirety from the mature infructescence. (b) Upon imbibition, the M^+ seed diaspore produces mucilage from the outer cell walls of the seed coat epidermal layers, forming conical papillae of up to 200 μm . (c) By contrast, germination of the IND fruit diaspore is a slower process, in part mediated by pericarp-imposed dormancy. A single M^- seed remains enclosed within the winged IND fruit, unless they are released by external mechanical means, and the radicle protrudes from within the pericarp. Bars, 1 mm. (d) Characteristic stony-slope and steppe habitat of *A. arabicum*, taken in the Kırşehir Province in the central Anatolian region of Turkey. (e) Climate diagram of sites in Turkey from which *A. arabicum* has been collected. The maximum (solid red) and minimum (solid blue) temperatures of an average day for every month are shown. The averages of the hottest day (dashed red) and coldest night (dashed blue) of each month from the last 30 yr are also shown. The dashed magenta line indicates the mean monthly temperature. Mean monthly precipitation (bars) is shown. All climate data were obtained from Meteoblue (developed at the University of Basel, Switzerland, based on weather forecast models of the National Oceanic and Atmospheric Administration and National Centers for Environmental Prediction) from a total of 25 specimens archived at the Global Biodiversity Information Facility (GBIF.org, <https://doi.org/10.15468/dl.w63b7k>; accessed 31 January 2018). Data are means \pm 1 SE. Numbers above the climate diagram indicate typical life cycle stages of diaspore persistence in seed bank (1,5), germination and seedling establishment (2), vegetative, flowering, and reproductive growth (3), and diaspore dispersal and plant senescence (4). (f) Seasonal variation of mean maximum (red) and mean minimum (blue) temperatures at low (800 m) and high (2200 m) elevations that support *A. arabicum* growth. Data are means \pm 1 SE.

diaspores, dispersed by abscission (Fig. 1a). Various morphological properties that may be influencing M^+ seed and IND fruit dispersal were all significantly different (Table 1). While freshly harvested mature M^+ seeds germinated readily within 2 d at 14°C, IND fruit germination required at least 2–4 wk (Fig. 1b,c; Table 1). Further to this, most of the M^+ seeds but none of the IND fruits germinated at 20°C, which suggests differences in dormancy and temperature responses of the dimorphic

diaspores. This difference in diaspore germinability is mediated, at least in part, by a 34-fold higher ABA concentration in the IND fruits than in the M^+ seeds (Table 1). This difference is associated with an ABA concentration in M^- seeds that is double that in M^+ seeds, combined with a very high ABA concentration of the pericarp. The low germinability of the IND fruits, therefore, seems to constitute a case of ABA-mediated and pericarp-enhanced dormancy. These differences, combined with

Table 1 Comparative dispersal and biophysical properties of *Aethionema arabicum* dimorphic diaspores.

	Diaspore		
	M ⁺	IND	M ⁻ †
Mass (mg)	0.34 ± 0.7 ^b	1053.5 ± 2.4 ^a	0.27 ± 0.6 ^c
Surface area (mm ²)	1.7 ± 0.2 ^c	53.9 ± 9.9 ^a	2.1 ± 0.3 ^b
Height (µm)	1099 ± 66 ^b	5764 ± 530 ^a	1125 ± 67 ^b
Width (µm)	580 ± 45 ^b	4614 ± 527 ^a	680 ± 55 ^b
Depth (µm)	500 ± 56 ^a	516 ± 51 ^a	354 ± 26 ^b
T ₅₀ at 14°C (h)	41.4 ± 0.8 ^b	364.2 ± 10.2 ^{a†}	49.6 ± 7.4 ^a
ABA (pmol per diaspore)	0.16 ± 0.06	5.47 ± 0.29 [§]	0.34 ± 0.08

Dry mass, surface area, biometrics and germinability, and abscisic acid (ABA) concentration are shown for the multiple mucilaginous (M⁺) seed and indehiscent (IND) fruit diaspores. Note that nonmucilaginous (M⁻) seeds, obtained by mechanical removal from the IND fruits, were used as a comparison to reveal the roles of the IND pericarp.

†Not a diaspore in nature, extracted from IND fruit for experimental comparison.

‡T₅₀ for half of the population, while the other half remained dormant for at least 1 month (Lenser *et al.*, 2016). T₅₀, time taken for cumulative germination to reach 50% of its maximum. *n* = 8, each with 100 replicate seeds (mass); 60 seeds (surface area, height, width and depth); three Petri dishes, each with 20 replicate seeds (T₅₀); five each with 50 mg diaspores (ABA). ANOVAs were performed on each of the variables. The *F*-statistic was significant for each ANOVA (*P* < 0.05). Within each series for a given variable, values followed by the same letter do not differ (Tukey's honest significant difference, *P* < 0.05).

§ABA concentration of one IND pericarp is 5.31 ± 0.25 pmol per diaspore.

the observed plasticity in DEH/IND fruit ratios and numbers (Lenser *et al.*, 2016) and the unstudied dispersal mechanisms of its dimorphic diaspores, are expected to support the adaptation of *A. arabicum* in its natural habitat and climate.

Aethionema arabicum is described as a poorly competitive species, and typically grows in dry locations near fields, in steppes, and on stony slopes and screes with highly eroded calcareous substrate (Fig. 1d) (Davis, 1965; Babaç, 2004; Sunar *et al.*, 2016; Delcheva & Bancheva, 2017; Mohammadin *et al.*, 2018). In the Anatolian peninsula, it grows at 600–2700 m elevation. Using the locations of 25 accessions, we have generated climate diagrams for the seasonal changes in precipitation, minimal and maximal temperatures at average elevation, as well as at low and high elevations (Fig. 1e,f). Germination, seedling establishment, and vegetative growth occur early in spring, flowering in April to June, and fruit maturation and diaspore dispersal during the dry summer and the wetter autumn (Fig. 1e). The distinct morphology of the dimorphic diaspores (Table 1) suggests that they have distinct roles and biophysical dispersal mechanisms linked to the climatic regime of the region.

Dimorphic fruit biomechanics

A comparative biomechanical analysis of DEH and IND fruit valve separation at low and high RH values (simulating the dry summer and wetter autumn) revealed, first, that DEH and IND fruits differed fundamentally in their dehiscence behaviour

(Fig. 2). Plant biomechanics is an integral component of the abiotic interactions of plants with gravity, wind and soil. Tensile tests determine the force needed to elongate a sample to its breaking point and provide insight into its material properties. The maximal force and the elasticity associated with separating the fruit valves were more than twofold lower for DEH than for IND fruits (Fig. 2a,b). DEH fruit force–displacement curves show a progressive failure with a sequence of force drops. This ‘composite’-type failure for DEH fruits, together with the lower maximal force, demonstrates that dehiscence is indeed the M⁺ seed dispersal mechanism operating for this fruit morph. Dehiscence required to disperse the M⁺ seeds was triggered in any humidity condition (Fig. 2c). By contrast, the IND fruit diaspore, for which detachment by abscission is the dispersal mechanism (Fig. 1a), shows a completely different profile. After a preloading phase, the force–displacement curve shows a linear region and no distinct plastic deformation (‘brittle’-type failure) (Fig. 2e). The maximal force and elasticity are dependent on the humidity conditions (Fig. 2c). The finding that they are significantly lower in high-humidity conditions is consistent with the role of fruit valve splitting to aid radicle emergence during IND fruit germination (Fig. 1c). These contrasting biomechanical properties of the dimorphic fruits, therefore, support dehiscence and abscission, respectively, as distinct mechanisms for the M⁺ seed and IND fruit dispersal.

Also in agreement with IND fruit dispersal by abscission is the fact that the force required to remove dry IND fruits from *A. arabicum* plants is approx. six-fold lower than that required to remove dry DEH fruits (Lenser *et al.*, 2016). To obtain evidence that this is also the case in humid conditions, to aid dispersal in autumn when precipitation increases (Fig. 1f), we investigated the effects of direct water droplet impacts on fruit abscission. While only 6 (± 1) water droplets (mean ± SE) were required to detach a ‘wet’ IND fruit by abscission, for a ‘wet’ DEH fruit, 97 (± 9) water droplets were required. In rare cases where M⁺ seeds were still attached to the replum after DEH fruit valve detachment had occurred (Fig. 1a), this process was also aided by rain: only 9 (± 4) water droplets were required to detach an M⁺ seed from the replum and, in 70% of the cases, this was achieved by a single water droplet. Dispersal by rain (ombrohydrochory) is therefore a likely mechanism for the dispersal of both dimorphic diaspores, but seems more important for the abscission of the IND diaspore.

IND fruits exhibit the greatest ability for wind dispersal

The wings, flat structure and large surface area (Fig. 1a,c; Table 1) of the IND fruit morph is indicative of an adaptation for dispersal by wind (anemochory). Mean descent rates (Fig. 3) of M⁺ seed and IND fruit diaspores, as well as for M⁻ seeds (used as comparison to reveal the roles of the IND-pericarp), were significantly different from one another (*F*_{2,297} = 438.1, *P* < 0.001). Intact IND fruits descended at the slowest rate, followed by M⁺ seeds (Fig. 3).

Quantified wind velocities in Anatolia are 1–4 m s⁻¹ (Apaydin *et al.*, 2011), and 4 m s⁻¹ currents are typically used in such wind dispersal experiments. We found that, as expected, because of the

Fig. 2 Biomechanics of dehiscent (DEH) and indehiscent (IND) *Aethionema arabicum* fruits. (a, b) Comparative maximum force (F_{max}) (a) and slope (approx. modulus of elasticity) (b) required to separate fruit valves from fruits under dry conditions. (c) Comparisons of F_{max} and slope in 17%, 65% and 100% relative humidities show a trend towards gradual decrease in stiffness in both fruits, while F_{max} also decreases in the IND fruit but remains unchanged in the DEH fruit. (d, e) Characteristic force–displacement curves of mechanical tests in which fruit dehiscence occurred in *A. arabicum*, revealing distinct fracture biomechanical properties of slow, gradual failure of the DEH fruit (d), and sudden, complete failure for the IND fruit (e). $n = 30$. Error bars ± 1 SEM.

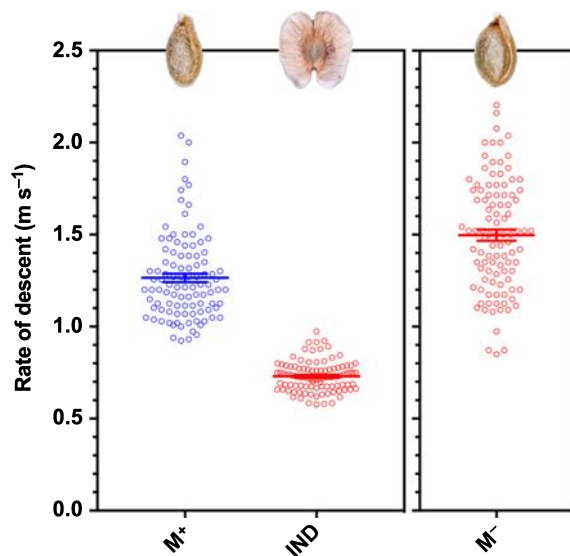
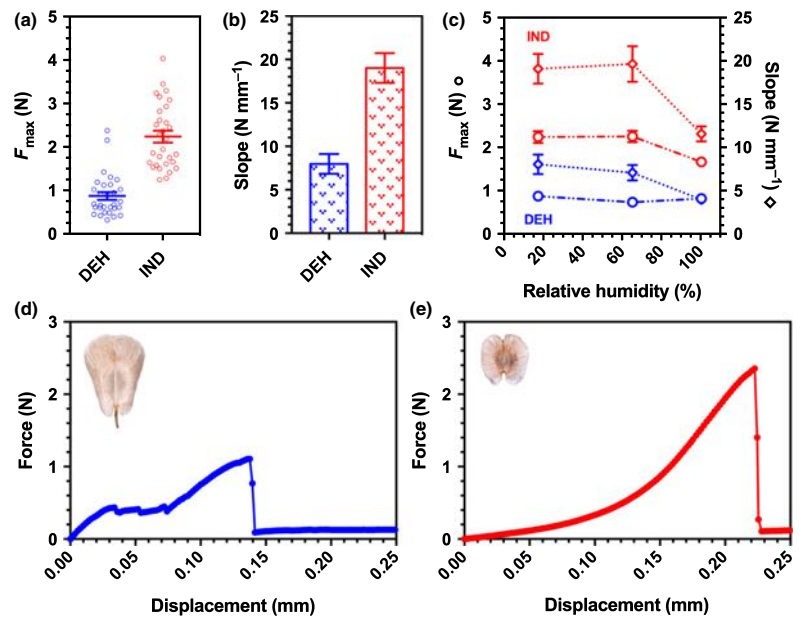


Fig. 3 Comparative fall rates of *Aethionema arabicum* diaspores during descent. Mean rate of descent ($m s^{-1}$) of multiple mucilaginous (M^+) seed diaspores and intact indehiscent (IND) fruit diaspores when released from a height of 1.08 m in still air. IND fruits required greater time to fall, confirming that the pericarp can be regarded as an adaptation for wind dispersal. The fall rates of nonmucilaginous (M^-) seeds (mechanically removed from IND fruits) are shown for comparison. Differences between M^+ seed and IND fruit diaspores are significant ($P < 0.001$). $n = 100$. Error bars ± 1 SEM.

wings, IND fruits (mean \pm SD = 286.6 ± 7.2 cm) dispersed further than M^+ seeds (78.4 ± 3.7 cm). In cases where M^+ seeds imbibe while attached to the replum of DEH fruits (after fruit

valve detachment) but do not disperse, redried M^+ seeds were also included in the analysis. Dispersal of redried M^+ seeds exhibited a ‘seed shadow’ with a mean distance of 197.3 cm (Fig. 4). These results demonstrate that IND fruits, with $c. 3$ m mean and $c. 5$ m maximum dispersal distance, exhibit the greatest ability for anemochorous dispersal. Although wind dispersal is more efficient over flat and uniform terrain, the IND fruit morph may have the potential for lateral and upward dispersal by gusts of wind in slope and scree habitats (Fig. 1d).

Evidence for restricted secondary dispersal (antitelechory) in M^+ seeds

Once dispersed from the mother plant (primary dispersal), the behaviour and interaction of diaspores with their substrata may restrict (antitelechory) secondary dispersal, a multistep process that further extends the dispersal distance from the parent plant. Mechanisms that thereby support antitelechory may explain the contrasting differences between M^+ seed and IND fruit dispersal. Assessing the behaviour of dry and imbibed *A. arabicum* diaspores on sandy substrate, we found striking differences between the dimorphic diaspores regarding the adherence potential of sand particles and its effects on diaspore mass. Comparisons of the initial (without contact with sand) and final (with sand particles attached) masses of the diaspores showed there was a significant interaction between the effects of diaspore morph (M^+ seed vs IND fruit), state (dry vs imbibed), and sand substrate (dry vs water-saturated) on the relative increase in mass ($F_{2,24} = 10.325$, $P < 0.001$). For M^+ seeds, a striking increase in mass ($P < 0.001$) was evident, while for IND fruits no such abundant adherence of sand particles was evident (Fig. 5). The comparison with M^- seeds demonstrated that this difference is a result of the adherence

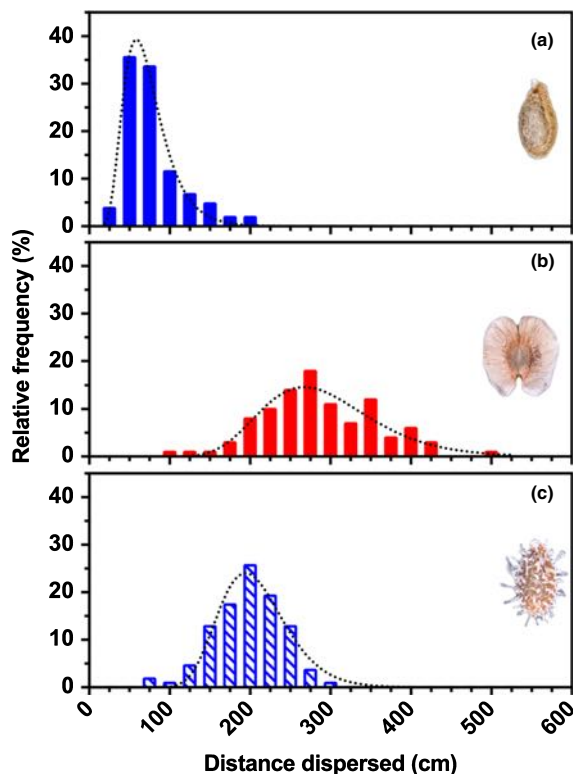


Fig. 4 Frequency distribution patterns ('seed dispersal shadows') of the dispersibility of *Aethionema arabicum* diaspores from the mother plant. (a, b) The dispersibilities of dry multiple mucilaginous (M^+) seed (a) and dry indehiscent (IND) fruit diaspores (b) differ significantly ($F_{2,313} = 437.2$, $P < 0.001$) in a 4 m s^{-1} continuous current of air. M^+ seeds achieve only short-distance dispersal from the mother plant, while the longer-distance dispersibility of IND fruit diaspores may influence colonization patterns in new steppe habitats. (c) Comparisons are made to rare cases where M^+ seeds imbibe while still attached to the replum, and are subsequently re-dried and then dispersed. $n = 100$. Dotted lines indicate log-normal curves fitted to individual frequency distributions.

of substrate particles via the production of M^+ seed coat mucilage (Figs 1b, 5). In contrast to M^+ seeds, M^- seeds only produce a thin mucilage layer and the outer surface of the IND pericarp is mucilage-free (Fig. 1c). The striking increase in M^+ seed mass therefore restricts its secondary dispersal and constitutes a mechanism for antitelechory.

To investigate the mechanisms via which *A. arabicum* diaspores may promote or restrict dispersal by water currents (nautohydrochory), we simulated diaspore displacement by surface water runoff events using a sandpaper-sloped surface. The distances travelled varied significantly among diaspores ($F_{4,495} = 143.3$, $P < 0.001$) (Fig. 6a). The IND fruit morph was 1.8- to six-fold further displaced compared to the M^+ seed morph in its different states (dry, re-dried, imbibed). The comparison with the nonmucilaginous M^- seed, which is similar in size and shape (Table 1), demonstrates that the reduced nautohydrochoric properties of the M^+ seed diaspore are also a result of seed coat mucilage extrusion.

As IND fruit dispersal does not appear to be restricted by surface water runoff, we wanted to compare the buoyancy potential of the *A. arabicum* dimorphic diaspores. There was a highly significant time \times diaspore type interaction ($F_{64,160} = 24.84$, $P < 0.001$; Fig. 6b) over the experimental period. The mean percentage of floating diaspores across 11 d differed significantly between M^+ seeds in different states (dry, re-dried, imbibed) and IND fruits ($F_{1,364} = 4.3$, $P < 0.05$). Most marked differences between diaspores occurred within the first 30 min; all re-dried and imbibed M^+ seeds were sinking rapidly, and only *c.* 45% of the dry M^+ seeds (but 100% of the IND fruits) remained floating (Fig. 6b). Dry M^+ seeds were progressively sinking (0% floating after *c.* 4 d), while IND fruits remained floating for many days (100% after 4 d, and $> 50\%$ after 11 d; Fig. 6b). Taken together, this comparison strongly suggests that IND fruits are adapted for dispersal in space (telechory) and time (pericarp-mediated dormancy), whereas M^+ seeds possess mechanisms to remain in the direct vicinity of mother plants (antitelechory).

Discussion

Distinct dispersal and dormancy mechanisms of dimorphic diaspores

Our biomechanical, ecophysiological, and morphological comparison of the *A. arabicum* dimorphic diaspores revealed that they correspond to distinct abiotic dispersal modes and agents. The biophysical properties of the M^+ seed diaspore support antitelechoric mechanisms to anchor the dispersed M^+ seed in the direct vicinity of the mother plant. By contrast, the biophysical properties of the winged IND fruit diaspore support telechoric mechanisms (by wind and water), favouring local population dispersal over longer distances. Whereas diaspore dispersal of monomorphic species can only employ the dispersal mode evolved for their single diaspore type, heteromorphic species have evolved an array of distinct dispersal and dormancy adaptations, proposed to provide a bet-hedging strategy to cope with the spatiotemporal variability of their unpredictable habitats (Imbert, 2002; Baskin *et al.*, 2013, 2014; Willis *et al.*, 2014; Lu *et al.*, 2015). In the Brassicaceae *Cakile* spp. and *Diptychocarpus strictus*, each fruit is fragmented to give rise to different morphs and, therefore, the ratio between the morphs is developmentally constrained (Cordazzo, 2006; Lu *et al.*, 2010, 2015). By contrast, the *A. arabicum* dimorphic diaspores derive from distinct fruits, and both the diaspore ratios and numbers can change in response to ambient temperature during reproduction (Lenser *et al.*, 2016). The *A. arabicum* dimorphic system hence provides a blend of bet-hedging and plasticity, which allows it to modulate dispersal ability and germinability in response to environmental cues. We discuss here how this relates to the native habitat and climate (Fig. 1), and reveal properties of its diaspores as adaptations to distinct dispersal mechanisms.

That ABA is a key hormone, mediating the distinct environmental responses to control germination timing by dormancy mechanisms, is well established (Finch-Savage & Leubner-Metzger, 2006), but nothing was known about differences in the

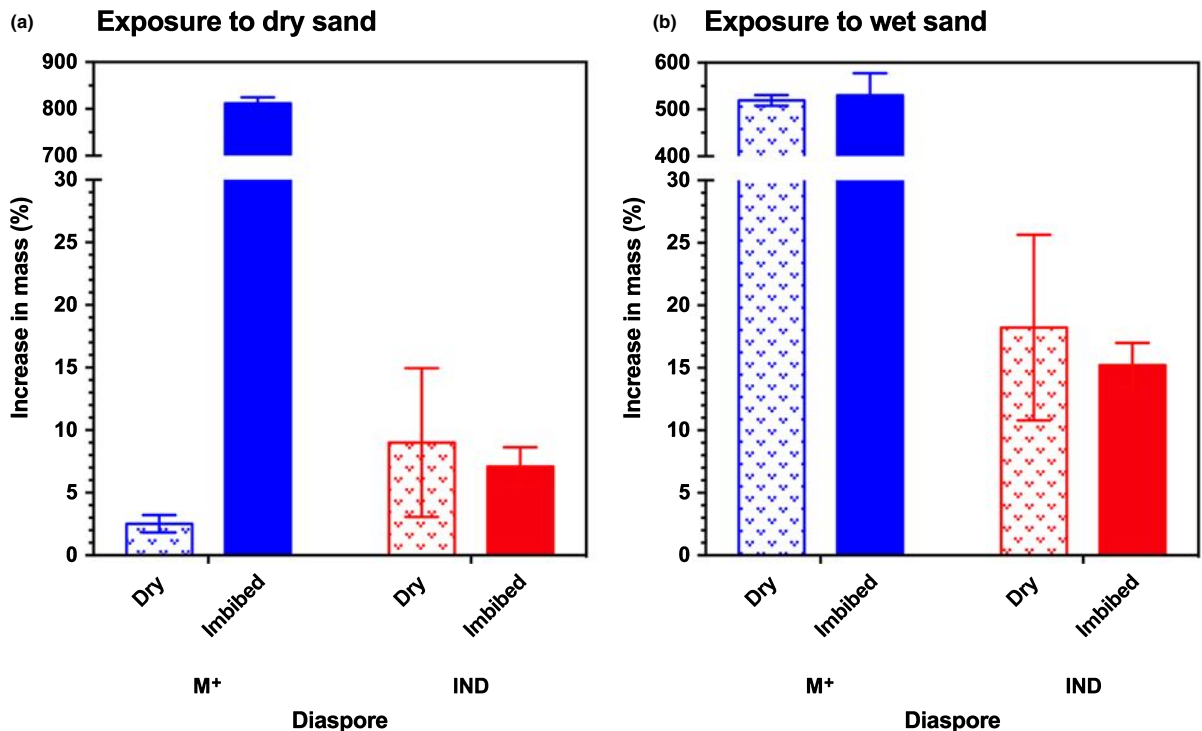


Fig. 5 Comparative behaviour of *Aethionema arabicum* diaspores on fine-grained sandy soil substrata. (a, b) Relative changes in mass of dry and imbibed multiple mucilaginous (M^+) seed and indehiscent (IND) fruit diaspores upon exposure to dry (a) and water-saturated (b) sand. By comparing the initial and final weights of the diaspores, a percentage was obtained by which the mass of the dispersal unit had been increased by adherent sand particles, thus illustrating the effectiveness of mucilage production in M^+ seed diaspores as a means of antitelechory. The unchanged mass of IND fruits suggests the fruit diaspores retain high dispersibility. $n = 3$, each with 25 replicates. Error bars ± 1 SEM.

ABA content of dimorphic diaspores in *A. arabicum*. We found that a 34-fold higher endogenous ABA concentration in the IND fruit diaspore compared with the M^+ seed diaspore is consistent with the low germinability (high degree of dormancy, HD₀) of the IND fruit and the higher germinability (low degree of dormancy, LD₀) of the M^+ seed diaspore. Also, the ABA concentrations in M^- seeds were higher than in M^+ seeds, but much of the ABA was contained in the pericarp. High ABA concentrations controlling germination timing are also known from dry fruits of monomorphic species (Benech-Arnold *et al.*, 1999; Hermann *et al.*, 2007; Chen *et al.*, 2008). The finding of high ABA concentrations in the IND pericarp is consistent with a key role in the pericarp-mediated dormancy mechanism.

M^+ seed diaspore properties support antitelechory

Flowering and reproductive development in April–June lead to diaspore dispersal during the dry summer and wetter autumn (Fig. 1e), after which the (annual) mother plant dies. In agreement with the idea that these conditions aid dispersal, our biomechanical analysis shows that M^+ seed dispersal via dehiscence (fruit valve separation leading to fruit opening) of DEH fruits occurs easily in both dry and humid conditions (Fig. 2). Fruit opening by dehiscence is the default trait in the Brassicaceae

(Mühlhausen *et al.*, 2013), and dehiscence upon wetting has generally been associated with plants adapted to arid environments (Gutterman, 2002; Pufal *et al.*, 2010). Our finding that *A. arabicum* DEH fruit dehiscence can occur in both dry and humid conditions supports the view that M^+ seed dispersal can be temporally staggered from the late dry summer to the wetter autumn. Upon DEH fruit dehiscence, the majority of M^+ seeds detach from the replum and undergo primary dispersal in close vicinity to the mother plant. Together with their lower ABA concentration and dormancy, germination of the M^+ seeds will ensure the progeny sustains its presence in favourable locations.

The phenomenon of mucilage production, known as myxospermy, is commonly understood to serve as an anchorage and adherence mechanism for seed retention; it is of particular importance for species inhabiting arid regions where moisture is often a limiting factor (Yang *et al.*, 2012). We have shown that the dispersal distance of M^+ seeds is significantly restricted in wet conditions (Figs 5, 6). M^+ seeds have the capacity to travel only short distances via runoff water (Fig. 6a). Our findings, therefore, support the view that myxospermy provides an antitelechoric mechanism by retaining the M^+ seed in favourable microclimates. Interactions with substrata provide a further means of adhesion and retention (Fig. 5). The relative increase in mass of the dry M^+ seed, in particular when exposed to wet sand, illustrates the

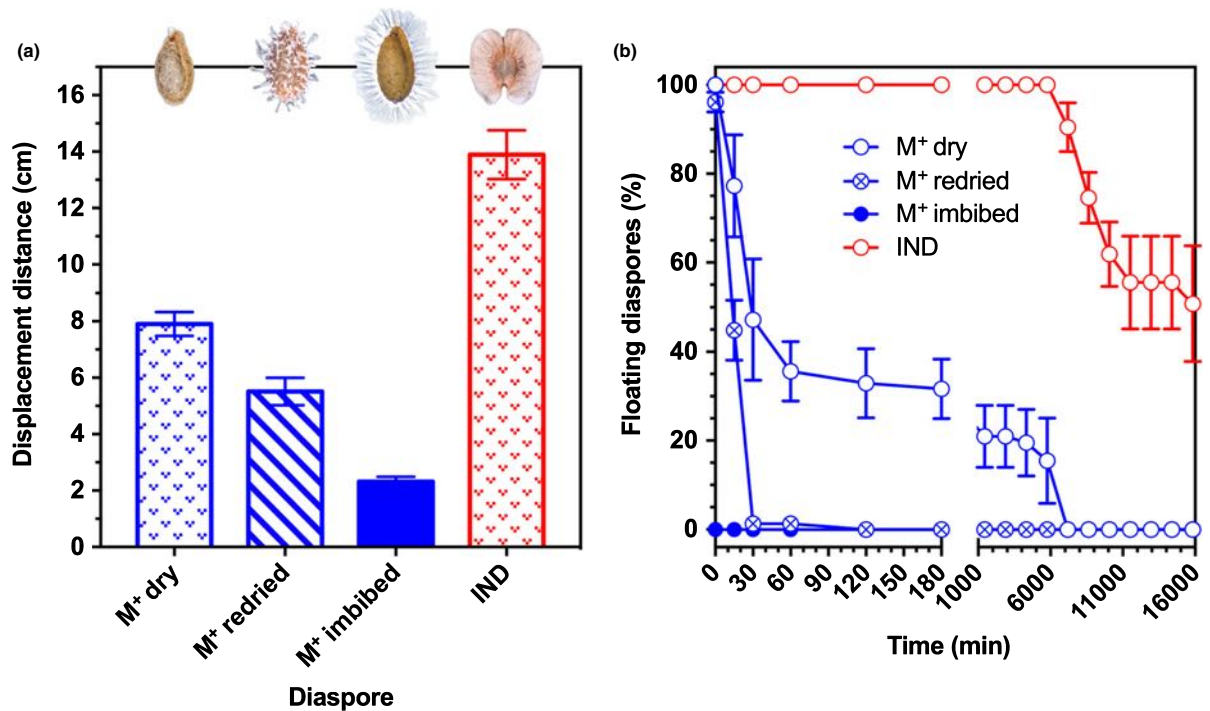


Fig. 6 Surface water runoff displacement and buoyancy of *Aethionema arabicum* fruit and seed diaspores. (a) Distance displaced by surface water runoff across a sloped sandpaper plate of dry, redried and imbibed multiple mucilaginous (M^+) seeds, in comparison to indehiscent (IND) fruits. Nonmucilaginous (M^-) seeds (not shown), when manually excised from the IND fruit, were displaced by 32.3 ± 1.9 cm. $n = 100$. Error bars ± 1 SEM. *Post hoc* pairwise comparisons confirmed that the dimorphic diaspores were statistically different from each other ($P < 0.001$). (b) Buoyancy of *A. arabicum* seed and fruit diaspores. Dry M^+ seeds, redried M^+ seeds, and imbibed M^+ seeds show progressive sinking as a result of mucilage extrusion. IND fruit diaspores, by contrast, start to sink after 5 d of shaking, while all M^- seeds (not shown) remained floating at the end of the experimental treatment. Symbols are offset on the x-axis for clarity. $n = 3$, each with 25 replicates. Error bars ± 1 SEM.

effectiveness of antitelechoric seed coat mucilage production (Grubert, 1974). This repression of dispersal is an adaptive mechanism, but it does not exclude rare cases of long-distance transport by exozoochory (Mummenhoff & Franzke, 2007). Dispersal of the M^+ seed diaspore therefore allows persistence in relatively stable environments by repeated establishment in few favourable sites. Nondispersed seeds may remain enclosed within DEH fruits and their spatiotemporal dispersal may be staggered by later rain events. Further analyses combining ecophysiological and genetic tools will shed light on the role and evolutionary advantages of seed coat mucilage production in *A. arabicum*.

Adaptive features of IND diaspores support telechory

In contrast to the M^+ seed, the adaptive features of the deeper dormant IND fruit morph promote telechory by wind and water. The convergent evolution of indehiscence within the Brassicaceae was associated with the evolution of pericarp features that enhance dispersal as well as an abscission zone on the joint between fruit segments in *Cakile* (Willis *et al.*, 2014). Fruit traits associated with greater dispersal ability, that is, indehiscence plus pericarp features, were also associated with the evolution of larger

seeds. In agreement with a greater dispersal ability (compared with the M^+ seed), the *A. arabicum* IND fruit morph is indeed characterized by pericarp features that enhance dispersal, but it is not associated with an increased M^- seed size (Table 1). The IND fruit morph also does not contain a joint, but the abscission zone that attaches it to the plant is well developed (Lenser *et al.*, 2016). In agreement with its dispersal by abscission (Fig. 1a), the force required to remove IND fruits from *A. arabicum* plants is approximately sixfold lower than that required for DEH fruits in dry conditions, and *c.* 16-fold lower than that for abscission triggered by rain (ombrohydrochory). This allows wind dispersal by abscission of IND fruits in dry conditions late in summer, and a further enhanced IND fruit abscission in wetter conditions in autumn. Consistent with supporting telechoric mechanisms is a wider wind dispersal kernel and a > 500-fold greater buoyancy of IND fruits compared with M^+ seeds.

Although plant species with anemochorous diaspores exhibit a cosmopolitan distribution, wind dispersal in itself is regarded as a derived dispersal mechanism (van der Pijl, 1982). Structurally, the wings of the IND pericarp confer rigidity with a large surface area and low mass (Table 1). Wing-loading for IND fruits is therefore relatively low (data not shown). The

fruit valves of the pericarp comprise anatomically dead tissue filled with air which is fully permeable for water. However, the chemical constitution of the M^- seed coat, presence of small air pockets in the outer walls of the epidermal cells, or hydrophobic properties of the pericarp may prevent excessive moisture absorbance and confer enhanced buoyancy properties (Fig. 5b). Observations of mature infructescences during humid conditions suggest that IND fruit abscission may not be the first step in its dispersal; moisture-induced movements (hygrochasy) of fruit pedicels (Lenser *et al.*, 2016) facilitate maximal exposure to forces enabling abscission and dispersal by wind and rain. This mechanism, present in a number of desert annuals, may correlate diaspore dispersal to rain events, which ensure optimal germination conditions (Guterman, 1993). In addition, the presence of densely cytoplasmic cells at the base of the fruit–pedicel junction in the IND fruit morph allows programmed abscission in response to such developmental and environmental cues. All these properties are consistent with IND fruit adaptations for telechoric dispersal and may be interpreted as a more opportunistic strategy to permit longer-distance range dispersal, including over the hilly terrain in the native habitat of *A. arabicum*.

Ecological significance of *A. arabicum* diaspore dimorphism

A complex evolutionary interdependence between dormancy and dispersal influences population structure and demography via interactions among multiple traits and selective processes (de Casas *et al.*, 2015). The dimorphic seed dispersal strategy in *A. arabicum* represents a fascinating tradeoff between promoting telechory (IND fruit diaspores) and antitelechory (M^+ seed diaspores). As in most described heteromorphic systems, in *A. arabicum* one of the diaspores (IND fruit) has a high degree of dormancy (HDo, i.e. low germinability), whereas the other diaspore (M^+ seed) has a low degree of dormancy (LDo). The observed difference in germinability is consistent with our finding that the IND fruit (HDo) has a higher ABA concentration than does the M^+ seed (LDo). Interestingly, whereas in most systems the HDo is combined with a low dispersal ability (LDi) and the LDo with a high dispersal ability (HDi) (Lu *et al.*, 2013, 2015; Baskin *et al.*, 2014), our biophysical and biochemical analysis of abiotic dispersal and dormancy properties revealed that this is different in *A. arabicum*. We found that the more abundant, myxospermous M^+ seed diaspore combines LDi–LDo, while the IND fruit diaspore combines HDi–HDo. The altered dispersal and dormancy properties of the IND fruit morph are almost exclusively conferred by the distinct pericarp features and the high ABA concentration of the IND diaspore.

Dispersal and dormancy provide two bet-hedging strategies which can evolve under fluctuations in the environmental conditions in space and time (Volis & Bohrer, 2013; de Casas *et al.*, 2015). There is extensive theoretical literature on this subject, from which the general picture emerges in many cases that these strategies are negatively associated (Buoro & Carlson, 2014; de Casas *et al.*, 2015). One of these two strategies tends to be

dominant: high dispersal associates with low dormancy, and low dispersal with high dormancy. However, much of this depends on the details of the models used. A further selective force emerges from the effects of local competition and the inclusive fitness effects that this brings. For example, in a structured deme model, in which dormancy and dispersal are allowed to evolve together, selection favours nondispersing seeds to have low dormancy (Vitalis *et al.*, 2013). A possible explanation for the evolution of HDo/HDi morphs was hypothesized by Buoro & Carlson (2014) and de Casas *et al.* (2015), who argued that the joint evolution of dispersal and dormancy can be explained by environmental correlation. Spatially uncorrelated environments lead to high dispersal, and temporally uncorrelated environments to high dormancy. If indeed environments in the natural habitat of *A. arabicum* are both spatially and temporally uncorrelated, this might explain the observed pattern for the IND morph: high dormancy coupled with high dispersal.

A further, more empirically grounded, explanation is that, in *A. arabicum*, the seed ontology links HDi to HDo. The altered dispersal and dormancy properties of the IND fruit morph are almost exclusively conferred by the distinct pericarp features. In many fruit diaspores, the evolution of HDi pericarp features is associated with an increased seed size (Willis *et al.*, 2014), but we found that this is not the case in *A. arabicum*. If selection for high dispersal variants is the dominant force, it will then go together with high dormancy. The LDi–LDo M^+ seed and HDi–HDo IND fruit diaspores may therefore have evolved as an adaptation to semiarid habitats with varied topography, which creates microclimates by elevation in mountain belts such as the South Anatolian Taurus (Apaydin *et al.*, 2011).

Mechanistic modelling of diaspore dispersal by wind over hilly terrain revealed that even gentle topography introduced considerable variability in the distance and direction of dispersal as a result of local turbulences (Trakhtenbrot *et al.*, 2014). Most alpine plant species have a limited capacity for diaspore dispersal beyond 10 m, and time their germination and seedling emergence with seasonal temperature regimes (Ohsawa *et al.*, 2007; Mondoni *et al.*, 2012). The winged, symmetrical fruit valve membranes, together with a localized concentration of mass (M^- seed), contribute to high IND fruit dispersal ability in air currents. Thus, through the act of thermal convection currents and air flows typically experienced in scree slope habitats, a vertical up-current may result in a large fall time for such a winged diaspore. This contrasts with the mother-site (or safe-site) theory, originally proposed by Zohary (1937), which predicts the putative low benefit of dispersal in harsh and unpredictable environments, where dispersal and repeated establishment in local favourable sites ensure persistence of plant species and populations, but rather suggests a species that is persisting in linked sink habitats through dispersal between these sinks (Jansen & Yoshimura, 1998).

Our working hypothesis is that the plasticity of *A. arabicum* to alter the ratios and numbers of the dimorphic diaspores in response to temperature during the reproductive phase, combined with the anemochorous dispersal ability of the IND fruit diaspore, supports the longer-distance dispersal over hilly

terrain. In mountainous environments, there is considerable variation in habitat at a relatively small scale: plants at higher altitude tend to be in a more exposed, harsh and unpredictable environment that is comparatively devoid of intense competition. Ambient temperature may act as a reliable clue to a habitat's altitude, thus allowing plants to sense which habitat they are in; by altering the ratio of seed morphs with temperature, *A. arabicum* can adjust its dispersal strategy to risks and fluctuations in the differing habitat conditions. Future ecological work in the field is required to test this hypothesis by analysing the phenology of *A. arabicum* seedling emergence and the relative numbers of the distinct dimorphic diaspores in relation to elevation.

Conclusions

The fascinating morphological, biophysical, hormonal and ecological adaptations of the diaspore dimorphism in *A. arabicum* reveal that they support telechory and antitelechory as contrasting dispersal strategies. The *A. arabicum* dimorphic diaspore system is distinct from most other heteromorphic species in several key features. First, it exhibits plasticity in response to the reproduction temperature in producing distinct numbers and ratios of the dimorphic diaspores. Second, for the myxospermous M⁺ seed diaspore, low dispersal ability is combined with low dormancy (LDi-LDo) to support antitelechory. Third, for the IND fruit diaspore, high dispersal ability is combined with high dormancy (HDi-HDo) to support telechory by wind and water as dispersal agents. Furthermore, these key differences in the dispersal ability and germinability of the dimorphic diaspores are conferred on the IND fruit diaspore by specific pericarp-derived features and high ABA concentration. Only the IND fruit diaspore can provide longer-range dispersal by wind and water. We propose that the unique features of the *A. arabicum* diaspore dimorphism and its phenotypic plasticity evolved as a bet-hedging adaptation for survival in semiarid habitats and high elevational scree-slope environments.

Acknowledgements







This work is part of the ERA-CAPS 'SeedAdapt' consortium project (www.seedadapt.eu) and was supported by a Natural Environment Research Council (NERC) Doctoral Training Partnership (DTP) studentship to WA (NE/L002485/1), by grants from the Biotechnology and Biological Sciences Research Council (BBSRC) to GL-M (BB/M00192X/1 and BB/M000583/1), a BBSRC DTP studentship to BN (BB/M011178/1), and from the Deutsche Forschungsgemeinschaft (DFG) to KM (MU 1137/12-1). We would like to thank members of the SeedAdapt consortium for useful discussions, the Botanical Garden of the University of Osnabrück for assistance with seed production, and S. Clausen, N. Wiegand, F. Przesdzink and U. Coja for help with dispersal experiments. We further acknowledge critical reading of the manuscript by J. Chandler, J. Hourston and S. Bhattacharya. Photography credits: A. Voegele (infructescence, Fig. 1a) and B. Özüdoğru (Fig. 1d). All data

presented or analysed are included in this published article or are available from the corresponding authors.

Author contributions

KM, KS, WA, TS and GL-M planned and designed the research; KS, WA and TS performed experiments; WA, KS, TS, GL-M and KM analysed and interpreted the data; BN and VAAJ formulated the hypothesis that temperature provides the cue for elevation, leading to adaptive plasticity of diaspore ratio; WA, TS, GL-M and KM wrote the manuscript; all authors revised and approved the final article. WA, KS, GL-M and KM contributed equally to this work.

ORCID

Waheed Arshad  <http://orcid.org/0000-0002-9413-2279>
 Vincent A. A. Jansen  <http://orcid.org/0000-0002-6518-2090>
 Gerhard Leubner-Metzger  <http://orcid.org/0000-0002-6045-8713>
 Klaus Mummenhoff  <http://orcid.org/0000-0002-8449-1593>
 Bethany Nichols  <http://orcid.org/0000-0003-1280-2070>
 Tina Steinbrecher  <http://orcid.org/0000-0003-3282-6029>

References

- Apaydin H, Anli AS, Ozturk F. 2011. Evaluation of topographical and geographical effects on some climatic parameters in the Central Anatolia Region of Turkey. *International Journal of Climatology* 31: 1264–1279.
- Avino M, Kramer EM, Donohue K, Hammel AJ, Hall JC. 2012. Understanding the basis of a novel fruit type in Brassicaceae: conservation and deviation in expression patterns of six genes. *EvoDevo* 3: 20.
- Babaç MT. 2004. Possibility of an information system on plants of South-West Asia with particular reference to the Turkish plants data service (TÜBIVES). *Turkish Journal of Botany* 28: 119–127.
- Baskin CC, Baskin JM. 2014. *Seeds: ecology, biogeography, and evolution of dormancy and germination*. San Diego, CA, USA: Elsevier.
- Baskin JM, Lu JJ, Baskin CC, Tan DY. 2013. The necessity for testing germination of fresh seeds in studies on diaspore heteromorphism as a life-history strategy. *Seed Science Research* 23: 83–88.
- Baskin JM, Lu JJ, Baskin CC, Tan DY, Wang L. 2014. Diaspore dispersal ability and degree of dormancy in heteromorphic species of cold deserts of northwest China: a review. *Perspectives in Plant Ecology, Evolution and Systematics* 16: 93–99.
- Benech-Arnold RL, Giallorenzi MC, Frank J, Rodriguez V. 1999. Termination of hull-imposed dormancy in developing barley grains is correlated with changes in embryonic ABA levels and sensitivity. *Seed Science Research* 9: 39–47.
- Box GE, Cox DR. 1964. An analysis of transformations. *Journal of the Royal Statistical Society. Series B (Methodological)* 26: 211–252.
- Buoro M, Carlson SM. 2014. Life-history syndromes: integrating dispersal through space and time. *Ecology Letters* 17: 756–767.
- de Casas RR, Donohue K, Venable DL, Cheptou P-O. 2015. Gene-flow through space and time: dispersal, dormancy and adaptation to changing environments. *Evolutionary Ecology* 29: 813–831.
- Chen S-Y, Kuo S-R, Chien C-T. 2008. Roles of gibberellins and abscisic acid in dormancy and germination of red bayberry (*Myrica rubra*) seeds. *Tree Physiology* 28: 1431–1439.
- Cordazzo CV. 2006. Seed characteristics and dispersal of dimorphic fruit segments of *Cakile maritima* Scopoli (Brassicaceae) population of southern Brazilian coastal dunes. *Brazilian Journal of Botany* 29: 259–265.

- Davis PH. 1965. *Flora of Turkey and the East Aegean Islands*. Edinburgh, UK: Edinburgh University Press.
- Delcheva MH, Bancheva ST. 2017. *Aethionema arabicum* Andr. ex DC. (Cruciferae) in Bulgaria – *in situ* and *ex situ* conservation. *Annual of Sofia University "St. Kliment Ohridski"* 101: 80–88.
- Donohue K, Rubio de Casas R, Burghardt L, Kovach K, Willis CG. 2010. Germination, postgermination adaptation, and species ecological ranges. *Annual Review of Ecology, Evolution, and Systematics* 41: 293–319.
- Dubois J, Cheptou P-O. 2012. Competition/colonization syndrome mediated by early germination in non-dispersing achenes in the heteromorphic species *Crepis sancta*. *Annals of Botany* 110: 1245–1251.
- Fahn A, Werker E. 1972. Anatomical mechanisms of seed dispersal. In: Kozlowski TT, ed. *Seed biology: importance, development, and germination*. New York, NY, USA: Academic Press, 151–221.
- Finch-Savage WE, Leubner-Metzger G. 2006. Seed dormancy and the control of germination. *New Phytologist* 171: 501–523.
- Franzke A, Lysak MA, Al-Shehbaz IA, Koch MA, Mummenhoff K. 2011. Cabbage family affairs: the evolutionary history of Brassicaceae. *Trends in Plant Science* 16: 108–116.
- García-Fayos P, Bochet E, Cerdá A. 2010. Seed removal susceptibility through soil erosion shapes vegetation composition. *Plant and Soil* 334: 289–297.
- Grubert M. 1974. Studies on the distribution of myxospermy among seeds and fruits of Angiospermae and its ecological importance. *Acta Biologica Venezuelica* 8: 315–551.
- Gutterman Y. 1993. Seed germination in desert plants. In: Cloudsley-Thompson JL, ed. *Adaptations of desert organisms*. Heidelberg, Germany: Springer, 1–253.
- Gutterman Y. 2002. *Survival strategies of annual desert plants*. Berlin, Germany: Springer-Verlag.
- Haudry A, Platts AE, Vello E, Hoen DR, Leclercq M, Williamson RJ, Forczek E, Joly-Lopez Z, Steffen JG, Hazzouri KM *et al.* 2013. An atlas of over 90,000 conserved noncoding sequences provides insight into crucifer regulatory regions. *Nature Genetics* 45: 891–898.
- Hermann K, Meinhard J, Dobrev P, Linkies A, Pesek B, Heß B, Machácková I, Fischer U, Leubner-Metzger G. 2007. 1-Aminocyclopropane-1-carboxylic acid and abscisic acid during the germination of sugar beet (*Beta vulgaris* L.): a comparative study of fruits and seeds. *Journal of Experimental Botany* 58: 3047–3060.
- Imbert E. 2002. Ecological consequences and ontogeny of seed heteromorphism. *Perspectives in Plant Ecology, Evolution and Systematics* 5: 13–36.
- Jansen VAA, Yoshimura J. 1998. Populations can persist in an environment consisting of sink habitats only. *Proceedings of the National Academy of Sciences, USA* 95: 3696–3698.
- Jiménez-Moreno G, Alçiçek H, Alçiçek MC, van den Hoek Ostende L, Wesselingh FP. 2015. Vegetation and climate changes during the late Pliocene and early Pleistocene in SW Anatolia, Turkey. *Quaternary Research* 84: 448–456.
- Kessler R, Stuppy W. 2012. *Seeds: time capsules of life*. San Rafael, CA, USA: Earth Aware Editions.
- Larson-Johnson K. 2016. Phylogenetic investigation of the complex evolutionary history of dispersal mode and diversification rates across living and fossil Fagales. *New Phytologist* 209: 418–435.
- Lenser T, Graeber K, Cevik ÖS, Adigüzel N, Dönmez AA, Grosche C, Kettermann M, Mayland-Quellhorst S, Mérai Z, Mohammadin S *et al.* 2016. Developmental control and plasticity of fruit and seed dimorphism in *Aethionema arabicum*. *Plant Physiology* 172: 1691–1707.
- Lenser T, Tarkovská D, Novák O, Wilhelmsson PK, Bennett T, Rensing SA, Strnad M, Theißen G. 2018. When the BRANCHED network bears fruit: how carpic dominance causes fruit dimorphism in *Aethionema*. *Plant Journal* 94: 352–371.
- Linkies A, Graeber K, Knight C, Leubner-Metzger G. 2010. The evolution of seeds. *New Phytologist* 186: 817–831.
- Lu JJ, Tan DY, Baskin JM, Baskin CC. 2010. Fruit and seed heteromorphism in the cold desert annual ephemeral *Diptychocarpus strictus* (Brassicaceae) and possible adaptive significance. *Annals of Botany* 105: 999–1014.
- Lu JJ, Tan DY, Baskin JM, Baskin CC. 2013. Trade-offs between seed dispersal and dormancy in an amphibasicarpic cold desert annual. *Annals of Botany* 112: 1815–1827.
- Lu JJ, Tan DY, Baskin JM, Baskin CC. 2015. Post-release fates of seeds in dehiscent and indehiscent siliques of the diaspore heteromorphic species *Diptychocarpus strictus* (Brassicaceae). *Perspectives in Plant Ecology, Evolution and Systematics* 17: 255–262.
- Mandák B, Pyšek P. 2001. Fruit dispersal and seed banks in *Atriplex sagittata*: the role of heterocarpy. *Journal of Ecology* 89: 159–165.
- Mohammadin S, Peterse K, van de Kerke SJ, Chatrou LW, Dönmez AA, Mummenhoff K, Pires JC, Edger PP, Al-Shehbaz IA, Schranz ME. 2017. Anatolian origins and diversification of *Aethionema*, the sister lineage of the core Brassicaceae. *American Journal of Botany* 104: 1042–1054.
- Mohammadin S, Wang W, Liu T, Moazzeni H, Ertugrul K, Uysal T, Christodoulou CS, Edger PP, Pires JC, Wright SI *et al.* 2018. Genome-wide nucleotide diversity and associations with geography, ploidy level and glucosinolate profiles in *Aethionema arabicum* (Brassicaceae). *Plant Systematics and Evolution* 304: 1–12.
- Mondoni A, Rossi G, Orsenigo S, Probert RJ. 2012. Climate warming could shift the timing of seed germination in alpine plants. *Annals of Botany* 110: 155–164.
- Mühlhausen A, Lenser T, Mummenhoff K, Theißen G. 2013. Evidence that an evolutionary transition from dehiscent to indehiscent fruits in *Lepidium* (Brassicaceae) was caused by a change in the control of valve margin identity genes. *Plant Journal* 73: 824–835.
- Mühlhausen A, Polster A, Theissen G, Mummenhoff K. 2010. Evolution of fruit dehiscence in Brassicaceae: examples from *Aethionema* and *Lepidium*. *Acta Horticulturae* 867: 207–219.
- Mummenhoff K, Franzke A. 2007. Gone with the bird: Late tertiary and quaternary intercontinental long-distance dispersal and allopolyploidization in plants. *Systematics and Biodiversity* 5: 255–260.
- Ohsawa T, Tsuda Y, Saito Y, Sawada H, Lde Y. 2007. Steep slopes promote downhill dispersal of *Quercus crispula* seeds and weaken the fine-scale genetic structure of seedling populations. *Annals of Forest Science* 64: 405–412.
- van der Pijl L. 1982. *Principles of dispersal in higher plants*. Berlin/Heidelberg, Germany: Springer-Verlag.
- Pufal G, Ryan KG, Garnock-Jones P. 2010. Hygrochastic capsule dehiscence in New Zealand alpine *Veronica* (Plantaginaceae). *American Journal of Botany* 97: 1413–1423.
- Ramesh K, Matloob A, Aslam F, Florentine SK, Chauhan BS. 2017. Weeds in a changing climate: vulnerabilities, consequences, and implications for future weed management. *Frontiers in Plant Science* 8: Article 95.
- Ridley H. 1930. *The dispersal of plants throughout the world*. Ashford, UK: Reeve.
- Robledo-Arnuncio JJ, Klein EK, Muller-Landau HC, Santamaría L. 2014. Space, time and complexity in plant dispersal ecology. *Movement Ecology* 2: 16.
- Şekercioğlu ÇH, Anderson S, Akçay E, Bilgin R, Can ÖE, Semiz G, Tavşanoğlu Ç, Yokeş MB, Soyumert A, İpekdal K *et al.* 2011. Turkey's globally important biodiversity in crisis. *Biological Conservation* 144: 2752–2769.
- Slatkin M. 1974. Hedging one's evolutionary bets. *Nature* 250: 704–705.
- Sorensen AE. 1978. Somatic polymorphism and seed dispersal. *Nature* 276: 174–176.
- Sperber K, Steinbrecher T, Graeber K, Scherer G, Clausung S, Wiegand N, Hourston JE, Kurre R, Leubner-Metzger G, Mummenhoff K. 2017. Fruit fracture biomechanics and the release of *Lepidium didymum* pericarp-imposed mechanical dormancy by fungi. *Nature Communications* 8: 1868.
- Steinbrecher T, Leubner-Metzger G. 2017. The biomechanics of seed germination. *Journal of Experimental Botany* 68: 765–783.
- Sun Y, Tan DY, Baskin CC, Baskin JM. 2012. Role of mucilage in seed dispersal and germination of the annual ephemeral *Alyssum minus* (Brassicaceae). *Australian Journal of Botany* 60: 439–449.
- Sunar S, Yıldırım N, Sengül M, Agar G. 2016. Genetic diversity and relationships detected by ISSR and RAPD analysis among *Aethionema* species growing in Eastern Anatolia (Turkey). *Comptes Rendus Biologies* 339: 147–151.
- Thuiller W, Lavorel S, Araújo MB, Sykes MT, Prentice IC. 2005. Climate change threats to plant diversity in Europe. *Proceedings of the National Academy of Sciences, USA* 102: 8245–8250.
- Trakhtenbrot A, Katul G, Nathan R. 2014. Mechanistic modeling of seed dispersal by wind over hilly terrain. *Ecological Modelling* 274: 29–40.
- Truscott AM, Soulsby C, Palmer SCF, Newell L, Hulme PE. 2006. The dispersal characteristics of the invasive plant *Mimulus guttatus* and the

- ecological significance of increased occurrence of high-flow events. *Journal of Ecology* **94**: 1080–1091.
- Venable DL. 1985. The evolutionary ecology of seed heteromorphism. *American Naturalist* **126**: 577–595.
- Venables WN, Ripley BD. 2002. *Modern applied statistics with S*. New York, NY, USA: Springer.
- Vitalis R, Rousset F, Kobayashi Y, Olivieri I, Gandon S. 2013. The joint evolution of dispersal and dormancy in a metapopulation with local extinctions and kin competition. *Evolution* **67**: 1676–1691.
- Volis S, Bohrer G. 2013. Joint evolution of seed traits along an aridity gradient: seed size and dormancy are not two substitutable evolutionary traits in temporally heterogeneous environment. *New Phytologist* **197**: 655–667.
- Walck JL, Hidayati SN, Dixon KW, Thompson KEN, Poschlod P. 2011. Climate change and plant regeneration from seed. *Global Change Biology* **17**: 2145–2161.
- Willis C, Hall J, Rubio de Casas R, Wang T, Donohue K. 2014. Diversification and the evolution of dispersal ability in the tribe Brassicaceae (Brassicaceae). *Annals of Botany* **114**: 1675–1686.
- Yang X, Baskin JM, Baskin CC, Huang Z. 2012. More than just a coating: ecological importance, taxonomic occurrence and phylogenetic relationships of seed coat mucilage. *Perspectives in Plant Ecology, Evolution and Systematics* **14**: 434–442.
- Zohary M. 1937. Die verbreitungsökologischen Verhältnisse der Pflanzen Palästinas. *Beihfte zum Botanischen Centralblatt* **56**: 1–155.



About New Phytologist

- *New Phytologist* is an electronic (online-only) journal owned by the New Phytologist Trust, a **not-for-profit organization** dedicated to the promotion of plant science, facilitating projects from symposia to free access for our Tansley reviews and Tansley insights.
- Regular papers, Letters, Research reviews, Rapid reports and both Modelling/Theory and Methods papers are encouraged. We are committed to rapid processing, from online submission through to publication 'as ready' via *Early View* – our average time to decision is <26 days. There are **no page or colour charges** and a PDF version will be provided for each article.
- The journal is available online at Wiley Online Library. Visit www.newphytologist.com to search the articles and register for table of contents email alerts.
- If you have any questions, do get in touch with Central Office (np-centraloffice@lancaster.ac.uk) or, if it is more convenient, our USA Office (np-usaoffice@lancaster.ac.uk)
- For submission instructions, subscription and all the latest information visit www.newphytologist.com

4. Dimorphic fruit fracture biomechanics

4.1 Paper as published in *Botany*

Chapter 4 addresses fundamental questions on dimorphic fruit fracturing biomechanics, and uses interdisciplinary methods to reach mechanistic insight to link structure and function of fruit-related traits in *Ae. arabicum*. The behaviour of plants subjected to forces and displacements at various hierarchical levels represents an integral component of how plants function within the limits set by their physical environment. Using comparative analyses of fruit fracture biomechanics, fracture surface morphology, and internal fruit anatomy, the material and morpho-anatomical properties of the dimorphic fruits of *Ae. arabicum* are analysed in greater detail. Biomechanical observations are linked to the presence of a separation layer along the valve-replum boundary in dehiscent fruits, while indehiscent fruits have numerous fibres with spiral thickening that link their winged valves at the adaxial surface.

The results of biomechanical tests and fracture morphologies were published in *Botany* (formerly the *Canadian Journal of Botany*) under the title “Fracture of the dimorphic fruits of *Aethionema arabicum* (Brassicaceae)” (DOI: 10.1139/cjb-2019-0014). The paper was published within a Plant Biomechanics special issue, related to the 9th International Plant Biomechanics Conference (Montréal, Canada), and is presented here in its full form.

4.2 Author contributions

All experiments, sample preparation, and data analysis were performed by W Arshad. The concepts and narrative of the manuscript were conceived by W Arshad. The proposal (ID: 20180809) for synchrotron radiation beamtime at the Swiss Light Source was prepared by W Arshad and is provided in Appendix 9.3.

F Marone provided technical expertise at the Paul Scherrer Institut, Villigen, Switzerland (during Synchrotron Radiation X-ray Tomographic Microscopy). Project supervision was provided by T Steinbrecher (Royal Holloway University of London, UK), ME Collinson (Royal Holloway University of London, UK), and G Leubner-Metzger (Royal Holloway University of London, UK).

W Arshad was the lead author of this manuscript, prepared all figures, and wrote the majority of the text. W Arshad prepared all manuscript components for submission, wrote the covering letter to *Botany*, and co-ordinated the revision process with all co-authors.

Fracture of the dimorphic fruits of *Aethionema arabicum* (Brassicaceae)¹

Waheed Arshad, Federica Marone, Margaret E. Collinson, Gerhard Leubner-Metzger, and Tina Steinbrecher

Abstract: Fruits exhibit highly diversified morphology, and are arguably one of the most highly specialised organs to have evolved in higher plants. Fruits range in morphological, biomechanical, and textural properties, often as adaptations for their respective dispersal strategy. While most plant species possess monomorphic (of a single type) fruit and seeds, here we focus on *Aethionema arabicum* (L.) Andr. ex DC. (Brassicaceae). Its production of two distinct fruit (dehiscent and indehiscent) and seed types on the same individual plant provides a unique model system with which to study structural and functional aspects of dimorphism. Using comparative analyses of fruit fracture biomechanics, fracture surface morphology, and internal fruit anatomy, we reveal that the dimorphic fruits of *A. arabicum* exhibit clear material, morpho-anatomical, and adaptive properties underlying their fracture behaviour. A separation layer along the valve–replum boundary is present in dehiscent fruit, whereas indehiscent fruit have numerous fibres with spiral thickening, linking their winged valves at the adaxial surface. Our study evaluates the biomechanics underlying fruit-opening mechanisms in a heteromorphic plant species. Elucidating dimorphic traits aids our understanding of adaptive biomechanical morphologies that function as a bet-hedging strategy in the context of seed and fruit dispersal within spatially and temporally stochastic environments.

Key words: diaspore dispersal, heteromorphy, pericarp biomechanics, silique anatomy, SRXTM, strain energy.

Résumé : Les fruit présentent une morphologie hautement diversifiée et ils constituent probablement un des organes les plus hautement spécialisés ayant évolué chez les plantes supérieures. Les fruit varient en ce qui concerne leurs propriétés morphologiques, biomécaniques et texturales, souvent comme adaptations de leurs stratégies respectives de dispersion. Alors que la plupart des espèces de plantes possèdent des fruit et graines monomorphes (d'un type unique), les auteurs se concentrent ici sur *Aethionema arabicum* (L.) Andr. ex DC. (Brassicaceae). Sa production de deux types distincts de fruit (déhiscent et indéhiscent) et de graines chez le même individu fournit un système modèle unique sur lequel étudier les aspects structuraux et fonctionnels du dimorphisme. À l'aide d'analyses comparatives de la biomécanique de la fracture du fruit, de la morphologie à la surface de la fracture et de l'anatomie interne du fruit, les auteurs révèlent que les fruit dimorphes d'*A. arabicum* présentent des propriétés matérielles, morpho-anatomiques et adaptatives claires qui sous-tendent le fonctionnement de la fracture. Une couche de séparation le long de la frontière valve–replum est présente chez les fruit déhiscent, alors que les fruit indéhiscent possèdent de nombreuses fibres avec un épaississement hélicoïdal, liant leurs valves ailées à la surface adaxiale. Cette étude évalue la biomécanique qui sous-tend les mécanismes d'ouverture du fruit chez les espèces végétales hétéromorphes. L'élucidation des traits dimorphes contribue à notre compréhension des morphologies biomécaniques adaptatives qui fonctionnent comme une stratégie de « bet-hedging » dans le contexte de la dispersion des graines et des fruit à l'intérieur d'environnements spatialement et temporellement stochastiques. [Traduit par la Rédaction]

Mots-clés : dispersion des diaspores, hétéromorphie, biomécanique du péricarpe, anatomie de la silique, microscope à rayonnement synchrotrique et tomographie aux rayons X, énergie de déformation.

Received 21 January 2019. Accepted 8 June 2019.

W. Arshad and T. Steinbrecher. School of Biological Sciences, Royal Holloway University of London, Egham, Surrey, TW20 0EX, UK.
F. Marone. Swiss Light Source, Paul Scherrer Institute, CH-5232 Villigen, Switzerland.

M.E. Collinson. Department of Earth Sciences, Royal Holloway University of London, Egham, Surrey TW20 0EX, UK.

G. Leubner-Metzger. School of Biological Sciences, Royal Holloway University of London, Egham, Surrey, TW20 0EX, UK; Laboratory of Growth Regulators, Centre of the Region Haná for Biotechnological and Agricultural Research, Palacký University and Institute of Experimental Botany, Academy of Sciences of the Czech Republic, 78371 Olomouc, Czech Republic.

Corresponding author: Tina Steinbrecher (email: tina.steinbrecher@rhul.ac.uk).

¹This Note is part of a Special Issue from the 9th International Plant Biomechanics Conference (9–14 August 2018, McGill University). Copyright remains with the author(s) or their institution(s). This work is licensed under a [Creative Commons Attribution 4.0 International License](https://creativecommons.org/licenses/by/4.0/) (CC BY 4.0), which permits unrestricted use, distribution, and reproduction in any medium, provided the original author(s) and source are credited.

Introduction

Across the plant kingdom, fruits are highly diversified in their morphology, representing remarkable botanical architecture and reproductive ingenuity — from the giant pumpkins of *Cucurbita maxima* (Cucurbitaceae), to the microscopic fruit of *Wolffia* (Araceae) duckweeds, which are no larger than 300 μm . The fruit is arguably one of the most highly specialised organs to have evolved in higher plants, mediating the maturation and dispersal of seeds, and representing the end of the reproductive cycle in angiosperms (Ferrández et al. 1999; Linkies et al. 2010).

Fruits may range in biomechanical and textural properties from being fleshy and fibrous, to dry and papery. Dry fruits are broadly classified as either indehiscent, in which the pericarp (mature ovary wall) remains closed at maturity, or dehiscent, in which the fruit splits or opens in some manner to release or expose the seed(s) (Spjut 1994). A classic example of the latter category, is in the cabbage family (Brassicaceae). Brassicaceae comprises species with great economic importance for food, fodder, industrial crops, and ornamentals. It also includes important model plants such as *Arabidopsis*, *Brassica*, *Lepidium*, and *Boechera* species (Heywood et al. 2007; Mummenhoff et al. 2008; Hohmann et al. 2015; Christenhusz et al. 2017). Typical fruit morphology within Brassicaceae consists of dehiscent, dry siliques (“capsules”), formed by a pistil composed of two or more carpels with persistent membranous placental tissue (septum). During seed dispersal, the pericarp valves detach from the replum along a separation layer, with varying dehiscence patterns (Fig. 1a) that exemplify evolutionarily labile morphologies.

Although the silique (or silicula) is the dominant fruit “bauplan” within the Brassicaceae, there are many morpho-anatomical variations possessing diagnostic and taxonomic characters (Koch et al. 2003; Hall et al. 2006). Fruit shape diversity in the Brassicaceae is generated by varying patterns of anisotropy, leading to fruit with angustiseptate (compressed at a right angle to the septum), latiseptate (compressed parallel to the septum), or unflattened (terete or angled in cross section) three-dimensional shapes (Koch et al. 2003; Beentje 2010; Eldridge et al. 2016). Computational modelling has provided a simplified framework for this diversity in Brassicaceae fruit shapes (Eldridge et al. 2016). Dehiscent fruits are considered to represent the ancestral fruit type in Brassicaceae species, with indehiscent fruit evolving independently in 20 tribes (Hall et al. 2011; Mühlhausen et al. 2013). For example, most of the species in the large genus *Lepidium* have dehiscent fruit, but indehiscent and didymous *Lepidium* fruit types evolved several times independently within this genus (Mummenhoff et al. 2008; Sperber et al. 2017). Even more specialised fruit morphology is exemplified by heteroarthrocarpic fruit belonging to *Cakile* spp. in the tribe Brassicaceae, where joints separate the fruit transversely into distinct proximal and dis-

tal segments (Hall et al. 2011; Willis et al. 2014). Thus, it is clear the morphological diversity within Brassicaceae family provides several fruitful avenues to study biomechanical form and function related to seed dispersal (Dinneny and Yanofsky 2005; Mühlhausen et al. 2013; Sperber et al. 2017).

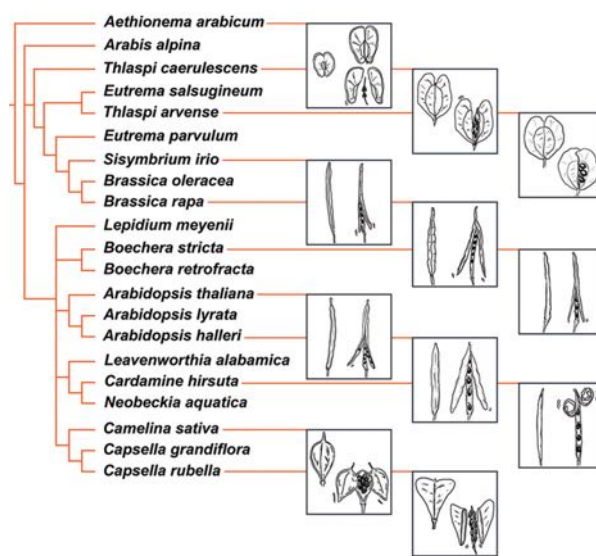
Most plant species possess monomorphic (of a single type) diaspores. However, a number of species exhibit fruit and seed heteromorphism (heterodiaspory), where a given trait exhibits a clear bimodal (dimorphism) or multimodal (heteromorphism) distribution (Imbert 2002; Baskin and Baskin 2014). Such intra-individual variation can often occur within the same fruiting head (infructescence) and be associated with distinct morpho-physiological properties (Baskin et al. 2014; Lenser et al. 2016; Liu et al. 2018; Bhattacharya et al. 2019). The phenomenon of heterodiaspory is of particular importance for relatively short-lived species in spatio-temporally unpredictable environments, and may function as a bet-hedging survival strategy (Venable 1985), particularly in species distributed in desert, saline, and other frequently-disturbed habitats (Imbert 2002; Baskin and Baskin 2014).

In this study, we focus on the dimorphic species *Aethionema arabicum* (L.) Andr. ex DC., a small, annual, herbaceous species belonging to the earliest diverging sister tribe (Aethionemeae) within the Brassicaceae (Franzke et al. 2011; Hohmann et al. 2015; Mohammadin et al. 2017). The genus *Aethionema* occurs mainly in the western Irano-Turanian region, an often-hypothesised cradle of the Brassicaceae (Hedge 1976; Al-Shehbaz et al. 2006; Beilstein et al. 2006; Mandáková et al. 2017). This divergence is thought to have occurred sometime during the Eocene (ca. 34–56 Ma) (Franzke et al. 2011; Hohmann et al. 2015; Mohammadin et al. 2017). *Aethionema arabicum* is characterised by two types of fruit and seeds produced on the same individual infructescence (Fig. 1b): dehiscent (DEH) fruit with 2–6 mucilaginous (M^+) seeds, and indehiscent (IND) fruit each containing a single non-mucilaginous (M^-) seed (Lenser et al. 2016). Dehiscence of the DEH fruit morph causes local dispersal of M^+ seeds, which adhere to substrates via seed-coat mucilage upon imbibition. M^+ seeds possess low dormancy and likely represent an anti-telechorous dispersal mechanism. In comparison, the more dormant IND fruit abscises from the mother plant in its entirety, and has the capacity to disperse longer distances (telechory) via wind and water (Arshad et al. 2019). The production of no intermediate morphs, together with a published genome sequence (Haudry et al. 2013), contributes to the suitability of *A. arabicum* as an excellent model system for fruit and seed dimorphism (Lenser et al. 2018; Mohammadin et al. 2018; Arshad et al. 2019; Wilhelmsson et al. 2019).

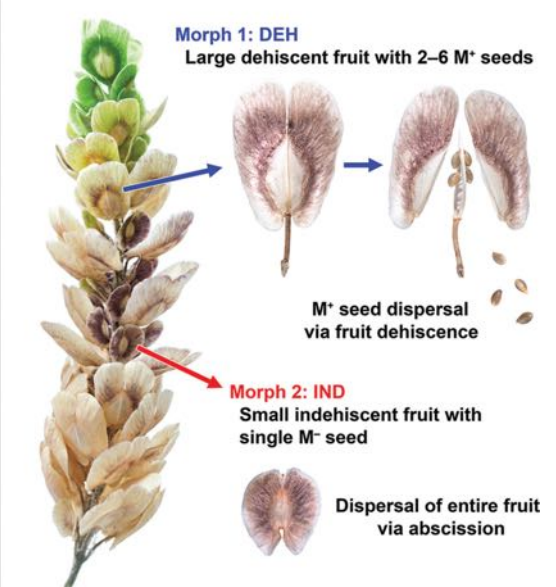
Little is known about the factors influencing fruit valve opening and the fracture behaviour of the two *A. arabicum* morphs. In this study, we elucidate the bio-

Fig. 1. (a) The diversity of fruit fracture mechanisms within members of the Brassicaceae. Depicted are the phylogenetic relationships of various “model” species, together with schematic panels illustrating typical mature fruit prior to (left) and during (right) fruit fracture. The mature fruit may be indehiscent (such as the M^- single-seeded fruit morph in *Aethionema arabicum*), rarely transversely articulate with indehiscent and dehiscent segments (heteroarthrocarpic, such as *Cakile* spp., not shown), or more typically a two-locular dehiscent capsule with a placental partition (septum) bordered by a replum. Schematic illustrations not to scale. Phylogeny according to [Nikolov and Tsiantis \(2017\)](#). (b) The fruit dimorphism in *A. arabicum* is characterised by dehiscent (DEH) fruit with 2–6 mucilaginous (M^+) seeds, and indehiscent (IND) fruit each containing a single non-mucilaginous (M^-) seed. Both fruit morphs are produced on the same individual infructescence. While dehiscence of the DEH fruit morph causes local dispersal of M^+ seeds, the IND fruit abscises from the mother plant in its entirety. [Colour online.]

a Fruit fracture mechanisms in the Brassicaceae



b Fruit dimorphism in *Aethionema arabicum*



mechanical properties during fruit fracture, the fruit valve surface morphology, and the internal fruit anatomy. The morphotype-specific fruit properties are discussed in the context of seed and fruit (diaspore) dispersal mechanisms within the spatially and temporally stochastic environments in which *A. arabicum* survives.

Materials and methods

Fruit valve tensile testing and energy absorption relations

Data from [Arshad et al. \(2019\)](#) were re-analysed to obtain the energy absorption of fruit valve separation. Mature, dry fruit of *Aethionema arabicum* (Turkish accession ES1020, obtained from Eric Schranz, Wageningen University and Research Centre) ([Wilhelmsson et al. 2019](#)) were clamped on each side of the fruit wing, leaving a 2 mm gap between the jaws of a single-column tensile testing machine (Zwick Roell ZwickiLine Z0.5, Ulm, Germany) configured with a 200 N load cell. A constant speed for separation was set at 1 mm·min⁻¹. Force-displacement data were obtained using 30 replicates from three mature main branch infructescences. All of the fruit were freshly harvested from plants grown un-

der long-day conditions (16 h, 20 °C : 8 h, 18 °C; light : dark) in a glasshouse, and mechanically tested at room temperature (20 °C) and 31% relative humidity. The total area under the resultant force-displacement curve was calculated as the mechanical energy consumed by the pericarp in straining it to its fracture point. Using a digital camera (Canon EOS 5D Mark II, fitted with a EF 100 mm f/2.8 macro lens) and Fiji ([Schindelin et al. 2012](#)), the area representing the pericarp fracture zone was determined for 50 manually separated replicates each of DEH and IND fruit. An unpaired two-sample *t* test was carried out using R version 3.5.1 (R Foundation for Statistical Computing, Vienna, Austria).

Scanning electron microscopy (SEM) analysis of fractured fruit valve surfaces

Mature, dry fruit pericarps of both *A. arabicum* morphs were mounted on 12.5 mm Cambridge aluminium specimen stubs, using conductive putty (Lennox Educational, Dublin, Ireland) or two-component epoxy (Araldite®; Huntsman Advanced Materials GmbH, Switzerland). Samples were sputter-coated with a 40 nm thickness of

gold or gold–palladium using a Polaron SEM Coating Unit E5100 (Bio-Rad Microscience Division, Watford, UK). Pericarp fracture surfaces were studied using SEM (Hitachi S-3000N, Japan) at an acceleration voltage of 20 kV, with images subsequently contrast adjusted in Adobe Photoshop CC.

Synchrotron-based radiation X-ray tomographic microscopy (SRXTM) of fracture zones

Mature, dry fruit were fixed in 3% glutaraldehyde plus 4% formaldehyde in 0.1 mol/L piperazine-*N,N'*-bis(2-ethanesulfonic acid) (PIPES) buffer at pH 7.2, for 3 h. The samples were then rinsed twice for 10 min with 0.1 mol/L PIPES, before dehydration in five changes of ethanol (30%, 50%, 70%, 95%, 100%). Samples were critical-point dried (Balzers CPD-030; Bal-Tec, Germany) using ethanol as the intermediate fluid and CO₂ as the transitional fluid. Dehiscent and indehiscent fruit samples were mounted onto 3 mm diameter brass pin stubs using two-component epoxy (Araldite) and imaged at the TOMographic Microscopy and Coherent rAdiology experimentTs (TOMCAT) beamline of the Swiss Light Source, Paul Scherrer Institute (Stampanoni et al. 2006). Data were acquired using a 10× objective and a sCMOS camera (PCO.edge; PCO, Kelheim, Germany), with an exposure time of 80 ms at 12 keV (isotropic voxel dimensions = 0.65 μm). A total of 1501 projections were acquired equi-angularly over 180°, post-processed and reconstructed using a Fourier-based algorithm (Marone and Stampanoni 2012). For verification, three replicates were examined for each fruit morph. Axial tomographic slice data derived from the scans were analysed and manipulated using Avizo™ 9.5.0 (ThermoFisher Scientific, Visualization Science Group Inc., Burlington, Massachusetts, USA) for Windows 10 Pro 64-bit, and contrast adjusted in Adobe Photoshop CC.

Results

Distinct biomechanical events lead to dimorphic fruit failure

To investigate the biomaterial profiles underlying fruit opening mechanisms of the two distinct fruit morphs in *A. arabicum* (DEH and IND), a uniaxial tensile test was performed. Such tests determine the resistance of the component against elongation, and thus enable the derivation of several key material properties and parameters of the tested material (Farquhar and Zhao 2006; Steinbrecher and Leubner-Metzger 2017). We observed two modes of fruit fracture and characterised the force–displacement curves associated with the distinct morphs (Fig. 2). Fruit from the DEH morph were typified by force–displacement curves exhibiting an initial elastic and plastic deformation, followed by a pre-failure event (Fig. 2a). This fracturing event typically initiated at the valve–replum border adjacent to the fruit–pedicel junction, extending along the longitudinal axis of the replum. The crack wake was temporarily held together

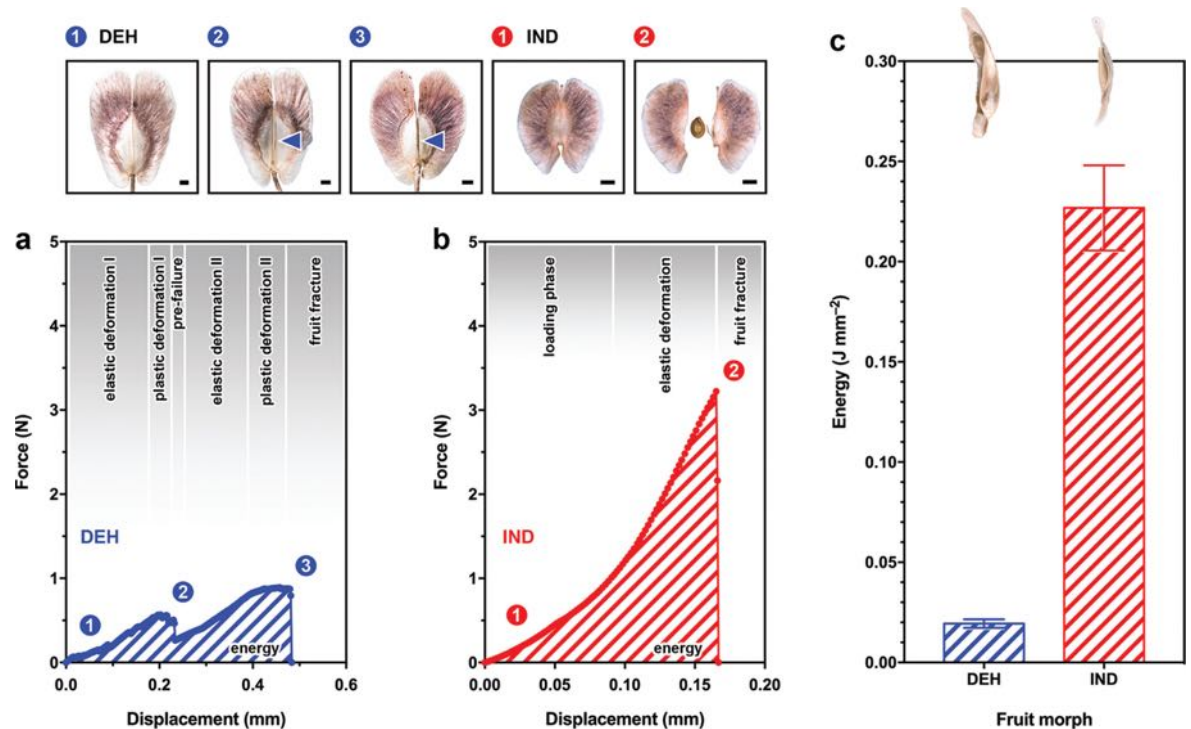
before a second elastic and plastic deformation phase, preceding complete fruit fracture after which no further change in force was detected. In contrast, IND fruit were characterised by a consistent loading phase, comprising non-uniform deformation of the pericarp prior to uniform and linear elastic deformation leading to fruit fracture (Fig. 2b).

The force–displacement curves for DEH fruit show the typical biomechanical response for loading of a benignly “ductile” and elastic material, which can be deformed in multiple stages without causing a complete fracture of the material. The DEH fruit are initially compliant and exhibit a degree of flexibility as the load is increased (Fig. 2a). The more brittle IND fruit, however, failed with less deformation when subjected to loading, with, on average, a 2.6-times higher force. Thus, the dissimilarities in the mechanism and ability of the dimorphic fruit to resist the extension of the initial crack are profound. The comparative biomechanical properties between fruit morphs were also associated with significant differences in the mean mechanical energy consumed by the pericarp in straining it to its failure point ($t_{58} = -9.704$, $P < 0.001$, $d = 2.5$) (Fig. 2c). The energy taken up by each sample is represented by the total area underneath the force–displacement curve up to failure (Hourston et al. 2017; Steinbrecher and Leubner-Metzger 2017). The IND fruit (mean ± SE = 0.227 J·mm⁻² ± 0.02) had a ca. 12-fold increase compared with DEH fruit (0.019 ± 0.002). Taken together, results show that fruit valve opening in *A. arabicum* has two clear biomaterial and mechanical energy profiles, associated unequivocally with the two morphs.

Comparative fracture surface morphology reveals distinct properties of the fruit endocarp

Because the fruit exhibit clear biomechanical failure patterns, pericarp fracture surface morphology was investigated to determine whether it contributed to the observed fruit failure patterns. At the macroscopic level, experimentally fractured valves revealed the replum and septum typical for dehiscent brassicaceous siliques in the DEH morph (Fig. 3a), while experimentally fractured valves in the IND morph (Fig. 3f) revealed a fruit with a dysfunctional replum and lacking a septum. Scanning electron microscopy (SEM) revealed structural differences at several hierarchical levels of organisation. During the fracturing process, the internal tissues of the two fruit morphs split in two distinct ways; the comparatively even structure of the DEH pericarp fracture surface contrasted with the uneven structure of the IND pericarp fracture surface, which often had protrusions at the valve edge (Fig. 3g). In the DEH fruit, an exocarp layer of thick-walled cells, together with a thin-walled mesocarp and endocarp were visible at the fractured edge (Figs. 3c–3e). Both adaxial and abaxial surfaces were identical in morphology (Figs. 3c and 3d). Furthermore, the region of follicle splitting along the replum during de-

Fig. 2. Biomechanical changes during dehiscent (DEH) and indehiscent (IND) fruit fracture in *Aethionema arabicum*. (a and b) Typical force–displacement curves of mechanical tests during fruit valve separation in *A. arabicum*, revealing two contrasting fracture patterns. While DEH (a) fruit exhibit a multistage slow, gradual failure with distinct deformation events at the valve–replum border (blue arrowheads on panels 2 and 3), IND (b) fruit in contrast show a sudden and complete failure preceded by a characteristic loading phase. Numbered panels above force-displacement curves and the corresponding photographs illustrate the process of DEH (1, 2, 3 in blue) and IND (1, 2 in red) fruit fracturing. Scale bars = 1 mm. (c) Comparative means of pericarp-specific mechanical energy consumed during the separation of fruit valves from fruit differ significantly ($t_{58} = -9.704$, $P < 0.001$, $d = 2.5$) between DEH and IND morphs. $N = 30$. Error bars ± 1 standard error of the mean. Data are normalised relative to the mean area of the fracture zone (DEH, $6.94 \pm 0.14 \text{ mm}^2$; IND, 0.87 ± 0.03). [Colour online.]



hiscence exhibits a concave surface (Fig. 3e). The IND fruit pericarp morphology, in contrast, exhibited a different structure (Figs. 3h–3j). At the abaxial margin (Fig. 3h), the valve fracture surface appeared consistently “rough” in texture and comprised cell walls that had been mechanically torn. At the adaxial margin (Figs. 3i and 3j), the endocarp consisted of a very distinct thick-walled single cell layer, oriented at a perpendicular angle to the longitudinal axis of the fruit. Here, numerous fibres with spiral thickening (Figs. 3i and 3j) can be seen to run across the adaxial surface, where they were previously connected across the two halves of the pericarp. Thus, there are clear fracture surface morphologies, at various hierarchical levels, which underlie the two observed fruit fracturing behaviours.

Comparative internal anatomy confirms absence of a separation layer in IND fruit

To explore the internal anatomy of the dimorphic fruit, we conducted non-destructive investigations of the internal structure of mature fruit prior to the onset of

ripening, with a particular focus at the region of fruit failure. Reconstructed digital sections (orthoslices) obtained by SRXTM revealed high resolution cell and tissue details (Fig. 4) without destruction of the sample or risk of artefacts associated with traditional histology (Betz et al. 2007; Smith et al. 2009). Differences, otherwise determined by tissue and cell wall composition, were highlighted by varying X-ray attenuation. Our schematic interpretation of fruit layers (Figs. 4c and 4d) indicates that cells of the exocarp, mesocarp, and endocarp layers were all readily distinguishable in the digital sections from both fruit morphs. Two distinct layers of the endocarp were observed; endocarp *a* (*ena*) comprised an inner epidermis of longitudinally elongated, thin-walled cells, while a subepidermal endocarp *b* (*enb*) layer consisted of one to three layers of tightly packed, isodiametric cells. These observations correlate with the thick cell-walled endocarp layer of the IND fruit, as observed by SEM (Fig. 3j), which leads to the fibres with spiral thickening after fracturing.

Fig. 3. Morphology of the experimentally fractured valves underlying the observed biomechanical differences between dehiscent (DEH) and indehiscent (IND) fruit of *Aethionema arabicum*. Macroscopic features of separated fruit indicate the presence of a replum and septum in DEH fruit (a), while a dysfunctional replum and lack of septum characterise IND fruit (f and g). SEM images of the abaxial (c and h) and adaxial (d, e, i, and j) edges of fractured pericarps indicate the even structure of DEH pericarp fracture surface, in comparison with the uneven structure of IND pericarp fracture surface. Both abaxial and adaxial fracture surfaces of DEH pericarps are identical in morphology (c and d). The distinct thick-walled IND fruit endocarp layer (l and j) possesses numerous fibres with spiral thickening (j, arrowhead) across the adaxial fracture surface, where they were previously connected across the two halves of the pericarp. Scale bars = 1 mm (a, f); 100 μ m (b, g); and 20 μ m (c-e, h-j). SEM, scanning electron microscopy; M⁺, mucilaginous; M⁻, non-mucilaginous; ex, exocarp; ms, mesocarp; en, endocarp. [Colour online.]

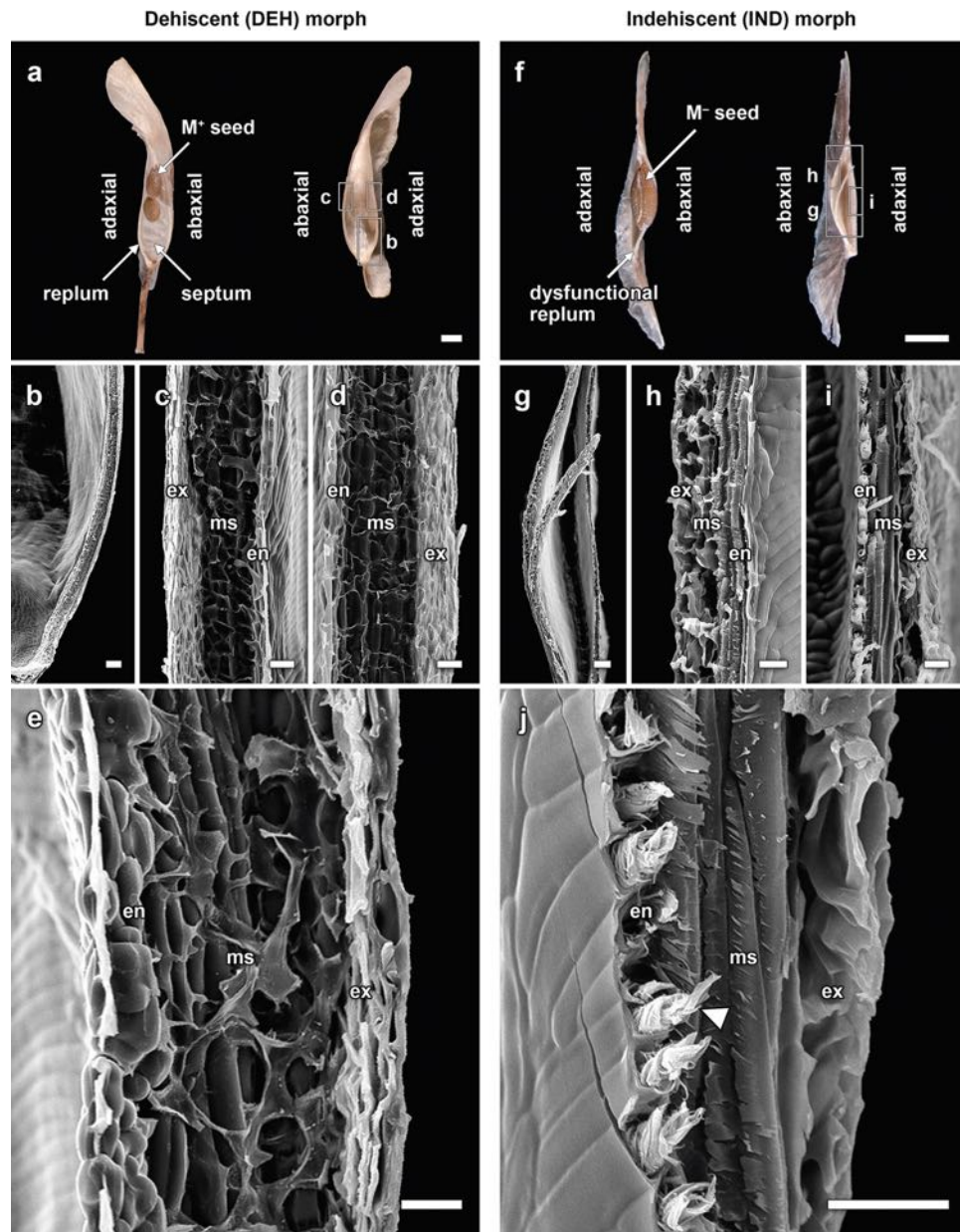
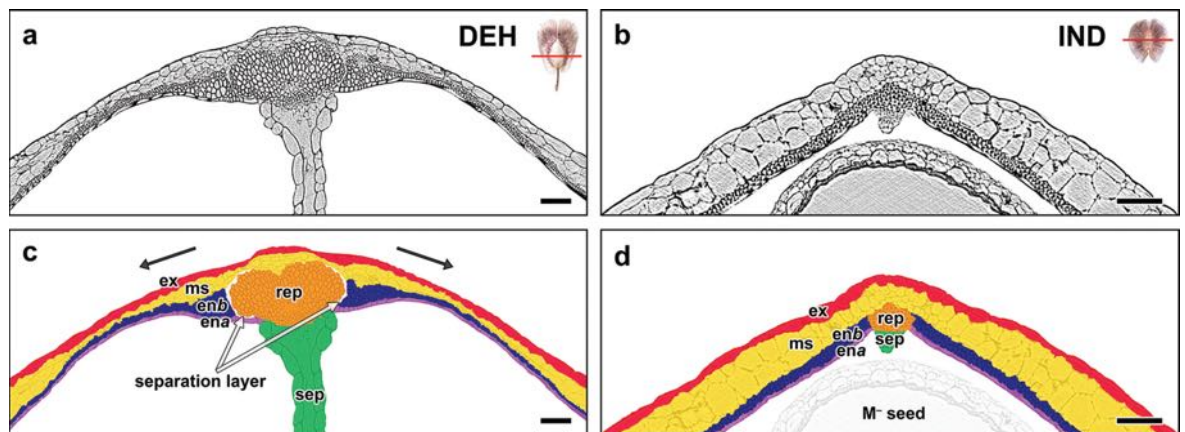


Fig. 4. Comparative SRXTM results obtained from digital transverse sections of mature *Aethionema arabicum* dehiscent (DEH) (a) and indehiscent (IND) (b) fruit with schematic representations (c and d) at the valve–replum region. Inset fruit (not to scale) depict the region from which the slice is taken. The exocarp and outer epidermis (ex), two to three cell layers of mesocarp (ms), and two zones within the endocarp plus inner epidermis (ena and enb) can be distinguished in the fruit valves. A “separation layer” at the valve margin, extending in continuity around the replum when the fruit is further dried, allows DEH fruit valves to detach from the replum. Thus, the endocarp (enb), valve margins, and regions of the mesocarp, together with cell-wall degradation in the ena layer, contribute to “pod-shattering” biomechanics during DEH fruit dehiscence. Arrows indicate proposed directionality of DEH fruit drying tensions, which contribute to rain-mediated seed dispersal (ombrohydrochory). The IND fruit, characterised by its absence of a separation layer (“dehiscence zone”) and septum, does not undergo this highly co-ordinated process, instead retaining a single seed within the pericarp during dispersal. Scale bar = 75 μ m. SRXTM, synchrotron radiation X-ray tomographic microscopy; M⁻, non-mucilaginous.



The *A. arabicum* DEH morph is typical for many brassicaceous siliques, in that the margins of the two carpels and the parietal placentae, between which the septum is attached, form a replum. However, of particular significance is the separation between cells of the replum and endocarp layers (ena and enb) in the DEH fruit morph (Figs. 4a and 4c). This distinct tissue “separation layer” forms part of the “dehiscence zone”, extending along the entire longitudinal axis of the pericarp at the valve–replum boundary. In contrast, tissue organisation within the IND morph pericarp is distinctly different (Figs. 4b and 4d). The mesocarp contributes to a distinct layer composed of large cells, with more densely-packed cells adjacent to the comparatively smaller, dysfunctional replum. The IND morph appears unilocular and only the remnants of a septum persist; the ovary thus contained a single ovule (M⁻ seed; Figs. 4b and 4d). Although there is a comparatively reduced replum, cells of the endocarp and the replum were not separated by a dehiscence zone, instead forming a continuous layer. Furthermore, while the enb layer becomes multilayered proximal to the replum in the DEH morph, only a few cell-layers are present in the enb in the IND morph. Thus, the absence of a “separation layer” or “dehiscence zone”, as well as septum absence, are major differences in the internal anatomy of the IND morph pericarp.

Discussion

Distinct fracture biomechanics of dimorphic fruit

The integration of biomechanics and mechanobiology has been a significant methodological advancement to

address questions in plant sciences, and has seen a renaissance over recent decades (Read and Stokes 2006; Moulia 2013). Our biomechanical evaluation of fruit opening mechanisms of a heteromorphic plant species links pericarp-specific properties to adaptive seed and fruit dispersal. In contrast to the single fruit fracture mechanism — and associated dispersal strategy — of monomorphic plants, the distinct biomechanical profiles for the *Aethionema arabicum* fruit morphs are correlated with their adaptations for different modes of dispersal (Arshad et al. 2019). Our comparisons of fruit fracture biomechanics, and the morpho-anatomical features that contribute to the observed patterns, show that the behaviours are unequivocally associated with the two fruit morphs. Under natural conditions, it is hypothesised that recurring forces from raindrop impacts and (or) wind on the DEH fruit most likely induce fatigue crack growth along the replum. DEH fruit exhibit a multistaged biomechanical response, with several ranges of linear behaviour during pericarp opening, whereas the IND pericarp provides a more brittle breaking behaviour and prolonged loading phase requiring a significantly higher opening energy (Fig. 2c). Torn-out structures (IND fruit, Fig. 3g) indicate that friction between cell layers had to be overcome during the fruit fracture process, creating the “rough” fracture surface texture. As previously described by Beismann et al. (2000), shearing cell layers during the tearing process may contribute to the toughness of the material. The winged, dispersal-

enhancing feature of the IND pericarp allows the seed to remain encased during dispersal (Arshad et al. 2019); however, as a rare adaptation for long-range dispersal in desert plants, pericarp “wings” may also serve as a protective measure against the adverse environment during germination and seedling establishment (Ellner and Shmida 1981).

That fruit opening in monomorphic Brassicaceae fruit is dependent on the positioning and formation of the valve margin and its dehiscence zone is well-established (Spence et al. 1996; Avino et al. 2012), but little is known about differences in the opening mechanisms operating in heteromorphic fruit. We found that the IND fruit lacks the distinctive anatomical organisation present in typical dehiscent siliques, and that the cells of the endocarp layers form a continuous band around the replum, thus preventing fruit dehiscence. The IND fruit pericarp, therefore, not only confers enhanced dispersal ability and degree of dormancy (Arshad et al. 2019), but also a mechanism for remaining as a closed disseminule after dispersal. This may suggest that pericarp-mediated dormancy in the *A. arabicum* system may be partly physically and physiologically imposed on M⁻ seeds. In the indehiscent fruit of *Lepidium didymum* (Brassicaceae), Sperber et al. (2017) found that the thick, hard pericarp imposed a mechanical constraint on the germination of encased seeds by influencing water uptake patterns into seeds inside fruit valves, and that fungi induced selective weakening of pericarp tissue (at distinct predetermined zones), lowering its mechanical resistance to breakage. The mechanisms by which the *A. arabicum* IND pericarp may impose a mechanical constraint to full water uptake by the M⁻ seed is little investigated. Ongoing ecophysiological, biomechanical, and molecular analyses on the influence of the pericarp tissue during and after IND fruit germination should shed light on its specific role.

The presented fruit fracture biomechanics prompts questions on the contrasting development and molecular regulation underpinning the morph-specific determination of *A. arabicum* fruit. Within the Brassicaceae, the evolutionary transition from dehiscent to indehiscent fruit has been investigated in *Lepidium*, where both dehiscent and indehiscent fruit are produced (Mummenhoff et al. 2008; Mühlhausen et al. 2013). Anatomical changes at the valve–replum border were connected with altered expression patterns of various genes orthologous to the known fruit developmental genes in *Arabidopsis*, including *ALCATRAZ* (*ALC*), *INDEHISCENT* (*IND*), *SHATTERPROOF1* (*SHP1*), and *SHATTERPROOF2* (*SHP2*) (Rajani and Sundaresan 2001; Liljegren et al. 2004; Ballester and Ferrandiz 2017). Orthologues were shown to be expressed in the dehiscence zone-forming fruit valve margin of *Lepidium campestre* dehiscent fruit, whereas in the corresponding tissue of *L. appelianum* indehiscent fruit, expression patterns were down-regulated (Mühlhausen et al. 2013). Indeed, in *A. arabicum*, expression analyses in mature fruit

have previously revealed that the orthologue *IND* (which is involved in the differentiation of the separation layer and acts as the key regulator in controlling valve margin specification) was down-regulated in IND fruit compared with DEH fruit (Lenser et al. 2016). The genetic pathways operating in DEH and IND fruit therefore indicate an avenue for more detailed developmental and molecular time-course characterisations in *A. arabicum*, particularly with reference to valve-margin-specific and dehiscence zone identity genes (Avino et al. 2012; Lenser et al. 2018).

Our microscopy approaches indicated fundamental differences in the structure and organisation of fruit valve layers. Combining SEM with non-invasive and non-destructive methods such as SRXTM provides new possibilities for the visualisation and analysis of the external and internal structure of fossil and extant plant material (Friis et al. 2014; Benedict et al. 2015). Such imaging solves problems associated with cutting or histological sectioning by minimising the introduction of artefacts (e.g., tears, gaps), and allows multiple planes of section through the same specimen to be acquired at high quality resolution (Smith et al. 2009; Adams et al. 2016). In addition to the absence of a dehiscence zone, the identification of valve tissue morphology was of particular significance at the adaxial fracture surface. As structural differences in the valves are associated with the mode of fracturing, the IND fruit tissue organisation could perhaps be interpreted as a remnant of a once active dehiscence apparatus (Fahn and Zohary 1955). Differential timing of anisotropic growth patterns, in turn coordinating the development of fruit growth and maturation leading to dispersal, may also influence the anatomical organisation and material properties observed between DEH and IND fruit. The dimorphic fruit in *A. arabicum* therefore provide an ideal system with which to model post-fertilisation gynoecium growth and shape formation, as has been demonstrated in the monomorphic *Capsella rubella* (Eldridge et al. 2016), to identify tissue-specific activities required to obtain the two distinct morphologies.

Hypothesis for fracturing biomechanics and dispersal in natural conditions

The semi-arid environment in which *A. arabicum* grows is characterised by highly variable rainfall in space and in time, and therefore presents challenging climatic and edaphic conditions for plant growth (Arshad et al. 2019). At the macroscale this may include sporadic rain events, with high precipitation rates over relatively small spatial scales, while at the microscale, topographic factors and soil surfaces are thought to contribute to the variability of water availability (Kigel 1995). The contrasting morpho-anatomical and biomechanical properties of *A. arabicum* fruit contribute to bet-hedging adaptations for successful dispersal in the scree and steppe habitats of Anatolia (Arshad et al. 2019). Prior to dehiscence, the DEH fruit pericarp dries as the fruit approaches matu-

urity. Our working hypothesis is that the highly coordinated events causing tissue separation and endocarp lignification create spring-like tensions in the mature DEH fruit, the elastic energy from which is retained during the dry period until rain-induced (ombrohydrochory) impact events cause “pod-shattering” and M⁺ seed dispersal to occur. This is consistent with the passive, drying forces acting on microstructures that have been demonstrated during fruit and seed dispersal of other species (Elbaum and Abraham 2014). For example, the shedding of living twigs (in *Salix* spp. and *Populus* spp.) provides a reproductive mechanism (via twig dispersal and subsequent establishment in new habitats) that also relies on fracture mechanics. The relative roughness of the twig fracture surface in the genus *Salix* correlates with the classification of brittle and non-brittle species (Beismann et al. 2000).

Dehiscence upon wetting has generally been associated with plants adapted to arid environments (Gutterman 2002; Pufal et al. 2010), and the work of fracture is typically negatively correlated with moisture content (Farquhar and Zhao 2006). Tensions are created due to the differential drying of the parenchymatic and sclerenchymatic tissues of the pericarp, while degeneration of the middle lamellae of the separation layer cells (via cell wall degrading enzymes) forms a pre-determined breaking zone along the longitudinal axis. This, together with moisture-induced (hygrochastic) movements of fruit pedicels (Lenser et al. 2016), is thought to contribute to the distinct biomechanical fracture mechanism observed in DEH fruit. The mature IND fruit, in contrast, abscises from the mother plant in its entirety and thus has inherently different biotic and abiotic factors influencing its pericarp fracture biomechanics. Post-dispersal time-lapse data obtained during seedling establishment (not shown) suggest that IND fruit valve separation only occurs after completion of germination, as a result of radicle protrusion between two adjoining pericarp valves.

Conclusions

The species richness and divergent fruit shapes in the Brassicaceae provide an invaluable framework to address questions on seed and fruit dispersal. Here, we have shown that the dimorphic fruit fracture patterns in *Aethionema arabicum* are associated with distinct morpho-anatomical features influencing the deformation behaviours of the pericarp during opening. A distinct “separation layer” along the DEH fruit valve–replum boundary contributed to the multistaged fracture events leading to failure. In contrast, IND fruit were shown to possess a distinct endocarp layer with spirally thickened fibres linking its winged valves at the adaxial surface. This, and a lack of a dehiscence zone, mediate the more brittle material properties of IND fruit valves. The *A. arabicum* dimorphic system illustrates how biomechanics approaches can be successfully combined with internal and

external imaging techniques, to understand the underlying causes for dispersal-related phenomena. The presented anatomical observations across a range of hierarchical levels contribute to our understanding of dimorphic structures and functions, and further support our knowledge of how these interact as bet-hedging adaptations to the physical environment. Together with recently published (Lenser et al. 2018; Wilhelmsson et al. 2019) and future molecular work into the mechanisms of the diaspore dimorphism in *A. arabicum*, the integration of biomechanics and imaging makes it an exciting time to study fruit- and dispersal-related properties by moving beyond *Arabidopsis* and other monomorphic plants.

Acknowledgements

We thank Patricia Goggin and the Imaging and Microscopy Centre (University of Southampton) for assistance with the sample preparation for SEM and SRXTM, and Sharon Gibbons (Earth Sciences, Royal Holloway University of London) for assistance with SEM. We also acknowledge the Paul Scherrer Institut, Villigen, Switzerland, for provision of synchrotron radiation beamtime (Proposal ID: 20180809) at the TOMCAT beamline of the Swiss Light Source to T.S. (Principal Investigator) and Co-Investigators (W.A., M.E.C., G.L.-M.). **List of author contributions:** W.A. and T.S. planned and designed the research; W.A., F.M., and T.S. performed the experiments; W.A., M.E.C., G.L.-M., and T.S. analysed and interpreted the data; W.A., G.L.-M., and T.S. wrote the manuscript; all of the authors revised and approved the final article. **Funding information:** This work originated from the ERA-CAPS “SeedAdapt” consortium project (www.seedadapt.eu) and was supported by a Natural Environment Research Council (NERC) Doctoral Training Grant to W.A. (grant no. NE/L002485/1), and by the Biotechnology and Biological Sciences Research Council (BBSRC) to T.S. and G.L.-M. (grant nos. BB/M00192X/1 and BB/M000583/1). **Data availability statement:** All data presented or analysed are included in this published article as described in detail in the main text and figure legends or are available from the authors.

References

- Adams, N.F., Collinson, M.E., Smith, S.Y., Bamford, M.K., Forest, F., Malakasi, P., et al. 2016. X-rays and virtual taphonomy resolve the first *Cissus* (Vitaceae) macrofossils from Africa as early-diverging members of the genus. *Am. J. Bot.* **103**(9): 1657–1677. doi:10.3732/ajb.1600177. PMID:27647420.
- Al-Shehbaz, I.A., Beilstein, M.A., and Kellogg, E.A. 2006. Systematics and phylogeny of the Brassicaceae (Cruciferae): an overview. *Plant Syst. Evol.* **259**: 89–120. doi:10.1007/s00606-006-0415-z.
- Arshad, W., Sperber, K., Steinbrecher, T., Nichols, B., Jansen, V.A., Leubner-Metzger, G., and Mummenhoff, K. 2019. Dispersal biophysics and adaptive significance of dimorphic diaspores in the annual *Aethionema arabicum* (Brassicaceae). *New Phytol.* **221**(3): 1434–1446. doi:10.1111/nph.15490. PMID:30230555.
- Avino, M., Kramer, E.M., Donohue, K., Hammel, A.J., and Hall, J.C. 2012. Understanding the basis of a novel fruit type in Brassicaceae: conservation and deviation in expression pat-

- terms of six genes. *EvoDevo*, **3**(1): 20. doi:10.1186/2041-9139-3-20. PMID:22943452.
- Ballester, P., and Ferrandiz, C. 2017. Shattering fruit: variations on a dehiscent theme. *Curr. Opin. Plant Biol.* **35**: 68–75. doi:10.1016/j.pbi.2016.11.008. PMID:27888713.
- Baskin, C.C., and Baskin, J.M. 2014. Seeds: ecology, biogeography, and evolution of dormancy and germination. 2nd ed. Elsevier.
- Baskin, J.M., Lu, J.J., Baskin, C.C., Tan, D.Y., and Wang, L. 2014. Diaspore dispersal ability and degree of dormancy in heteromorphic species of cold deserts of northwest China: a review. *Perspect. Plant Ecol.* **16**(2): 93–99. doi:10.1016/j.ppees.2014.02.004.
- Beentje, H. 2010. The Kew plant glossary: an illustrated dictionary of plant terms. Royal Botanic Gardens, Kew, UK.
- Beilstein, M.A., Al-Shehbaz, I.A., and Kellogg, E.A. 2006. Brassicaceae phylogeny and trichome evolution. *Am. J. Bot.* **93**(4): 607–619. doi:10.3732/ajb.93.4.607. PMID:21646222.
- Beismann, H., Wilhelmi, H., Baillères, H., Spatz, H.C., Bogenrieder, A., and Speck, T. 2000. Brittleness of twig bases in the genus *Salix*: fracture mechanics and ecological relevance. *J. Exp. Bot.* **51**(344): 617–633. doi:10.1093/jexbot/51.344.617. PMID:10938818.
- Benedict, J.C., Smith, S.Y., Collinson, M.E., Leong-Škorničková, J., Specht, C.D., Marone, F., et al. 2015. Seed morphology and anatomy and its utility in recognizing subfamilies and tribes of Zingiberaceae. *Am. J. Bot.* **102**(11): 1814–1841. doi:10.3732/ajb.1500300. PMID:26507111.
- Betz, O., Wegst, U., Weide, D., Heethoff, M., Helfen, L., Lee, W.K., and Cloetens, P. 2007. Imaging applications of synchrotron X-ray phase-contrast microtomography in biological morphology and biomaterials science. I. General aspects of the technique and its advantages in the analysis of millimeter-sized arthropod structure. *J. Microsc.* **227**(1): 51–71. doi:10.1111/j.1365-2818.2007.01785.x. PMID:17635659.
- Bhattacharya, S., Mayland-Quellhorst, S., Müller, C., and Mummenhoff, K. 2019. Two-tier morpho-chemical defence tactic in *Aethionema* via fruit morph plasticity and glucosinolates allocation in diaspores. *Plant Cell Environ.* **42**(4): 1381–1392. doi:10.1111/pce.13462. PMID:30316198.
- Christenhusz, M.J.M., Fay, M.F., and Chase, M.W. 2017. Plants of the world: an illustrated encyclopedia of vascular plants. Kew Publishing and The University of Chicago Press, Royal Botanic Gardens, Kew, UK.
- Dinnyeny, J.R., and Yanofsky, M.F. 2005. Drawing lines and borders: how the dehiscent fruit of *Arabidopsis* is patterned. *BioEssays*, **27**(1): 42–49. doi:10.1002/bies.20165. PMID:15612035.
- Elbaum, R., and Abraham, Y. 2014. Insights into the microstructures of hygroscopic movement in plant seed dispersal. *Plant Sci.* **223**: 124–133. doi:10.1016/j.plantsci.2014.03.014. PMID:24767122.
- Eldridge, T., Łangowski, Ł., Stacey, N., Jantzen, F., Moubayidin, L., Sicard, A., et al. 2016. Fruit shape diversity in the Brassicaceae is generated by varying patterns of anisotropy. *Development*, **143**(18): 3394–3406. doi:10.1242/dev.135327. PMID:27624834.
- Ellner, S., and Shmida, A. 1981. Why are adaptations for long-range seed dispersal rare in desert plants? *Oecologia*, **51**(1): 133–144. doi:10.1007/BF00344663. PMID:28310320.
- Fahn, A., and Zohary, M. 1955. On the pericarpial structure of the legumen, its evolution and relation to dehiscence. *Phytomorphology*, **5**: 99–111.
- Farquhar, T., and Zhao, Y. 2006. Fracture mechanics and its relevance to botanical structures. *Am. J. Bot.* **93**(10): 1449–1454. doi:10.3732/ajb.93.10.1449. PMID:21642092.
- Ferrándiz, C., Pelaz, S., and Yanofsky, M.F. 1999. Control of carpel and fruit development in *Arabidopsis*. *Annu. Rev. Biochem.* **68**(1): 321–354. doi:10.1146/annurev.biochem.68.1.321. PMID:10872453.
- Franzke, A., Lysak, M.A., Al-Shehbaz, I.A., Koch, M.A., and Mummenhoff, K. 2011. Cabbage family affairs: the evolutionary history of Brassicaceae. *Trends Plant Sci.* **16**(2): 108–116. doi:10.1016/j.tplants.2010.11.005. PMID:21177137.
- Friis, E.M., Marone, F., Pedersen, K.R., Crane, P.R., and Stampanoni, M. 2014. Three-dimensional visualization of fossil flowers, fruit, seeds, and other plant remains using synchrotron radiation X-ray tomographic microscopy (SRXTM): new insights into Cretaceous plant diversity. *J. Paleontol.* **88**(4): 684–701. doi:10.1666/13-099.
- Gutterman, Y. 2002. Survival strategies of annual desert plants. Adaptations of desert organisms. Springer-Verlag, Berlin, Germany.
- Hall, J.C., Tisdale, T.E., Donohue, K., and Kramer, E.M. 2006. Developmental basis of an anatomical novelty: heteroarthrocarpy in *Cakile lanceolata* and *Erucaria erucarioides* (Brassicaceae). *Int. J. Plant Sci.* **167**(4): 771–789. doi:10.1086/504928.
- Hall, J.C., Tisdale, T.E., Donohue, K., Wheeler, A., Al-Yahya, M.A., and Kramer, E.M. 2011. Convergent evolution of a complex fruit structure in the tribe Brassicaceae (Brassicaceae). *Am. J. Bot.* **98**(12): 1989–2003. doi:10.3732/ajb.1100203. PMID:22081414.
- Haudry, A., Platts, A.E., Vello, E., Hoen, D.R., Leclercq, M., Williamson, R.J., et al. 2013. An atlas of over 90,000 conserved noncoding sequences provides insight into crucifer regulatory regions. *Nat. Genet.* **45**(8): 891–898. doi:10.1038/ng.2684. PMID:23817568.
- Hedge, I. 1976. A systematic and geographical survey of the Old World Cruciferae. In *The biology and chemistry of the Cruciferae*. Edited by J.G. Vaughan and A.J. MacLeod. Academic Press, London, UK. pp. 1–45.
- Heywood, V.H., Brummitt, R.K., Culham, A., and Seberg, O. 2007. Flowering plant families of the world. Firefly Books Ltd., Royal Botanic Gardens, Kew, UK.
- Hohmann, N., Wolf, E.M., Lysak, M.A., and Koch, M.A. 2015. A time-calibrated road map of Brassicaceae species radiation and evolutionary history. *Plant Cell*, **27**: 2770–2784. doi:10.1105/tpc.15.00482. PMID:26410304.
- Hourston, J.E., Ignatz, M., Reith, M., Leubner-Metzger, G., and Steinbrecher, T. 2017. Biomechanical properties of wheat grains: the implications on milling. *J.R. Soc. Interface*, **14**(126): 20160828. doi:10.1098/rsif.2016.0828.
- Imbert, E. 2002. Ecological consequences and ontogeny of seed heteromorphism. *Perspect. Plant Ecol.* **5**(1): 13–36. doi:10.1078/1433-8319-00021.
- Kigel, J. 1995. Seed germination in arid and semiarid regions. In *Seed Development and Germination*. Edited by J. Kigel and G. Galili. Marcel Dekker, Inc. pp. 645–699.
- Koch, M., Al-Shehbaz, I.A., and Mummenhoff, K. 2003. Molecular systematics, evolution, and population biology in the mustard family (Brassicaceae). *Ann. Mo. Bot. Gard.* **90**(2): 151–171. doi:10.2307/3298580.
- Lenser, T., Graeber, K., Cevik, Ö.S., Adigüzel, N., Dönmez, A.A., Grosche, C., et al. 2016. Developmental control and plasticity of fruit and seed dimorphism in *Aethionema arabicum*. *Plant Physiol.* **172**(3): 1691–1707. doi:10.1104/pp.16.00838. PMID:27702842.
- Lenser, T., Tarkowská, D., Novák, O., Wilhelmsson, P., Bennett, T., Rensing, S.A., et al. 2018. When the BRANCHED network bears fruit: How carpic dominance causes fruit dimorphism in *Aethionema*. *Plant J.* **94**: 352–371. doi:10.1111/tipj.13861. PMID:29418033.
- Liljegren, S.J., Roeder, A.H.K., Kempin, S.A., Gremski, K., Østergaard, L., Guimil, S., et al. 2004. Control of fruit patterning in *Arabidopsis* by INDEHISCENT. *Cell*, **116**(6): 843–853. doi:10.1016/S0092-8674(04)00217-X. PMID:15035986.
- Linkies, A., Graeber, K., Knight, C., and Leubner-Metzger, G. 2010. The evolution of seeds. *New Phytol.* **186**(4): 817–831. doi:10.1111/j.1469-8137.2010.03249.x. PMID:20406407.

- Liu, H.F., Liu, T., Han, Z.Q., Luo, N., Liu, Z.C., and Hao, X.R. 2018. Germination heterochrony in annual plants of *Salsola* L.: an effective survival strategy in changing environments. *Sci. Rep.* **8**: 6576. doi:10.1038/s41598-018-23319-0. PMID:29700346.
- Mandáková, T., Hloušková, P., German, D.A., and Lysak, M.A. 2017. Monophyletic origin and evolution of the largest crucifer genomes. *Plant Physiol.* **174**: 2062–2071. doi:10.1104/pp.17.00457. PMID:28667048.
- Marone, F., and Stampanoni, M. 2012. Regridding reconstruction algorithm for real-time tomographic imaging. *J. Synchrotron Radiat.* **19**(6): 1029–1037. doi:10.1107/S0909049512032864. PMID:23093766.
- Mohammadin, S., Peterse, K., van de Kerke, S.J., Chatrou, L.W., Dönmez, A.A., Mummenhoff, K., et al. 2017. Anatolian origins and diversification of *Aethionema*, the sister lineage of the core Brassicaceae. *Am. J. Bot.* **104**(7): 1042–1054. doi:10.3732/ajb.1700091. PMID:28743759.
- Mohammadin, S., Wang, W., Liu, T., Moazzeni, H., Ertugrul, K., Uysal, T., et al. 2018. Genome-wide nucleotide diversity and associations with geography, ploidy level and glucosinolate profiles in *Aethionema arabicum* (Brassicaceae). *Plant Syst. Evol.* **304**(5): 619–630. doi:10.1007/s00606-018-1494-3.
- Mouliá, B. 2013. Plant biomechanics and mechanobiology are convergent paths to flourishing interdisciplinary research. *J. Exp. Bot.* **64**(15): 4617–4633. doi:10.1093/jxb/ert320. PMID:24193603.
- Mühlhausen, A., Lenser, T., Mummenhoff, K., and Theißen, G. 2013. Evidence that an evolutionary transition from dehiscent to indehiscent fruit in *Lepidium* (Brassicaceae) was caused by a change in the control of valve margin identity genes. *Plant J.* **73**(5): 824–835. doi:10.1111/tpj.12079. PMID:23173897.
- Mummenhoff, K., Polster, A., Mühlhausen, A., and Theißen, G. 2008. *Lepidium* as a model system for studying the evolution of fruit development in Brassicaceae. *J. Exp. Bot.* **60**(5): 1503–1513. doi:10.1093/jxb/ern304. PMID:19052256.
- Nikolov, L.A., and Tsiantis, M. 2017. Using mustard genomes to explore the genetic basis of evolutionary change. *Curr. Opin. Plant Biol.* **36**: 119–128. doi:10.1016/j.pbi.2017.02.005. PMID:28285128.
- Pufal, G., Ryan, K.G., and Garnock-Jones, P. 2010. Hygrochastic capsule dehiscence in New Zealand alpine *Veronica* (Plantaginaceae). *Am. J. Bot.* **97**(9): 1413–1423. doi:10.3732/ajb.1000066. PMID:21616895.
- Rajani, S., and Sundaresan, V. 2001. The *Arabidopsis* mycBHLH gene *ALCATRAZ* enables cell separation in fruit dehiscence. *Curr. Biol.* **11**(24): 1914–1922. doi:10.1016/S0960-9822(01)00593-0. PMID:11747817.
- Read, J., and Stokes, A. 2006. Plant biomechanics in an ecological context. *Am. J. Bot.* **93**(10): 1546–1565. doi:10.3732/ajb.93.10.1546. PMID:21642101.
- Schindelin, J., Arganda-Carreras, I., Frise, E., Kaynig, V., Longair, M., Pietzsch, T., et al. 2012. Fiji: an open-source platform for biological-image analysis. *Nat. Methods*, **9**: 676–682. doi:10.1038/nmeth.2019. PMID:22743772.
- Smith, S.Y., Collinson, M.E., Rudall, P.J., Simpson, D.A., Marone, F., and Stampanoni, M. 2009. Virtual taphonomy using synchrotron tomographic microscopy reveals cryptic features and internal structure of modern and fossil plants. *Proc. Natl. Acad. Sci. U.S.A.* **106**(29): 12013–12018. doi:10.1073/pnas.0901468106. PMID:19574457.
- Spence, J., Vercher, Y., Gates, P., and Harris, N. 1996. ‘Pod shatter’ in *Arabidopsis thaliana*, *Brassica napus*, and *B. juncea*. *J. Microsc.* **181**(2): 195–203. doi:10.1046/j.1365-2818.1996.111391.x.
- Sperber, K., Steinbrecher, T., Graeber, K., Scherer, G., Clausing, S., Wiegand, N., et al. 2017. Fruit fracture biomechanics and the release of *Lepidium didymum* pericarp-imposed mechanical dormancy by fungi. *Nat. Commun.* **8**: 1868. doi:10.1038/s41467-017-02051-9. PMID:29192192.
- Spjut, R.W. 1994. A systematic treatment of fruit types. *Mem. N.Y. Bot. Gard.* **70**: 1–182.
- Stampanoni, M., Groso, A., Isenegger, A., Mikuljan, G., Chen, Q., Bertrand, A., et al. 2006. Trends in synchrotron-based tomographic imaging: the SLS experience. *In* *Developments in X-ray Tomography*, V. International Society for Optics and Photonics. pp. U199–U212.
- Steinbrecher, T., and Leubner-Metzger, G. 2017. The biomechanics of seed germination. *J. Exp. Bot.* **68**(4): 765–783. doi:10.1093/jxb/erw428. PMID:27927995.
- Venable, D.L. 1985. The evolutionary ecology of seed heteromorphism. *Am. Nat.* **126**(5): 577–595. doi:10.1086/284440.
- Wilhelmsson, P., Chandler, J., Fernandez-Pozo, N., Graeber, K., Ullrich, K., Arshad, W., et al. 2019. Usability of reference-free transcriptome assemblies for detection of differential expression: a case study on *Aethionema arabicum* dimorphic seeds. *BMC Genomics*, **20**: 95. doi:10.1186/s12864-019-5452-4. PMID:30700268.
- Willis, C., Hall, J., Rubio de Casas, R., Wang, T., and Donohue, K. 2014. Diversification and the evolution of dispersal ability in the tribe Brassicaceae (Brassicaceae). *Ann. Bot.* **114**(8): 1675–1686. doi:10.1093/aob/mcu196. PMID:25342656.

5. Molecular regulation of dimorphic seed coat development

5.1 Manuscript in advanced stages for intended submission to *Plant Cell*

Chapter 5 explores the molecular mechanisms underpinning dimorphic seed coat development. A comparative tomographic imaging and transcriptomic approach was used to address questions of morph-specific developmental differences during seed coat differentiation and mucilage production in *Ae. arabicum*.

The transition from an unfertilised ovule to a readily-dispersed seed propagule represents a highly vulnerable but key developmental process which, coupled with the differentiation of ovule integuments into the mature seed coat, impacts on the facilitation of dispersal, dormancy control, and regulation of germination. In this manuscript, the underpinning mechanisms governing development into distinct morphs are explored. Time-course characterisations reveal a co-ordinated framework of morph-specific changes in internal anatomy of developing gynoecia, which correlate with altered regulatory patterns of genes involved in the differentiation of epidermal cells, and pectin and/or cellulose biosynthesis. Establishing the framework for mucilage-producing seed coat development within a dimorphic species contributes to establishing *Ae. arabicum* as an excellent system with which to explore differential patterns of cell differentiation, biosynthesis and secretion of mucilage polysaccharides.

5.2 Author contributions

Experiments were performed in collaboration with SeedAdapt partner institutions. Synchrotron-based Radiation X-ray Tomographic Microscopy (SRXTM) of reproductive development was performed by W Arshad, T Steinbrecher, and F Marone who provided technical expertise at the Paul Scherrer Institut, Villigen, Switzerland. As described in Section 4.2, the proposal (Appendix 9.3) for beamtime was prepared by W Arshad. Samples for RNA-seq analysis were prepared by T Lenser, and sequence libraries processed by P Wilhelmsson and SA Rensing using an established bioinformatics pipeline (Wilhelmsson *et al.*, 2019).

All data (including RNA-seq) were analysed by W Arshad, with assistance from J Chandler for GO term and promoter motif analyses and ME Perez for optimisation of quantitative RT-PCR. The concepts and narrative of the manuscript were conceived by W Arshad. Project supervision was provided by ME Collinson (Royal Holloway University of London, UK), W Stuppy (Botanischer Garten der Ruhr-Universität Bochum, Germany), G Theißen (Friedrich Schiller University, Jena, Germany), and G Leubner (Royal Holloway University of London, UK).

W Arshad was the lead author of this manuscript, prepared all figures, conducted all analyses, and wrote the majority of the text. The manuscript, as presented here, is in advanced stages for submission to *Plant Cell* as a Regular Research Article. This submission is intended for the end of 2020.

1 **A tale of two morphs: developmental patterns and mechanisms of bet-hedging**
2 **diaspores in the dimorphic model *Aethionema arabicum* (Brassicaceae)** ^[CC-BY]

3

4 **Waheed Arshad¹, Teresa Lenser², Per KI Wilhelmsson³, Jake O Chandler¹, Tina**
5 **Steinbrecher¹, Federica Marone⁴, Marta Pérez Suarez¹, Margaret E Collinson⁵,**
6 **Wolfgang Stuppy⁶, Stefan A Rensing³, Günter Theißen², Gerhard Leubner-**
7 **Metzger^{†1,7}**

8

9 **Author affiliations**

10 ¹ School of Biological Sciences, Royal Holloway University of London, Egham,
11 Surrey, TW20 0EX, United Kingdom; Web: “The Seed Biology Place” –
12 www.seedbiology.eu

13

14 ² Department of Genetics, Friedrich Schiller University, 07743 Jena, Germany

15

16 ³ Plant Cell Biology, Faculty of Biology, University of Marburg, 35043 Marburg,
17 Germany

18

19 ⁴ Swiss Light Source, Paul Scherrer Institute, CH-5232 Villigen, Switzerland

20

21 ⁵ Department of Earth Sciences, Royal Holloway University of London, Egham,
22 Surrey TW20 0EX, United Kingdom

23

24 ⁶ Botanischer Garten der Ruhr-Universität Bochum, Universitätsstraße 150, D-44780,
25 Bochum, Germany

26

27 ⁷ Laboratory of Growth Regulators, Centre of the Region Haná for Biotechnological
28 and Agricultural Research, Palacký University and Institute of Experimental Botany,
29 Academy of Sciences of the Czech Republic, 78371 Olomouc, Czech Republic

30

31 ^[CC-BY] Article free via Creative Commons CC-BY 4.0 licence.

32

33 [†] **Corresponding author email:** gerhard.leubner@rhul.ac.uk

34 **Funding information**

35 This work originated from the ERA-CAPS “SeedAdapt” consortium project
36 (www.seedadapt.eu) and was supported by a Natural Environment Research Council
37 (NERC) Doctoral Training Grant to W.A. (grant no. NE/L002485/1), by the Deutsche
38 Forschungsgemeinschaft (DFG) to G.T. (TH 417/10-1) and S.A.R. (RE 1697/8-1), and
39 by the Biotechnology and Biological Sciences Research Council (BBSRC) to T.S. and
40 G.L.-M. (grant nos. BB/M00192X/1 and BB/M000583/1).

41

42 **List of author contributions**

43 WA, TL, GT and GL-M planned and designed the research; WA, TL, TS and FM
44 performed experiments; WA, TL, PKIW, JOC, TS, MEC, WS, FM, MPS, GT, SR and
45 GL-M analysed and interpreted data; WA wrote the manuscript.

46

47 **ORCID**s

48 Waheed Arshad: 0000-0002-9413-2279

49 Teresa Lenser: n/a

50 Per KI Wilhelmsson: 0000-0002-8578-3387

51 Jake O Chandler: 0000-0003-0955-9241

52 Tina Steinbrecher: 0000-0003-3282-6029

53 Federica Marone: 0000-0002-3467-8763

54 Marta Pérez Suarez: 0000-0002-6802-205X

55 Margaret E Collinson: n/a

56 Wolfgang Stuppy: n/a

57 Günter Theißen: 0000-0003-4854-8692

58 Stefan A Rensing: 0000-0002-0225-873X

59 Gerhard Leubner-Metzger: 0000-0002-6045-8713

60

61 **Acknowledgements**

62 We thank Patricia Goggin and the Imaging and Microscopy Centre (University of
63 Southampton) for assistance with SEM and SRXTM sample preparation, and Sharon
64 Gibbons (Earth Sciences, Royal Holloway University of London) for assistance with
65 SEM. We also acknowledge the Paul Scherrer Institut, Villigen, Switzerland for
66 provision of synchrotron radiation beamtime (Proposal ID: 20180809) at the

67 TOMCAT beamline of the Swiss Light Source. We thank all members of the
68 “SeedAdapt” consortium project (www.seedadapt.eu) for fruitful discussions.

69

70 **Abstract**

71 The developmental transition from an unfertilised ovule to a dispersed seed propagule
72 represents a highly vulnerable but key process which, coupled with the differentiation
73 of ovule integuments into the mature seed coat, impacts on the facilitation of dispersal,
74 dormancy control, and regulation of germination. We explore the underpinning
75 mechanisms governing fruit and seed (diaspore) development in
76 *Aethionema arabicum*, a member of the earliest diverging lineage of the Brassicaceae
77 family. One of its intriguing adaptations is the production and dispersal of
78 morphologically distinct, mucilaginous and non-mucilaginous seeds on the same plant
79 (heteromorphism). Here, we combine novel tomographic imaging with developmental
80 transcriptomics to understand the process of seed coat mucilage production and its
81 regulation within a dimorphic system. Synchrotron-based radiation X-ray tomographic
82 microscopy revealed a co-ordinated framework of morph-specific changes in internal
83 anatomy of developing gynoecia, which correlated with altered regulatory patterns of
84 genes involved in the differentiation of epidermal cells, and pectin and/or cellulose
85 biosynthesis. Elucidating the molecular framework for mucilage-producing seed coat
86 development furthers use of *Ae. arabicum* as a valuable dimorphic model system to
87 understand bet-hedging strategies in semi-arid environments, timely in the face of
88 global climatic change.

89

90 **Key words**

91 *Aethionema arabicum*, bet-hedging, developmental anatomy, diaspore dimorphism,
92 mucilage synthesis, reproductive development, seed coat mucilage, synchrotron
93 radiation X-ray tomographic microscopy

94

95 **Introduction.**

96

97 Fruit and seed development represents a crucial reproductive phase for angiosperms;
98 the transition from an unfertilised ovule to a dispersed seed propagule is a highly
99 vulnerable but key developmental process leading to successful maturation, dispersal,
100 and eventual seedling establishment of a plant species (Gutterman, 2000; Finch-
101 Savage & Leubner-Metzger, 2006). Angiosperm dispersal units – here: fruits and seeds
102 (diaspores) – thus support the distribution and early life history of the progeny, and
103 are particularly important for annual plant species whose life-cycle is entirely
104 dependent on successful production of, and regeneration from, the seed (Linkies *et al.*,
105 2010).

106

107 Coupled with the maturation of the angiosperm fruit is the development of the seed,
108 the embryo of which is protected by the seed coat during embryogenesis. Double
109 fertilisation not only commences embryogenesis and nutritive endosperm
110 development, but also the differentiation of ovule integuments into the mature seed
111 coat. Some of the most dramatic cellular changes occur within these specialised
112 maternal cells, and have impacts on the facilitation of dispersal, dormancy control, and
113 regulation of germination (Koorneef *et al.*, 2002; Haughn & Chaudhury, 2005; Finch-
114 Savage & Leubner-Metzger, 2006; Arshad *et al.*, 2019). Large amounts of mucilage
115 accumulation around the seed, a phenomenon called “myxospermy”, is especially
116 common in species-rich and geographically widely distributed rosid and asterid
117 families (Grubert, 1974; Yang *et al.*, 2012). Mucilage may exhibit various inter- and
118 intra-specific morphologies (Western, 2012; Voiniciuc *et al.*, 2016; Golz *et al.*, 2018).
119 The composition of mucilage varies between species, but a polysaccharidic cell wall-
120 like structure with large amounts of rhamnogalacturonan I (RGI) pectin domains and
121 smaller amounts of homogalacturonan (HG) pectin domains, cellulose, and
122 hemicelluloses are typical (Haughn & Chaudhury, 2005; Haughn & Western, 2012;
123 Voiniciuc *et al.*, 2015). The main ecological adaptation of mucilaginous seed coats
124 may be in facilitating imbibition and maintenance of moisture for growth in water-
125 deficient environments (Huang *et al.*, 2000). Mucilage may also reduce germination
126 rates by impeding the diffusion of oxygen (Witztum *et al.*, 1969), as well as aid or
127 restrict fruit and seed dispersal (Lobova *et al.*, 2003; Arshad *et al.*, 2019).

128 Diaspore development in many plant model systems is monomorphic – *i.e.* only a
129 single type of fruit and/or seed is produced in individuals and populations. While
130 diaspores from populations, individual plants, or individual inflorescences can vary
131 continuously, they may also exhibit heteromorphism, whereby two or more distinctly
132 different types of diaspores are produced (Harper, 1977; Mandák, 1997; Imbert, 2002).
133 Several heteromorphic systems are well described in the literature, particularly with
134 respect to a given morphological or physiological trait (Baskin & Baskin, 2014).
135 However, little is known about the underpinning mechanisms governing diaspore
136 development into distinct morphs. Understanding how new morphologies, organs, or
137 body plans arise is one of the most fascinating questions in evolutionary
138 developmental (evo-devo) plant biology. Within the Brassicaceae, which includes the
139 models *Arabidopsis*, *Brassica*, *Lepidium* and *Boechera* (Couvreur *et al.*, 2009;
140 Franzke *et al.*, 2011), the typical monomorphic dehiscent fruit containing
141 mucilaginous seeds is representative of the default “bauplan” from more than three
142 thousand species of the family (Mühlhausen *et al.*, 2013). In a few genera, however,
143 heteromorphic fruits evolved as an adaptive bet-hedging strategy to deal with the
144 spatio-temporal variability in favourable conditions (Gutterman, 2002; Lu *et al.*, 2010;
145 Ward, 2016).

146

147 Here, we exploit the dimorphism in *Aethionema arabicum*, an annual member of the
148 earliest diverging sister tribe (Aethionemeae) within the Brassicaceae (Franzke *et al.*,
149 2011; Hohmann *et al.*, 2015; Mohammadin *et al.*, 2017). Two morphs of fruits and
150 seeds are produced on the same individual infructescence (Fig. 1a). Dehiscent (DEH)
151 fruits develop 4–6 non-deep dormant, mucilaginous (M^+) seeds. The surface of the dry
152 M^+ seed coat is visible as an array of compressed, large circular-hexagonal cell outlines
153 with thickened cell walls, representing mucilage-producing, conical papillae (Fig. 1b)
154 irreversibly extruded upon seed imbibition (Lenser *et al.*, 2016). In contrast,
155 indehiscent (IND) fruits each contain a single, pericarp-imposed deep dormant non-
156 mucilaginous (M^-) seed (Fig. 1b). Moreover, the two *Ae. arabicum* morphs differ in a
157 number of developmental, morpho-physiological, and dispersal-related traits (Lenser
158 *et al.*, 2016; Bhattacharya *et al.*, 2018; Lenser *et al.*, 2018; Arshad *et al.*, 2019). While
159 the multiple-seeded DEH fruits are predominantly produced on main flowering
160 branches, single-seeded IND fruits in contrast are favoured on higher-order side

161 branches (Lenser *et al.*, 2018). No intermediate morphs are produced. A genome
162 sequence is available (Haudry *et al.*, 2013), making *Ae. arabicum* a valuable model
163 system for diaspora dimorphism (Mohammadin *et al.*, 2018; Wilhelmsson *et al.*,
164 2019).

165

166 The adaptive significance of *Ae. arabicum* seed coat mucilage is hypothesised (Arshad
167 *et al.*, 2019; Arshad *et al.*, 2020), but the molecular framework underpinning
168 development of its dimorphic seed and seed coat characteristics remains unknown.
169 Studies of *Arabidopsis thaliana* (hereafter *Arabidopsis*) seed coat mucilage indicate
170 there is a complex transcriptional network regulating development of the outer ovule
171 integument and differentiation of mucilage secretory cells (North *et al.*, 2014; Francoz
172 *et al.*, 2015). Among the well-described transcription factors (TFs) involved are
173 pleiotropic WD40-repeat proteins, MYB, and basic helix-loop-helix (bHLH) TFs,
174 playing a key role in normal epidermal cell differentiation, mucilage production, and
175 release. The multimeric WD40–bHLH–MYB complex consisting of ENHANCER OF
176 GLABRA3 (EGL3), MYB5, TRANSPARENT TESTA2 and 8 (TT2 and TT8), and
177 TRANSPARENT TESTA GLABRA1 (TTG1) has been shown, together with
178 APETALA2 (AP2), to modulate the expression of two transcriptional sub-pathways
179 through GLABRA2 (GL2) and TTG2 (Western *et al.*, 2004; Gonzalez *et al.*, 2009). In
180 addition, *MYB61* also functions in a distinct genetic pathway to promote the
181 accumulation of linear rhamnogalacturonans in the seed coat during early seed
182 development (Penfield *et al.*, 2001). How this delicate network including its
183 downstream targets may be regulated within a dimorphic system is not known. In
184 particular, the biodiversity of seed development, and its impacts on early-life history
185 transitioning with respect to environmental adaptation, are currently poorly understood
186 and require extension to more diverse species beyond the monomorphic *Arabidopsis*.

187

188 In this study, comparative tomographic imaging and transcriptomic approaches are
189 used to address questions of morph-specific developmental differences during seed
190 coat differentiation and mucilage production in *Ae. arabicum*. The DEH fruit and
191 multiple M⁺ seed diaspora syndrome is considered the typical trait combination,
192 similar to *Arabidopsis*, while the alternative diaspora type (IND fruit and M⁻ seed)
193 confers an additional program. We propose the unique seed coat dimorphism as an

194 excellent model system for study of the regulation of epidermal cell differentiation and
195 mucilage biosynthesis. Elucidating the underlying molecular framework of the
196 dimorphic diaspore syndrome is key to understanding differential regulation of bet-
197 hedging survival strategies in challenging environments, timely in the face of global
198 climatic change.

199

200 **Results**

201

202 *Gynoecial, but not floral, development in Aethionema arabicum exhibits clear*
203 *dimorphism*

204 To establish key developmental events during the transition from bud to fruit, a
205 sequential account of the structural formation of reproductive organs was detailed in
206 reference to homologous events in *Arabidopsis* (Smyth *et al.*, 1990; Roeder &
207 Yanofsky, 2006). In *Ae. arabicum*, wild-type fruit development follows a comparable
208 pattern at initial stages from primordial bud formation to floral morphogenesis (Fig.
209 1c). To the point of anthesis, morphologies of flowers that would later produce DEH
210 and IND fruits appeared phenotypically identical. Analysis of pollen showed grains do
211 not differ between morphs (Fig. S1), and aniline blue-stained pollen tubes show no
212 difference between morphs (Lenser *et al.*, 2018). While petals and sepals readily
213 abscised from the IND morph at 3–4 DAP, perianth withering in the DEH morph did
214 not occur until 6 DAP, despite initiation of lateral fruit elongation. Thus, floral
215 development until early stages of gynoecial expansion appears phenotypically
216 monomorphic. Beyond this, fruits became clearly dimorphic in their development
217 when pericarp tissue began expansion; similarly, there was no deviation in the
218 commitment to development of a specific morph (Fig. 1c). Comparison of fruit
219 maturation patterns, showed that onset of DEH silicle yellowing (37 DAP) was
220 approximately 7 days earlier than in the IND fruit morph (43 DAP). Thus, fruit
221 maturation into a dispersal-ready propagule seemingly occurred at a faster rate for the
222 IND morph. This time-course allowed the identification of key events (Fig. 1c) prior
223 to, and soon after, phenotypic morph separation.

224

225 *Synchrotron Radiation X-ray Tomographic Microscopy reveals a co-ordinated time-*
226 *course of morph-specific changes in internal anatomy*

227 To explore the internal anatomy underlying the morph-specific phenotypic changes,
228 we performed non-destructive synchrotron-based X-ray tomographic microscopy
229 (SRXTM) during the time-course of reproductive development. Reconstructed digital
230 sections obtained by SRXTM at 0, 1, 7 and 40 DAP provided excellent cell and tissue
231 details (Fig. 2). Floral buds (0 DAP) exhibited a morphologically-distinct gynoecium
232 (two congenitally fused carpels), and immature stamens (four medial and two short).
233 Four anatropous ovules (Fig. 2b, c) were visible in buds from both morphs. Ovules at
234 anthesis (Fig. 2f, g) in both DEH (Fig. 2f) and IND (Fig. 2g) morphs exhibit
235 differentiated internal structures of an identical nature. External morphologies of the
236 bud (Fig. 2a, d) and flower (Fig. 2e, h) were also consistently monomorphic. Within
237 immature fruits (~7 DAP), DEH fruits possessed four to six fertilised ovules, while
238 IND fruits possessed only one.

239

240 Seed integuments showed considerable morph-specific differences at ~7 DAP, namely
241 in the development and secretion of mucilage between the outer primary wall and the
242 protoplast (in a ring around the area where starch granules are located within the cell)
243 (Fig. 2j, k). This secretion resulted in a ring-shaped mucilage pocket (Fig. 2k). The
244 developing M^- seed coat comprised a more distinct, inner epidermal layer as well as
245 multiple outer cell layers undergoing differentiation within the outer integument (Fig.
246 2l). At ~40 DAP, the outermost epidermal layer formed large mucilage secretory cells
247 in the case of mucilaginous seeds (M^+) from the DEH fruit morph (Fig. 2q), but a thin
248 outer epidermal layer lacking mucilage secretory cells in the single (M^-) seed (Fig. 2r)
249 of the IND fruit. Only several collapsed cell layers and an inner integument remaining
250 of relatively thick-walled cells (Fig. 2r) remained in the developed M^- seed coat.

251

252 Also evident were significant changes associated with the gynoecium and internal fruit
253 anatomy. Flowers developing into an IND fruit possessed four ovules at anthesis and,
254 consistent with Lenser *et al.* (2018), we observed that three of those had been aborted
255 post-fertilisation. The endocarp layers were in continuity with the cells of the replum
256 in the IND morph, while in the mature DEH fruit, a dehiscence zone separated lignified
257 cells of the replum from those of the endocarp layer on the inside of the fruit valves
258 (Arshad *et al.*, 2020). A replum was not observed in IND fruits which, in addition,
259 lacked a septum between the two parietal placentae. Thus, the tomography revealed

260 clear similarities in ovule and outer epidermal cell morphology during the early
261 developmental transition from bud to flower, but revealed major differences arising at
262 7 DAP and becoming very obvious at 40 DAP.

263

264 *Dimorphic changes to the ovule wall occur rapidly after fertilisation*

265 A temporal histological analysis of isolated gynoecia post-fertilisation indicated the
266 more exact timing of changes to the wall of the ovules within developing fruits. The
267 asymmetric growth of a single seed within IND fruits pushed the septum towards the
268 side of the opposing seed chamber at 2–3 DAP, seemingly resulting in the rupture of
269 the septum and “fusion” of the two locules (Fig. S2f). Unlike *Arabidopsis* (the mature
270 ovule of which is amphitropous), the mature ovule in *Ae. arabicum* appeared
271 anatropous; the micropyle is bent towards the funicle to which the body of the ovule
272 is united. The inner integument consisted of multiple layers of parenchymatous cells
273 during early seed development (Fig. S2a–f), but later appeared as one or two layers of
274 crushed palisade cells (Fig. S2g–j). By 5 DAP, outer integuments had started
275 differentiation into mucilage secretory cells in M⁺ seeds only. Thus, the observed
276 morphological changes associated with the transition of the integuments into the
277 mature seed coat indicate that, at the same time as external differences between morphs
278 become visible at 2–3 DAP, the developmental program guiding seed coat mucilage
279 development also becomes morph-specific. In addition to the changes in fruit anatomy
280 (Fig. S3), this implies several regulatory processes are acting at the onset of
281 fertilisation to drive seed and fruit dimorphism.

282

283 *Comparative RNA-Sequencing analyses reveal transcriptomic differences associated*
284 *with cell- and morphogenesis-related processes during early morph-transitioning*

285 The lack of morph-specific external differences at the bud and flower stage makes
286 comparative analysis of morph differentiation difficult; however, flowers harvested
287 from undisturbed 2nd-order branches produce more than 95% IND fruits, and flowers
288 harvested from the main branch of plants, where all side branches are constantly
289 removed, produce more than 95% DEH fruits (Lenser *et al.*, 2016; Lenser *et al.*, 2018).
290 This local separation of fruit morphs allowed direct morph-specific comparisons
291 during reproductive development. Replicate RNA-Seq samples clustered tightly by
292 organ (Fig. 3a) and by morph (Fig. 3b), as observed in a principal component (PC)

293 analysis on the 500 genes with highest variance. The majority of the variability in the
294 data was explained by PC1 (67.18%), while PC2 and PC3 explained 22.62% and
295 4.82% respectively. An unsupervised hierarchical clustering approach based on
296 Euclidean distance measures, revealed the high similarity of bud samples from DEH
297 and IND morphs (Fig. 3d). However, while flower samples also clustered by morph,
298 these samples were more similar in their transcriptional profile to bud samples than to
299 fruit samples (Fig. 3d). These results suggest that the developmental trajectory of
300 *Ae. arabicum* morphs is strongly evident from their transcriptional profile at the post-
301 fertilisation flower stage, but not at the bud stage of development.

302

303 Morph-specific differential expression analysis detected significant differences at the
304 three harvested stages (Fig. 4). A total of 16,243 genes were found to be differentially
305 expressed in IND vs. DEH samples (8,012 up-regulated and 8,231 down-regulated).
306 After filtering genes showing a $|\log_2(\text{fold change})| > 2$ and adjusted P value < 0.05 ,
307 the highest number of morph-specific differentially expressed genes (DEGs) were
308 found at the flower stage (862 up-regulated and 599 down-regulated; Fig. 4b). Among
309 these, were 16 DEGs (0.7%) shared between bud and flower samples (Fig. 4c). Similar
310 to the GO term enrichment, WRKY- and HOMEODOMAIN-RELATED PROMOTER MOTIF
311 were significantly enriched in the promoters of DEGs up in IND samples in comparison to
312 DEH (data not shown). Consistent with Lenser *et al.* (2018), we detected the *Ae.*
313 *arabicum* orthologue encoding the HOMEODOMAIN-RELATED PROMOTER MOTIF 21
314 (AA33G00123), whose transcription is positively regulated by the TEOSINTE
315 BRANCHED1, CYCLOIDEA, PCF (TCP) transcription factor BRANCHED1
316 (BRC1). We also detected the orthologue LATE EMBRYOGENESIS ABUNDANT
317 (LEA) 4-1, which, along with other LEA proteins, typically accumulate in response to
318 low water availability imposed during development.

319

320 Analysis of gene ontology (GO) terms associated with up- and down-regulated
321 transcripts during development, showed significantly over- and under-represented
322 GO-terms of each class [Biological Process (BP), Molecular Function (MF) and
323 Cellular Component (CC)]. Morph-specific GO comparisons at the flower stage using
324 Fisher's exact test (fdr corrected P value of 0.05), revealed that pollination-, cell wall
325 growth-, and cell differentiation-related BPs showed highest significance in the BP

326 GO-bias list of IND samples, while glucosinolate-, secondary metabolite-, and
327 phytohormone-related biosynthetic processes were significant BPs in BP GO-bias list
328 of DEH samples. Among the 26 shared BPs, some of the most significant terms belong
329 to high-level categories such as “developmental growth” (GO:0048589), “cell wall
330 organization or biogenesis” (GO:0071554), and “cell wall modification”
331 (GO:0042545) (comprehensive lists of BP terms associated with the DEG sets are
332 provided in Supplementary Table 1). We therefore focussed downstream analyses on
333 the molecular mechanisms which give rise to the unique cellular layers surrounding
334 developing and mature dimorphic seeds.

335

336 *Transcriptional profiles indicate altered regulatory patterns during differentiation of*
337 *outer seed coat integuments*

338 Since both the SRXTM and histological approaches confirmed key differences in
339 patterns of mucilage synthesis, we hypothesised that the transcriptional network
340 underpinning seed coat development in the M⁻ seed may be altered with respect to
341 genes involved in (i) the differentiation of integuments and epidermises, and (ii) pectin
342 and/or cellulose biosynthesis. A developmental scheme was created (Fig. S4) based
343 on a literature search for orthologous genes and/or proteins necessary for “normal”
344 mucilage development, synthesis, modification, and release (summarised in Fig. 5).
345 RNA-Seq data from 0 and 1 DAP show altered expression patterns for key
346 developmental events in seed coat formation. Among these genes was *AP2*, required
347 for the expression of the WRKY TF *TTG2* and the homeobox TF *GL2*, both of which
348 act in the early stages of integument and epidermal cell differentiation. *TTG2* and *GL2*
349 expression requires the WD40–bHLH–MYB transcription complex (formed from
350 *EGL3*, *MYB5*, *TT2*, *TT8* and *TTG1*), expression of which did not exhibit a morph-
351 specific difference from RNA-Seq data (Fig. 5). This implies that, while the
352 monomorphic formation of ovules from both morphs may be regulated by this
353 multimeric TF complex, seed coat differences are manifested downstream.

354

355 Consistent with our hypothesis, the expression patterns of genes encoding enzymes
356 specifically associated with the synthesis of pectic polysaccharides, namely in
357 repeating the disaccharides rhamnose and galacturonic acid to form RGI, showed a
358 decrease in samples developing M⁻ seeds in comparison to M⁺ (Fig. 5). Among these

359 DEGs, was the orthologue of MUM4/RHM2 rhamnose synthase, showing a 1.5-fold
360 increase in M⁺ vs M⁻. Interestingly, *Arabidopsis mum4-rhm2* mutants show reduced
361 accumulation of mucilage polysaccharides (Usadel *et al.*, 2004; Western *et al.*, 2004).
362 Also downregulated in M⁻ vs. M⁺ was the orthologue of galacturonosyltransferase
363 (GAUT) family glycosyltransferase GATL5, required to add UDP-L-Rha or UDP-D-
364 GalA to an oligo- or polysaccharide acceptor (North *et al.*, 2014). Genes encoding
365 enzymes involved in cellulose and secondary cell wall synthesis also show a morph-
366 specific response. Development of conical papillae, as observed specifically in the M⁺
367 seed coat, requires cellulose synthase (CESA) subunits for secondary cell wall
368 development (Mendu *et al.*, 2011a; Mendu *et al.*, 2011b). Both CESA2,
369 MUM3/CESA5 and RADIAL SWELLING 3 (RSW3), whose mutants in *Arabidopsis*
370 show little secreted mucilage after imbibition (Burn *et al.*, 2002), had increasing trends
371 in M⁺ samples. DEGs involved in both mucilage and papillae production, therefore
372 suggest key regulatory events guide morph-specific changes observed during M⁺ and
373 M⁻ seed development.

374

375 *Elevated GL2 and MYB61 transcript abundances, together with CESA subunits,*
376 *correlate with mucilaginous seed morph development*

377 To independently validate the expression of morph-specific genes during
378 development, a higher-resolution time course was sampled from plants grown
379 completely undisturbed. qRT-PCR data obtained at 0, 1, 3, and 10 DAP (Fig. 6)
380 confirmed that transcript abundance of the orthologue *GL2* was indeed significantly
381 higher in M⁺ (DEH fruit) samples, while a similar time-dependent trend was observed
382 with *MYB61*. Abundance of TTG1, part of the multimeric WD40-bHLH-MYB
383 complex, and MUM4/RHM2, a downstream target of *GL2*, did not show dramatic
384 increases. Interestingly, transcript abundance of the *Ae. arabicum* orthologue of
385 PME16, whose mutants in *Arabidopsis* show a delay in mucilage release and an
386 unbroken outer primary cell wall (Saez-Aguayo *et al.*, 2013), shows a tendency
387 towards increasing in M⁺ samples in comparison to M⁻. We also observed a strong
388 time-dependent increase in expression associated with genes involved in cellulose
389 synthesis (Fig. 6). After 10 DAP, *CESA2* and *MUM3/CESA5* orthologues showed a 4-
390 fold and 2-fold increase, respectively, in comparison to developing M⁻ seeds (IND
391 samples). Taken together, these data suggest that numerous key regulatory elements

392 are driving the reduced M⁻ seed coat biosynthesis of pectin and cellulosic columellae
393 in comparison to M⁺ seeds.

394

395 *Post-fertilisation ovule abortion within IND fruits may involve genes associated with*
396 *defective embryogenesis*

397 Given the systematic abortion of seeds during IND fruit development (Fig. S2, S3),
398 we examined RNA-Seq data for candidate DEGs that may be involved with this co-
399 ordinated process preceding single M⁻ seed development. Forward genetic screens in
400 *Arabidopsis* identified genes involved in female gametogenesis and early embryo
401 development, highlighting several maternal effect embryo arrest (MEE) mutants
402 associated with defects in embryo sac development (Pagnussat *et al.*, 2005). Of the
403 nine identified orthologues of *Arabidopsis* MEEs (Fig. 7a), only expression levels of
404 the *Ae. arabicum* orthologues of DEGs *MEE14* and *MEE59* showed an increase
405 specifically within IND flower samples. The *ca.* 9-fold and 1.5-fold increase,
406 respectively, detected from normalised RNA-Seq data was further investigated by
407 qRT-PCR using independently-grown samples at higher temporal resolution (Fig. 7b).
408 Interestingly, a time-dependent increase in expression was consistent for IND samples
409 (developing a single seed) in comparison to DEH samples (developing multiple seeds).
410 Though IND transcript abundances showed considerable variation at the flower (1
411 DAP) stage, expression levels showed a dramatic morph-specific difference at 3 DAP,
412 where *MEE14* and *MEE59* expression correlates well with the timing of ovule abortion
413 as observed by histology (Fig. 7c, S2). As three ovules within the IND fruit are aborted
414 at an early zygotic stage around 2–3 days post-fertilisation, it is speculated that MEE
415 proteins may play a role in this highly morph-specific co-ordinated process.

416

417 **Discussion and Conclusions**

418

419 *Sticking to bet-hedging adaptations in semi-arid conditions*

420 Ephemeral plant phenology and associated germination-regulation mechanisms
421 requires morphological and physiological adaptations, as well as phenotypic plasticity,
422 to maintain ecological success (Mulroy & Rundel, 1977). In the dimorphic
423 *Ae. arabicum* system, this is partly achieved by its unique fruit and seed characteristics
424 that give rise to diaspores optimally adapted as differential survival strategies (Arshad
425 *et al.*, 2019; Arshad *et al.*, 2020). Our comparative anatomical and molecular analyses
426 of the early reproductive development leading to seed dispersal revealed two distinct
427 regulatory processes that likely underpin seed morph development. At the seed level,
428 the controlled abortion of three fertilised ovules and comparatively reduced
429 development of mucilage and mucilage papillae contributed to its unique dimorphic
430 strategy. This is in contrast to the developmental framework acting in the
431 monomorphic *Arabidopsis* (Haughn & Western, 2012). That the *Ae. arabicum*
432 dimorphic seeds derive exclusively from distinct fruits, and that both the diaspore
433 ratios exhibit phenotypic plasticity in response to ambient temperature experienced
434 during reproduction (Lenser *et al.*, 2016), is hence an exceptional example of an
435 adaptive bet-hedging strategy. We propose here how the underpinning molecular
436 mechanisms within the M⁻ seed in IND fruits may act through a distinct developmental
437 program.

438

439 The framework for mucilage-producing seed coat development and descriptions of the
440 events leading up to seed coat maturation has been characterised in only a small
441 number of taxa (Yang *et al.*, 2012). Among the Brassicaceae species possessing
442 myxospermous seeds, *Arabidopsis* has emerged as an important model, and a body of
443 literature has focussed on characterising its seed coat development (Windsor *et al.*,
444 2000; Francoz *et al.*, 2015; Golz *et al.*, 2018). Here, we describe the morphological
445 and developmental changes that occur during differentiation of *Ae. arabicum*
446 dimorphic seed coat integuments. Analysis of delicate plant material during
447 development was greatly enhanced by the application of critical-point drying and
448 SRXTM, both of which allowed high-resolution anatomical detail in multiple planes
449 of digital section without technical issues encountered during traditional destructive

450 histological approaches (Smith *et al.*, 2009; Friis *et al.*, 2014). The present study
451 demonstrated remarkable organ- and tissue-level similarities in internal and external
452 bud and floral morphologies, while highlighting prominent differences associated with
453 seeds (and indeed fruits) at later developmental stages, readily recognised in the
454 absence of folding or tearing artefacts derived from tissue embedding, sectioning, and
455 mounting. Thus, the presented findings provide the most accurate morph-specific
456 volumetric investigations of *Ae. arabicum* to date, and shows suitability of SRXTM
457 for a variety of evo-devo questions for modern plant taxa.

458

459 Mucilaginous seed coats exist with varying morphologies. In the desert-inhabiting
460 *Blepharis persica* (Acanthaceae), the extrusion of large multicellular seed coat hairs,
461 whose primary walls are composed of cellulose microfibrils in a uronic gel, act as
462 protective measure during rain-mediated dispersal and as a lubricant for radicle
463 penetration (Witztum *et al.*, 1969). Similarly, in *Ruellia strepens* (Acanthaceae), the
464 seed coat epidermis is formed by unicellular hairs which, upon imbibition, release
465 mucilage (Schnepf & Deichgräber, 1983). The pectin- and cellulose-rich nature of *Ae.*
466 *arabicum* seed coat mucilage, evident from staining with ruthenium red and methylene
467 blue, was coupled with densely-covered thread-like projections in M⁺ seeds only. Such
468 projections were absent in the M⁻ seed, where concentrated regions of pectin around
469 the radicle may have a role in altering the cell wall chemistry, to facilitate radicle
470 lubrication and protrusion through the IND fruit during germination. Previous data
471 (Arshad *et al.*, 2019) have shown that the biophysical properties of the M⁺ seed support
472 anti-telechorous (dispersal prevention) mechanisms to anchor the dispersed M⁺ seed
473 in direct vicinity of the mother plant. In contrast, the winged IND fruit diaspore support
474 telechorous (dispersal promotion) mechanisms. As the IND pericarp itself may act as
475 a water-retaining structure facilitating germination (Lenser *et al.*, 2016), the
476 requirement for a mucilaginous seed coat may thus have been “lost” through the course
477 of evolutionary adaptation favouring telechory. In this case, the protective function is
478 constructed out of maternal tissue, rather than embryo or gametophyte tissue.

479

480 *Conservation of plant resources through targeted ovule abortion and decreased*
481 *indehiscent pericarp development*

482 A diverse set of genes is involved in gametophyte development, controlling functions
483 between fertilisation and early embryo development (Pagnussat *et al.*, 2005). A
484 number of mutants exhibiting fertilised embryo sacs, but with very early arrest of
485 embryo development, have been identified in *Arabidopsis*. Among the DEGs
486 upregulated in IND flowers in comparison to DEH flowers were orthologues of
487 *Arabidopsis* genes identified as having defects in endosperm development leading to
488 developmental arrest at the one-cell zygotic stage (Pagnussat *et al.*, 2005). Expression
489 of two MEE orthologues (*MEE14* and *MEE59*) in *Ae. arabicum* were found to
490 correlate with the timing of ovule abortion observed only in IND fruits. Interestingly,
491 mutants defective in early embryo development also showed disrupted genes encoding
492 TFs belonging to the MYB, WRKY, and TCP families (Pagnussat *et al.*, 2005). That
493 we see an increase in MYB- and WRKY-related promotor motifs in IND flowers, in
494 comparison to DEH flowers, may indicate that there are many potential signal
495 transduction components mediating this complex and morph-specific process during
496 ovule abortion and early regulation of seed coat development.

497

498 Particularly under “stressful” abiotic environmental conditions, developing pollen,
499 ovules, and/or embryos are known to be aborted in many angiosperms as a result of
500 differential regulation of plant resources for reproduction (Sun *et al.*, 2004).
501 Interestingly, during reproduction under elevated temperatures, heat stress caused
502 significant decreases in the total number of reproductive organs in *Ae. arabicum*
503 (Lenser *et al.*, 2016). Though this typically occurs through several physiological
504 processes, from impaired meiosis and pollen germination to reduced ovule viability
505 and low pollen grain retention (Hasanuzzaman *et al.*, 2013), here we propose that the
506 mucilaginous seed morph production (within DEH fruits) is preferential under
507 elevated abiotic stress conditions. When different temperatures during flowering and
508 fruit/seed development (reproduction temperatures) were compared, there were a
509 similar number of M⁺ seed diaspores of *ca.* 430 (20°C) and *ca.* 360 (25°C) per plant,
510 but the number of IND fruit diaspores decreased six-fold from *ca.* 480 (20°C) to *ca.*
511 80 (25°C) at the warmer reproduction temperature (Lenser *et al.*, 2016). This plasticity
512 at different maternal growth temperatures, implies there may be different

513 developmental cues prompting M⁺ and M⁻ seed development (and thus DEH and IND
514 fruit morphogenesis). Exactly how the incidence of ovule abortion may be linked with
515 temperature-influenced fruit and seed development, including the imposed maternal
516 effects on seed germination and dormancy, remains unknown.

517

518 An early hypothesis by Lloyd *et al.* (1980) predicted that flowers, gametophytes, and
519 embryos would vary in their advancement through the adjustment of maternal
520 resources during reproductive development; abortion of ovules (and senescence of
521 embryos) acts as a conservation of resources, thereby minimising unnecessary
522 expenditure at early developmental stages. In the IND fruit, the allocation of resources
523 is instead shifted into pericarp-related developmental processes which, in turn, permit
524 the longer-distance dispersal of the entire diaspore in comparison to locally-dispersing
525 M⁺ seeds (Arshad *et al.*, 2019). By this hypothesis, one might expect more IND fruits
526 to be produced in increased stress conditions. However, through the adjustment of
527 reproduction and resource allocation during stress, *Ae. arabicum* plants appear to
528 respond to harsh environmental conditions by increasing reproductive output to
529 produce multiple-seeded DEH fruits. Production of a greater number of seeds per fruit
530 may be considered as more of a “safe” bet-hedging strategy to maintain enough seed
531 progeny for the next generation. Since the decision on which seed and fruit morph to
532 develop is determined fairly late, this may provide one of the reasons why all ovules
533 within both fruit morphs are initially fertilised and systematically aborted post-anthesis
534 (Lenser *et al.*, 2018). Testing this hypothesis by monitoring resource allocation to
535 ovules and embryos during development under normal and stressed growth conditions
536 would elucidate this precise and highly specific developmental process.

537

538 In addition to the seed coat-specific processes acting on M⁺ and M⁻ seeds, there may
539 be fruit developmental cross-talk involving the molecular regulation of branching-
540 related morph determination. It is thought that a pre-existing network regulates carpic
541 dominance in *Ae. arabicum*; DEH fruits occur primarily on the main branch, can be
542 induced by the removal of side branches, and thus develop preferentially as the
543 dominant plant reproductive organ. In contrast, IND fruits develop under growth
544 inhibitory conditions (Lenser *et al.*, 2018). The regulation of this primigenic
545 dominance acts through an accumulation balance of the plant growth hormones auxin

546 and cytokinin within flowers, as well as with the transcript abundance of BRC1,
547 encoding a TF known for its conserved function as a branching repressor (Lenser *et*
548 *al.*, 2018). In our study, we observed that transcript abundance of the *Ae. arabicum*
549 orthologue of HOMEBOX-LEUCINE ZIPPER PROTEIN 21 (AA33G00123),
550 positively regulated by BRC1, is accumulated in IND morph flowers. Together with
551 HOMEBOX PROTEIN 40 (HB40) and HOMEBOX PROTEIN 53 (HB53), these
552 genes are known to enhance *9-CIS-EPOXICAROTENOID DIOXIGENASE (NCED)*
553 expression, triggering abscisic acid (ABA) accumulation, and causing suppression of
554 bud development (González-Grandío *et al.*, 2017). Though ABA is not yet fully
555 integrated into current models of the hormonal control of shoot branching, ABA has
556 been classically associated with dormancy in seeds and buds in many different species
557 (Yao & Finlayson, 2015; Lenser *et al.*, 2018). That we see increased dormancy of M⁻
558 seeds (extracted from IND fruits) in comparison to M⁺ seeds (Lenser *et al.*, 2016)
559 supports these observations. We therefore hypothesise that there is a likely correlation
560 or interconnected regulation between the co-expression networks underpinning carpic
561 dominance, fruit morphogenesis, and seed development in *Ae. arabicum*.

562

563 *Seed coat epidermis in Aethionema arabicum as a dimorphic model system*

564 Our understanding of the genetic processes associated with reproductive development
565 has been greatly advanced in recent years through mechanistic and functional analyses
566 of gene expression in mutant phenotypes. We have shown that the unique seed
567 dimorphism in *Ae. arabicum* provides an excellent system with which to establish
568 patterns in the regulation of cell differentiation, biosynthesis and secretion of mucilage
569 polysaccharides. The future isolation and characterisation of seed coat-specific
570 mutants in *Ae. arabicum* should improve our understanding of the co-expression
571 network underlying this process, and provide a further insight into its link with morph-
572 specific fruit development. By elucidating the fundamental mechanisms and complex
573 dynamics modulating fruit and seed development, particularly in response to ambient
574 temperature experienced during reproduction, our findings within a dimorphic model
575 system provide an alternative avenue for seed developmental research. Given the
576 distribution of myxospermous seed-producing species in regions most threatened by
577 climate change, our understanding of the molecular and genetic basis of mucilage, as
578 the seed-environment interface, is therefore of great importance.

579 **Methods**

580

581 *Plant material and experimental growth conditions*

582 Mature plants of *Aethionema arabicum* (L.) Andr. ex DC. were grown from accession
583 ES1020 (obtained from Eric Schranz, Wageningen University and Research Centre),
584 in Levington compost with added horticultural grade sand (F₂ + S), under long-day
585 conditions (16 h light/20°C and 8 h dark/18°C) in a greenhouse. The day after
586 pollination (DAP) was defined phenotypically as the time at which the flowers open
587 (anthesis) and the four long stamens extend over the gynoecium.

588

589 *Synchrotron-based Radiation X-ray Tomographic Microscopy (SRXTM) of*
590 *reproductive development*

591 Five replicate buds, flowers, immature (~7–10 DAP) fruits, and mature (~30–40 DAP)
592 fruits were fixed in 3% glutaraldehyde plus 4% formaldehyde in 0.1 M piperazine-
593 *N,N'*-bis(2-ethanesulfonic acid) (PIPES) buffer at pH 7.2. Samples were then rinsed
594 with 0.1 M PIPES, and dehydrated in five changes of EtOH (30%, 50%, 70%, 95%,
595 100%). Samples were critical point dried (Balzers CPD-030, Bal-Tec, Germany),
596 mounted onto 3 mm diameter brass pin stubs using 2-component epoxy (Araldite[®],
597 Huntsman Advanced Materials GmbH, Switzerland), and imaged at the TOMographic
598 Microscopy and Coherent radiology experimentTs (TOMCAT) beamline of the Swiss
599 Light Source, Paul Scherrer Institute, Villigen, Switzerland (Stampanoni *et al.*, 2006).
600 Data were acquired using a 10× objective and a sCMOS camera (PCO.edge, PCO,
601 Kelheim, Germany), with an exposure time of 80 ms at 12 keV. Projections were post-
602 processed and reconstructed using a Fourier-based algorithm (Marone & Stampanoni,
603 2012). Tomographic slice data derived from the scans were analysed using Avizo[™]
604 9.5.0 (Thermo Scientific[™], Visualization Science Group Inc., Burlington, MA) for
605 Windows 10 Pro 64-bit, and contrast adjusted in Adobe Photoshop Lightroom CC.

606

607 *Whole seed staining and developmental analysis of seed coat differentiation*

608 Whole M⁺ and M⁻ seeds were imbibed in 0.01% (w/v) ruthenium red (Sigma-Aldrich,
609 11103-72-3) or 0.01% (w/v) methylene blue (VWR, 3470.0025) for two minutes, then
610 visualised under a Leica MZ-125 stereomicroscope. Developing gynoecia from 0 to 7
611 DAP were harvested and fixed in vacuum-infiltrated FAA fixation solution (2%

612 formaldehyde, 5% glacial acetic acid, 60% EtOH, 0.1% Tween-20) at 4°C for 24 h.
613 After sample dehydration and clearing using HistoClear™, samples were transferred
614 into fresh melted paraffin and embedded into Peel-A-Way® moulds. A Microm HM
615 355 S rotary microtome (Walldorf, Germany) and Leica 819 low-profile disposable
616 blades were used to prepare 6 µm sections, which were mounted on glass slides using
617 Mayer's egg albumin solution, and deparaffinised using HistoClear™ and EtOH.
618 Slides were stained using 0.05% toluidine blue, and inspected using a Nikon Eclipse
619 (Ni-E) upright motorised microscope (Nikon, Japan). Photographs were acquired
620 using Nikon Imaging Software (NIS) Elements Basic Research (v4.2), and contrast
621 adjusted using Adobe Photoshop Lightroom CC.

622

623 *RNA extraction for RNA-Seq*

624 Floral buds (0 DAP), flowers at anthesis (1 DAP), and fruits (~30 DAP) at their full
625 length (prior to the onset of yellowing and drying) were harvested from second-order
626 branches of plants that grew undisturbed (IND) or from the main branch of plants
627 where side branches were constantly removed during development (DEH), as
628 previously described (Lenser *et al.*, 2018). Total RNA was isolated from 50 mg of bud,
629 flower, and fruit tissue using QIAzol Lysis Reagent (Qiagen, Hilden, Germany).
630 Genomic DNA was removed by DNaseI (Roche, Mannheim, Germany) digestion in
631 solution, followed by RNA purification using RNeasy Mini spin columns (QIAGEN,
632 Hilden, Germany). RNA quantity and purity were determined using a NanoDrop™
633 spectrophotometer (ND-1000, ThermoScientific™, Delaware, USA) and Agilent 2100
634 Bioanalyzer with the RNA 6000 Nano Kit (Agilent Technologies, CA, USA) using the
635 2100 Expert Software to calculate RNA Integrity Number (RIN) values. Four
636 biological replicate RNA samples were used for downstream applications. Sequencing
637 was performed at the Vienna BioCenter Core Facilities (VBCF) Next Generation
638 Sequencing Unit, Vienna, Austria (www.vbcf.ac.at). Libraries were sequenced in 50-
639 bp single-end mode on Illumina® HiSeq 2000 Analyzers using the manufacturer's
640 standard cluster generation and sequencing protocols.

641

642 *RNA-Seq, data trimming, filtering, and analysis*

643 The cDNA sequence libraries were processed, including data trimming, filtering, read
644 mapping and feature counting, as previously described (Wilhelmsson *et al.*, 2019).

645 Raw RNA-Seq reads were quality control checked (FastQC), processed to remove
646 adapters and low-quality bases (Trimmomatic, PrinSeq), and cleaned reads mapped
647 (GSNAP) to the *Aethionema arabicum* genome v2.5 (Haudry *et al.*, 2013). After
648 normalisation, genome-mapped reads were compared at each developmental stage
649 using *R* (R Core Team, 2013) and the Bioconductor package DESeq2 (Love *et al.*,
650 2014; Huber *et al.*, 2015), to identify differentially expressed genes using an adjusted
651 *P*-value (FDR) cut-off for optimising the independent filtering set to 0.05. Principal
652 Component Analyses (PCAs) and clustered heat-maps were created using a custom
653 script and the pheatmap (Kolde, 2015) package in *R*. Indehiscent samples were
654 compared against dehiscent samples (baseline) in all comparisons.

655

656 *Gene Ontology (GO) term and promotor motif analyses*

657 Transcripts of *Aethionema arabicum* genome (v2.5) were annotated with GO terms as
658 previously described (Wilhelmsson *et al.*, 2019). GO term enrichment was analysed
659 with the topGO Bioconductor package (Huber *et al.*, 2015; Alexa & Rahnenfuhrer,
660 2016), using the classic method and fisher test. Enriched promoter motifs from the
661 *Arabidopsis* DNA affinity purification motif database (O'Malley *et al.*, 2016) were
662 identified using Analysis of Motif Enrichment (AME) in MEME Suite 5.0.4, with
663 DEG promoter sequences used as the primary sequences and all promoter sequences
664 used as the control sequences (average odds score with fisher's exact test) (Bailey *et al.*,
665 2009; Buske *et al.*, 2010). Promoter sequences were defined as -1000 and +100
666 base pairs from the transcription start site based on *Ae. arabicum* genome (v2.5)
667 mRNA annotation.

668

669 *Identification of gene orthologs*

670 Orthologs of *Arabidopsis thaliana* genes were identified in *Ae. arabicum*
671 (Supplementary Table 2) by searching query sequences with BLASTP (Altschul *et al.*,
672 1990) against a plant-specific protein database. To detect homologous sequences,
673 results were filtered for adequate query coverage and amino acid similarity (Rost,
674 1999). Sequence data from *Ae. arabicum* are available in the CoGe database
675 (<https://genomevolution.org/coge/>) under the following genome ID: v2.5, id33968.

676

677

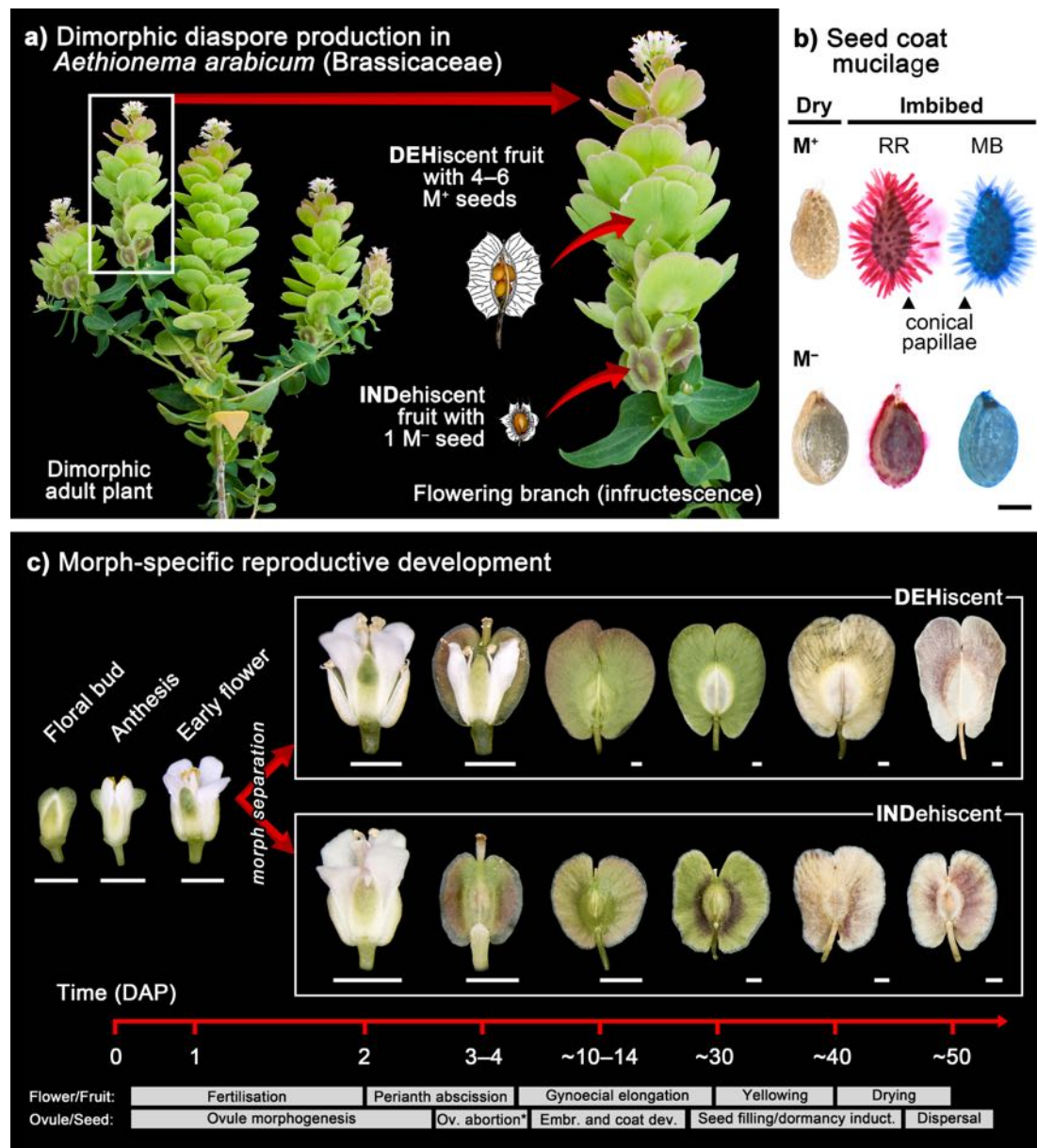
678 *Gene expression analysis via quantitative RT-PCR*

679 Floral buds (0 DAP), and flowers at 1, 3, and 10 DAP were harvested from second-
680 order branches (indehiscent) or from the main branch (dehiscent) of multiple
681 undisturbed plants. Tissue was frozen in liquid nitrogen, and ground using a Precellys®
682 24 tissue homogeniser (Bertin Instruments). RNA was extracted using methods
683 described for RNA-Seq. The quantity and purity of RNA was determined using an
684 Agilent 2100 Bioanalyzer with the RNA 6000 Nano Kit (Agilent Technologies, CA,
685 USA), using the 2100 Expert Software to calculate RNA Integrity Number (RIN)
686 values. One µg DNase I-treated RNA was used for cDNA synthesis with random
687 hexamer primers, using the Invitrogen™ SuperScript™ III First-Strand Synthesis
688 System (Thermo Scientific).

689

690 qRT-PCR reactions were performed in a CFX96 Touch™ Real-Time PCR Detection
691 System (Bio-Rad), using ABSolute qPCR SYBR Green Mix (Thermo Scientific) and
692 primer pairs listed in Supplementary Table 3, with the following parameters: 95°C for
693 15 min, 40 cycles with 95°C for 15 sec, and 60°C for 30 sec, and 72°C for 30 sec, then
694 65°C for 31 sec. Melt-curve analysis verified the absence of primer-dimer artefacts
695 and amplification of a single product from each qPCR assay. PCR efficiencies and C_q
696 values were calculated using Real-time PCR Miner algorithm (Zhao & Fernald, 2005;
697 Graeber *et al.*, 2011) using raw fluorescence data as input. The geometric mean of
698 *Aethionema* orthologues of ADAPTIN FAMILY PROTEIN (AearAFP,
699 AA44G00404), CALCINEURIN-LIKE METALLO-PHOSPHOESTERASE
700 SUPERFAMILY PROTEIN (AearCMSP, AA10G00283), and the unknown protein
701 AA19G00315 (AearAA19G00315) was used as reference for normalisation. All qRT-
702 PCR experiments were performed using five independent biological replicates.
703 Statistical analysis was performed using GraphPad Prism (v.7.0a; San Diego, CA,
704 USA), using a two-way ANOVA with a Šidák's *post-hoc* correction for multiple
705 comparisons.

706



709

710

711 **Figure 1: Fruit and seed dimorphism in *Aethionema arabicum* (Brassicaceae).**

712 Mature individual plant showing presence of two morphologically-distinct fruit types

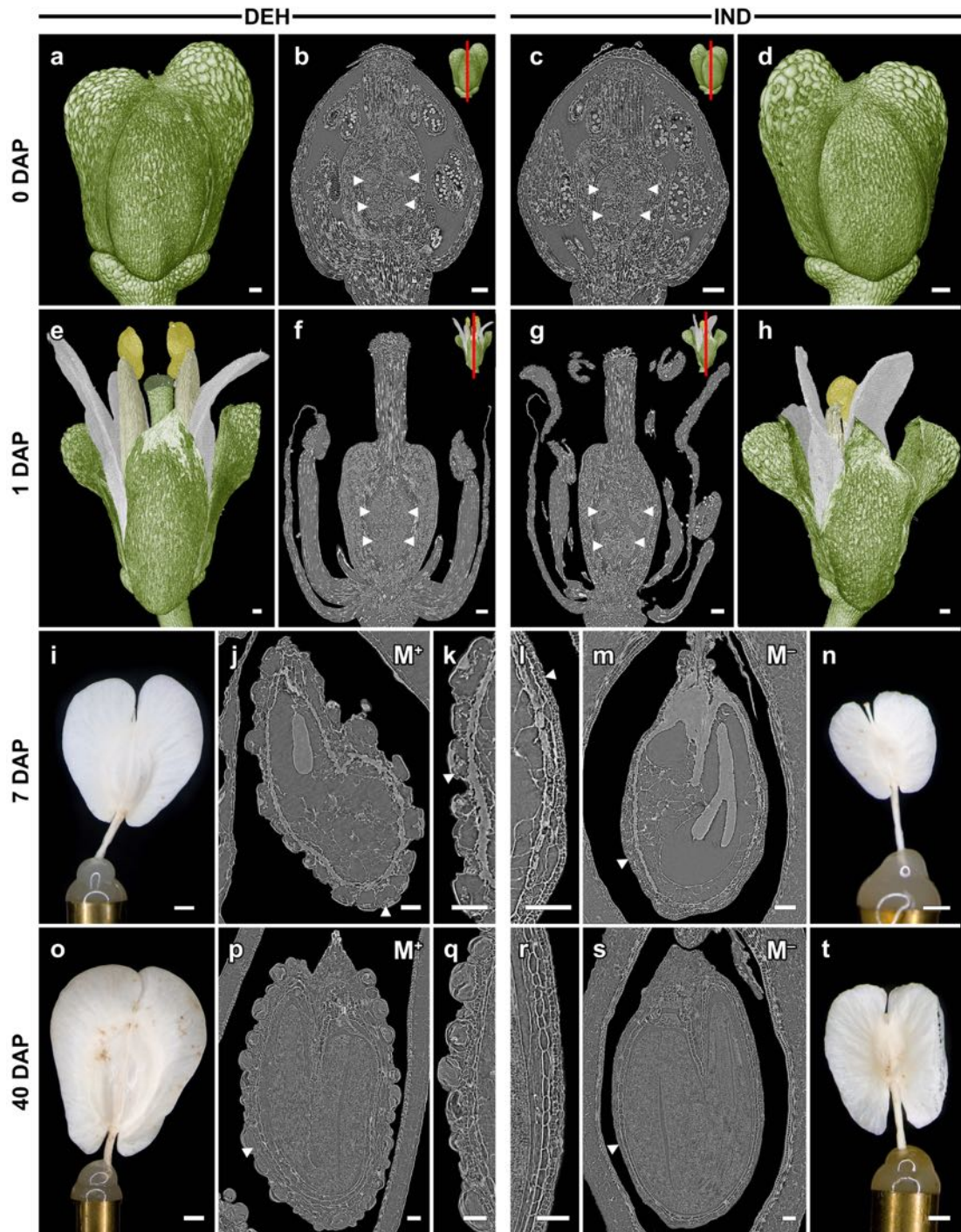
713 on the same infructescence. Large, dehiscent (DEH) fruits contain 4–6 seed diaspores

714 which produce mucilage (M⁺) upon imbibition. Small, indehiscent (IND) fruits contain715 a single non-mucilaginous (M⁻) seed only. There are no intermediate fruit or seed716 morphs. **(b)** Staining with ruthenium-red (RR, 0.01%) and methylene blue (MB,

717 0.01%) shows mature seeds from DEH fruits contain a pectin- and cellulose-rich,

718 mucilage-forming epidermal cell layer which extrudes as conical papillae upon

719 imbibition. In contrast, mature seeds manually excised from IND fruits possess a
720 smooth, ± “non-mucilaginous” outermost seed coat layer. (c) The two fruit types have
721 distinct patterns of reproductive development. Floral buds and flowers at anthesis
722 (time at which self-pollination occurs) are phenotypically identical. Morph-specific
723 differences become first evident two days after pollination (DAP), when fruit tissue
724 growth extends beyond sepals in DEH fruits, while IND fruits remain concealed by
725 outer floral organs. At 3–4 DAP, there is abscission of sepals and petals from both
726 fruit morphs. Fruits elongate (4–30 DAP) through both cell expansion and cell
727 division, before reaching their full length at 30 DAP, after which the fruit yellows (40
728 DAP) before drying. Scale bars = 1 mm. Abbreviations: **ov** = ovule; **embr** = embryo;
729 **dev** = development; **induct** = induction.
730

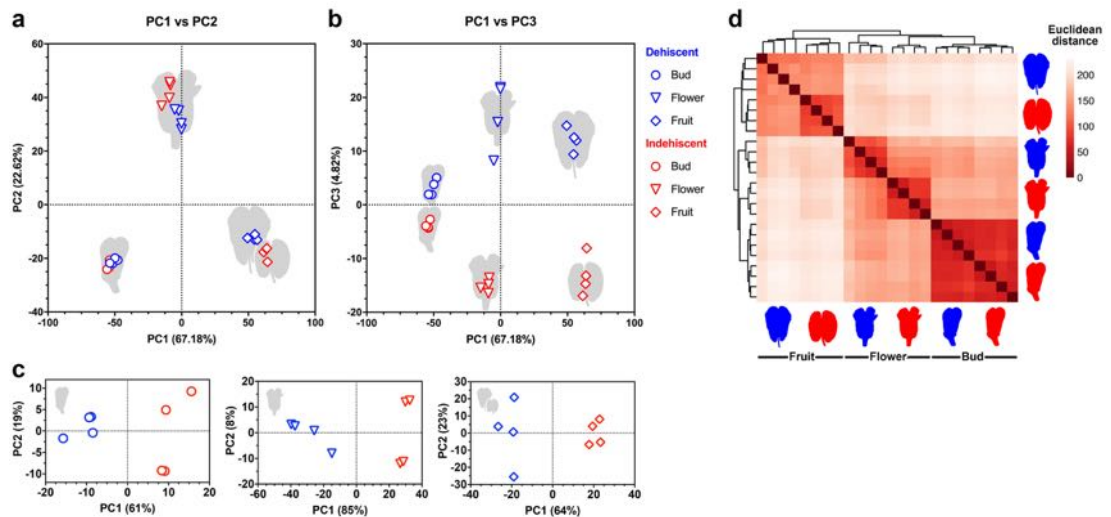


731

732

733 **Figure 2: Comparative SRXTM results obtained during diaspore development in**
 734 **the dehiscent (DEH) and indehiscent (IND) fruits of *Aethionema arabicum*, with**
 735 **3D surface (isosurface) representations and longitudinal slices through volumes**
 736 **depicting seed and coat development at the respective stage. (a–d) Floral buds,**
 737 **showing morphologically-distinct gynoecium (consisting of two congenitally fused**
 738 **carpels), medial and short stamens. Four anatropous ovules (arrowheads) are present**

739 in buds from both morphs. (**e–h**) Anthesis, the time at which the flower opens and self-
740 pollinates. Ovules (arrowheads) are completely developed and anthers extend above
741 the top of the stigma. Both DEH (**f**) and IND (**g**) morphs exhibit differentiated internal
742 structures of an identical nature, with ovules possessing the same nucellus size,
743 number of integument layers, and ovule shape despite developing into different fruit
744 morphs. (**i–n**) Immature fruits (*ca.* 7 days after pollination [DAP]) from the DEH (**i, j,**
745 **k**) and IND (**l, m, n**) morphs. Outer and inner integuments (**k, l, q, r**) show
746 considerable morph-specific differences (arrowheads), namely in the development and
747 secretion of mucilage between the outer primary wall and the protoplast (in a ring
748 around the area where starch granules are located). (**o–t**) Mature fruits (*ca.* 40 DAP)
749 from the DEH (**o–q**) and IND (**r–t**) morphs. Shown are seeds at full maturation, the
750 outermost epidermal layer of which forms large mucilage secretory cells in the case of
751 mucilaginous seeds (M^+) from the DEH fruit morph (**q**), but a thin layer of mucilage
752 in the single non-mucilaginous (M^-) seed (**r**) of the IND fruit. Scale bars = 75 μm (**a–**
753 **h, j–m, p–s**) or 1 mm (**i, n, o, t**). Abbreviations: **SRXTM** = synchrotron radiation X-
754 ray tomographic microscopy; M^+ = mucilaginous; M^- = non-mucilaginous.



755

756

757 **Figure 3: Comparative RNA-Seq analysis of transcriptome dynamics during**

758 **morph-specific reproductive development in *Aethionema arabicum*.** (a–b)

759 Unbiased principal component analysis (PCA) of morph-specific fruit development

760 mRNA transcriptome data. The PCA plots are based on the top 500 genes by variance

761 across all samples, using approximately homoscedastic Variance Stabilising

762 Transformed (VST) counts. Comparison of variable loadings on (a) PC1 vs. PC2 and

763 (b) PC1 vs. PC3 reveal samples group in an organ-specific and morph-specific manner,

764 respectively, with (c) clustering of biological replicates indicating the variation

765 dominating the signal. (d) Unsupervised hierarchical clustering using VST count

766 values, with heat map displaying a computed sample (Euclidean) distance matrix,

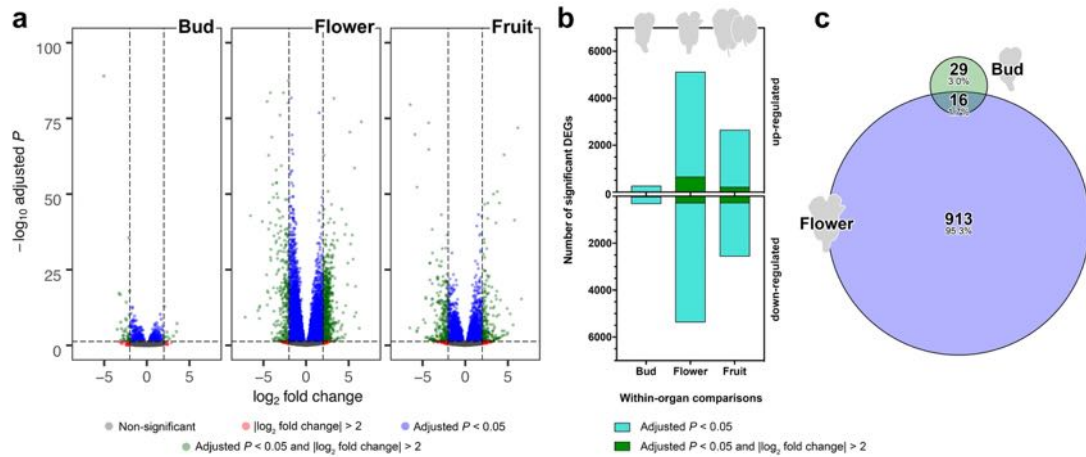
767 reveals the high similarity of bud samples from dehiscent (DEH) and indehiscent

768 (IND) morphs. Flower samples also cluster by morph, and are more similar in their

769 transcriptional profile to bud samples than to fruit samples. At each stage of

770 reproductive development, N = 4. Colours of bud, flower, and fruit schematics indicate

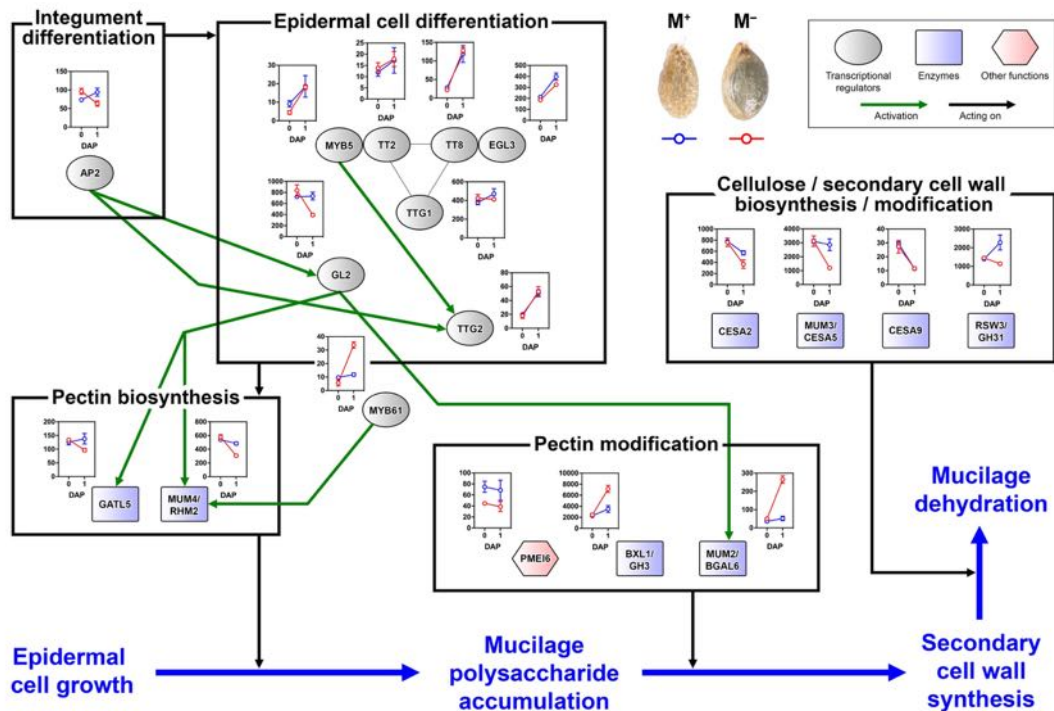
771 developmental morph (DEH = blue, IND = red).



772

773

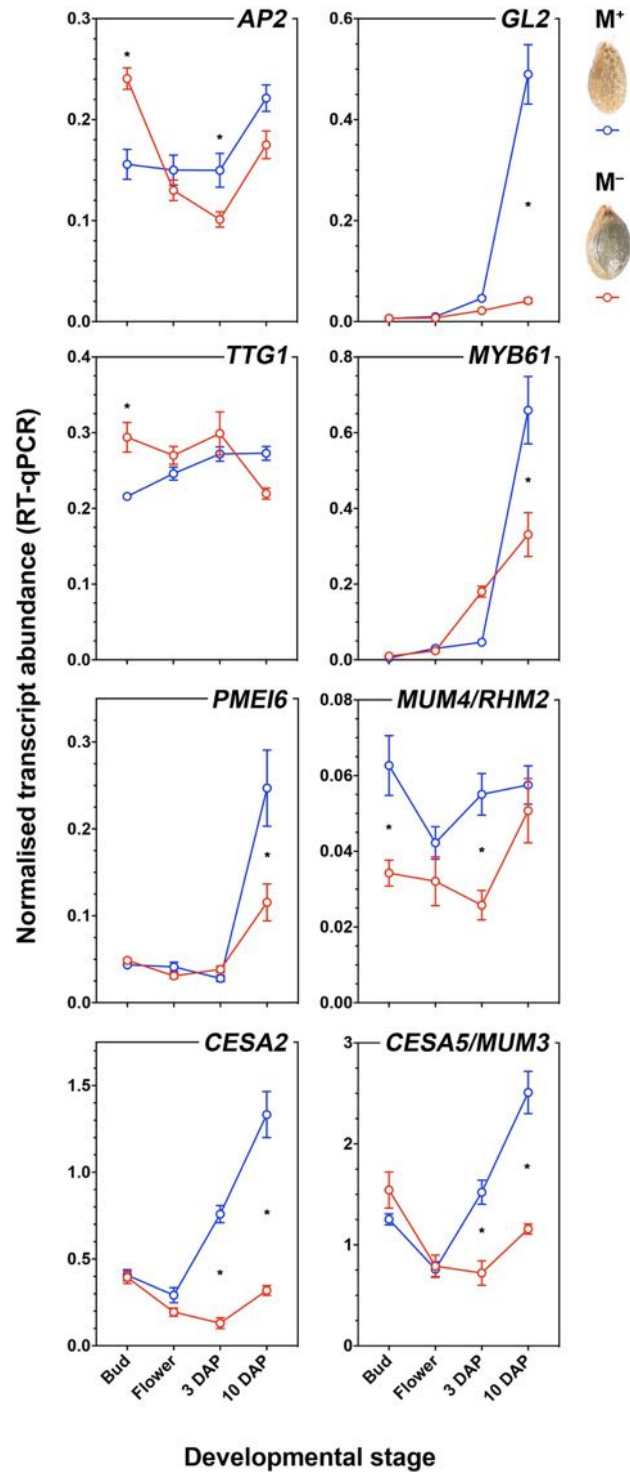
774 **Figure 4: Differential expression analysis of morph-specific transcripts across**
 775 **reproductive development in *Aethionema arabicum*.** (a) RNA-Seq volcano plots of
 776 differential expression between *Ae. arabicum* morphs at bud, flower, and fruit
 777 developmental stages. Transcripts exhibiting a $|\log_2$ (fold change) > 2 and adjusted
 778 P value < 0.05 were considered differentially expressed genes (DEGs). P values were
 779 generated with a negative binominal generalised linear model in DESeq2. (b)
 780 Summary of total (cyan) and $|\log_2$ (fold change) | significant (green) up- and down-
 781 regulated transcripts based on morph-specific pairwise comparisons within each
 782 developmental time point. Shown are the transcriptional changes of indehiscent (IND)
 783 samples, with dehiscent (DEH) samples set as the reference level. (c) Area-
 784 proportional Venn diagram depicting the numbers of organ-specific and shared DEGs
 785 across bud and flower stages.



786

787

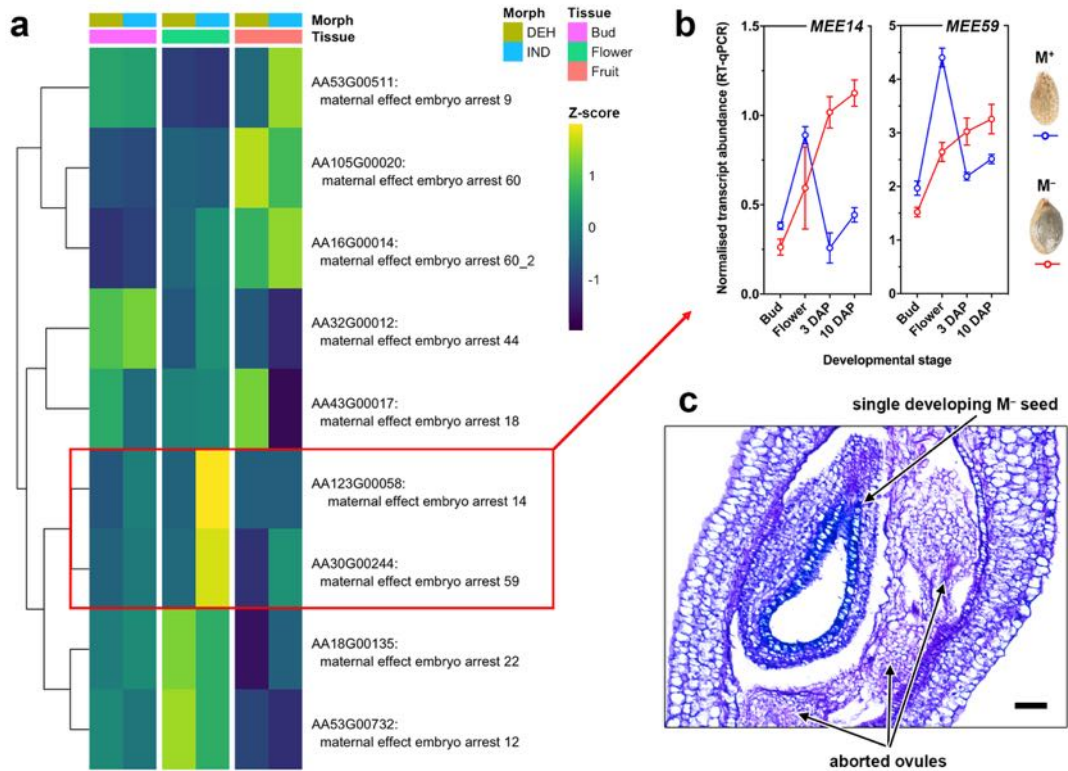
788 **Figure 5: Summary of proposed regulatory network underpinning epidermal cell**
 789 **differentiation during morph-specific mucilage development in**
 790 *Aethionema arabicum*. Shown are normalised transcript abundances for *Ae. arabicum*
 791 orthologues at 0 and 1 days after pollination (DAP), obtained from samples containing
 792 seeds developing mucilaginous seed coats (M⁺, blue) and “non-mucilaginous” seed
 793 coats (M⁻, red). Rounded grey nodes represent transcription factors, square blue nodes
 794 represent enzymes, and the hexagonal orange node represents a gene or protein with
 795 other functions. Shown are major changes associated with differentiation of the
 796 integument and epidermal cells that give rise to the biosynthesis and modification of
 797 pectin, and later cellulose and secondary cell wall synthesis. Arrows represent
 798 experimentally-verified activated or repressed expression regulatory relations derived
 799 from *Arabidopsis* literature (for a full list of references, see Fig. S4 and Supplementary
 800 Table 2).



801

802 **Figure 6: RT-qPCR expression analysis of genes involved in morph-specific seed**
 803 **coat development in *Aethionema arabicum*.** Shown are morph-specific differences
 804 in RT-qPCR expression of orthologues of major transcription factors and enzymes
 805 involved in mucilaginous seed coat development: *APETALA2* (*AP2*), *GLABRA2*
 806 (*GL2*), *TRANSPARENT TESTA GLABRA 1* (*TTG1*), *MYB DOMAIN PROTEIN 61*

807 (*MYB61*), *PECTIN METHYLESTERASE INHIBITOR6 (PMEI6)*, *MUCILAGE-*
808 *MODIFIED 4 / RHAMNOSE BIOSYNTHESIS 2 (MUM4/RHM2)*, *CELLULOSE*
809 *SYNTHASE 2 (CESA2)* and *CELLULOSE SYNTHASE 5 (CESA5/MUM3)*. Within each
810 time point, a * indicates a significant difference between mucilaginous seed (M⁺,
811 derived from dehiscent samples) and non-mucilaginous seed (M⁻, derived from
812 indehiscent samples) morphs based on two-way ANOVA, followed by Šídák's
813 multiple comparisons *post-hoc* test ($P < 0.05$). Dry seeds are depicted in the key (for
814 clearer visual differences, see Fig. 1).



815

816

817 **Figure 7: Ovule abortion in *Aethionema arabicum* indehiscent (IND) fruits.**

818 (a) Clustered heatmap using the mean Z-score of the expression of nine identified

819 *MATERNAL EFFECT EMBRYO ARREST* orthologues derived from RNA-Seq data.

820 Only the transcript abundance of the *Ae. arabicum* orthologue of *MEE14* and *MEE59*

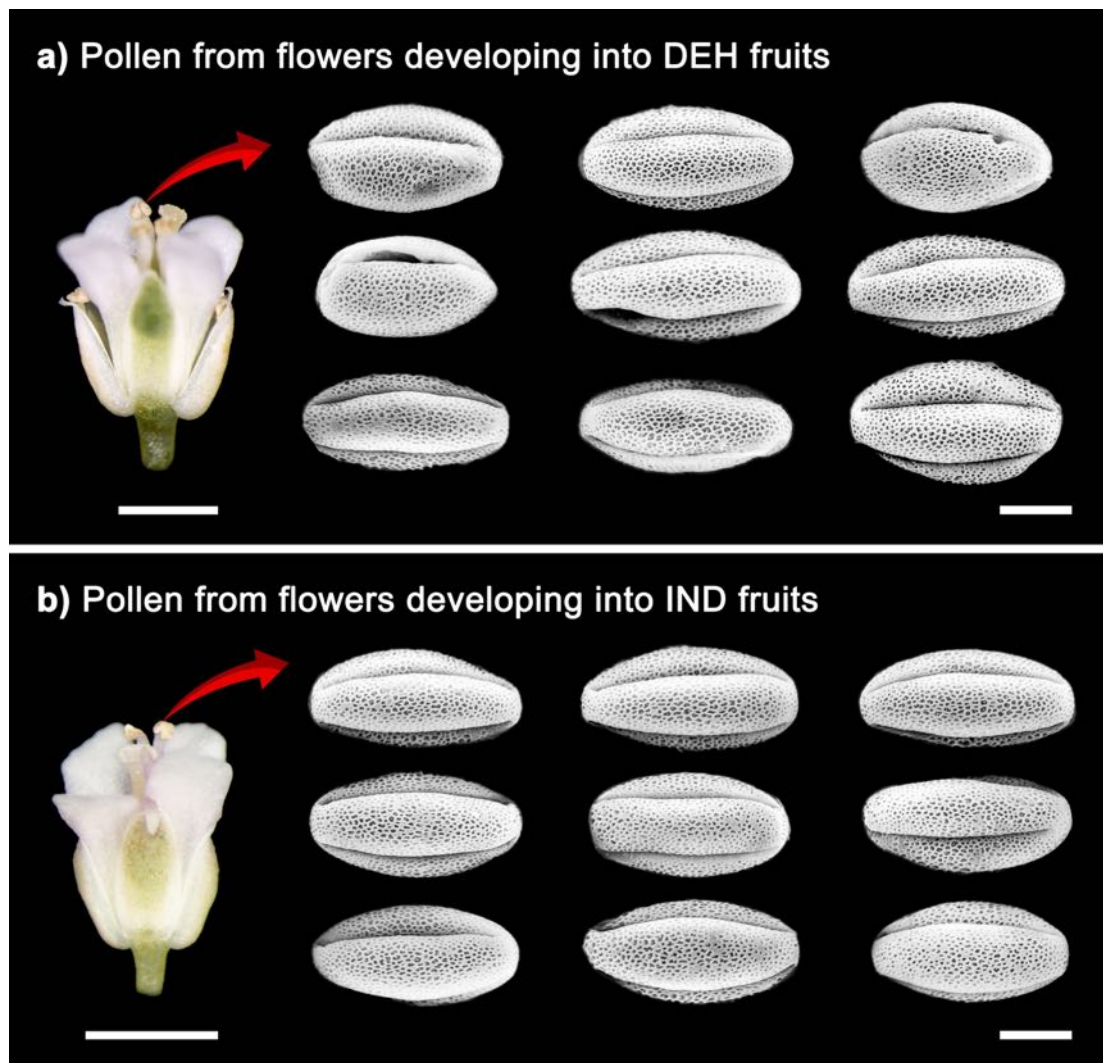
821 correlates with the timing of controlled embryonic arrest (abortion) within indehiscent

822 (IND) fruits around 2–3 days after pollination, as verified by RT-qPCR analysis (b)

823 using independently-grown biological samples. N = 5 (RT-qPCR) and 4 (RNA-Seq).

824 Error bars = ± 1 standard error of the mean. (c) A toluidine-blue (0.05%) stained 6 μm

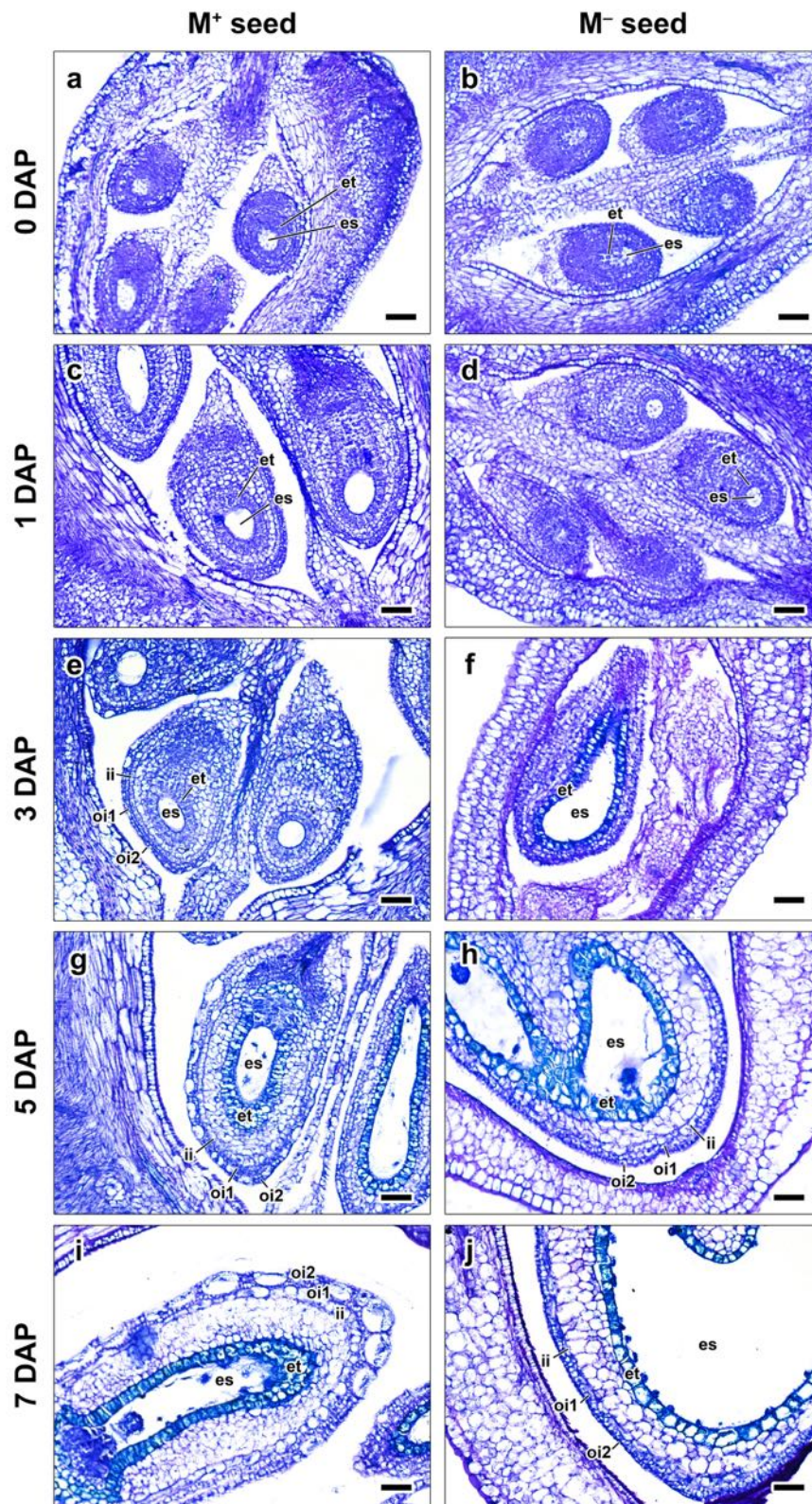
825 thick section depicts the abortion of three ovules in IND gynoecia at 3 DAP.



828

829

830 **Figure S1: Comparative Scanning Electron Microscopy (SEM) analysis of pollen**
831 **grains from *Aethionema arabicum* flowers at anthesis.** Comparative morphology of
832 pollen from flowers developing into (a) dehiscent (DEH) fruits and into (b)
833 indehiscent (IND) fruits. Shown is the range of variation of individual pollen grains in
834 equatorial views, all of which exhibit a largely isopolar, prolate–perprolate shape
835 (polar axis : equatorial diameter ratio). All pollen grains are tricolpate, have reticulate
836 exine sculpturing, and do not differ between morphs. Scale bars = 1 mm (flowers) and
837 10 μ m (pollen).

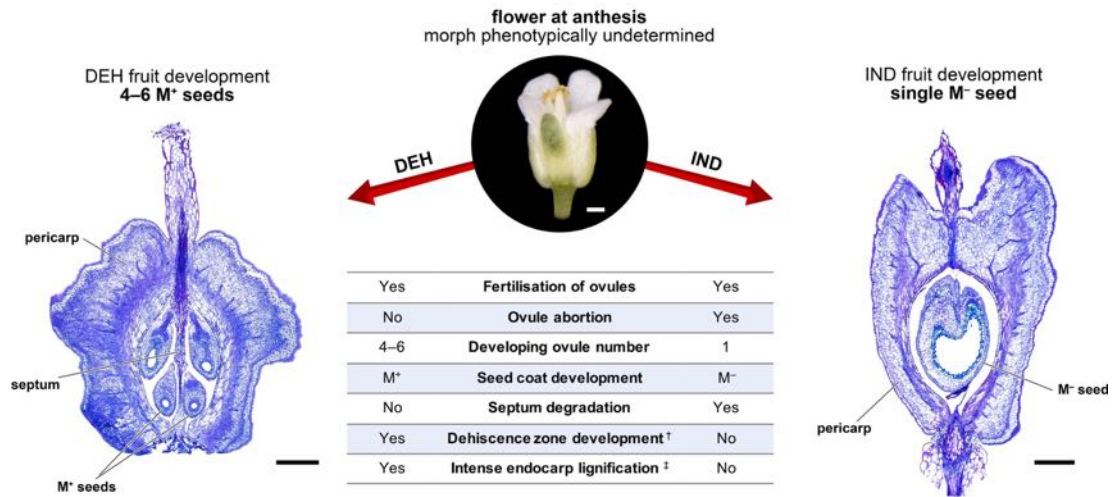


838

839

840 **Figure S2: Comparative analysis of morph-specific ovule anatomy during early**
 841 **stages of *Aethionema arabicum* fruit growth after pollination.** Shown are 6 μ m
 842 thick longitudinal sections through ovules stained with toluidine blue at 0, 1, 3, 5 and

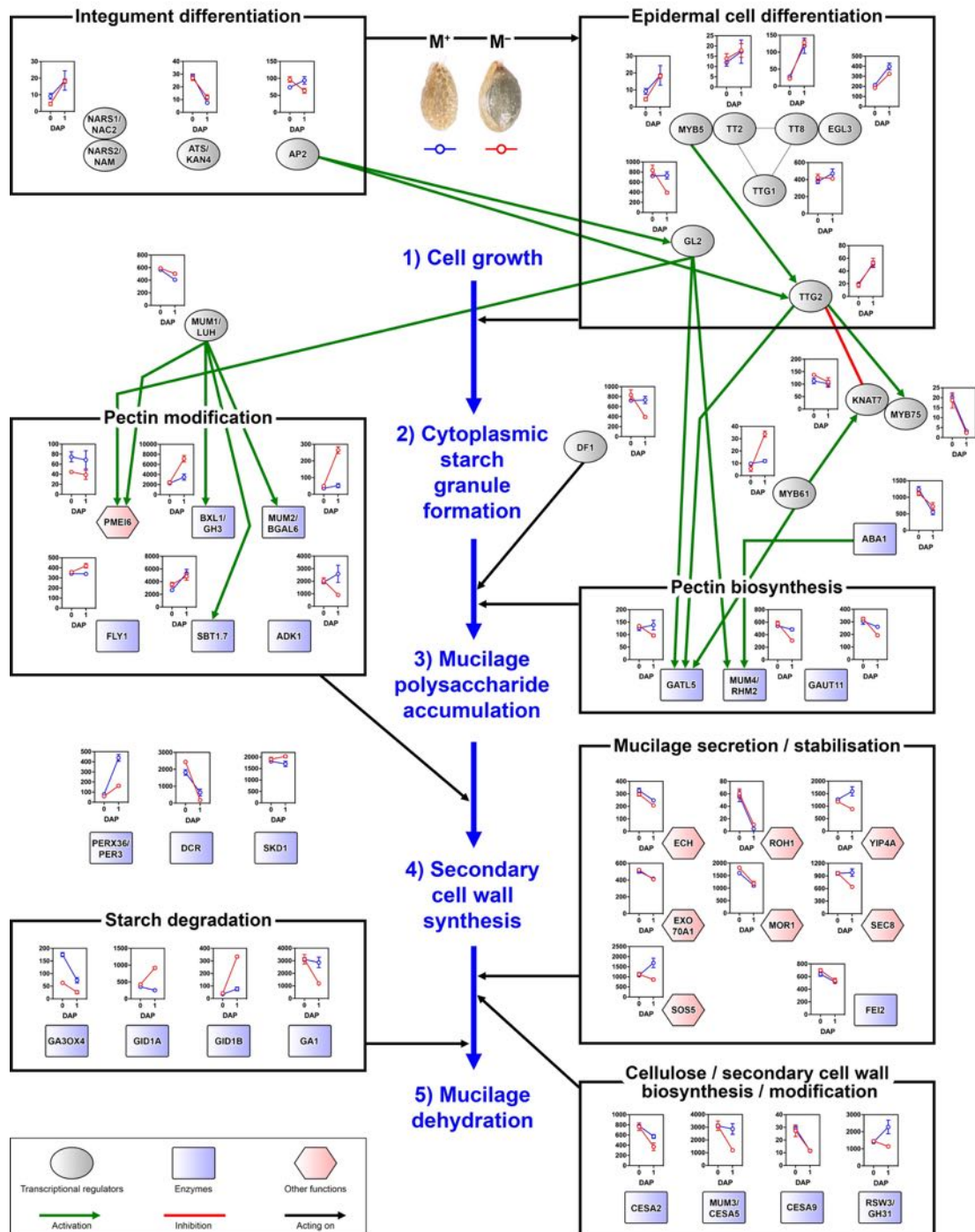
843 7 days after pollination (DAP). Seeds within dehiscent fruits develop mucilaginous
844 (M^+) seed coats (**a, c, e, g, i**), while the single seed within indehiscent fruits (**b, d, f, h,**
845 **j**) develops a non-mucilaginous (M^-) seed coat. Both morphs start with 4–6 ovules,
846 and IND fruits undergo an abortive process at 2–3 DAP, where programmed cell death
847 of three ovules (**f**) and septum leads to the development of only a single seed. Scale
848 bars = 50 μm . Abbreviations: **et** = endothelium; **es** = embryo sac; **ii** = inner integument;
849 **oi1** = inner epidermis of the outer integument; **oi2** = outer epidermis of the outer
850 integument.



851

852

853 **Figure S3: Summary of morph-specific anatomical changes associated with**
 854 **development of dehiscent (DEH) and indehiscent (IND) *Aethionema arabicum***
 855 **fruits.** The morph transition from a flower, whose morph is phenotypically
 856 undeterminable, into a DEH or IND fruit (at two days after pollination [DAP]) is
 857 coupled with a multitude of gynoecial changes associated with the ovules, carpels,
 858 septum, and pericarp tissue. These changes lead to the development of non-deep
 859 dormant, mucilaginous (M⁺) seeds in DEH fruits, and the pericarp-imposed deep
 860 dormant, single non-mucilaginous (M⁻) seed in IND fruits. Shown are 6 μm thick
 861 longitudinal sections of fruits at ~5 DAP, stained with toluidine blue. Scale bars =
 862 300 μm. [†]Arshad *et al.* (2019a). [‡]Lenser *et al.* (2016).



863

864

865 **Figure S4: Hypothesised regulatory network underpinning epidermal cell**
 866 **differentiation during morph-specific seed coat development in *Aethionema***
 867 ***arabicum*.** Shown are normalised transcript abundances for *Ae. arabicum* orthologues
 868 at 0 and 1 days after pollination (DAP), obtained from samples containing seeds
 869 developing mucilaginous seed coats (M⁺, blue) and “non-mucilaginous” seed coats

870 (M^- , red). Rounded grey nodes represent transcription factors, square blue nodes
871 represent enzymes, and hexagonal orange nodes represent genes and/or proteins with
872 other functions. Arrows represent experimentally-verified activated or repressed
873 expression regulatory relations derived from *Arabidopsis thaliana*. Genes and/or
874 proteins associated with mucilage phenotypes were retrieved from Francoz *et al.*
875 (2015), classified among eight categories (Supplementary Table 2). This model was
876 developed from existing models in the following literature: Western (2012); North *et*
877 *al.* (2014); Francoz *et al.* (2015).

878 **References**

879

880 **Alexa A, Rahnenfuhrer J. 2016.** topGO: Enrichment Analysis for Gene Ontology.

881 *R package version 2.32.0.*

882 **Altschul SF, Gish W, Miller W, Myers EW, Lipman DJ. 1990.** Basic local
883 alignment search tool. *Journal of Molecular Biology* **215**(3): 403–410.

884 **Arshad W, Marone F, Collinson M, Leubner-Metzger G, Steinbrecher T. 2020.**

885 Fracture of the dimorphic fruits of *Aethionema arabicum* (Brassicaceae).

886 *Botany* **98**: 65–75.

887 **Arshad W, Sperber K, Steinbrecher T, Nichols B, Jansen V, Leubner-Metzger**

888 **G, Mummenhoff K. 2019.** Dispersal biophysics and adaptive significance of

889 dimorphic diaspores in the annual *Aethionema arabicum* (Brassicaceae). *New*

890 *Phytologist* **221**(3): 1434–1446.

891 **Bailey TL, Boden M, Buske FA, Frith M, Grant CE, Clementi L, Ren J, Li**

892 **WW, Noble WS. 2009.** MEME SUITE: Tools for motif discovery and

893 searching. *Nucleic Acids Research* **37**: W202–W208.

894 **Baskin CC, Baskin JM. 2014.** *Seeds: Ecology, Biogeography, and Evolution of*

895 *Dormancy and Germination*: Elsevier.

896 **Bhattacharya S, Mayland-Quellhorst S, Müller C, Mummenhoff K. 2018.** Two-

897 tier morpho-chemical defence tactic in *Aethionema* via fruit morph plasticity

898 and glucosinolates allocation in diaspores. *Plant, Cell & Environment* **42**(4):

899 1381–1392.

900 **Burn JE, Hurley UA, Birch RJ, Arioli T, Cork A, Williamson RE. 2002.** The

901 cellulose-deficient *Arabidopsis* mutant *rsw3* is defective in a gene encoding a

902 putative glucosidase II, an enzyme processing N-glycans during ER quality

903 control. *The Plant Journal* **32**(6): 949–960.

904 **Buske FA, Bodén M, Bauer DC, Bailey TL. 2010.** Assigning roles to DNA

905 regulatory motifs using comparative genomics. *Bioinformatics* **26**(7): 860–

906 866.

907 **Couvreur TLP, Franzke A, Al-Shehbaz IA, Bakker FT, Koch MA,**

908 **Mummenhoff K. 2009.** Molecular phylogenetics, temporal diversification

909 and principles of evolution in the mustard family (Brassicaceae). *Molecular*

910 *Biology and Evolution* **27**(1): 55–71.

911 **Finch-Savage WE, Leubner-Metzger G. 2006.** Seed dormancy and the control of

912 germination. *New Phytologist* **171**(3): 501–523.

913 **Francoz E, Ranocha P, Burlat V, Dunand C. 2015.** Arabidopsis seed mucilage

914 secretory cells: regulation and dynamics. *Trends in Plant Science* **20**(8): 515–

915 524.

916 **Franzke A, Lysak MA, Al-Shehbaz IA, Koch MA, Mummenhoff K. 2011.**

917 Cabbage family affairs: the evolutionary history of Brassicaceae. *Trends in*

918 *Plant Science* **16**(2): 108–116.

919 **Friis EM, Marone F, Pedersen KR, Crane PR, Stampanoni M. 2014.** Three-

920 dimensional visualization of fossil flowers, fruits, seeds, and other plant

921 remains using synchrotron radiation X-ray tomographic microscopy

922 (SRXTM): new insights into Cretaceous plant diversity. *Journal of*

923 *Paleontology* **88**(4): 684–701.

924 **Golz JF, Allen PJ, Li SF, Parish RW, Jayawardana NU, Bacic A, Doblin MS.**

925 **2018.** Layers of regulation – Insights into the role of transcription factors

- 926 controlling mucilage production in the *Arabidopsis* seed coat. *Plant Science*
 927 **272**: 179–192.
- 928 **Gonzalez A, Mendenhall J, Huo Y, Lloyd A. 2009.** TTG1 complex MYBs, MYB5
 929 and TT2, control outer seed coat differentiation. *Developmental Biology*
 930 **325**(2): 412–421.
- 931 **González-Grandío E, Pajoro A, Franco-Zorrilla JM, Tarancón C, Immink**
 932 **RGH, Cubas P. 2017.** Abscisic acid signaling is controlled by a
 933 *BRANCHED1/HD-ZIP* cascade in *Arabidopsis* axillary buds. *Proceedings of*
 934 *the National Academy of Sciences* **114**(2): E245–E254.
- 935 **Graeber K, Linkies A, Wood ATA, Leubner-Metzger G. 2011.** A guideline to
 936 family-wide comparative state-of-the-art quantitative RT-PCR analysis
 937 exemplified with a Brassicaceae cross-species seed germination case study.
 938 *The Plant Cell* **23**(6): 2045–2063.
- 939 **Grubert M. 1974.** Studies on the distribution of myxospermy among seeds and
 940 fruits of Angiospermae and its ecological importance. *Acta Biologica*
 941 *Venezuelica* **8**(3–4): 315–551.
- 942 **Gutterman Y. 2000.** Environmental factors and survival strategies of annual plant
 943 species in the Negev Desert, Israel. *Plant Species Biology* **15**(2): 113–125.
- 944 **Gutterman Y. 2002.** *Survival Strategies of Annual Desert Plants*. Berlin: Springer-
 945 Verlag.
- 946 **Harper JL. 1977.** *Population Biology of Plants*. Caldwell, New Jersey: The
 947 Blackburn Press.
- 948 **Hasanuzzaman M, Nahar K, Alam MM, Roychowdhury R, Fujita M. 2013.**
 949 Physiological, biochemical, and molecular mechanisms of heat stress
 950 tolerance in plants. *International Journal of Molecular Sciences* **14**(5): 9643–
 951 9684.
- 952 **Haudry A, Platts AE, Vello E, Hoen DR, Leclercq M, Williamson RJ, Forczek**
 953 **E, Joly-Lopez Z, Steffen JG, Hazzouri KM, et al. 2013.** An atlas of over
 954 90,000 conserved noncoding sequences provides insight into crucifer
 955 regulatory regions. *Nature Genetics* **45**(8): 891–898.
- 956 **Haughn G, Chaudhury A. 2005.** Genetic analysis of seed coat development in
 957 *Arabidopsis*. *Trends in Plant Science* **10**(10): 472–477.
- 958 **Haughn G, Western T. 2012.** *Arabidopsis* seed coat mucilage is a specialized cell
 959 wall that can be used as a model for genetic analysis of plant cell wall
 960 structure and function. *Frontiers in Plant Science* **3**(64): 1–5.
- 961 **Hohmann N, Wolf EM, Lysak MA, Koch MA. 2015.** A time-calibrated road map
 962 of Brassicaceae species radiation and evolutionary history. *The Plant Cell* **27**:
 963 2770–2784.
- 964 **Huang Z, Gutterman Y, Hu Z. 2000.** Structure and function of mucilaginous
 965 achenes of *Artemisia monosperma* inhabiting the Negev Desert of Israel.
 966 *Israel Journal of Plant Sciences* **48**(4): 255–266.
- 967 **Huber W, Carey VJ, Gentleman R, Anders S, Carlson M, Carvalho BS, Bravo**
 968 **HC, Davis S, Gatto L, Girke T. 2015.** Orchestrating high-throughput
 969 genomic analysis with Bioconductor. *Nature Methods* **12**(2): 115–121.
- 970 **Imbert E. 2002.** Ecological consequences and ontogeny of seed heteromorphism.
 971 *Perspectives in Plant Ecology, Evolution and Systematics* **5**(1): 13–36.
- 972 **Kolde R. 2015.** pheatmap: Pretty Heatmaps. *R package version 1.0.12*.
- 973 **Koornneef M, Bentsink L, Hilhorst H. 2002.** Seed dormancy and germination.
 974 *Current Opinion in Plant Biology* **5**(1): 33–36.

- 975 **Lenser T, Graeber K, Cevik ÖS, Adigüzel N, Dönmez AA, Grosche C,**
976 **Kettermann M, Mayland-Quellhorst S, Mérai Z, Mohammadin S, et al.**
977 **2016.** Developmental control and plasticity of fruit and seed dimorphism in
978 *Aethionema arabicum*. *Plant Physiology* **172**(3): 1691–1707.
- 979 **Lenser T, Tarkowská D, Novák O, Wilhelmsson P, Bennett T, Rensing SA,**
980 **Strnad M, Theißen G. 2018.** When the BRANCHED network bears fruit:
981 How carpic dominance causes fruit dimorphism in *Aethionema*. *The Plant*
982 *Journal* **94**: 352–371.
- 983 **Linkies A, Graeber K, Knight C, Leubner-Metzger G. 2010.** The evolution of
984 seeds. *New Phytologist* **186**(4): 817–831.
- 985 **Lloyd D, Webb C, Primack R. 1980.** Sexual strategies in plants. *New Phytologist*
986 **86**(1): 81–92.
- 987 **Lobova TA, Mori SA, Blanchard F, Peckham H, Charles-Dominique P. 2003.**
988 *Cecropia* as a food resource for bats in French Guiana and the significance of
989 fruit structure in seed dispersal and longevity. *American Journal of Botany*
990 **90**(3): 388–403.
- 991 **Love MI, Huber W, Anders S. 2014.** Moderated estimation of fold change and
992 dispersion for RNA-seq data with DESeq2. *Genome Biology* **15**: 550.
- 993 **Lu JJ, Tan DY, Baskin JM, Baskin CC. 2010.** Fruit and seed heteromorphism in
994 the cold desert annual ephemeral *Diptychocarpus strictus* (Brassicaceae) and
995 possible adaptive significance. *Annals of Botany* **105**(6): 999–1014.
- 996 **Mandák B. 1997.** Seed heteromorphism and the life cycle of plants: a literature
997 review. *Preslia, Praha* **69**: 129–159.
- 998 **Marone F, Stampanoni M. 2012.** Regridding reconstruction algorithm for real-time
999 tomographic imaging. *Journal of Synchrotron Radiation* **19**(6): 1029–1037.
- 1000 **Mendu V, Griffiths JS, Persson S, Stork J, Downie AB, Voiniciuc C, Haughn**
1001 **GW, DeBolt S. 2011a.** Subfunctionalization of cellulose synthases in seed
1002 coat epidermal cells mediates secondary radial wall synthesis and mucilage
1003 attachment. *Plant Physiology* **157**(1): 441–453.
- 1004 **Mendu V, Stork J, Harris D, DeBolt S. 2011b.** Cellulose synthesis in two
1005 secondary cell wall processes in a single cell type. *Plant Signaling &*
1006 *Behavior* **6**(11): 1638–1643.
- 1007 **Mohammadin S, Peterse K, van de Kerke SJ, Chatrou LW, Dönmez AA,**
1008 **Mummenhoff K, Pires JC, Edger PP, Al-Shehbaz IA, Schranz ME. 2017.**
1009 Anatolian origins and diversification of *Aethionema*, the sister lineage of the
1010 core Brassicaceae. *American Journal of Botany* **104**(7): 1042–1054.
- 1011 **Mohammadin S, Wang W, Liu T, Moazzeni H, Ertugrul K, Uysal T,**
1012 **Christodoulou CS, Edger PP, Pires JC, Wright SI, et al. 2018.** Genome-
1013 wide nucleotide diversity and associations with geography, ploidy level and
1014 glucosinolate profiles in *Aethionema arabicum* (Brassicaceae). *Plant*
1015 *Systematics and Evolution* **304**(5): 619–630.
- 1016 **Mühlhausen A, Lenser T, Mummenhoff K, Theißen G. 2013.** Evidence that an
1017 evolutionary transition from dehiscent to indehiscent fruits in *Lepidium*
1018 (Brassicaceae) was caused by a change in the control of valve margin identity
1019 genes. *The Plant Journal* **73**(5): 824–835.
- 1020 **Mulroy TW, Rundel PW. 1977.** Annual plants: Adaptations to desert environments.
1021 *Bioscience* **27**(2): 109–114.
- 1022 **North HM, Berger A, Saez-Aguayo S, Ralet M-C. 2014.** Understanding
1023 polysaccharide production and properties using seed coat mutants: future

- 1024 perspectives for the exploitation of natural variants. *Annals of Botany* **114**(6):
 1025 1251–1263.
- 1026 **O'Malley RC, Huang S-sC, Song L, Lewsey MG, Bartlett A, Nery JR, Galli M,**
 1027 **Gallavotti A, Ecker JR. 2016.** Cistrome and episcistrome features shape the
 1028 regulatory DNA landscape. *Cell* **165**(5): 1280–1292.
- 1029 **Pagnussat GC, Yu H-J, Ngo QA, Rajani S, Mayalagu S, Johnson CS, Capron A,**
 1030 **Xie L-F, Ye D, Sundaresan V. 2005.** Genetic and molecular identification of
 1031 genes required for female gametophyte development and function in
 1032 *Arabidopsis*. *Development* **132**(3): 603–614.
- 1033 **Penfield S, Meissner RC, Shoue DA, Carpita NC, Bevan MW. 2001.** *MYB61* is
 1034 required for mucilage deposition and extrusion in the *Arabidopsis* seed coat.
 1035 *The Plant Cell* **13**(12): 2777–2791.
- 1036 **R Core Team. 2013.** *R: A language and environment for statistical computing.*
- 1037 **Roeder AH, Yanofsky MF. 2006.** Fruit development in *Arabidopsis*. *Arabidopsis*
 1038 *Book 4*: e0075.
- 1039 **Rost B. 1999.** Twilight zone of protein sequence alignments. *Protein Engineering*
 1040 **12**(2): 85–94.
- 1041 **Saez-Aguayo S, Ralet M-C, Berger A, Botran L, Ropartz D, Marion-Poll A,**
 1042 **North HM. 2013.** PECTIN METHYLESTERASE INHIBITOR6 promotes
 1043 *Arabidopsis* mucilage release by limiting methylesterification of
 1044 homogalacturonan in seed coat epidermal cells. *The Plant Cell* **25**(1): 308–
 1045 323.
- 1046 **Schnepf E, Deichgräber G. 1983.** Structure and formation of fibrillar mucilages in
 1047 seed epidermis cells. *Protoplasma* **114**(3): 222–234.
- 1048 **Smith SY, Collinson ME, Rudall PJ, Simpson DA, Marone F, Stampanoni M.**
 1049 **2009.** Virtual taphonomy using synchrotron tomographic microscopy reveals
 1050 cryptic features and internal structure of modern and fossil plants.
 1051 *Proceedings of the National Academy of Sciences* **106**(29): 12013–12018.
- 1052 **Smyth DR, Bowman JL, Meyerowitz EM. 1990.** Early flower development in
 1053 *Arabidopsis*. *The Plant Cell* **2**(8): 755–767.
- 1054 **Stampanoni M, Groso A, Isenegger A, Mikuljan G, Chen Q, Bertrand A,**
 1055 **Henein S, Betemps R, Frommherz U, Böhler P, et al. 2006.** Trends in
 1056 synchrotron-based tomographic imaging: the SLS experience. *Developments*
 1057 *in X-ray Tomography V*: International Society for Optics and Photonics.
 1058 U199–U212.
- 1059 **Sun K, Hunt K, Hauser BA. 2004.** Ovule abortion in *Arabidopsis* triggered by
 1060 stress. *Plant Physiology* **135**(4): 2358–2367.
- 1061 **Usadel B, Kuschinsky AM, Rosso MG, Eckermann N, Pauly M. 2004.** *RHM2* is
 1062 involved in mucilage pectin synthesis and is required for the development of
 1063 the seed coat in *Arabidopsis*. *Plant Physiology* **134**(1): 286–295.
- 1064 **Voiniciuc C, Yang B, Schmidt MH-W, Günl M, Usadel B. 2015.** Starting to gel:
 1065 how *Arabidopsis* seed coat epidermal cells produce specialized secondary
 1066 cell walls. *International Journal of Molecular Sciences* **16**(2): 3452–3473.
- 1067 **Voiniciuc C, Zimmermann E, Schmidt MH-W, Günl M, Fu L, North HM,**
 1068 **Usadel B. 2016.** Extensive natural variation in *Arabidopsis* seed mucilage
 1069 structure. *Frontiers in Plant Science* **7**(803): 1–14.
- 1070 **Ward D. 2016.** *The Biology of Deserts*: Oxford University Press.
- 1071 **Western TL. 2012.** The sticky tale of seed coat mucilages: production, genetics, and
 1072 role in seed germination and dispersal. *Seed Science Research* **22**: 1–25.

- 1073 **Western TL, Young DS, Dean GH, Tan WL, Samuels AL, Haughn GW. 2004.**
1074 *MUCILAGE-MODIFIED4* encodes a putative pectin biosynthetic enzyme
1075 developmentally regulated by *APETALA2*, *TRANSPARENT TESTA*
1076 *GLABRA1*, and *GLABRA2* in the Arabidopsis seed coat. *Plant Physiology*
1077 **134**(1): 296–306.
- 1078 **Wilhelmsson P, Chandler J, Fernandez-Pozo N, Graeber K, Ullrich K, Arshad**
1079 **W, Khan S, Hofberger J, Buchta K, Edger P, et al. 2019.** Usability of
1080 reference-free transcriptome assemblies for detection of differential
1081 expression: a case study on *Aethionema arabicum* dimorphic seeds. *BMC*
1082 *Genomics* **20**: 1–25.
- 1083 **Windsor JB, Symonds VV, Mendenhall J, Lloyd AM. 2000.** Arabidopsis seed
1084 coat development: morphological differentiation of the outer integument. *The*
1085 *Plant Journal* **22**(6): 483–493.
- 1086 **Witztum A, Gutterman Y, Evenari M. 1969.** Integumentary mucilage as an
1087 oxygen barrier during germination of *Blepharis persica* (Burm.) Kuntze.
1088 *Botanical Gazette* **130**(4): 238–241.
- 1089 **Yang X, Baskin JM, Baskin CC, Huang Z. 2012.** More than just a coating:
1090 Ecological importance, taxonomic occurrence and phylogenetic relationships
1091 of seed coat mucilage. *Perspectives in Plant Ecology, Evolution and*
1092 *Systematics* **14**(6): 434–442.
- 1093 **Yao C, Finlayson SA. 2015.** Abscisic acid is a general negative regulator of
1094 Arabidopsis axillary bud growth. *Plant Physiol* **169**(1): 611–626.
- 1095 **Zhao S, Fernald RD. 2005.** Comprehensive algorithm for quantitative real-time
1096 polymerase chain reaction. *Journal of Computational Biology* **12**(8): 1047–
1097 1064.
1098

1099 **Supplementary Table 1:** Summary of significantly under- and over-represented GO
 1100 terms (Biological Processes only) associated with DEG lists at each morph-specific
 1101 developmental time point comparison (IND vs. DEH).
 1102

GO.ID	Term	Annotated	Significant	Expected	Fisher	FDR
GO:0080058	protein deglutathionylation	3	1	0	0.002	1
GO:0071836	nectar secretion	6	1	0	0.0041	1
GO:0007623	circadian rhythm	170	2	0.12	0.0056	1
GO:0048511	rhythmic process	179	2	0.12	0.0062	1
GO:0015770	sucrose transport	13	1	0.01	0.0088	1
GO:0015766	disaccharide transport	16	1	0.01	0.0108	1
GO:0015772	oligosaccharide transport	16	1	0.01	0.0108	1
GO:0048574	long-day photoperiodism, flowering	30	1	0.02	0.0202	1
GO:0048571	long-day photoperiodism	32	1	0.02	0.0216	1
GO:0006457	protein folding	344	2	0.23	0.0217	1
GO:0018298	protein-chromophore linkage	36	1	0.02	0.0243	1
GO:0009911	positive regulation of flower developmen...	40	1	0.03	0.0269	1
GO:0002238	response to molecule of fungal origin	42	1	0.03	0.0282	1
GO:0006662	glycerol ether metabolic process	42	1	0.03	0.0282	1
GO:0018904	ether metabolic process	44	1	0.03	0.0296	1
GO:0048608	reproductive structure development	1899	4	1.29	0.0307	1
GO:0061458	reproductive system development	1899	4	1.29	0.0307	1
GO:0009414	response to water deprivation	433	2	0.29	0.0334	1
GO:0009415	response to water	438	2	0.3	0.0341	1
GO:2000243	positive regulation of reproductive proc...	52	1	0.04	0.0349	1
GO:0042752	regulation of circadian rhythm	54	1	0.04	0.0362	1
GO:0009416	response to light stimulus	1227	3	0.84	0.0447	1
GO:0048582	positive regulation of post-embryonic de...	71	1	0.05	0.0473	1

1103

a) Buds: BPs up in IND vs. DEH

1104

1105

1106 **Supplementary Table 1: (cont.)**

GO.ID	Term	Annotated	Significant	Expected	Fisher	FDR
GO:0009866	induced systemic resistance, ethylene me...	3	1	0	0.0037	1
GO:0043619	regulation of transcription from RNA pol...	3	1	0	0.0037	1
GO:0006979	response to oxidative stress	550	4	0.67	0.0039	1
GO:0009871	jasmonic acid and ethylene-dependent sys...	4	1	0	0.0049	1
GO:0043618	regulation of transcription from RNA pol...	4	1	0	0.0049	1
GO:0043620	regulation of DNA-templated transcriptio...	4	1	0	0.0049	1
GO:2000068	regulation of defense response to insect	4	1	0	0.0049	1
GO:0051090	regulation of DNA binding transcription ...	9	1	0.01	0.011	1
GO:0009861	jasmonic acid and ethylene-dependent sys...	12	1	0.01	0.0146	1
GO:0006535	cysteine biosynthetic process from serin...	13	1	0.02	0.0158	1
GO:0015743	malate transport	14	1	0.02	0.017	1
GO:0015740	C4-dicarboxylate transport	15	1	0.02	0.0182	1
GO:0009873	ethylene-activated signaling pathway	176	2	0.22	0.0193	1
GO:0000103	sulfate assimilation	18	1	0.02	0.0218	1
GO:0071369	cellular response to ethylene stimulus	194	2	0.24	0.0231	1
GO:0005992	trehalose biosynthetic process	20	1	0.02	0.0242	1
GO:0005991	trehalose metabolic process	21	1	0.03	0.0254	1
GO:0000160	phosphorelay signal transduction system	212	2	0.26	0.0273	1
GO:0006835	dicarboxylic acid transport	29	1	0.04	0.035	1
GO:0009992	cellular water homeostasis	29	1	0.04	0.035	1
GO:0006884	cell volume homeostasis	30	1	0.04	0.0362	1
GO:0006563	L-serine metabolic process	31	1	0.04	0.0373	1
GO:0009269	response to desiccation	32	1	0.04	0.0385	1
GO:0009682	induced systemic resistance	32	1	0.04	0.0385	1
GO:0030104	water homeostasis	33	1	0.04	0.0397	1
GO:0002213	defense response to insect	34	1	0.04	0.0409	1
GO:0002218	activation of innate immune response	37	1	0.05	0.0444	1
GO:0002253	activation of immune response	37	1	0.05	0.0444	1
GO:0046351	disaccharide biosynthetic process	38	1	0.05	0.0456	1

1107

b) Buds: BPs down in IND vs. DEH

1108

1109 **Supplementary Table 1: (cont.)**

GO.ID	Term	Annotated	Significant	Expected	Fisher	FDR
GO:0009860	pollen tube growth	266	57	8.19	0	0
GO:0048868	pollen tube development	314	61	9.67	0	0
GO:0009856	pollination	360	62	11.08	3.30E-29	5.04E-26
GO:0044706	multi-multicellular organism process	361	62	11.11	3.90E-29	5.04E-26
GO:0009827	plant-type cell wall modification	227	46	6.99	6.30E-25	5.69E-22
GO:0009932	cell tip growth	374	58	11.51	6.60E-25	5.69E-22
GO:0000904	cell morphogenesis involved in different...	447	59	13.76	1.20E-21	8.86E-19
GO:0048588	developmental cell growth	479	61	14.74	1.40E-21	9.05E-19
GO:0009826	unidimensional cell growth	531	64	16.35	2.60E-21	1.49E-18
GO:0042545	cell wall modification	397	55	12.22	3.10E-21	1.60E-18
GO:0060560	developmental growth involved in morphog...	641	67	19.73	6.60E-19	3.10E-16
GO:0009664	plant-type cell wall organization	423	51	13.02	4.10E-17	1.77E-14
GO:0016049	cell growth	789	70	24.29	6.50E-16	2.58E-13
GO:0048468	cell development	710	65	21.86	1.80E-15	6.65E-13
GO:0071669	plant-type cell wall organization or bio...	557	55	17.15	1.40E-14	4.82E-12
GO:0000902	cell morphogenesis	762	66	23.46	1.60E-14	5.17E-12
GO:0032989	cellular component morphogenesis	815	68	25.09	3.70E-14	1.13E-11
GO:0048589	developmental growth	866	70	26.66	7.10E-14	2.04E-11
GO:0071555	cell wall organization	830	68	25.55	9.00E-14	2.45E-11
GO:0045229	external encapsulating structure organiz...	885	70	27.24	2.10E-13	5.43E-11
GO:0009723	response to ethylene	440	46	13.54	3.20E-13	7.88E-11
GO:0001101	response to acid chemical	1669	102	51.37	4.60E-12	1.08E-09
GO:0040007	growth	1076	75	33.12	1.40E-11	3.15E-09
GO:0071554	cell wall organization or biogenesis	1157	78	35.61	2.60E-11	5.60E-09
GO:0051704	multi-organism process	2179	120	67.07	3.80E-11	7.86E-09
GO:0010200	response to chitin	437	40	13.45	7.00E-10	1.39E-07
GO:1901700	response to oxygen-containing compound	2472	127	76.09	8.50E-10	1.63E-07
GO:0009725	response to hormone	1990	108	61.26	1.20E-09	2.14E-07
GO:0009753	response to jasmonic acid	521	44	16.04	1.20E-09	2.14E-07
GO:0009719	response to endogenous stimulus	2001	108	61.59	1.70E-09	2.93E-07
GO:1901698	response to nitrogen compound	840	59	25.86	2.10E-09	3.50E-07
GO:0030048	actin filament-based movement	80	16	2.46	2.20E-09	3.55E-07
GO:0080092	regulation of pollen tube growth	21	9	0.65	4.90E-09	7.68E-07
GO:0010243	response to organonitrogen compound	471	40	14.5	6.20E-09	9.43E-07
GO:0030154	cell differentiation	1184	73	36.45	6.60E-09	9.75E-07
GO:0010769	regulation of cell morphogenesis involve...	24	9	0.74	2.00E-08	2.87E-06

1110

1111

c) Flowers: BPs up in IND vs. DEH

1112 **Supplementary Table 1: (cont.)**

GO.ID	Term	Annotated	Significant	Expected	Fisher	FDR
GO:1901659	glycosyl compound biosynthetic process	215	21	2.91	1.40E-12	7.24E-09
GO:0016144	S-glycoside biosynthetic process	176	18	2.39	2.80E-11	3.62E-08
GO:0019758	glucosinolate biosynthetic process	176	18	2.39	2.80E-11	3.62E-08
GO:0019761	glucosinolate biosynthetic process	176	18	2.39	2.80E-11	3.62E-08
GO:1901657	glycosyl compound metabolic process	298	22	4.04	1.10E-10	1.10E-07
GO:0016143	S-glycoside metabolic process	222	19	3.01	1.70E-10	1.10E-07
GO:0019757	glucosinolate metabolic process	222	19	3.01	1.70E-10	1.10E-07
GO:0019760	glucosinolate metabolic process	222	19	3.01	1.70E-10	1.10E-07
GO:0044550	secondary metabolite biosynthetic proces...	389	24	5.27	5.70E-10	3.27E-07
GO:0044272	sulfur compound biosynthetic process	538	26	7.29	1.80E-08	9.30E-06
GO:0006790	sulfur compound metabolic process	799	32	10.83	3.20E-08	1.50E-05
GO:0009851	auxin biosynthetic process	125	11	1.69	1.00E-06	0.00043075
GO:0009684	indoleacetic acid biosynthetic process	102	10	1.38	1.20E-06	0.00047714
GO:0009683	indoleacetic acid metabolic process	103	10	1.4	1.30E-06	0.00047998
GO:0034754	cellular hormone metabolic process	163	12	2.21	2.20E-06	0.00075812
GO:0009850	auxin metabolic process	145	11	1.97	4.50E-06	0.00145378
GO:0042435	indole-containing compound biosynthetic ...	122	10	1.65	6.20E-06	0.00188516
GO:0042430	indole-containing compound metabolic pro...	151	11	2.05	6.60E-06	0.0018953
GO:0010817	regulation of hormone levels	981	31	13.29	8.50E-06	0.00222267
GO:0019748	secondary metabolic process	698	25	9.46	8.60E-06	0.00222267
GO:1901605	alpha-amino acid metabolic process	612	23	8.29	9.40E-06	0.00231374
GO:0008652	cellular amino acid biosynthetic process	520	20	7.05	2.70E-05	0.00634377
GO:1901607	alpha-amino acid biosynthetic process	453	18	6.14	4.50E-05	0.01011326
GO:0065008	regulation of biological quality	1789	44	24.24	5.50E-05	0.01184563
GO:0006520	cellular amino acid metabolic process	794	25	10.76	7.30E-05	0.01509348
GO:0000103	sulfate assimilation	18	4	0.24	8.60E-05	0.01709746
GO:0042446	hormone biosynthetic process	758	24	10.27	9.50E-05	0.01818722
GO:0042445	hormone metabolic process	829	25	11.23	0.00015	0.02769107
GO:0000096	sulfur amino acid metabolic process	374	15	5.07	0.00018	0.03001355
GO:0000097	sulfur amino acid biosynthetic process	333	14	4.51	0.00018	0.03001355
GO:0042178	xenobiotic catabolic process	2	2	0.03	0.00018	0.03001355
GO:0019344	cysteine biosynthetic process	218	11	2.95	0.00019	0.03069094
GO:0008361	regulation of cell size	91	7	1.23	0.00023	0.03602636
GO:0006534	cysteine metabolic process	227	11	3.08	0.00027	0.04104794
GO:0009070	serine family amino acid biosynthetic pr...	230	11	3.12	3.00E-04	0.04430571
GO:0071555	cell wall organization	830	24	11.25	0.00037	0.05312583

1113

1114

d) Flowers: BPs down in IND vs. DEH

1115 **Supplementary Table 1: (cont.)**

GO.ID	Term	Annotated	Significant	Expected	Fisher	FDR
GO:0042546	cell wall biogenesis	392	26	3.9	1.30E-14	5.86E-11
GO:0010413	glucuronoxylan metabolic process	184	19	1.83	2.30E-14	5.86E-11
GO:0045492	xylan biosynthetic process	188	19	1.87	3.40E-14	5.86E-11
GO:0045491	xylan metabolic process	193	19	1.92	5.50E-14	7.11E-11
GO:0010410	hemicellulose metabolic process	204	19	2.03	1.50E-13	9.69E-11
GO:0044038	cell wall macromolecule biosynthetic pro...	204	19	2.03	1.50E-13	9.69E-11
GO:0070589	cellular component macromolecule biosynt...	204	19	2.03	1.50E-13	9.69E-11
GO:0070592	cell wall polysaccharide biosynthetic pr...	204	19	2.03	1.50E-13	9.69E-11
GO:0010383	cell wall polysaccharide metabolic proces...	252	19	2.51	6.70E-12	3.85E-09
GO:0044036	cell wall macromolecule metabolic proces...	329	20	3.27	9.00E-11	4.65E-08
GO:2000652	regulation of secondary cell wall biogen...	20	7	0.2	5.80E-10	2.73E-07
GO:0071554	cell wall organization or biogenesis	1157	35	11.5	1.80E-09	7.16E-07
GO:1903338	regulation of cell wall organization or ...	23	7	0.23	1.80E-09	7.16E-07
GO:0009834	plant-type secondary cell wall biogenesi...	63	8	0.63	1.90E-07	7.02E-05
GO:0044264	cellular polysaccharide metabolic proces...	686	23	6.82	2.80E-07	9.65E-05
GO:0009698	phenylpropanoid metabolic process	204	12	2.03	9.00E-07	0.00029076
GO:0009832	plant-type cell wall biogenesis	212	12	2.11	1.40E-06	0.00042568
GO:0000271	polysaccharide biosynthetic process	645	21	6.41	1.60E-06	0.00045947
GO:0001101	response to acid chemical	1669	37	16.59	1.80E-06	0.00046521
GO:0009699	phenylpropanoid biosynthetic process	145	10	1.44	1.80E-06	0.00046521
GO:0033692	cellular polysaccharide biosynthetic pro...	545	19	5.42	1.90E-06	0.00046767
GO:0006355	regulation of transcription, DNA-templat...	2207	44	21.94	2.50E-06	0.00053844
GO:1903506	regulation of nucleic acid-templated tra...	2207	44	21.94	2.50E-06	0.00053844
GO:2001141	regulation of RNA biosynthetic process	2207	44	21.94	2.50E-06	0.00053844
GO:0051252	regulation of RNA metabolic process	2235	44	22.22	3.50E-06	0.00072366
GO:1901700	response to oxygen-containing compound	2472	47	24.58	3.70E-06	0.00073559
GO:0005976	polysaccharide metabolic process	860	24	8.55	4.00E-06	0.00076578
GO:0034637	cellular carbohydrate biosynthetic proce...	585	19	5.82	5.40E-06	0.00099688
GO:0009889	regulation of biosynthetic process	2594	48	25.79	6.00E-06	0.00106945
GO:0044262	cellular carbohydrate metabolic process	832	23	8.27	7.60E-06	0.00130948
GO:0006351	transcription, DNA-templated	2483	46	24.69	1.00E-05	0.00161531
GO:0097659	nucleic acid-templated transcription	2485	46	24.71	1.00E-05	0.00161531
GO:0032774	RNA biosynthetic process	2492	46	24.78	1.10E-05	0.001723
GO:0019219	regulation of nucleobase-containing comp...	2346	44	23.33	1.20E-05	0.00182435
GO:0050794	regulation of cellular process	4754	72	47.27	1.50E-05	0.00221529
GO:0009808	lignin metabolic process	83	7	0.83	1.80E-05	0.0025845

1116

1117

e) **Fruits: BPs up in IND vs. DEH**

1118 **Supplementary Table 1: (cont.)**

GO.ID	Term	Annotated	Significant	Expected	Fisher	FDR
GO:1901700	response to oxygen-containing compound	2472	68	30.3	1.10E-11	4.14E-08
GO:0010200	response to chitin	437	26	5.36	2.30E-11	4.14E-08
GO:0009725	response to hormone	1990	59	24.39	2.50E-11	4.14E-08
GO:0009719	response to endogenous stimulus	2001	59	24.53	3.20E-11	4.14E-08
GO:0010243	response to organonitrogen compound	471	26	5.77	1.20E-10	1.24E-07
GO:0010033	response to organic substance	2954	73	36.21	2.30E-10	1.98E-07
GO:0032870	cellular response to hormone stimulus	1137	40	13.94	8.40E-10	6.20E-07
GO:0071495	cellular response to endogenous stimulus	1147	40	14.06	1.10E-09	6.89E-07
GO:0006952	defense response	1619	49	19.85	1.20E-09	6.89E-07
GO:0042221	response to chemical	3903	85	47.84	2.00E-09	9.48E-07
GO:0009612	response to mechanical stimulus	59	10	0.72	2.20E-09	9.48E-07
GO:1901698	response to nitrogen compound	840	33	10.3	2.20E-09	9.48E-07
GO:0009755	hormone-mediated signaling pathway	979	35	12	7.90E-09	3.14E-06
GO:0042493	response to drug	1138	38	13.95	1.00E-08	3.69E-06
GO:0070887	cellular response to chemical stimulus	1577	46	19.33	1.40E-08	4.52E-06
GO:0071310	cellular response to organic substance	1469	44	18.01	1.40E-08	4.52E-06
GO:0009611	response to wounding	363	20	4.45	2.10E-08	6.39E-06
GO:0001101	response to acid chemical	1669	47	20.46	2.80E-08	8.04E-06
GO:0042446	hormone biosynthetic process	758	29	9.29	4.30E-08	1.17E-05
GO:0014070	response to organic cyclic compound	919	32	11.27	7.10E-08	1.83E-05
GO:0042445	hormone metabolic process	829	30	10.16	8.40E-08	2.07E-05
GO:0050832	defense response to fungus	398	20	4.88	9.40E-08	2.21E-05
GO:0007165	signal transduction	2000	51	24.52	1.50E-07	3.37E-05
GO:0002679	respiratory burst involved in defense re...	120	11	1.47	2.50E-07	5.17E-05
GO:0045730	respiratory burst	120	11	1.47	2.50E-07	5.17E-05
GO:0023052	signaling	2057	51	25.22	3.70E-07	7.36E-05
GO:0050896	response to stimulus	6500	113	79.68	3.90E-07	7.47E-05
GO:0006950	response to stress	4020	80	49.28	5.90E-07	0.00010892
GO:1901701	cellular response to oxygen-containing c...	1029	32	12.61	9.00E-07	0.00016042
GO:0010817	regulation of hormone levels	981	31	12.03	9.80E-07	0.00016885
GO:0071229	cellular response to acid chemical	835	28	10.24	1.10E-06	0.00017768
GO:0007154	cell communication	2384	55	29.22	1.10E-06	0.00017768
GO:0009751	response to salicylic acid	521	21	6.39	1.70E-06	0.00026628
GO:0033993	response to lipid	948	29	11.62	4.40E-06	0.00066893
GO:0045088	regulation of innate immune response	476	19	5.83	6.20E-06	0.00091565
GO:0050776	regulation of immune response	477	19	5.85	6.40E-06	0.00091893

1119

1120

f) Fruits: BPs down in IND vs. DEH

1121

Supplementary Table 2: *Aethionema arabicum* orthologues of genes and/or proteins with mucilage phenotypes identified from *Arabidopsis*

1122

(derived from Francoz *et al.*, 2015), used to create a hypothesised regulatory network (Figs. 5 and S4) for mucilage biosynthesis.

1123

Pathway	<i>Arabidopsis thaliana</i> identifier	Gene	<i>Aethionema arabicum</i> identifier	TAIR10: other names	Amino acid identity with <i>Arabidopsis</i> orthologue (%)	Max score	Total score	Query cover	E value	Ident	Reference
Mucilage secretion / stabilisation	AT1G09540	MYB61	AA42G00001	ARABIDOPSIS THALIANA MYB DOMAIN PROTEIN 61, ATMYB61, MYB DOMAIN PROTEIN 61, MYB61	63.73%	416	416	100%	2.00E-146	63.73%	Penfield <i>et al.</i> (2001) <i>Plant Cell</i> 13: 2777-2791
	AT1G52880	NARS2/NAM	?	ANAC018, ARABIDOPSIS NAAC DOMAIN CONTAINING PROTEIN 18, ATNAM, NAAC-REGULATED SEED MORPH	0.00%						Huang <i>et al.</i> (2011) <i>Plant Physiol.</i> 156: 491-502
	AT1G56850	MYB75	AA39G00757	ARABIDOPSIS THALIANA PRODUCTION OF ANTHOCYANIN PIGMENT 1, ATMYB75, ATPAPT, MYB DOMAIN P	62.80%	270	270	98%	2.00E-91	62.80%	Bhargava <i>et al.</i> (2013) <i>Plant</i> 237: 1199-1211
	AT1G62990	KNAT7	AA53G001391	IRREGULAR XYLEM 11, IRX11, KNAT7, KNOTTED-LIKE HOMEBOX OF ARABIDOPSIS THALIANA 7	83.55%	511	511	100%	0	83.55%	Bhargava <i>et al.</i> (2013) <i>Plant</i> 237: 1199-1211
	AT1G63550	EGL3	AA53G001357	ATEGL3, ATMYC-2, EGL1, EGL3, ENHANCER OF GLABRA 3	75.89%	915	915	100%	0	75.89%	Gonzalez <i>et al.</i> (2009) <i>Dev. Biol.</i> 325: 412-421
	AT1G76880	DF1	AA31G002986	DF1	66.74%	519	608	92%	0	66.74%	Vasilevski <i>et al.</i> (2012) <i>Mol. Biosyst.</i> 8: 2566-2574
	AT1G79840	GL2	AA89G00008	GL2, GLABRA 2	81.11%	1250	1250	99%	0	81.11%	Westem <i>et al.</i> (2011) <i>Plant Physiol.</i> 127: 998-1011
	AT2G32700	MUM1/LUH	AA32G00448	LEUNIG, HOMOLOG, LUH, MUCILAGE-MODIFIED 1, MUM1	84.01%	1308	1308	100%	0	84.01%	Westem <i>et al.</i> (2011) <i>Plant Physiol.</i> 156: 491-502
	AT2G32760	TTG2/DLS1	AA60G00054	ATWRK44, DR, STRANGELOVE 1, DLS1, 1, TRANSPARENT TESTA GLABRA 2, TTG2, WRKY44	61.56%	489	489	99%	7.00E-173	61.56%	Johnson <i>et al.</i> (2002) <i>Plant Cell</i> 14: 1359-1375
	AT3G13540	MYB5	AA26G00051	ATMYB5, MYB DOMAIN PROTEIN 5, MYB5	69.83%	318	318	95%	1.00E-110	69.83%	Gonzalez <i>et al.</i> (2008) <i>Dev. Biol.</i> 325: 412-421
	AT3G13510	NARS1/NAC2	AA15G00071	ANAC096, ARABIDOPSIS NAAC DOMAIN CONTAINING PROTEIN 56, ATNAC2, NAAC DOMAIN CONTAINING PRO	66.49%	430	430	100%	2.00E-151	66.49%	Kumeda <i>et al.</i> (2008) <i>Plant Cell</i> 20: 2631-2642
	AT4G09820	TT8	AA21G00569	ATTT8, BHLH42, TRANSPARENT TESTA 8, TT8	75.83%	329	329	33%	6.00E-106	75.83%	Gonzalez <i>et al.</i> (2009) <i>Dev. Biol.</i> 325: 412-421; Baudry <i>et al.</i> (2006) <i>Plant J.</i> 46: 768-779
	AT4G21030	DOF4.2	?	ATDOF4.2, ATDOF4.2	0.00%						Zou <i>et al.</i> (2013) <i>Biochem. J.</i> 448: 373-388
	AT4G32551	LUG	?	LEUNIG, LUG, RONZ, ROTUNDA 2	0.00%						Walker <i>et al.</i> (2011) <i>Plant Physiol.</i> 156: 46-60; Bai <i>et al.</i> (2011) <i>J. Integr. Plant Biol.</i> 53: 399-408
	AT4G36920	AP2	AA30G00232	AP2, APETALA 2, ATP2, FL1, FLO, FLORAL MUTANT 2, FLOWER 1	68.39%	546	546	100%	0	68.39%	Westem <i>et al.</i> (2011) <i>Plant Physiol.</i> 127: 998-1011
AT5G24550	TTG1	AA13G00129	ATTTG1, TRANSPARENT TESTA GLABRA 1, TTG, TTG1, UNARMED 23, URM23	89.83%	637	637	100%	0	89.83%	Gonzalez <i>et al.</i> (2009) <i>Dev. Biol.</i> 325: 412-421; Westem <i>et al.</i> (2011) <i>Plant Physiol.</i> 127: 998-1011	
AT5G35550	TT2	AA64G00001	ATMYB23, ATTT2, MYB DOMAIN PROTEIN 23, MYB23, TRANSPARENT TESTA 2, TT2	70.61%	344	344	100%	8.00E-121	70.61%	Gonzalez <i>et al.</i> (2009) <i>Dev. Biol.</i> 325: 412-421	
AT5G40330	MYB23	AA87G00136	ATMYB23, ATMYB23, MYB DOMAIN PROTEIN 23, MYB23	68.35%	300	300	99%	2.00E-104	68.35%	Li <i>et al.</i> (2009) <i>Plant Cell</i> 21: 72-89; Matsui <i>et al.</i> (2005) <i>Plant Cell Physiol.</i> 46: 147-155	
AT5G42300	ATS/KAN4	AA30G00207	ABERRANT TESTA SHAPE, ATS, KAN4, KANADI 4	59.65%	270	270	98%	3.00E-91	59.65%	Leon-Klosterziel <i>et al.</i> (1994) <i>Plant Cell</i> 6: 385-392; McAbee <i>et al.</i> (2006) <i>Plant J.</i> 46: 522-531	
AT5G65410	ATHB23/ZFH2	AA40G00084	ARABIDOPSIS THALIANA HOMEBOX TRANSFERASE-LIKE 5, GATL5	53.97%	254	254	100%	4.00E-84	53.97%	Fuerrado <i>et al.</i> (2011) <i>Plant Cell</i> 23: 1772-1794	
AT5G66730	GATL5	AA80G00257	ENHYDROUS, ENY, IDDI, INDETERMINATE DOMAIN 1	76.80%	682	682	100%	0	76.80%	Fuerrado <i>et al.</i> (2011) <i>Plant Cell</i> 23: 1772-1794	
AT1G02720	GAU11	AA39G00047	GALACTURONOSYLTRANSFERASE 11, GAU11	80.18%	532	532	86%	0	80.18%	Kong <i>et al.</i> (2013) <i>Plant Physiol.</i> 163: 1203-1217	
AT1G18580	MOR1	AA39G00017	GALACTURONOSYLTRANSFERASE 11, GAU11	89.61%	998	998	100%	0	89.61%	Cattali <i>et al.</i> (2009) <i>Mol. Plant</i> 2: 1000-1014	
AT1G53500	MUM4/RHM2	AA15G00120	ARABIDOPSIS THALIANA MUCILAGE-MODIFIED 4, ARABIDOPSIS THALIANA RHAMNANOSE BIOSYNTHESIS 2,	92.04%	1249	1249	99%	0	92.04%	Westem <i>et al.</i> (2011) <i>Plant Physiol.</i> 164: 1842-1856	
AT5G22740	CSLA2	AA80G00287	ARABIDOPSIS THALIANA CELLULOSE SYNTHASE-LIKE A02, ARABIDOPSIS THALIANA CELLULOSE SYNTH	96.80%	1071	1071	100%	0	96.80%	Yu <i>et al.</i> (2014) <i>Plant Physiol.</i> 164: 1842-1856	
AT1G09330	ECH	AA21G00445	ECH, ECHINOA	80.57%	302	302	98%	2.00E-106	80.57%	Gendre <i>et al.</i> (2013) <i>Plant Cell</i> 25: 2633-2646; McFarlane <i>et al.</i> (2013) <i>Plant Cell Physiol.</i> 54: 1867-1880	
AT1G63930	ROH1	AA53G01338	FROM THE CZECH ROH MEANING CORNER, ROH1	92.18%	350	350	100%	6.00E-120	92.18%	Kulich <i>et al.</i> (2010) <i>New Phytol.</i> 188: 615-625	
AT2G18840	YIP4A	AA60G00177	YIP4A, YPTIRAB GTPASE INTERACTING PROTEIN 4A	89.51%	443	443	100%	6.00E-159	89.51%	Gendre <i>et al.</i> (2013) <i>Plant Cell</i> 25: 2633-2646	
AT2G35630	MOR1	AA90G00090	GEM1, MICROTUBULE ORGANIZATION 1, MOR1	90.70%	3618	3618	99%	0	90.70%	McFarlane <i>et al.</i> (2008) <i>Plant</i> 237: 1363-1375	
AT3G10380	SEC8	AA93G00210	ATSEC8, SEC8, SUBUNIT OF EXOCYST COMPLEX 8	91.44%	964	964	90%	0	91.44%	Kulich <i>et al.</i> (2010) <i>New Phytol.</i> 188: 615-625	
AT4G30260	YIP4B	?	YIP4B, YPTIRAB GTPASE INTERACTING PROTEIN 4B	0.00%						Gendre <i>et al.</i> (2013) <i>Plant Cell</i> 25: 2633-2646	
AT5G03540	EXO70A1	AA19G00229	ATEX070A1, EXO70A1, EXOCYST SUBUNIT EXO70 FAMILY PROTEIN A1	91.61%	1174	1174	98%	0	91.61%	Kulich <i>et al.</i> (2010) <i>New Phytol.</i> 188: 615-625	
AT2G47670	PME1B	AA21G00495	PECTIN METHYLSTERASE INTERACTING PROTEIN 4A	67.74%	239	239	91%	6.00E-81	67.74%	Saez-Aguayo <i>et al.</i> (2013) <i>Plant Cell</i> 25: 306-323	
AT3G09820	ADK1	AA60G00055	ADENOSINE KINASE 1, ADK1, ATADK1	83.56%	501	501	100%	0	83.56%	Moffatt <i>et al.</i> (2002) <i>Plant Physiol.</i> 128: 812-821	
AT4G28370	FLY1	AA22G00020	FLY1, FLYING SAUCER 1	86.92%	994	994	98%	0	86.92%	Voinicuc <i>et al.</i> (2013) <i>Plant Cell</i> 25: 944-959	
AT5G49360	BXL1/GH3	AA58G00011	ATBXL1, BETA-XYLOSIDASE 1, BXL1	86.93%	1387	1387	99%	0	86.93%	Aseovski <i>et al.</i> (2009) <i>Plant Physiol.</i> 150: 1219-1234	
AT5G38000	MUM2/BGAL6	AA40G00117	BETA-GALACTOSIDASE 6, BGAL6, MUCILAGE-MODIFIED 2, MUM2	89.72%	414	414	96%	3.00E-142	89.72%	Dean <i>et al.</i> (2007) <i>Plant Cell</i> 19: 4007-4021; Westem <i>et al.</i> (2011) <i>Plant Physiol.</i> 127: 998-1011	
AT2G35820	FEI2	AA90G00092	FEI2, FEI2	87.67%	1031	1031	100%	0	87.67%	Harpaaz-Saad <i>et al.</i> (2011) <i>Plant J.</i> 68: 941-953	
AT3G29810	COBL2	?	COBL2, COBRA-LIKE PROTEIN 2, PRECURSOR	0.00%						Ben-Dov <i>et al.</i> (2015) <i>Plant Physiol.</i> 167: 711-724	
AT3G46550	SOSS5	AA16G00041	FASCICULINE-LIKE ARABINOGLYCAN-PROTEIN 4, FLA4, SALT OVERLY SENSITIVE 5, SOSS5	85.25%	648	648	99%	0	85.25%	Harpaaz-Saad <i>et al.</i> (2011) <i>Plant J.</i> 68: 941-953; Griffiths <i>et al.</i> (2014) <i>Plant Physiol.</i> 165: 991-1004	
AT5G09870	MUM3/CEAS5	AA40G00210	CELLULOSE SYNTHASE 5, CEAS5, MUCILAGE-MODIFIED 3, MUM3	86.85%	1417	1417	67%	0	86.85%	Harpaaz-Saad <i>et al.</i> (2011) <i>Plant J.</i> 68: 941-953; Sullivan <i>et al.</i> (2011) <i>Plant Physiol.</i> 156: 1725-1739	
AT2G21770	CESA9	AA48G00095	CELLULOSE SYNTHASE A9, CESA9, CESA9	76.82%	1362	1362	96%	0.00E+00	76.82%	Stork <i>et al.</i> (2010) <i>Plant Physiol.</i> 153: 560-589; Mendau <i>et al.</i> (2011) <i>Plant Physiol.</i> 157: 441-453	
AT3G09920	PRX38/PER36	AA13G00026	PER36, PEROXIDASE 36, PRX36	72.49%	508	508	99%	0	72.49%	Kumeda <i>et al.</i> (2013) <i>Plant Cell</i> 25: 1355-1367	
AT4G39350	CEB2	AA20G00013	ATCEB2, AT-THA, CELLULOSE SYNTHASE A2, CESA2	89.65%	1936	1936	100%	0	89.65%	Mendu <i>et al.</i> (2011) <i>Plant Physiol.</i> 157: 441-453	
AT5G67360	SBSA1	AA41G00032	ARA12, SBS1, 7, SUBTILISIN-LIKE SERINE PROTEASE 17	87.57%	898	898	68%	0	87.57%	Rautengarten <i>et al.</i> (2008) <i>Plant J.</i> 54: 466-480	
AT1G79840	GA3OX4	AA31G00896	ATGID1A, GA INSENSITIVE DWARF1A, GID1A	67.04%	513	513	98%	0	67.04%	Kim <i>et al.</i> (2005) <i>Plant Cell</i> 17: 1317-1325	
AT1G30510	GID1A	AA10G00111	ATGID1A, GA INSENSITIVE DWARF1A, GID1A	67.04%	513	513	98%	0	67.04%	Kim <i>et al.</i> (2005) <i>Plant Cell</i> 17: 1317-1325	
AT1G30310	GAT1	AA61G00628	ATGID1B, GA INSENSITIVE DWARF1B, GID1B	85.12%	642	642	100%	0	85.12%	Kim <i>et al.</i> (2007) <i>Plant J.</i> 50: 959-966	
AT4G02780	GAT1	AA32G00309	ABC33, ARABIDOPSIS THALIANA ENT-COPAL-YL-DIPHOSPHATE SYNTHETASE 1, ATPCS1, CPP SYNTHASE	73.55%	1131	1131	94%	0	73.55%	Uchi <i>et al.</i> (2007) <i>Plant J.</i> 50: 959-966	
AT5G67030	SKB1	AA80G0025	ABA DEFICIENT 1, ABA1, ARABIDOPSIS THALIANA ABA DEFICIENT 1, ARABIDOPSIS THALIANA ZEAXANTHIN	85.16%	1149	1149	100%	0	85.16%	Karsen <i>et al.</i> (1983) <i>Plant</i> 157: 158-165	
AT2G27600	SKO1	AA32G00917	ATSKO1, SKO1, SUPPRESSOR OF K+ TRANSPORT GROWTH DEFECT11, VACUOLAR PROTEIN SORTING 4, V	96.32%	872	872	100%	0	96.32%	Shahrani <i>et al.</i> (2010) <i>Plant Signal Behav.</i> 5: 1308-1310	
AT5G21580	PRX56	AA40G00570	PEROXIDASE 56, PRX56	79.73%	503	503	100%	0	79.73%	Panikashvili <i>et al.</i> (2014) <i>Plant Signal Behav.</i> 9: e817734	
AT5G23400	DCR	AA51G00266	DCR, DEFECTIVE IN CUTICULAR RIDGES, EMBS3009, EMBRYO DEFECTIVE 3009, PELL3, PERMEABLE LEAVE	82.31%	226	226	29%	2.00E-46	82.31%	Ranikashvili <i>et al.</i> (2009) <i>Plant Physiol.</i> 151: 1773-1789; Rami <i>et al.</i> (2010) <i>J. Biol. Chem.</i> 285: 38337-38347	
AT5G63840	RSW3/GH31	AA46G00121	PRIORITY IN SWEET LIFE 5, PSL5, RADIAL SWELLING 3, RSW3	89.67%	1742	1742	99%	0	89.67%	Burn <i>et al.</i> (2002) <i>Plant J.</i> 32: 949-960	

1124 **Supplementary Table 3:** List of primers used for quantitative RT-PCR analysis.

1125

Name	<i>Aethionema arabicum</i> (genome v2.5) ID	Sequence (5' – 3')
AA19G00315_2 - 546 F	AA19G00315	TGGTGCACGTGAGCTCTTAG
AA19G00315_2 - 723 R		ATCTTTGGTGGGAGTGCTGG
AFP_1 - 415 F	AA44G00404	AGAACGGTGGCTGTAAGTGG
AFP_1 - 617 R		GATTCCTTTTCCCGGCATGC
CMSP_1 - 239 F	AA10G00283	TTGGTCCGGCTTTGTCTTTG
CMSP_1 - 445 R		CACCAAAGTTATCATGGTTTCCCC
AP2_1 - 271 F	AA30G00232	AAACGGTGAAAGCGGTTGTG
AP2_2 - 399 R		GAGCTCCGTGATCTTGGACC
GL2_1 - 377 F	AA89G00009	ATCCGGACGAGAAGCAAAGG
GL2_1 - 511 R		CTTTCAGCAGCGAGTTCTCG
MEEA14_1 - 121 F	AA123G00058	GTGGTTCGGTGTTCAGCAC
MEEA14_1 - 268 R		AGTCATCACCTTCCAGCGTC
MYB61_1 - 247 F	AA42G00001	GCAGTCCTCGGAAACAGATG
MYB61_1 - 421 R		TTGCAGAAGAAGTTGAAGCAGG
TTG1_1 - 274 F	AA13G00129	CTTCGTCGCTCATCTACCGG
TTG1_1 - 414 R		CAACGGTGACAGAACTCAC
CESA2_2 - 907 F	AA20G00013	TGTGAGATTTGGTTGCTGTTTC
CESA2_2 - 1,074 R		TGCTAATCCTGATGGCTTCCC
MUM3/CESA5_2 - 652 F	AA4G00210	CGAATGGAGGAATGGAAGCG
MUM3/CESA5_2 - 783 R		TCGTGATAACGGTTGCCTCC
MUM4/RHM2_1 - 1,469 F	AA15G00120	CAGAGGGGTCAGGGATTGG
MUM4/RHM2_1 - 1,640 R		ATGAAGTTTCGCGGGTTCTC
PMEI6_1 - 180 F	AA21G00495	TTCGCCATTCTCCTCTCTCG
PMEI6_1 - 293 R		CGCCGCGTTTTGAGTAAGAG
MEEA59_2 - 367 F	AA30G00244	GGTGAGGAGAGTGTAACCGC
MEEA59_2 - 454 R		CATTTGTCGCCGGATTCCC

1126

6. Effect of seed dimorphism on seedling physiology and abiotic stress tolerance

6.1 Introduction

Chapter 6 characterises the possible consequences of *Ae. arabicum* seed dimorphism on seedling survival under a range of abiotic stresses representative of an unpredictable environment, via a large-scale screening of developmental traits. The underlying hypothesis is that, though dry seed, seed germination, and seed dormancy traits show dimorphic responses, the seedling stage is not thought to exhibit dimorphism. Exposure to distinct temperature, water availability, and salt stress regimes was used to elucidate similarities and/or differences between M⁺ and M⁻ seedling phenotypes. In addition to physiological assays, a comprehensive transcriptome time-course dataset elucidates when, during the transition from germinating seeds to growing seedlings, differences in expression programmes are “reset”, or whether they remain present at a later physical or physiological seedling growth stage. Work presented in this chapter presents current knowledge and future research directions regarding seedling physiology in *Ae. arabicum*, and has thus not been prepared for publication.

6.1.1 *Dimorphic post-germination seedling growth*

Irrespective of the reason(s) underlying variations in diaspore size, morphology, colour *etc.* (discussed in Chapter 1.2), heteromorphic differences may confer effects on germination percentages, rates, and ultimately timing of

seedling growth and survival. Transcriptome differences are so far especially observed at the dry seed (Wilhelmsson *et al.*, 2019) and germination stage (Chandler *et al.*, unpublished), where the radicle emerges from the seed (M^+) or from the fruit (radicle of M^- seed protruding through IND pericarp). Following this very different strategy, seedlings grow to an adult dimorphic plant bearing both M^+ and M^- seeds, no matter of their “origin” (Lenser *et al.*, 2016). Some differences in life history stages of plants grown from different morphs of seed heteromorphic species exist in the literature (Mandák, 1997; Imbert, 2002; Yang *et al.*, 2014; Song *et al.*, 2017), but data showing how plants grown from different diaspore morphs perform as seedlings are lacking. Of particular interest is the effect of dimorphism on seedling physiology and seed proliferation of the offspring, derived from different seed morphs, under different environmental stresses (Mandák & Pyšek, 2005; Yao *et al.*, 2010).

Seedlings in the fruit and seed heteromorphic species *Diptychocarpus strictus* (Brassicaceae) did not show morph-specific effects on phenology, growth, morphology and survival after 20 days of growth. Plants derived from two seed morphs germinating in the same season or under the same watering schedule also did not differ in life history traits (Lu *et al.*, 2010; Lu *et al.*, 2014). However, in *Cakile* spp., where the heteromorphism is between proximal and distal segments of a fruit and its seeds, Zhang (1993) suggested both *C. edentula* seed germination and subsequent growth was dependent on seed mass rather than seed morph; plants derived from large seeds generally had larger leaf area, shoot to root ratio, biomass, and smaller leaf area ratio than those from small seeds. The adaptive significance of this dimorphism is that it increases

the probability of seedling emergence from different depths of seed burial; for example, it is thought sand accretion acts as a strong selective force in the evolution of large seed size, which in turn increases seedling survivability within shingle or dune shoreline microhabitats (Maun & Payne, 1989).

These phenotypes relate to vigour, a trait defined as “the sum of those properties that determine the activity and performance of seed lots of acceptable germination in a wide range of environments” (ISTA, 2015). Mimicking stressful environmental conditions unfavourable to seedling development via seedling vigour tests, allows the investigation of how seed lots withstand one or more of these stresses. These tests provide a better understanding of vigour as a trait defining the potential performance of viable seeds and their complex interactions with the environment (Finch-Savage & Bassel, 2015). The consequence of the *Ae. arabicum* seed dimorphism in the context of seedlings remains completely unknown.

Determining the degree to which seedling morphs differ in their abiotic stress responses assumes differences between seed morphs persist post-germination. However, data have shown that plants originating from M⁺ or M⁻ seeds are indistinguishable upon maturity (Lenser *et al.*, 2016). It is well documented that endosperm and cotyledon storage reserves, particularly lipids acting as the major metabolic substrate during germination, are critical for early growth during heterotrophic development of young seedlings (Elamrani *et al.*, 1992). Reserve utilisation and the autonomy conferred on seedling growth prior to emergence provide the ultimate link between

germination and autotrophic growth. It is during this particular stage that initial differences between *Ae. arabicum* M⁺ and M⁻ seeds are hypothesised to become less evident after completion of germination, “resetting” to an adult plant lacking the phenotypic differences present in earlier life cycle stages.

6.2 Aims and objectives

This chapter will test the raised hypotheses by investigating the possible consequences of the seed dimorphism (M⁺ vs. M⁻) on the emerging *Ae. arabicum* seedlings (Figure 6-1). The specific objectives were:

- to use quantitative imaging data to compare development of seedling growth in response to abiotic stress factors affecting establishment;
- to investigate the tissue-specific transcriptional profiles of seedlings through comparative time-course investigations of differentially expressed genes during germination and early seedling growth.

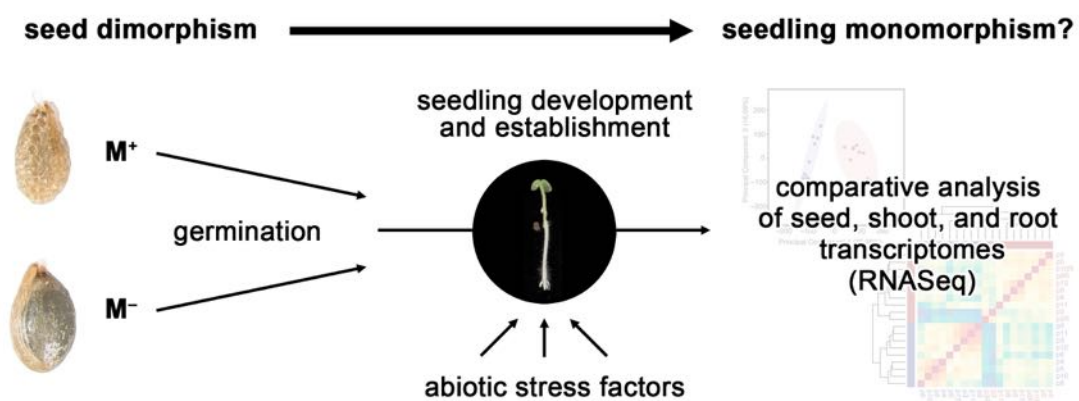


Figure 6-1: Schematic summary of proposed seedling work, investigating the effect of seed dimorphism on seedling physiology and abiotic stress tolerance during establishment. M⁺ = mucilaginous. M⁻ = non-mucilaginous.

6.3 Results

6.3.1 Germination optima based on temperature profiling

To first establish an optimal temperature for seedling growth, germination optima were investigated. Comparisons of final germination percentage (G_{\max}) and rates for cumulative germination to reach 50% of its maximum (GR_{50}) revealed an optimal temperature (T_{opt}) for M^+ , M^- , and IND fruits as 14°C (Figure 6-2). The IND fruit batch, however, exhibited some degree of dormancy across the temperature gradient; thus, the effects of abiotic stresses focussed on M^+ and M^- seeds (manually extracted from IND fruits) only.

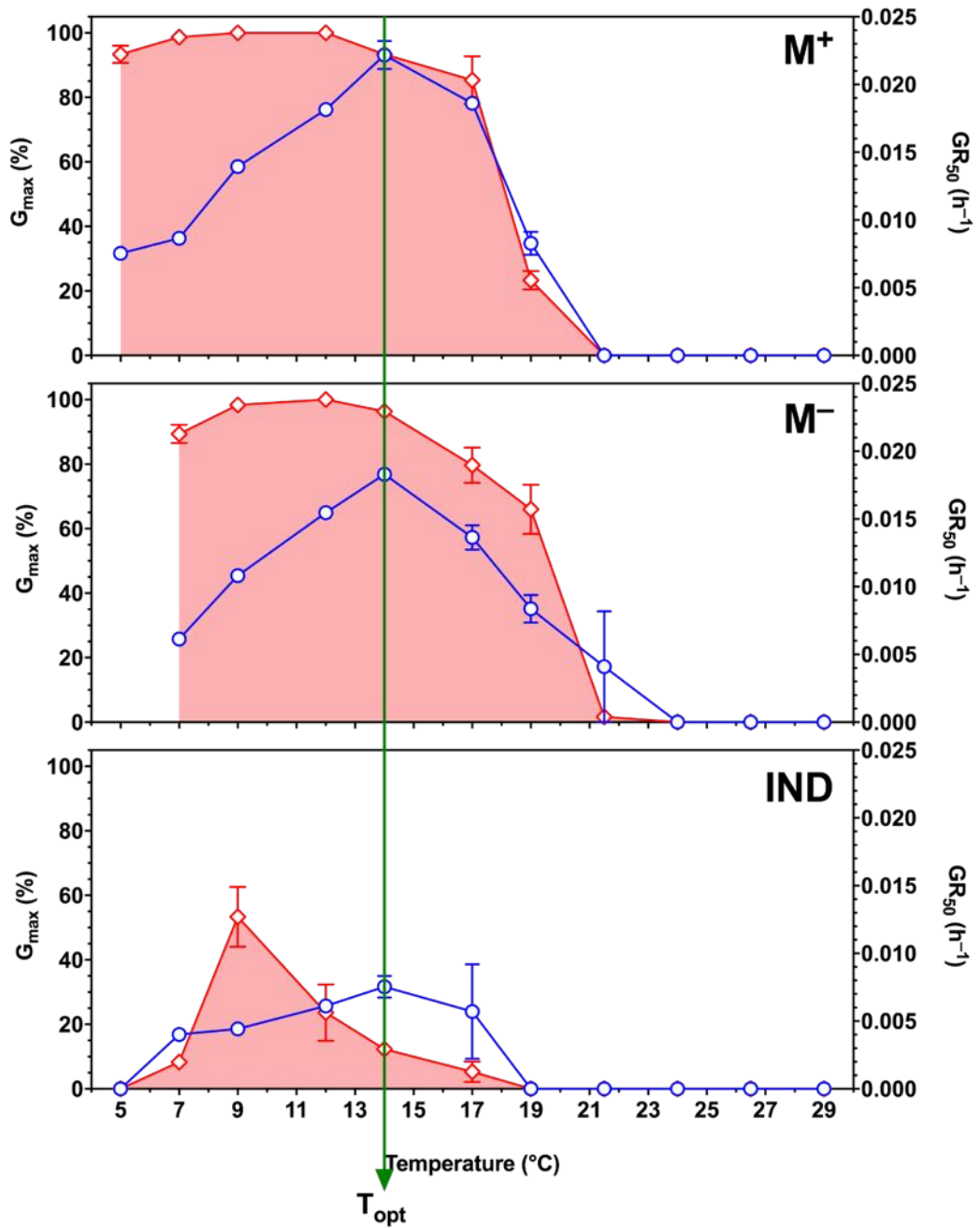


Figure 6-2: Temperature profile for freshly-harvested M⁺ seed, M⁻ seed, and IND fruit germination. Shown is the mean maximum germination percentage (○ G_{max}) and the rate until cumulative germination reached 50% of its maximum (◇ GR₅₀). The optimal temperature (T_{opt}) for completion of germination was considered as 14°C. Error bars = ± 1 SEM. N = 3, each with approx. 30 seeds.

6.3.2 Growth responses under water deficit (osmotic stress) conditions

To study the effect of osmotic stress on the growth of *Ae. arabicum* seedlings, M⁺ and M⁻ seeds that had just completed germination were transplanted onto plates with lowered water potentials using high-molecular weight polyethylene glycol (PEG). Since PEG cannot be mixed with molten agar at high concentrations, an overlay method was employed, allowing low water potentials in the already solid agar medium to be reproducibly attained (van der Weele *et al.*, 2000; Verslues & Bray, 2004).

After almost four weeks of vertical growth, seedling morphs did not differ in their total length and growth rates under three different concentrations of PEG (Figure 6-3). ANOVA revealed there were no significant morph-specific differences in seedling size at 10 mM ($P = 0.838$), 20 mM ($P = 0.818$), or 30 mM ($P = 0.157$) PEG. At control conditions, however, differences between M⁺ and M⁻ seedlings were observed ($P = 0.019$), which were found to be attributed to measurements taken at 6 ($P = 0.011$), 9 ($P = 0.017$), and 12 ($P = 0.047$) days only (Figure 6-3).

ANOVA of the growth rates revealed no differences between M⁺ and M⁻ seedlings across water potentials. Similar patterns of growth were observed at control ($P = 0.548$), 10 mM ($P = 0.994$), 20 mM ($P = 0.698$), and 30 mM ($P = 0.248$) conditions. Seedlings at control conditions potentially indicated longer M⁻ seedlings; however, that the growth rates showed no statistical differences suggests an absence of a morph-specific response to overall seedling growth under osmotic stress.

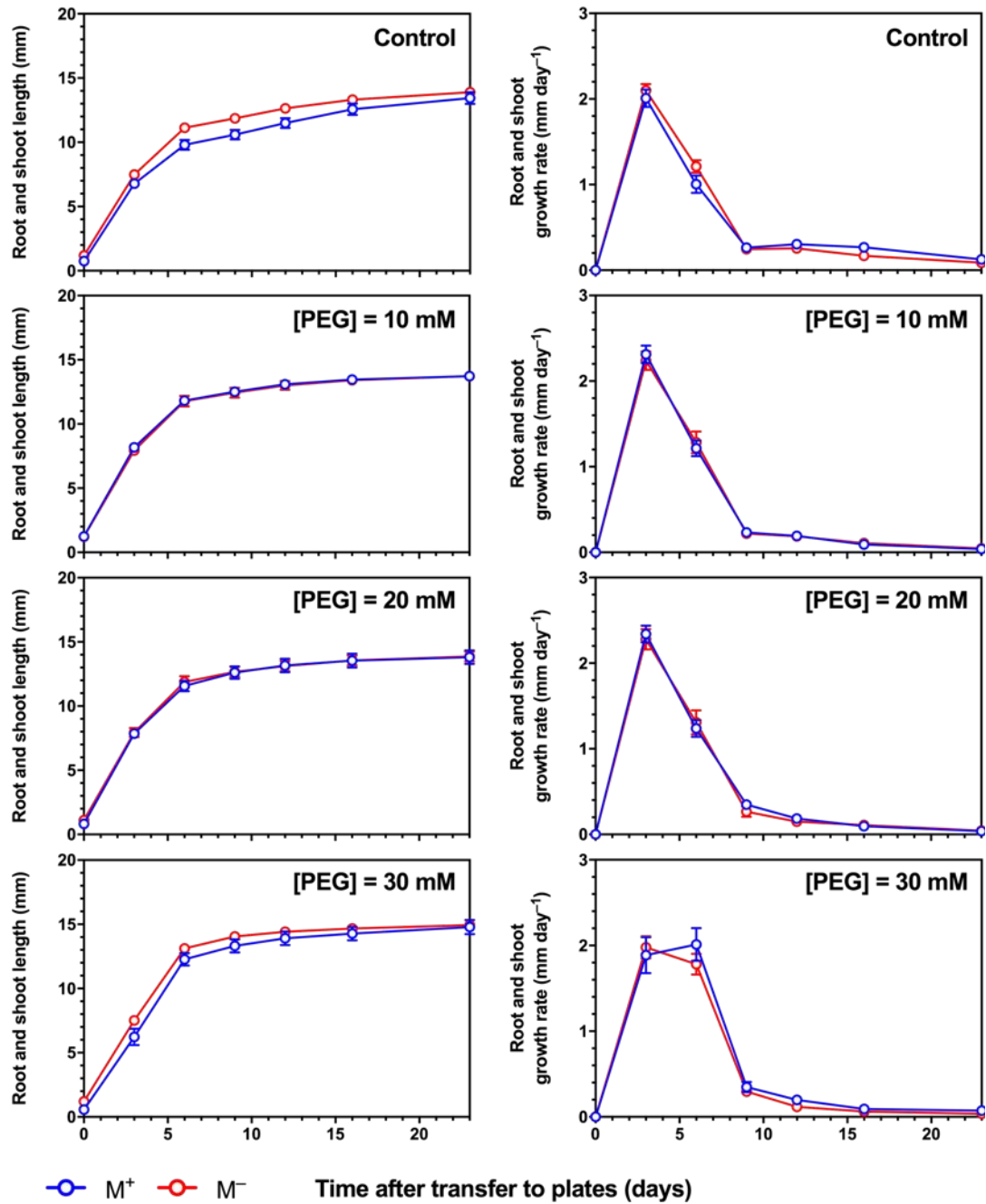


Figure 6-3: *Ae. arabicum* seedling growth responses to increasing concentrations of polyethylene glycol (PEG). The means of combined root and shoot lengths, and their associated growth rates, were calculated over an experimental period of 23 days. Error bars = ± 1 SEM. N = 3, each with 7 seedlings.

Root and shoot tissue were separated at the end of the experimental conditions. ANOVA revealed neither shoot fresh weights ($P = 0.145$) nor root fresh weights ($P = 0.502$) had a significant morph-specific difference at each PEG concentration, thereby supporting the seedling length and growth rate data above.

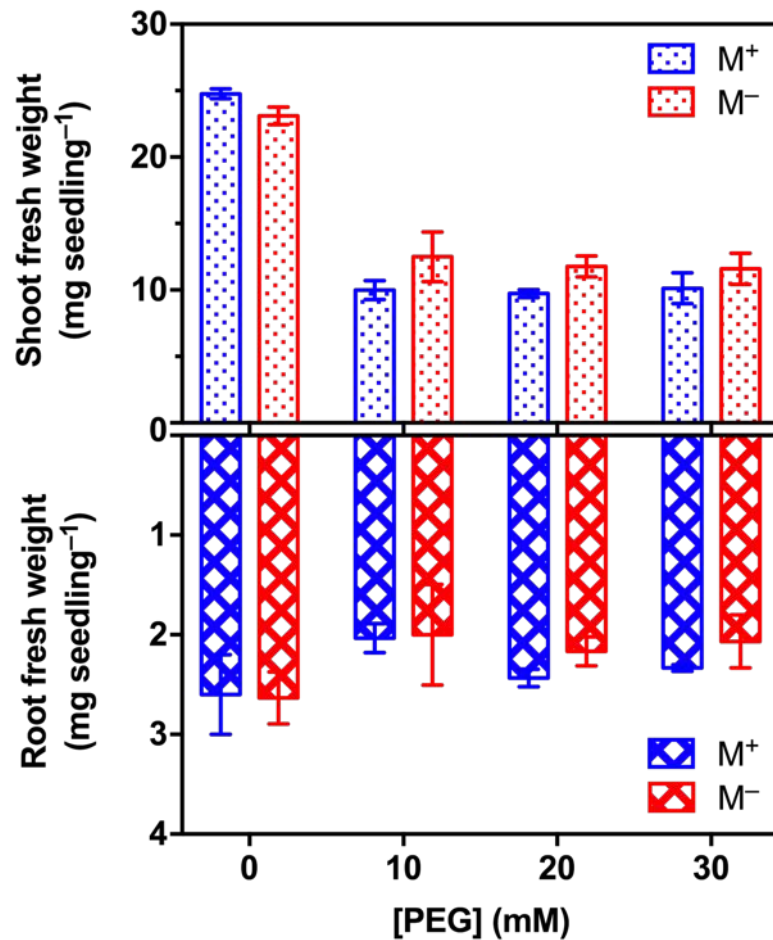


Figure 6-4: Mean fresh weights of separated root and shoot tissue from 31 day-old seedlings grown under different osmotic stress conditions using 0, 10, 20 and 30 mM polyethylene glycol (PEG). Error bars = ± 1 SEM. $N = 3$, each with 7 seedlings.

6.3.3 Growth responses under thermal stress conditions

The effects of thermal stress on the growth of *Ae. arabicum* seedlings were investigated using similar methods as employed for the osmotic stress assay. M⁺ and M⁻ seedlings grown at 14°C, 20°C, 24°C, 30°C and 35°C were compared for their root and shoot lengths and seedling growth rates. Though the total seedling length differed between morphs at 14°C ($P = 0.003$) and 20°C ($P = 0.025$), length under higher temperatures of 24°C ($P = 0.076$), 30°C ($P = 0.834$), and 35°C ($P = 0.123$) did not elicit such a morph-specific response.

Similarly, ANOVA of growth rates revealed that morph had no effect overall at 14°C ($P = 0.114$), 24°C ($P = 0.089$), 30°C ($P = 0.959$), or 35°C ($P = 0.217$), while at 20°C ($P = 0.027$), M⁺ seedlings grew at a faster rate than M⁻ seedlings.

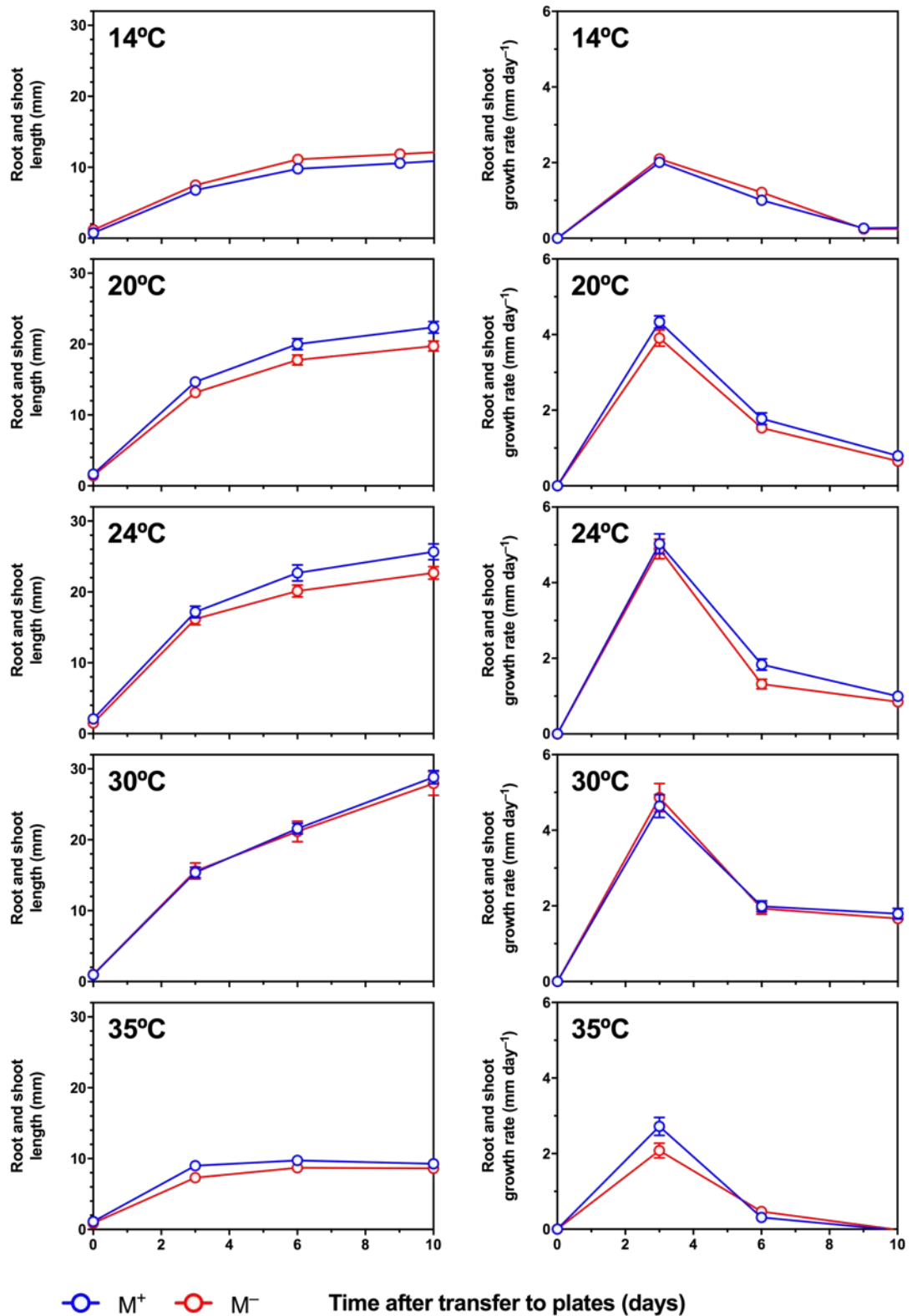


Figure 6-5: *Ae. arabicum* seedling growth responses to a range of constant growth temperatures. The mean of combined root and shoot lengths, and total seedling growth rates, were calculated over an experimental period of 10 days. Error bars = ± 1 SEM. N = 3, each with 7 seedlings.

Fresh and dry weights of separated root and shoot tissue (Figure 6-6) at the end of the experimental conditions (10 days), revealed a strong temperature response ($P < 0.001$), with highest masses observed at 30°C. There were no morph-specific differences in fresh ($P = 0.094$) and dry ($P = 0.068$) shoot masses across growth temperatures. In root tissues, ANOVA revealed that seed morph accounted for 1.36% of the total variance with fresh weight ($P = 0.026$), and 1.71% of the total variance with dry weight ($P = 0.019$). Though this effect is significant, the relatively small percentage of variability accounted for by seed morph implies a small effect size. Together with seedling lengths, growth rates, and fresh weights, the most optimal growth conditions were thus considered as 30°C.

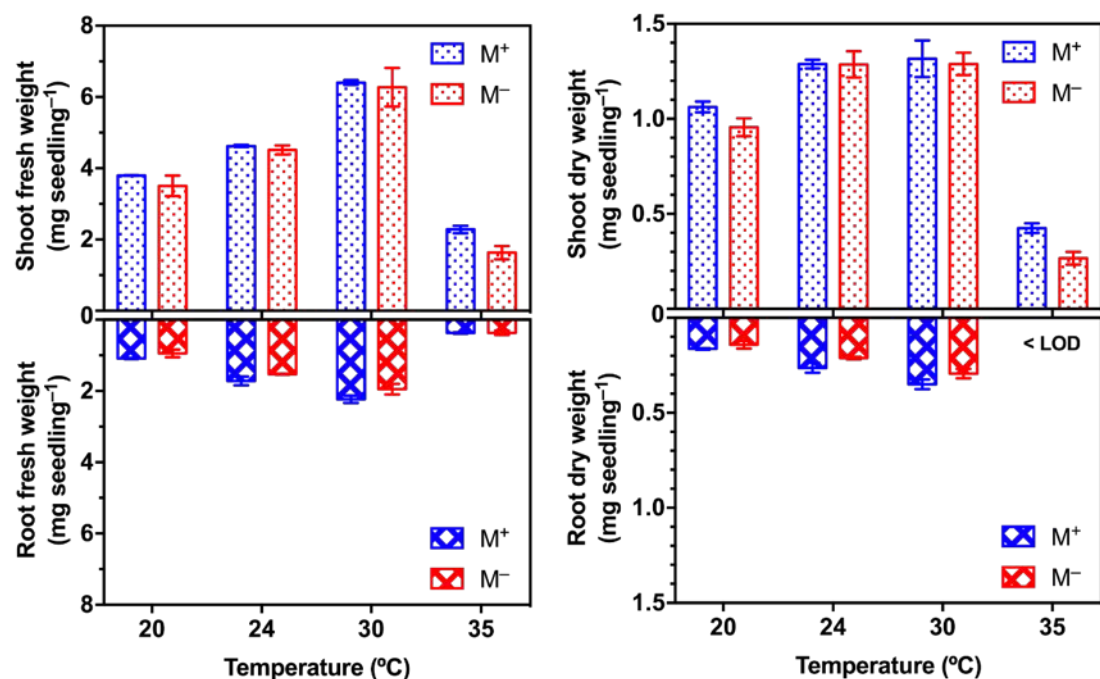


Figure 6-6: M⁺ and M⁻ seedling weights after 10 days of growth under temperatures representative of thermal stress. Shown are mean shoot and root fresh (A) and dry (B) weights. Error bars = ± 1 SEM. N = 3, each with 7 seedlings. LOD = limit of detection.

6.3.4 Basal thermotolerance of seedlings

At 35°C, there were slight indications that M⁺ seedlings had greater vigour, with a higher mean shoot fresh weight than M⁻ seedlings (Figure 6-6). This was exclusively for shoot tissue only. Prompted by this finding that M⁺ seedlings may exhibit more vigorous shoots, the two morphs were tested for their response to a period of elevated temperature. Termed basal thermotolerance, this represents the intrinsic tolerance of plants to heat stress, through direct exposure, without any conditioning pre-treatment (Halter *et al.*, 2016). This is distinct from acquired thermotolerance, attained by changes in gene expression induced by pre-treatment to modest, sublethal heat shock, which was not investigated in this study.

A 20-minute heat-shock exposure of 4 dos to 39°C, 42°C, 45°C, 48°C, 51°C caused varying degrees of damage to seedling viability (*i.e.* capability of surviving or establishing successfully). Quantification during the recovery period, based on a 5-point scoring system, showed that damage for both seedling morphs worsened with increasing temperatures (Figure 6-7). Overall, seed morph had a significant effect on survival across heat shock temperatures ($P = 0.005$). Only seedling viability at 45°C showed interesting responses ($P < 0.001$), in that M⁻ seedlings had a greater survivability than M⁺ seedlings (Figure 6-7a). Mean damage scores were also significantly different between morphs ($P < 0.001$), with M⁺ seedlings exhibiting a comparatively higher proportion of damaged seedlings than M⁻ under the same heat shock treatment temperature.

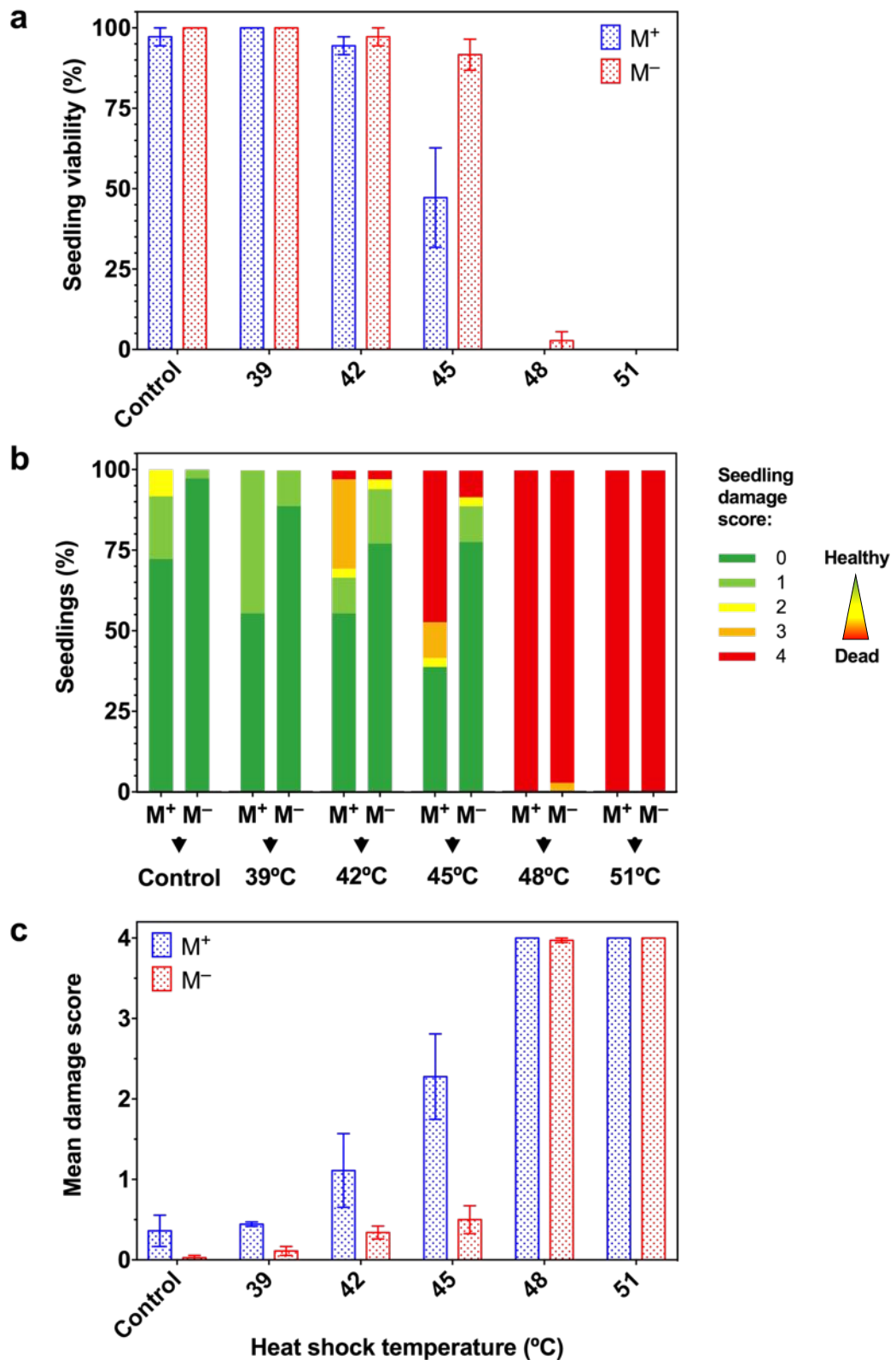


Figure 6-7: Basal thermotolerance assay for *Ae. arabicum* seedlings grown from M⁺ and M⁻ seeds. **a)** Mean seedling viability when exposed to increasing temperatures of heat shock treatment. **b)** Seedlings were scored using a 5-point classification (see 2.4.4), for which a mean damage score (**c**) was obtained. Bars in **a** and **c** represent ± 1 SEM. N = 3, each with 12 seedlings.

6.3.5 Time-course characterisation of chlorophyll content

Observations during previous seedling assays suggested there may be potential differences in chlorophyll content, and thus photosynthetic capacity, during early stages of seedling growth. ANOVA of seedling chlorophyll content under unstressed conditions showed evidence for a morph-specific difference in both chlorophyll *a* ($P = 0.008$) and *b* ($P = 0.005$) during a 12-day time-course (Figure 6-8).

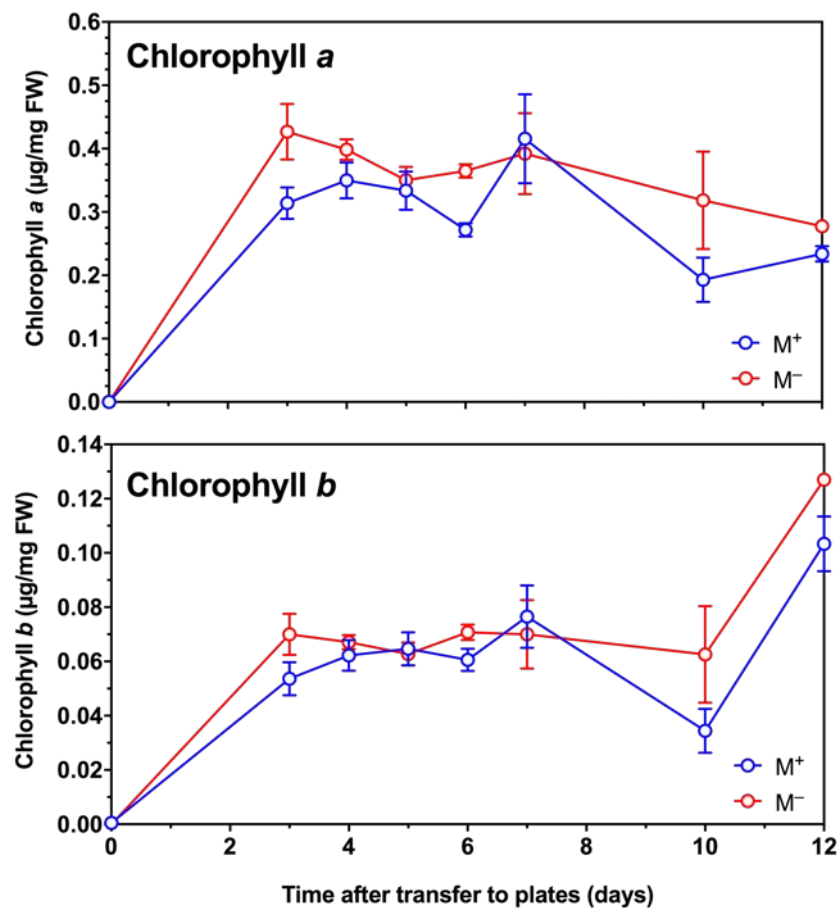


Figure 6-8: Time-course characterisation of chlorophyll *a* and *b* content during seedling growth of *Ae. arabicum* morphs. Shown are mean values obtained during 12 days of seedling establishment. Error bars = ± 1 SEM. $N = 3$, each with 10 replicate seedlings.

6.3.6 Growth responses under salinity stress

To determine the effects of salinity on seedling growth, a sodium chloride (NaCl) tolerance assay was developed. Preliminary data (Figure 6-9) suggested high sensitivity of *Ae. arabicum* seedlings to concentrations of NaCl greater than 100 mM, around which seedling survival was poor. Therefore four reduced concentrations (0 mM, 20 mM, 40 mM, and 60 mM) were selected for further comparative analyses.

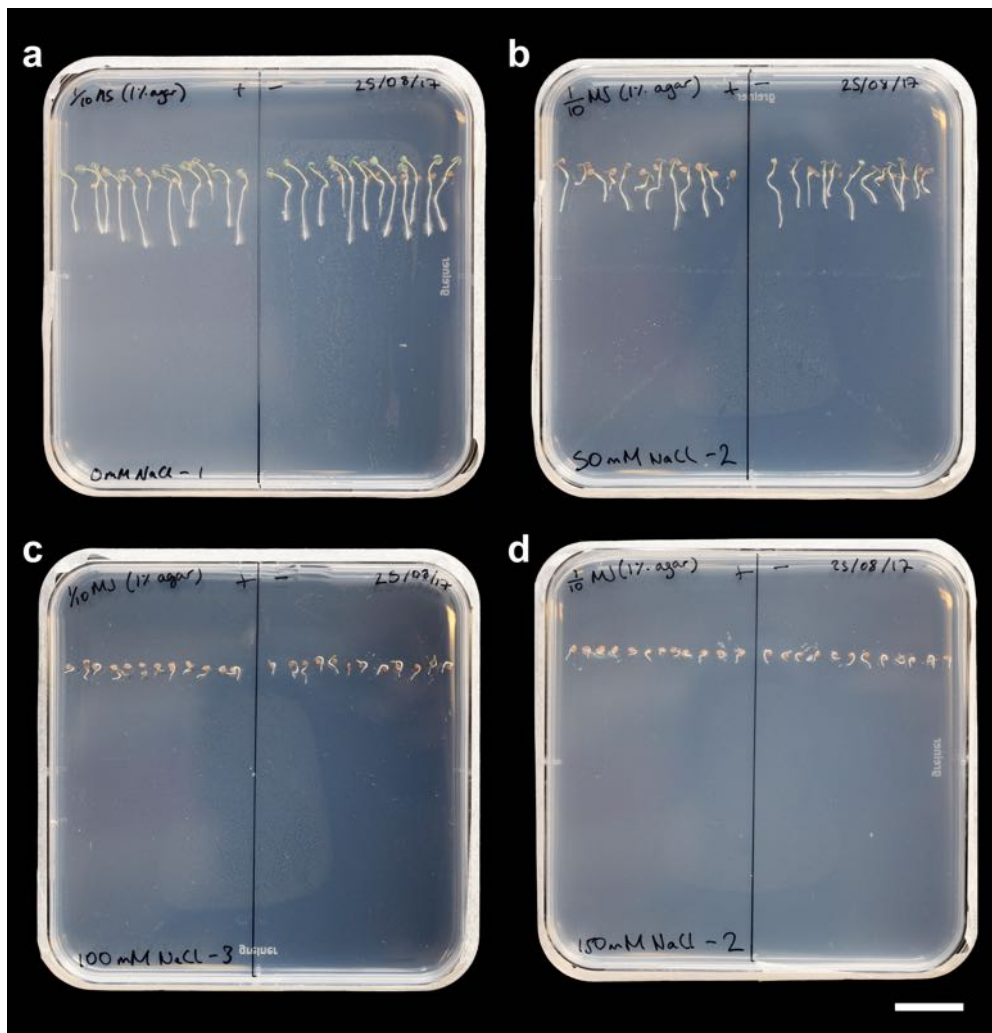


Figure 6-9: Representative growth plates of M⁺ and M⁻ seedlings grown under (a) control, (b) 50 mM, (c) 100 mM, and (d) 150 mM NaCl conditions. Given the poor survivability of seedlings at 100 mM and 150 mM NaCl, a modified assay was developed using revised concentrations. Scale bar = 20 mm.

Growth imaging analysis of seedlings subjected to salinity stress highlighted potential responses between morphs (Figure 6-10). ANOVA revealed there were no significant morph-specific differences in seedling size under control conditions ($P = 0.294$), but under 20 mM ($P < 0.001$), 40 mM ($P = 0.002$), and 60 mM ($P < 0.001$) NaCl, differences were particularly evident towards the end of the 10-day period. Similarly, ANOVA of the growth rates revealed significant differences at 20 mM ($P = 0.015$), 40 mM ($P < 0.001$), and 60 mM ($P < 0.001$) but not at control conditions ($P = 0.112$), thereby supporting the seedling length data.

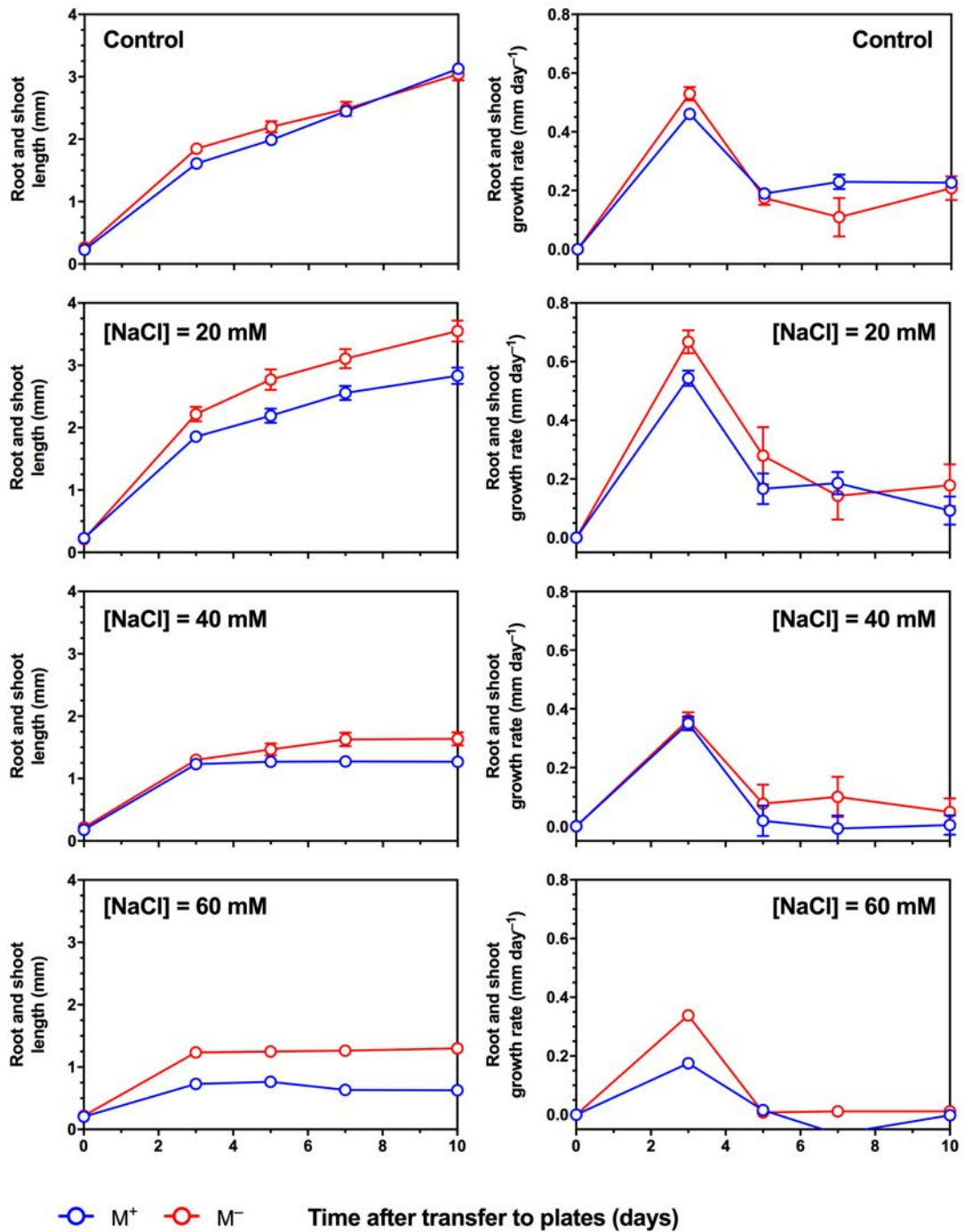


Figure 6-10: *Ae. arabicum* seedling growth responses to increasing concentrations of sodium chloride (NaCl). The means of total seedling length and growth rates were calculated over an experimental period of 10 days. Error bars = ± 1 SEM. N = 3, each with 12 seedlings.

While the addition of NaCl to the medium exposes plants to salt stress, the resultant effects on seedling growth are a combination of osmotic stress (NaCl

lowers the water potential of the medium) and Na⁺ toxicity, a particular consideration at high NaCl concentrations (Munns & Tester, 2008). To gain a better understanding of growth response to salinity stress in *Ae. arabicum* seedlings, we investigated whether the growth repression was induced by mannitol and LiCl (at approximately one tenth the concentration of NaCl), which are assumed to mimic the osmotic and the ionic component of salinity respectively (Tester & Davenport, 2003; Kazachkova *et al.*, 2016). Comparisons of seedlings grown under equivalent concentrations were largely consistent with previous assays, in that M⁺ and M⁻ seedlings did not differ ($P = 0.692$). However, the phenotype under NaCl more closely resembled that under mannitol, than to LiCl, suggesting the growth response was more likely the result of osmotic, but not ionic, stress.

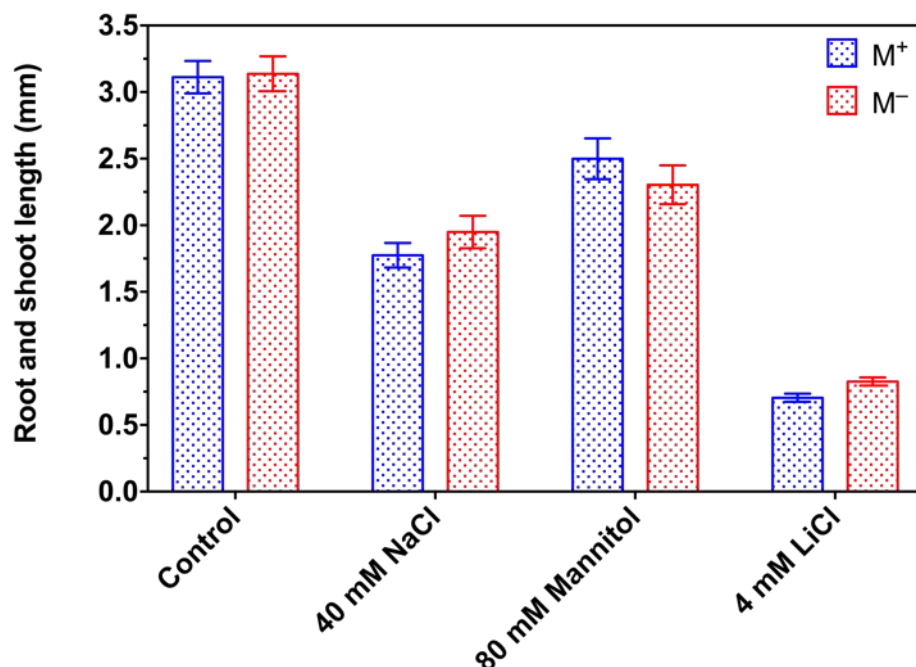


Figure 6-11: Comparisons of mean seedling length after 10 days of growth under different salt controls, which comprised sodium chloride (NaCl), mannitol, and lithium chloride (LiCl). Error bars = ± 1 SEM. N = 3, each with 12 seedlings.

6.3.7 Selection for RNA-sequencing

Given the apparent lack of phenotypic difference between M^+ and M^- seedlings grown under a range of abiotic stresses, a time-course transcriptome investigation was conducted during germination (where differences are known to exist) and seedling growth. Root and shoot tissue were harvested from samples at key physiological stages during completion of germination and early seedling establishment (Figure 6-12 and Figure 6-13).

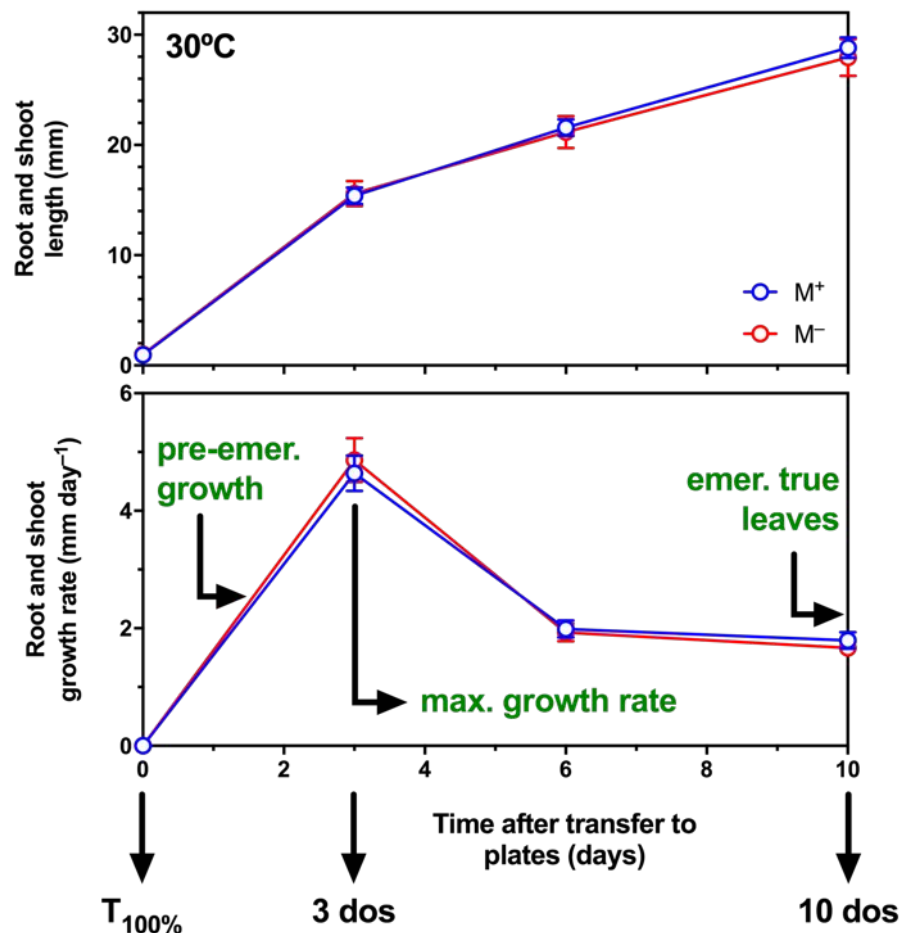


Figure 6-12: Seedling sample selection for RNA-seq. Four physiological time points were selected: $T_{1\%}$ = time at which radicle emergence of the seed population is 1% (not shown on figure), $T_{100\%}$ = completion of germination, 3 day old seedlings (dos) = time at which growth rate is at its maximum, 10 dos = time at which true leaf emergence occurs. At 3 and 10 dos, root and shoot tissue was harvested separately. Entire IND fruits at the same physical time points were also harvested.

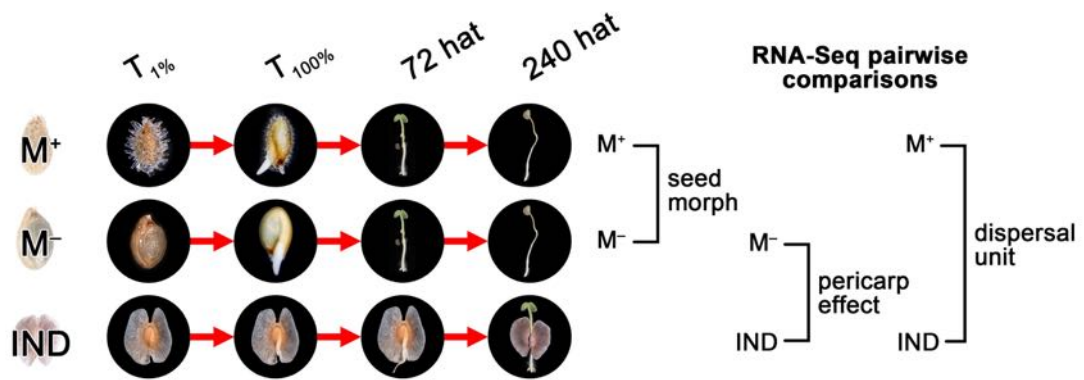


Figure 6-13: Overall experimental design for comparative RNA-seq analysis of seed germination and seedling establishment. Time-points were selected during completion of germination ($T_{1\%}$ and $T_{100\%}$), early (72 hat), and late (240 hat) seedling establishment. Within-root and within-shoot tissue pairwise comparisons were based on the effect of the morph (M^+ vs. M^-), the effect of the pericarp (M^- vs. IND), and the ecological dispersal unit (M^+ vs. IND).

6.3.8 Sample clustering and Principal Components Analysis

To provide insights into the association between samples, RNA-seq datasets were visualised using principal component analysis (PCA), based on the 500 genes with highest variance. Replicate RNA-seq samples clustered tightly by diaspore and by tissue type (Figure 6-14). As expected, three distinct clusters were separated primarily by the derivation of the samples from seed, root, or shoot tissue based on the first two components, explaining 48% and 44% of the variability, respectively. In this combined analysis (Figure 6-14), IND samples at $T_{100\%}$ remain distinct from all other tissues and time points.

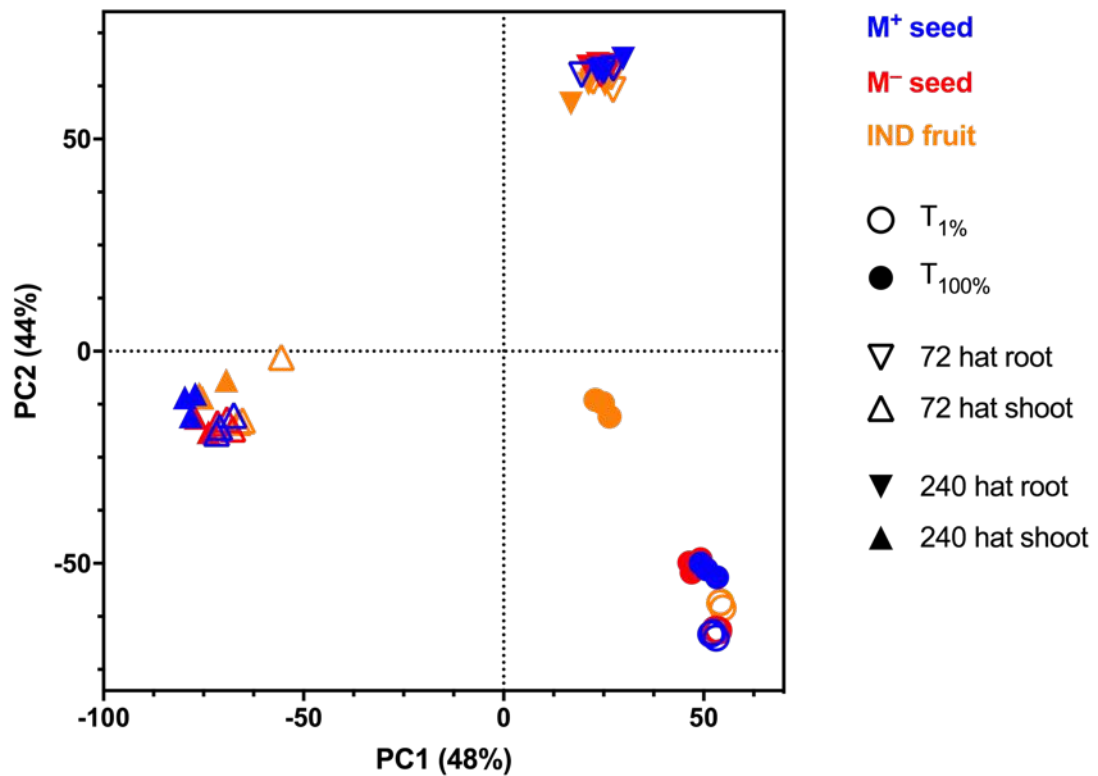


Figure 6-14: Principal Components (PC) analysis of RNA-seq samples obtained during M⁺ seed, M⁻ seed, and IND fruit germination and seedling establishment. Colours indicate morph, while symbols indicate seed, root, or shoot tissue at 1% germination (T_{1%}), 100% germination (T_{100%}), 72 or 240 hours after transfer (hat) to growth plates.

Separation of samples involved in key processes of germination (T_{1%} and T_{100%}), root establishment (72 and 240 hat), and shoot establishment (72 and 240 hat) revealed comparative transcriptome profiles between the morphs in greater detail (Figure 6-15). Clear differences were observed with IND samples, such that both T_{1%} samples and T_{100%} clustered as outliers, separately from M⁺ and M⁻ seed samples. M⁺ and M⁻ seed samples, however, showed tight correlations throughout the course of germination (Figure 6-15a).

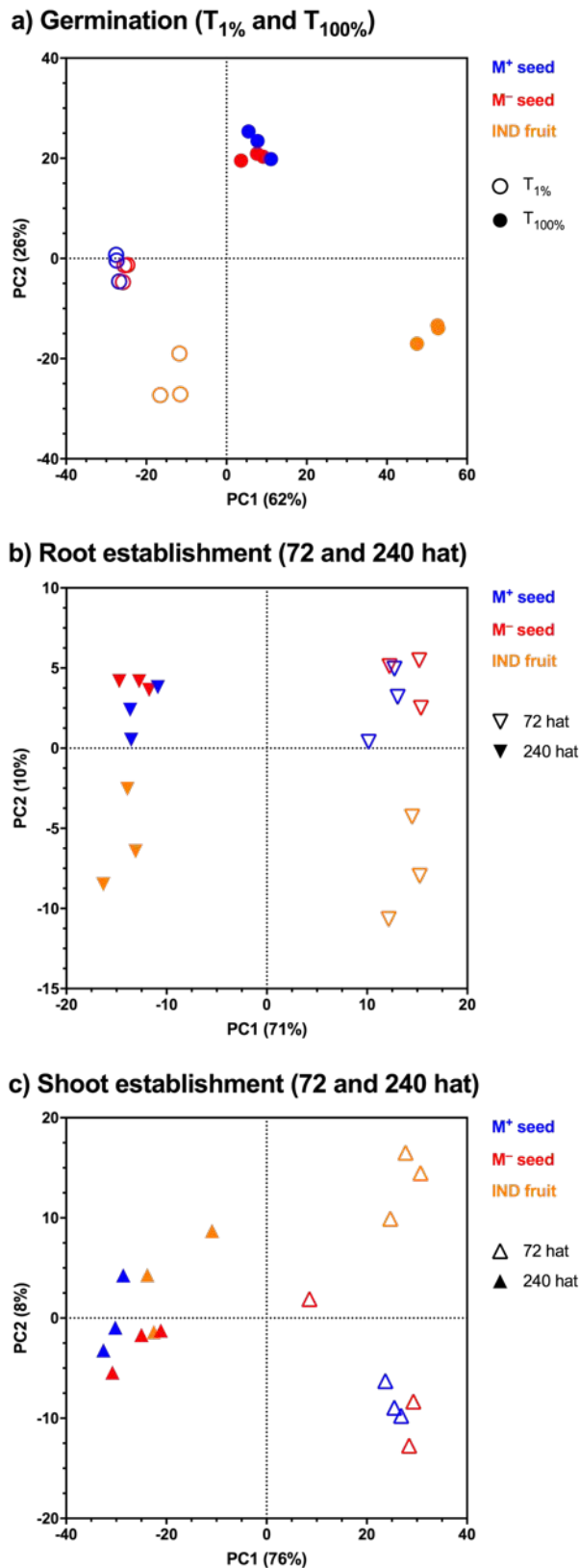


Figure 6-15: Principal Components (PC) analysis of RNA-seq samples obtained during M^+ seed, M^- seed, and IND fruit germination (**a**) and seedling establishment (**b** and **c**). Germination (**a**) comprises samples at $T_{1\%}$ and $T_{100\%}$, while both (**b**) root and (**c**) shoot establishment samples were obtained at 72 and 240 hours after transfer (hat) to growth plates.

As seedlings, differences between morphs appear to be smaller. M⁺ and M⁻ samples cluster together during the two time points during root (Figure 6-15b) and shoot (Figure 6-15c) establishment. IND root samples remain distinct from M⁺ and M⁻ samples. However, transcriptional profiles of IND shoot tissue suggest that, while samples at 72 h remain as a separate cluster, by 240 h there is a tendency towards greater similarity to M⁺ and M⁻ samples.

6.3.9 Differentially expressed gene detection and analysis

Cleaned RNA-seq reads mapped to the genome were further investigated and Differentially Expressed Genes (DEGs) detected in a strict consensus (overlap) approach (Wilhelmsson *et al.*, 2019). Pairwise-comparisons of M⁺ vs. M⁻ (seed only), M⁺ vs. IND (natural dispersal units), and M⁻ vs. IND (pericarp effect) allowed transcriptome exploration of the dimorphic syndrome during seed germination and seedling establishment. Comparisons showed that M⁺ and M⁻ transcriptomes became remarkably similar during completion of germination (Figure 6-16); a total of 180 and 55 DEGs were detected at T_{1%} and T_{100%} respectively, while after 72 h transcriptome differences were not as present in the root (0 DEGs) and shoot (1 DEG) stages. A clear tendency towards more identical transcriptomes is evident throughout germination and seedling establishment. By contrast, comparisons of DEGs between the natural diaspores, M⁺ vs. IND, showed a much higher number during germination. A total of 2,041 DEGs during T_{1%} increased to 2,682 by T_{100%}, thereafter reducing ~10-fold (roots) and 16-fold (shoots) by 72 h. By 240 h, the time of true leaf emergence for M⁺ seedlings, differences were only evident from 60 DEGs in root samples and 10 DEGs in shoot samples.

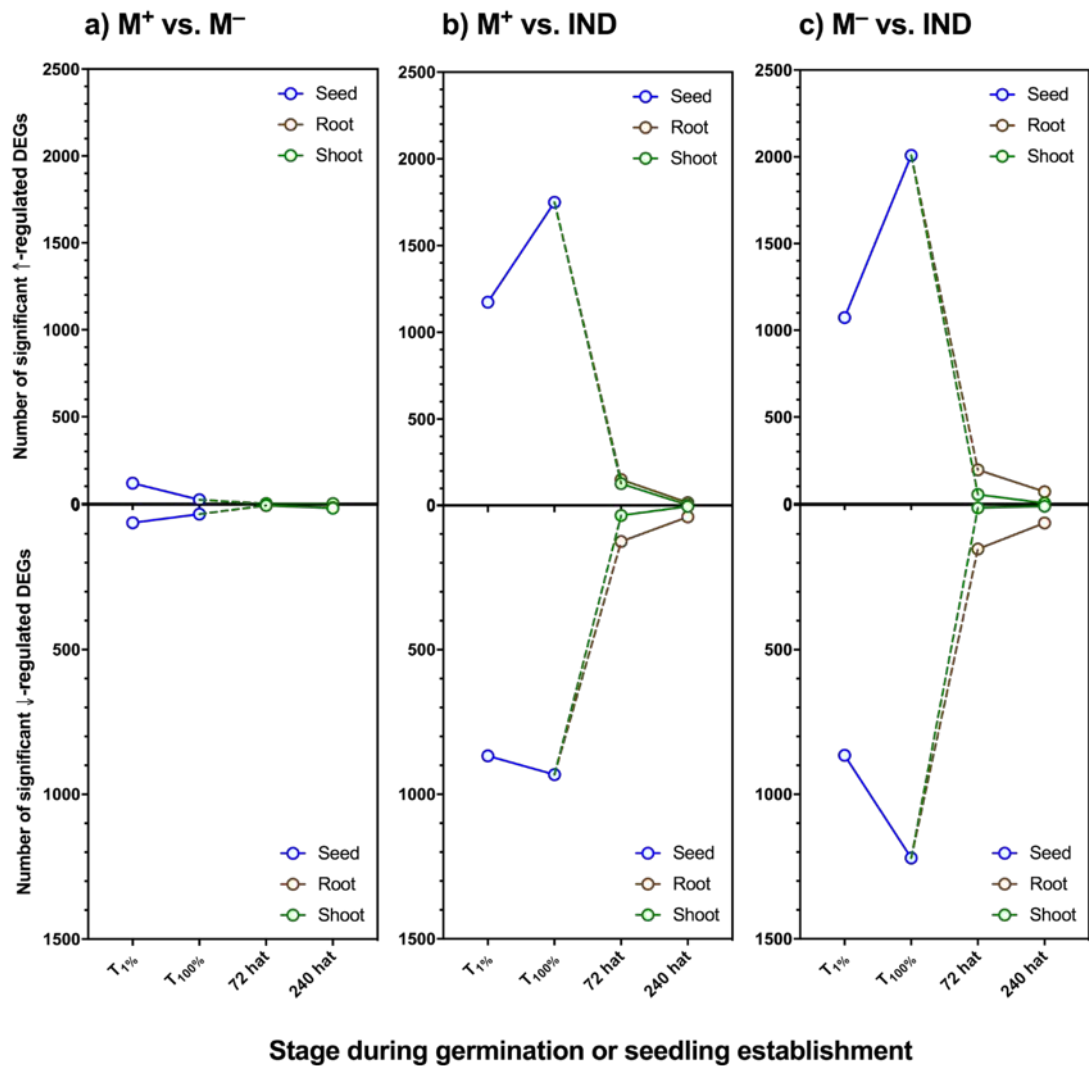


Figure 6-16:Total number of Differentially Expressed Genes (DEGs) detected during the developmental transition from germination to seedling establishment. Shown are DEGs up- (\uparrow) and down- (\downarrow) regulated based on pairwise comparisons of (a) M^+ vs. M^- , (b) M^+ vs. IND fruit, and (c) M^- vs. IND fruit. In all comparisons, the first treatment type was the baseline to which the second treatment was compared. The dashed line indicates a hypothetical trajectory of DEGs for the corresponding tissues.

Interestingly, a similar but more pronounced pattern of DEGs is observed between the comparison of the pericarp effect (M^- vs. IND) on M^- seed germination and seedling establishment (Figure 6-16). The number of DEGs at T_{1%} is similar to those detected in the M^+ comparison (2041 vs. 1938), but the greatest differences are observed at T_{100%} (= pre-emergence growth).

Here, up-regulated DEGs increase 1.9-fold, while down-regulated DEGs increase 1.4-fold. It is therefore at this physiological time-point at which transcriptome differences are greatest. As seedlings progress in root and shoot establishment, the pericarp imposes a total of 347 root-specific DEGs at 72 h, while shoot-specific DEGs are comparably lower (64). By 240 h, differences in shoot samples comprise 4 up- and 4 down-regulated DEGs, while 69 up- and 62 down-regulated DEGs are detected in the root tissues.

Taken together, these results suggest the tendency towards transcriptional “resetting” of seedling morphs. For the ecologically-relevant comparison (M⁺ vs. IND), these data suggest shoot resetting occurs earlier (by 72 h) and root resetting occurs later (differences still evident at 240 h), but clearly that resetting occurs in early seedlings during pre-emergence growth.

6.4 Discussion and conclusions

Growth and establishment of the seedling is a critical stage in the life cycle of a plant, among the most vulnerable to abiotic stresses (Leck *et al.*, 2008; Kranner *et al.*, 2010). In addition to dispersibility (Chapter 3 and 4), another possible adaptive response of the *Ae. arabicum* dimorphism may relate to an improvement in the emergence or establishment of its seedlings. While the seed dimorphism in *Ae. arabicum* is particularly highlighted in this thesis with respect to development of mucilage (Chapter 5), there are distinct gaps in our knowledge about post-germination growth and seedling responses to abiotic stresses. Development of a seed with (M⁺) and without mucilage (M⁻ seed extracted from IND fruits) allows direct comparisons of how two seed morphs, which exhibit distinct dry seed transcriptomes (Wilhelmsson *et al.*, 2019) and germination responses (Lenser *et al.*, 2016), can develop into adult plants lacking phenotypic differences.

In this chapter, a series of abiotic stress assays on *Ae. arabicum* seedlings demonstrated very few, if any, phenotypic differences in growth response. It was found that seedlings grown from M⁺ and M⁻ seed morphs exhibited very similar seedling lengths, growth rates, and tissue masses when grown under osmotic, thermal, and salinity stresses. There were possible indications that M⁺ and M⁻ seedling morphs respond differently to thermal (heat-shock) stress in particular. With a significantly higher growth rate of M⁺ seedlings at a constant 35°C, it may be expected that this morph is better adapted to elevated temperatures, or that the M⁻ seedling had a greater sensitivity to abiotic stresses in the absence of its protective fruit pericarp. This hypothesis was not

supported by the basal thermotolerance assay, which in contrast suggested that the M^- seedling was more tolerant than seedlings derived from the M^+ morph. Similarly, growth curves obtained under salinity stress revealed contrasting results and could be improved by ensuring individual seedlings are fully exposed to the plate medium. With this suggested improvement to the experimental set-up, a repetition of these assays with the IND morph and a greater number of seedling individuals will further elucidate morph-specific adaptability to abiotic stresses.

A detailed investigation through the detection of DEGs under “optimal” growth conditions highlighted key differences during the transition to seedling establishment. Transcriptional profiles of seed morph comparisons (M^+ vs. M^-) showed that the number of significant DEGs was greatest at early germination ($T_{1\%}$), with differences progressively diminishing. Mature dry seeds differ in size and mass, and the dry seed transcriptome of M^+ appears relatively more oriented towards translation of RNA and chromatin assembly, whereas the M^- seed morph transcriptome may be more oriented to post-transcriptional processing of RNA (Wilhelmsson *et al.*, 2019). These initial transcriptome differences, thought to be related to comparatively faster M^+ seed desiccation and maturation, were not detected after completion of germination. The robust DEG detection approach adopted in this chapter combined several methods to minimise false positives (Zhang *et al.*, 2014) and exclude genes of low abundance. Thus, the transcriptome “resetting” between M^+ and M^- morphs aligns with the observed abiotic stress phenotypes, occurring earlier in shoot tissue compared to later in root tissue.

By contrast, pairwise analyses yielded insight into the contribution of the pericarp to the transcriptome. The difference between seed morphs and the IND fruit became greatest at completion of germination, yet M⁻ seeds manually removed from their pericarps were more similar to the M⁺ seed transcriptome. These results provide clear evidence that the IND pericarp affects the transcriptional profile of the M⁻ seed, potentially through mediating a delay of radicle protrusion via biochemical and/or biomechanical means. It has previously been demonstrated that the IND fruit contains a 34-fold higher endogenous ABA concentration compared with the M⁺ seed, consistent with high degree of dormancy of the IND fruit and the low degree of dormancy of the M⁺ seed (Arshad *et al.*, 2019). Interestingly, pericarp-derived germination inhibitors have also been documented in the monomorphic *Laurus nobilis* (Lauraceae), such that there is complete inhibition in the presence of the pericarp, or potentially derived from inhibitors associated with the seed coat (Tilki, 2004; Sari *et al.*, 2006). An example within the Brassicaceae is with the indehiscent fruits of *Lepidium draba* and *L. appelianum*. Both isolated seeds and entire fruits were non-dormant in *L. appelianum*, while in *L. draba*, the pericarp conferred a coat-imposed chemical dormancy via ABA. This is thought to play a critical role in the “weediness” of this species and its timely germination (Mohammed *et al.*, 2019).

Given that the IND pericarp is permeable for water (Lenser *et al.*, 2016), it may be that the creation of an internal environment during imbibition, which keeps the M⁻ seed moist after a period of rainfall, extends the effective period over which germination is permissible, or alternatively permits seedling survival until

the next precipitation event by reducing the rate of desiccation within the fruit (Cousens *et al.*, 2009). Another explanation of the effect the IND pericarp may have during germination relates to a physical, biomechanical inhibition of radicle protrusion, in that the embryo does not have sufficient growth potential to overcome mechanical resistance of all seed-covering layers (Lu *et al.*, 2017). Within fruits of *Raphanus raphanistrum* (Brassicaceae), for example, low germination percentage of seeds may be caused by a combination of mechanical resistance of the indehiscent fruit *and* chemical inhibitors (Mekenian & Willemsen, 1975). Another example of the pericarp as a physical impediment, in the absence of water soluble germination inhibitors, is in the heterocarpic *Ceratocarpus heterocarpus* (Fumariaceae) (de Clavijo, 1994). Beyond the role of the IND pericarp in dispersal, pairwise comparisons between the natural diaspores (M⁺ vs. IND) and the effect of the pericarp (M⁻ vs. IND) hint at other differences influencing germination behaviour. Thus, further investigations are required regarding precisely how seed covering layers may interact with the germination process and seedling establishment phase in *Ae. arabicum*.

Based on the transcriptome “resetting” described in this chapter, there is a hypothesis that epigenomic changes occur during early seedling establishment. Such changes can be compared to plants that overwinter prior to flowering, when prolonged cold exposure induces chromatin modifications to regulate flowering regulatory genes and enable flowering in spring (Bouché *et al.*, 2017). For plants exhibiting these life-histories, the vernalised state must be reset to ensure that each growth and development cycle requires winter

cold exposure prior to flowering (Tao *et al.*, 2019). In *Ae. arabicum*, the epigenetic maintenance (or “memory”) of the dimorphic state may be lost during the transition to seedlings. To explore the reprogramming of epigenetic marks during early seedling development, examinations of DNA methylation and histone modifications are required to elucidate “native” transcriptome patterns which underpin those transitional changes. The analysis of the epigenome, together with the transcriptome, will therefore allow integrating different regulatory levels, highlighting DEGs which may be under epigenetic regulation and key factors exerting this control.

6.5 References

- Arshad W, Sperber K, Steinbrecher T, Nichols B, Jansen V, Leubner-Metzger G, Mummenhoff K. 2019.** Dispersal biophysics and adaptive significance of dimorphic diaspores in the annual *Aethionema arabicum* (Brassicaceae). *New Phytologist* **221**(3): 1434–1446.
- Bouché F, Woods DP, Amasino RM. 2017.** Winter memory throughout the plant kingdom: different paths to flowering. *Plant Physiology* **173**(1): 27–35.
- Chandler J, Wilhelmsson P, Graeber K, Arshad W, Mérai Z, Steinbrecher T, Mittelsten Scheid O, Strnad M, Schranz M, Rensing S, et al. unpublished.** SeedAdapt: Using large scale data to unravel the molecular mechanisms controlling germination and dormancy in *Aethionema arabicum* – a model species for diaspore heteromorphism.
- Cousens RD, Young KR, Tadayyon A. 2009.** The role of the persistent fruit wall in seed water regulation in *Raphanus raphanistrum* (Brassicaceae). *Annals of Botany* **105**(1): 101–108.
- de Clavijo ER. 1994.** Heterocarpy and seed polymorphism in *Ceratocarpus heterocarpus* (Fumariaceae). *International Journal of Plant Sciences* **155**(2): 196–202.
- Elamrani A, Raymond P, Saglio P. 1992.** Nature and utilization of seed reserves during germination and heterotrophic growth of young sugar beet seedlings. *Seed Science Research* **2**: 1–8.
- Finch-Savage WE, Bassel GW. 2015.** Seed vigour and crop establishment: extending performance beyond adaptation. *Journal of Experimental Botany* **67**(3): 567–591.
- Halter G, Simonetti N, Suguitan C, Helm K, Soroksky J, Waters ER. 2016.** Patterns of thermotolerance, chlorophyll fluorescence, and heat shock gene expression vary among four *Boechera* species and *Arabidopsis thaliana*. *Botany* **95**(1): 9–27.
- Imbert E. 2002.** Ecological consequences and ontogeny of seed heteromorphism. *Perspectives in Plant Ecology, Evolution and Systematics* **5**(1): 13–36.
- ISTA 2015.** International Rules for Seed Testing. Basserdorf, Switzerland: International Seed Testing Association.
- Kazachkova Y, Khan A, Acuña T, López-Díaz I, Carrera E, Khozin-Goldberg I, Fait A, Barak S. 2016.** Salt induces features of a dormancy-like state in seeds of *Eutrema (Thellungiella) salsugineum*, a halophytic relative of *Arabidopsis*. *Frontiers in Plant Science* **7**(1071): 1–18.
- Kranner I, Minibayeva FV, Beckett RP, Seal CE. 2010.** What is stress? Concepts, definitions and applications in seed science. *New Phytologist* **188**(3): 655–673.
- Leck MA, Parker VT, Simpson RL. 2008.** *Seedling Ecology and Evolution*. United States of America: Cambridge University Press, New York.
- Lenser T, Graeber K, Cevik ÖS, Adigüzel N, Dönmez AA, Grosche C, Kettermann M, Mayland-Quellhorst S, Mérai Z, Mohammadin S, et**

- al. 2016. Developmental control and plasticity of fruit and seed dimorphism in *Aethionema arabicum*. *Plant Physiology* **172**(3): 1691–1707.
- Lu JJ, Tan DY, Baskin CC, Baskin JM. 2017. Delayed dehiscence of the pericarp: role in germination and retention of viability of seeds of two cold desert annual Brassicaceae species. *Plant Biology* **19**(1): 14–22.
- Lu JJ, Tan DY, Baskin JM, Baskin CC. 2010. Fruit and seed heteromorphism in the cold desert annual ephemeral *Diptychocarpus strictus* (Brassicaceae) and possible adaptive significance. *Annals of Botany* **105**(6): 999–1014.
- Lu JJ, Tan DY, Baskin JM, Baskin CC. 2014. Germination season and watering regime, but not seed morph, affect life history traits in a cold desert diaspore-heteromorphic annual. *PLoS ONE* **9**(7): e102018.
- Mandák B. 1997. Seed heteromorphism and the life cycle of plants: a literature review. *Preslia, Praha* **69**: 129–159.
- Mandák B, Pyšek P. 2005. How does seed heteromorphism influence the life history stages of *Atriplex sagittata* (Chenopodiaceae)? *Flora – Morphology, Distribution, Functional Ecology of Plants* **200**(6): 516–526.
- Maun M, Payne A. 1989. Fruit and seed polymorphism and its relation to seedling growth in the genus *Cakile*. *Canadian Journal of Botany* **67**(9): 2743–2750.
- Mekenian MR, Willemssen RW. 1975. Germination characteristics of *Raphanus raphanistrum*. I. Laboratory studies. *Bulletin of the Torrey Botanical Club*: 243–252.
- Mohammed S, Turečková V, Tarkowská D, Strnad M, Mummenhoff K, Leubner-Metzger G. 2019. Pericarp-mediated chemical dormancy controls the fruit germination of the invasive hoary cress (*Lepidium draba*), but not of hairy whitetop (*Lepidium appelianum*). *Weed Science*: 1–12.
- Munns R, Tester M. 2008. Mechanisms of salinity tolerance. *Annual Review of Plant Biology* **59**: 651–681.
- Sari AO, Oguz B, Bilgic A. 2006. Breaking seed dormancy of laurel (*Laurus nobilis* L.). *New Forests* **31**(3): 403–408.
- Song J, Shi W, Liu R, Xu Y, Sui N, Zhou J, Feng G. 2017. The role of the seed coat in adaptation of dimorphic seeds of the euhalophyte *Suaeda salsa* to salinity. *Plant Species Biology* **32**(2): 107–114.
- Tao Z, Hu H, Luo X, Jia B, Du J, He Y. 2019. Embryonic resetting of the parental vernalized state by two B3 domain transcription factors in *Arabidopsis*. *Nature Plants* **5**(4): 424–435.
- Tester M, Davenport R. 2003. Na⁺ tolerance and Na⁺ transport in higher plants. *Annals of Botany* **91**(5): 503–527.
- Tilki F. 2004. Influence of pretreatment and desiccation on the germination of *Laurus nobilis* L. seeds. *Journal of Environmental Biology* **25**(2): 157–161.
- van der Weele CM, Spollen WG, Sharp RE, Baskin TI. 2000. Growth of *Arabidopsis thaliana* seedlings under water deficit studied by control of water potential in nutrient-agar media. *Journal of Experimental Botany* **51**(350): 1555–1562.

- Verslues PE, Bray EA. 2004.** *LWR1* and *LWR2* are required for osmoregulation and osmotic adjustment in *Arabidopsis*. *Plant Physiology* **136**(1): 2831–2842.
- Wilhelmsson P, Chandler J, Fernandez-Pozo N, Graeber K, Ullrich K, Arshad W, Khan S, Hofberger J, Buchta K, Edger P, et al. 2019.** Usability of reference-free transcriptome assemblies for detection of differential expression: a case study on *Aethionema arabicum* dimorphic seeds. *BMC Genomics* **20**: 1–25.
- Yang F, Baskin JM, Baskin CC, Yang X, Cao D, Huang Z. 2014.** Effects of germination time on seed morph ratio in a seed-dimorphic species and possible ecological significance. *Annals of Botany* **115**(1): 137–145.
- Yao S, Lan H, Zhang F. 2010.** Variation of seed heteromorphism in *Chenopodium album* and the effect of salinity stress on the descendants. *Annals of Botany* **105**(6): 1015–1025.
- Zhang J. 1993.** Seed dimorphism in relation to germination and growth of *Cakile edentula*. *Canadian Journal of Botany* **71**(9): 1231–1235.
- Zhang ZH, Jhaveri DJ, Marshall VM, Bauer DC, Edson J, Narayanan RK, Robinson GJ, Lundberg AE, Bartlett PF, Wray NR. 2014.** A comparative study of techniques for differential expression analysis on RNA-Seq data. *PLoS ONE* **9**(8): e103207.

7. Discussion and critical evaluation

7.1 Summary of findings

Morphological, physiological, and developmental traits that have evolved as adaptations to abiotic stress are particularly important for annual plants, whose new cycle is dependent on regeneration from seed. Heteromorphism as a bet-hedging strategy, provides one such mechanism to cope with semi-arid environments that bring about challenging climatic and edaphic conditions for plant growth. In this thesis, overall significant progress was made towards achieving the general aims and objectives outlined in Chapter 1.5, particularly with respect to traits involved in seed and fruit dispersal, seed coat development, and seedling establishment (Figure 7-1).

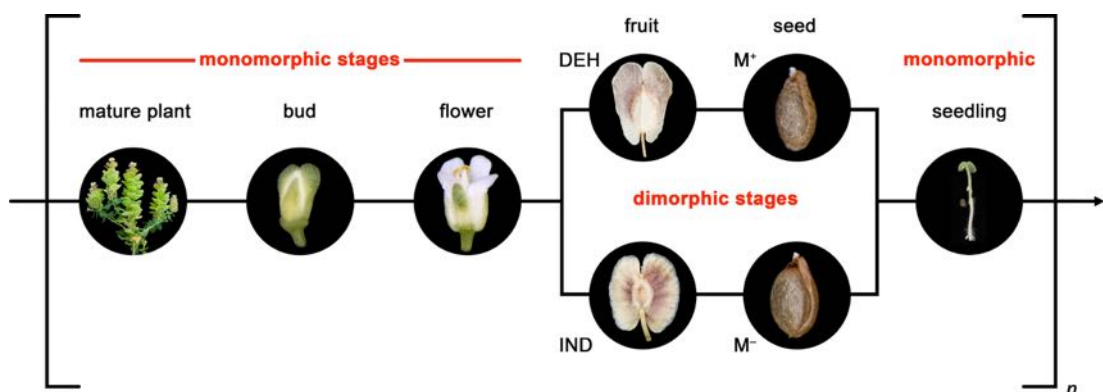


Figure 7-1: Summary of *Ae. arabicum* life-history stages elucidated in this thesis. The aims and objectives focussed on both monomorphic and dimorphic stages, which resulted in significant findings in relation to reproductive development (dimorphism), seed and fruit dispersal (dimorphism), and seedling establishment (monomorphism). DEH = dehiscent. IND = indehiscent. M⁺ = mucilaginous. M⁻ = non-mucilaginous.

In Chapter 3, it was found that morpho-physiological properties of *Ae. arabicum* diaspores support dimorphic dispersal mechanisms, namely by antitelechorous (adherence of M⁺ seed coat mucilage) and telechorous (longer-range fruit dispersal) mechanisms. For the IND fruit, distinct features imposed by the pericarp contributed to the dispersibility (via fruit aerodynamic properties) and ABA-mediated dormancy of the encased M⁻ seed. Chapter 3 also explored how dispersal and dormancy patterns may relate to the spatially and temporally uncorrelated environments in which *Ae. arabicum* grows, thereby supporting the hypothesis that heteromorphic ecophysiological properties influence the ability to persist in high-elevational scree-slope environments.

Exploring the structure and function of fruit-related traits, Chapter 4 revealed in greater detail how dimorphic patterns of fruit fracturing biomechanics could be explained by fracture surface morphology and internal fruit anatomy. A separation layer along the valve-replum boundary, typical for dehiscent fruits, was in contrast to the numerous, spirally-thickened fibres that linked winged IND fruit valves. This supported the hypothesis that anatomical properties link fruit fracture biomechanics with dehiscence and indehiscence syndromes relating to dispersal.

In Chapter 5, morph-specific differences in the context of seed coat development revealed dramatic changes within developing gynoecia. These differences were localised to the differentiation of ovule integuments, mucilage production, and post-fertilisation degradation of the septum (IND gynoecia

only), as documented through comparative high-resolution tomographic imaging. Developmental transcriptomics and an independent time-course validation revealed that expression of the transcription factors *GL2* and *MYB61*, in particular, were likely key regulatory elements driving the reduced M^- seed coat biosynthesis in comparison to M^+ seeds. Also revealed was the post-fertilisation ovule abortion within IND fruits, a highly-coordinated process which may be related to genes associated with defective embryogenesis.

Finally, in Chapter 6, development of seedlings in response to abiotic stress factors affecting establishment showed few differences between M^+ and M^- morphs. A time-course characterisation of tissue-specific transcriptional profiles suggested “resetting” occurs in early seedling pre-emergence growth, which may be earlier in shoot tissue compared to later in root tissue. That morph “resetting” occurs in *Ae. arabicum* seedlings is a phenomenon not described in other heteromorphic systems. These data also provided further insight into possible effects of the pericarp, in addition to ABA identified in Chapter 3, potentially through a developmental delay of seedling establishment.

7.2 Critical evaluation

7.2.1 *Dispersal ecology and the need for field-based validations*

Despite being a promising model for diaspora heteromorphism, no field data have been collected in this thesis. The working hypothesis derived from lab-based experiments is that e.g. ambient temperature may act as the sensory signal, to which the plastic fruit morph ratios can respond. To this effect, one

would expect there to be plasticity in the life history strategies based on phenology. For example, at lower altitudes, higher temperatures would prevent germination of the IND diaspore in summer months. Dispersal in autumn would be in favourable conditions (*i.e.* precipitation and temperature), but the pericarp-imposed dormancy would delay this germination. At low altitudes, germination would be possible in the winter, leading to earlier flowering in the season which means colder temperatures during the reproductive phase. At higher altitudes, germination would not be possible in winter due to colder temperatures, but germination in spring targets the reproductive phase to the warm summer season which ensures that appropriate numbers of both diaspores are produced. Thus, alternative strategies via stress-induced change in phenology and proportion of fruit morphs are particularly relevant at altitudinal extremes. To validate claims that environmental gradients regulate plasticity in vegetative and reproductive growth phenology, there is a requirement for field-based observations and integration of the climatic modelling presented in Chapter 3. This would also further support the selection of temperature regimes used in germination and seedling physiology experiments. Together with analyses of elevation-dependent climatic and edaphic factors, and how these may interact to create microclimates suitable for growth, a more complete picture of the species' ecology will emerge.

Also discussed is the high ABA concentration of the IND fruit diaspore which contributes to its delayed germinability. Though this implies a case of ABA-mediated and pericarp-enhanced dormancy, the precise dormancy mechanisms of IND fruits and the possible role of the pericarp in controlling

fruit germination timing remains unclear. Germination inhibitors in pericarp tissue are a frequent occurrence in desert species as a means to prevent germination after scarce and irregular rainfall, and only permit germination after a threshold amount has fallen (Kigel, 1995). In *Ae. arabicum*, there is insufficient evidence that pericarp ABA alone mediates this delay. Pericarp-imposed dormancy in *Ae. arabicum*, and several other studied Brassicaceae species, is also not due to complete water impermeability of seed-covering layers (Lenser *et al.*, 2016; Mohammed *et al.*, 2019). Thus, analyses of germination with- (IND fruit) and without-pericarp (M^- seed) using a more comprehensive chemical genetics (*e.g.* with hormone biosynthesis inhibitors) and hydrothermal time population-based threshold modelling (Finch-Savage & Leubner-Metzger, 2006) approaches are required to better understand IND fruit dormancy and germination. Since glucosinolate concentrations differ between *Ae. arabicum* fruit morphs at different ontogenetic stages (Bhattacharya *et al.*, 2018), the influence of biotic factors influencing the germination process also deserves further investigation.

7.2.2 *Imaging datasets as complementation to transcriptome studies*

Interdisciplinary methodological advances are crucial to the forefront of plant sciences, and work in this thesis reflects the integration of approaches at various hierarchical levels. Despite being more commonly applied to zoology (Smith *et al.*, 2009), the use of powerful imaging techniques in this project further supported the potential of synchrotron-based imaging methods for modern plant material. Structural data obtained of fruit- (Chapter 4) and seed- (Chapter 5) related traits proved that SRXTM is an excellent imaging system

to reveal exceptional details reconstructed in high resolution, with results rivalling those obtained using destructive techniques. Furthermore, videos of digital SRXTM tomograms have been obtained to aid those interpretations across multiple planes of section (supplemental data for manuscript submission of Chapter 5).

A major factor contributing to the success of the imaging was in the preparation of the analysed samples. Though fresh samples would have been preferable due to minimal manipulation of the tissue, a critical-point drying (CPD) approach (commonly used for electron microscopy) was instead employed. The large water content of developing gynoecia can cause interference and, since sample heating also occurs during imaging, would have likely caused artefacts through tissue shrinking or movement. Fixed and CPD specimens, which had not been subjected to deleterious surface tension effects through direct air-drying (Bray, 2000), could therefore be imaged directly.

Proof of concept studies were pivotal in optimising the sample preparation technique and determining spectral ranges that will interact with tissue to obtain the most accurate results. The nature of X-ray penetration and ionisation ability can cause significant damage to delicate specimens; the damage is dependent on the nature of the specimen (*e.g.* composition and state), as well as the imaging degree (*e.g.* rate of image acquisition and number of repeated scans). The plant materials studied in this thesis contained soft tissues, and therefore X-ray absorption was relatively poor (producing low contrast). Staining with agents that bind to lipids or proteins within tissue (*e.g.*

Lugol's iodine) can enhance contrast more generally, but their irreversible introduction complicates subsequent use of tissue (Strotton *et al.*, 2018). Furthermore, the efficacy of these agents in plant tissue remains relatively unstudied. Thus, images obtained for buds and flowers did not have the desirable resolution to separate tissues as well as in mature fruits and seeds, but still provided excellent volumetric investigations in Chapter 5 which could be contextualised with transcriptome analyses of reproductive development.

7.2.3 *Ecologically-relevant seedling comparisons*

The focus in Chapter 6 was on testing the hypothesis that M^+ and M^- seedling morphs are transcriptionally “reset” (and thus responses to abiotic stress are phenotypically similar). Since the IND fruit batch exhibited some degree of dormancy, the effects of abiotic stresses focussed on M^+ vs. M^- seeds for pragmatic reasons. Despite revealing responses specific to seed morphs, these comparisons do not fully reflect the natural dispersal units (M^+ vs. IND). The entire IND fruit represents the dispersal unit, and the M^- seed remains within the pericarp until fruit germination; in natural conditions, there is no evidence to suggest the pericarp is removed by external means. Furthermore, M^- seeds within IND fruits germinate slowly, but faster and more efficient germination is attained with seeds manually isolated from IND fruits. It is therefore unclear how the pericarp in particular may contribute to potential differences in abiotic stress tolerance.

The abiotic stress assays, though useful for screening morph-specific seedling responses, were perhaps not completely successful in determining the full

degree of differences. In part, this may be the result of sub-optimal experimental design due to time constraints of the project. This may also be due to certain technical challenges (e.g. reproducibly attaining low water potentials in already solid agar medium), or due to limited effectiveness of *in vitro* setups as a proxy for complex field stresses (Claeys *et al.*, 2014). Physiological effects of salinity stress, in particular, are complicated by the osmotic effect of the salt in the growth medium, and the toxic effect of the salt within the plant (Munns & Tester, 2008). Typically, there is a rapid response to the increase in external osmotic pressure, and a slower response due to Na⁺ accumulation. Use of LiCl (Tester & Davenport, 2003; Kazachkova *et al.*, 2016) in the assays employed in Chapter 6 does not adequately distinguish between short-term osmotic stress and longer-term ion toxicity (Shahzad *et al.*, 2016). To determine the specificity of seedling hypersensitivity, a range of different solutes should be tested (e.g. KCl [potassium chloride], LiCl, and CsCl [caesium chloride], and mannitol as an osmotic reagent) at the equivalent concentrations.

Despite this, however, there is little evidence to suggest that salinity may act as a major stress in the natural habitat of *Ae. arabicum*, as is the case for the heteromorphic species from the deserts of northern Xinjiang Province, China (Baskin *et al.*, 2014). Semi-arid deserts typically exhibit variations in incident radiation, temperature, and rainfall (Kigel, 1995). Therefore, a future approach to investigate *Ae. arabicum* seedling physiology should concentrate on more accurate determination of stresses imposed in their natural environment. Thereafter, characterising the expression patterns of stress-responsive

candidate genes, and whether these show dose-dependent responses, would form a more complete picture of the stress tolerance of the two morphs.

7.2.4 *Requirements of a transgenic approach for functional genomics*

The adaptive trans-generational plasticity of *Ae. arabicum* fruit morph production presents a valuable system for comparative studies of evolutionary and developmental genetics. In the absence of phenotypic differences in buds and flowers, an established experimental setup for the local separation of DEH and IND fruit morphs has led to fruit- (Lenser *et al.*, 2018) and seed-specific (Chapter 5) investigations. Fruit morphs are not distributed evenly throughout the plant (as in some other heteromorphic systems), and morphs can be selectively targeted based on 2nd-order branches of undisturbed plants (IND fruits) and main branches of plants whose side branches are constantly removed (DEH fruits). This, however, has the caveat that effects of wounding alone may be driving the formation of DEH fruits, and that positional effects alone may be driving the formation of IND fruits. Consequently, RNA-seq data obtained from this experimental approach have primarily been used as a screening method to identify candidate genes associated with seed coat development. The independent validation of gene expression patterns using a high-resolution time course sampled from plants grown completely undisturbed is therefore emphasised. That patterns of key regulatory elements followed similar trends, supports the raised hypotheses generated from the RNA-seq data discussed in Chapter 5.

Work from this thesis has also highlighted the need to establish a genetic transformation protocol for *Ae. arabicum*. To date, a transgenic approach is not yet possible (pers. comm. with SeedAdapt collaborators) and therefore experimental opportunities for functional genomics analysis are severely lacking. Functional data (e.g. about molecular mechanisms of mucilaginous seed coat formation) are currently limited to experiments derived from selective branch-cutting. Fruit- (e.g. Mühlhausen *et al.*, 2013) and seed-related (e.g. Penfield *et al.*, 2001) reverse genetics approaches will address this distinct gap in furthering *Ae. arabicum* as a model. As an example, the polarised deposition of mucilage polysaccharides precedes formation of the seed coat columella (Haughn & Western, 2012); *Arabidopsis* mutants which show a reduced mucilage accumulation phenotype (e.g. *gl2*, *ttg1*, and *mum4*) have mucilage and columellae present in the seed coat epidermis, but are reduced compared with that of wild-type (Western *et al.*, 2001). How seeds of these mutants in *Ae. arabicum* may differ in their morphology, particularly with respect to wild-type M⁻ seeds, would be an interesting comparison. A reverse genetics approach could also be used to explore the role of maternal effect embryo arrest (MEE) proteins during fruit and seed development; it would be similarly interesting if over-expression of genes encoding MEE proteins could lead to development of single M⁺ seeded DEH fruits and, conversely, if knock-outs could lead to development of multiple M⁻ seeded IND fruits.

Furthermore, a Recombinant Inbred Line (RIL) population derived from Cyprus and Turkey ecotypes is being developed as part of SeedAdapt (Nguyen *et al.*, 2019). A forward genetics approach, through genotyping RILs and the creation

of ethyl methanesulfonate (EMS) mutants, will identify Quantitative Trait Loci (QTLs) affecting the dimorphic diaspore syndromes, particularly in plants grown under abiotic stress. Since the conditions required for plant growth, the size of its genome, and the generation time of *Ae. arabicum* are similar to those of *Arabidopsis*, both forward and reverse genetic studies will therefore yield more mechanistic insights for specific genes and pathways.

7.3 Directions for future work

7.3.1 Compositional and functional analyses of seed coat mucilage

One area that remains to be explored is the analysis of seed coat mucilage composition. While a combination of pectins and heteroxylans are the predominant polymers detected, the chemical composition between myxospermous taxa can be highly variable (Western, 2012b). The pectinaceous nature of *Ae. arabicum* M⁺ seed coat mucilage is evident from both staining with ruthenium red and the metachromatic dye toluidine blue. In the M⁻ morph, concentrated regions of pectin may have a role in altering the cell wall chemistry, particularly around the radicle, which may facilitate radicle lubrication and protrusion through the IND fruit during germination. It is hypothesised that the M⁺ seed coat composition contains more than one type of mucilage, and that the two cell types have different properties. In several members of the Brassicaceae, the seed coat is comprised of an inner adherent mucilage layer, and an outer layer of columellae and cellulose rays (Western, 2012a). The epidermal cells which elongate with hydration in *Ae. arabicum* may contain mucilage comprising both homogalacturonans [α -(1→4)-linked D-galacturonic acid] concentrated in the columellae, and cellulose [β (1→4) linked

D-glucose units] concentrated in the smaller mucilaginous cells of the outer integument, potentially providing the structural integrity for the whole seed coat. The observed properties correlate well with the finding that cellulose promotes mucilage adhesion to the seed in *A. thaliana* (Harpaz-Saad *et al.*, 2011; Sullivan *et al.*, 2011). Removal of *Ae. arabicum* mucilage through vigorous shaking and extraction protocols involving a strong chelator, base or acid (e.g. Western *et al.*, 2001; North *et al.*, 2014), will liberate mucilage for further compositional and biochemical studies.

In this thesis, the anti-telechorous functions and interactions of M⁺ seeds with the soil-interface are well described, but the influence of seed coat mucilage on other aspects of seed physiology are not explored. There is particular scope for exploring the involvement of M⁺ seed coat mucilage in opportunistic DNA repair, which is of relevance in dehydrated conditions when dry seed embryos degenerate and nuclear and mitochondrial DNA suffers *in situ* damage (Huang *et al.*, 2007). Coupled with exposure to daily temperature oscillations, operational DNA repair mechanisms are important for seed longevity and long-term survival. In the desert shrub *Artemisia sphaerocephala* (Asteraceae), for example, seed mucilage may maintain seed viability through DNA repair during wet-dry cycling from night-time dew formation. In this way, despite hydration levels being too low for germination, genome integrity is retained (Elder *et al.*, 1987; Huang *et al.*, 2007; Yang *et al.*, 2011).

7.3.2 *Morph longevity and soil seed bank dynamics*

While *Ae. arabicum* emerges as a promising model for diaspore heteromorphism, the role of its two diaspore morphs in forming a seed bank is completely unknown. Active seasonal seed dormancy cycling, synchronising appropriate timing of germination and seedling emergence, is well understood for the monomorphic model *Arabidopsis thaliana* (Footitt *et al.*, 2011; Footitt *et al.*, 2015). However, it is not known how dimorphic species may differentially sense and integrate temporal (*e.g.* soil temperature and moisture) and spatial (*e.g.* light, nitrate, alternating temperatures) signals to alter the depth of diaspore dormancy.

Cyclic endogenous changes in seed dormancy has been reported for many annual weed species (Freas & Kemp, 1983; Baskin & Baskin, 1985; Gao *et al.*, 2018). Soil seed bank persistence, typically determined by dormancy and longevity traits, is thought to exhibit morph-specific differences in *Ae. arabicum*. Many longevity studies are based on seed storage under “room conditions”; the variability of favourable conditions at both micro- and macro-scales makes lab-based extrapolation to field-conditions problematic (Kigel, 1995). Once pericarp ABA leaching to the M⁻ seed is completed, or the impermeability barrier and mechanical restraints disappear, improper germination timing of the IND diaspore increases the risk of seedling death through immediate seed bank depletion or even density-dependent intraspecific competition (Cheplick, 1996). Thus, dormancy cycling may offer a solution for the need to limit germination to a specific season with suitable conditions, and for the maintenance of a persistent soil seed bank. This is of

particular relevance if the IND diaspore permits longer-distance dispersal to potentially unfavourable habitats. Comparisons of the seasonal dormancy cycling and longevity of *Ae. arabicum* diaspores (M^+ seed vs. IND fruit diaspore) will allow us to investigate and understand their long-term persistence in semi-arid environments.

7.3.3 Biophysical and material properties of the IND pericarp

That the IND fruit pericarp provides numerous adaptive features for dispersal and germination has been discussed in this thesis in detail. However, precisely how biophysical and biomaterial properties of the IND fruit coat determine dormancy (and potentially impact seed longevity) remains understudied. The pericarp acts as a mechanically-protective structure with complex tissue patterning that influences dehiscence behaviour. It also represents the interface with the ambient environment. More detailed biomechanical tests of the pericarp (e.g. compression, cyclic tensile- and stress-relaxation tests), coupled with tissue-specific puncture-force experiments during IND fruit germination, will shed light on IND-fruit vs. M^- seed germination. Together with quantification of seed dormancy and sensitivity states using plant hormones and specific hormone biosynthesis inhibitors (discussed in 7.2.1), this provides an important and relevant avenue for future work.

7.3.4 Integrative analysis of seedling transcriptomes with hormonomes

Combining the transcriptome with other large scale datasets, the role of phytohormones in relation to growth and developmental processes would be of immediate interest. Both auxins and cytokinins interact with each other to

promote and maintain several aspects of growth, with above- and below-ground interactions during biosynthesis, degradation, transport, and signalling (Schaller *et al.*, 2015). It is well known that indole-3-acetic acid (IAA), the most abundant auxin, is involved in a range of plant physiological processes (Tarkowská *et al.*, 2014). Cytokinins also have a wide spectrum of physiological effects, involving root growth (Riefler *et al.*, 2006), resistance to environmental stresses (Hare *et al.*, 1997), fruit and seed development (Mok, 1994; Lenser *et al.*, 2018). Tissue-specific comparisons of not only free hormone, but also of major metabolites and biosynthetic precursors, would provide complete understanding of the similarities or differences in IAA and cytokinin metabolism during dimorphic growth. Furthermore, with recent progress in analytical technologies, tissue- and cell-specific quantifications within an IND fruit would provide a fascinating insight into the seed-pericarp interaction, particularly with respect to leaching of inhibitors during germination. Combining large scale datasets (Todaka *et al.*, 2017) would therefore provide more mechanistic insight on how endogenous plant hormone concentrations and transcriptome responses may interact, notably during the “resetting” phase of early seedling development.

7.4 References

- Baskin JM, Baskin CC. 1985.** The annual dormancy cycle in buried weed seeds: a continuum. *Bioscience* **35**(8): 492–498.
- Baskin JM, Lu JJ, Baskin CC, Tan DY, Wang L. 2014.** Diaspore dispersal ability and degree of dormancy in heteromorphic species of cold deserts of northwest China: A review. *Perspectives in Plant Ecology, Evolution and Systematics* **16**(2): 93–99.
- Bhattacharya S, Mayland-Quellhorst S, Müller C, Mummenhoff K. 2018.** Two-tier morpho-chemical defence tactic in *Aethionema* via fruit morph plasticity and glucosinolates allocation in diaspores. *Plant, Cell & Environment* **42**(4): 1381–1392.
- Bray D 2000.** Critical Point Drying of Biological Specimens for Scanning Electron Microscopy. In: Williams JR, Clifford AA eds. *Supercritical Fluid Methods and Protocols*. Totowa, NJ: Humana Press, 235–243.
- Cheplick G. 1996.** Do seed germination patterns in cleistogamous annual grasses reduce the risk of sibling competition? *Journal of Ecology*: 247–255.
- Claeys H, Van Landeghem S, Dubois M, Maleux K, Inzé D. 2014.** What is stress? Dose-response effects in commonly used *in vitro* stress assays. *Plant Physiology* **165**(2): 519–527.
- Elder R, Dell'Aquila A, Mezzina M, Sarasin A, Osborne DJ. 1987.** DNA ligase in repair and replication in the embryos of rye, *Secale cereale*. *Mutation Research/Fundamental and Molecular Mechanisms of Mutagenesis* **181**(1): 61–71.
- Finch-Savage WE, Leubner-Metzger G. 2006.** Seed dormancy and the control of germination. *New Phytologist* **171**(3): 501–523.
- Footitt S, Douterelo-Soler I, Clay H, Finch-Savage WE. 2011.** Dormancy cycling in *Arabidopsis* seeds is controlled by seasonally distinct hormone-signaling pathways. *Proceedings of the National Academy of Sciences* **108**(50): 20236–20241.
- Footitt S, Müller K, Kermode AR, Finch-Savage WE. 2015.** Seed dormancy cycling in *Arabidopsis*: chromatin remodelling and regulation of DOG1 in response to seasonal environmental signals. *The Plant Journal* **81**(3): 413–425.
- Freas K, Kemp PR. 1983.** Some relationships between environmental reliability and seed dormancy in desert annual plants. *The Journal of Ecology*: 211–217.
- Gao R, Zhao R, Huang Z, Yang X, Wei X, He Z, Walck JL. 2018.** Soil temperature and moisture regulate seed dormancy cycling of a dune annual in a temperate desert. *Environmental and Experimental Botany* **155**: 688–694.
- Hare P, Cress W, Van Staden J. 1997.** The involvement of cytokinins in plant responses to environmental stress. *Plant Growth Regulation* **23**: 79–103.
- Harpaz-Saad S, McFarlane HE, Xu S, Divi UK, Forward B, Western TL, Kieber JJ. 2011.** Cellulose synthesis via the FEI2 RLK/SOS5 pathway

- and cellulose synthase 5 is required for the structure of seed coat mucilage in *Arabidopsis*. *The Plant Journal* **68**(6): 941–953.
- Haughn G, Western T. 2012.** Arabidopsis seed coat mucilage is a specialized cell wall that can be used as a model for genetic analysis of plant cell wall structure and function. *Frontiers in Plant Science* **3**(64): 1–5.
- Huang Z, Boubriak I, Osborne DJ, Dong M, Gutterman Y. 2007.** Possible role of pectin-containing mucilage and dew in repairing embryo DNA of seeds adapted to desert conditions. *Annals of Botany* **101**(2): 277–283.
- Kazachkova Y, Khan A, Acuña T, López-Díaz I, Carrera E, Khozin-Goldberg I, Fait A, Barak S. 2016.** Salt induces features of a dormancy-like state in seeds of *Eutrema (Thellungiella) salsugineum*, a halophytic relative of *Arabidopsis*. *Frontiers in Plant Science* **7**(1071): 1–18.
- Kigel J 1995.** Seed Germination in Arid and Semiarid Regions. In: Kigel J, Galili G eds. *Seed Development and Germination*: Marcel Dekker, Inc., 645–699.
- Lenser T, Graeber K, Cevik ÖS, Adigüzel N, Dönmez AA, Grosche C, Kettermann M, Mayland-Quellhorst S, Mérai Z, Mohammadin S, et al. 2016.** Developmental control and plasticity of fruit and seed dimorphism in *Aethionema arabicum*. *Plant Physiology* **172**(3): 1691–1707.
- Lenser T, Tarkowská D, Novák O, Wilhelmsson P, Bennett T, Rensing SA, Strnad M, Theißen G. 2018.** When the BRANCHED network bears fruit: How carpic dominance causes fruit dimorphism in *Aethionema*. *The Plant Journal* **94**: 352–371.
- Mohammed S, Turečková V, Tarkowská D, Strnad M, Mummenhoff K, Leubner-Metzger G. 2019.** Pericarp-mediated chemical dormancy controls the fruit germination of the invasive hoary cress (*Lepidium draba*), but not of hairy whitetop (*Lepidium appelianum*). *Weed Science*: 1–12.
- Mok MC 1994.** Cytokinins and Plant Development – An Overview. In: Mok DWS, Mok MC eds. *Cytokinins: Chemistry, Activity, and Function*. Boca Raton, USA: CRC Press, 155–166.
- Mühlhausen A, Lenser T, Mummenhoff K, Theißen G. 2013.** Evidence that an evolutionary transition from dehiscent to indehiscent fruits in *Lepidium* (Brassicaceae) was caused by a change in the control of valve margin identity genes. *The Plant Journal* **73**(5): 824–835.
- Munns R, Tester M. 2008.** Mechanisms of salinity tolerance. *Annual Review of Plant Biology* **59**: 651–681.
- Nguyen T-P, Mühlich C, Mohammadin S, van den Bergh E, Platts AE, Haas FB, Rensing SA, Schranz ME. 2019.** Genome improvement and genetic map construction for *Aethionema arabicum*, the first divergent branch in the Brassicaceae family. *bioRxiv*: 662684.
- North HM, Berger A, Saez-Aguayo S, Ralet M-C. 2014.** Understanding polysaccharide production and properties using seed coat mutants: future perspectives for the exploitation of natural variants. *Annals of Botany* **114**(6): 1251–1263.

- Penfield S, Meissner RC, Shoue DA, Carpita NC, Bevan MW. 2001.** MYB61 is required for mucilage deposition and extrusion in the Arabidopsis seed coat. *The Plant Cell* **13**(12): 2777–2791.
- Riefler M, Novak O, Strnad M, Schmölling T. 2006.** Arabidopsis cytokinin receptor mutants reveal functions in shoot growth, leaf senescence, seed size, germination, root development, and cytokinin metabolism. *The Plant Cell* **18**(1): 40–54.
- Schaller GE, Bishopp A, Kieber JJ. 2015.** The yin-yang of hormones: cytokinin and auxin interactions in plant development. *The Plant Cell* **27**(1): 44–63.
- Shahzad B, Tanveer M, Hassan W, Shah AN, Anjum SA, Cheema SA, Ali I. 2016.** Lithium toxicity in plants: Reasons, mechanisms and remediation possibilities—A review. *Plant Physiology and Biochemistry* **107**: 104–115.
- Smith SY, Collinson ME, Rudall PJ, Simpson DA, Marone F, Stampanoni M. 2009.** Virtual taphonomy using synchrotron tomographic microscopy reveals cryptic features and internal structure of modern and fossil plants. *Proceedings of the National Academy of Sciences* **106**(29): 12013–12018.
- Strotton MC, Bodey AJ, Wanelik K, Darrow MC, Medina E, Hobbs C, Rau C, Bradbury EJ. 2018.** Optimising complementary soft tissue synchrotron X-ray microtomography for reversibly-stained central nervous system samples. *Scientific Reports* **8**(1): 12017.
- Sullivan S, Ralet MC, Berger A, Diatloff E, Bischoff V, Gonneau M, Marion-Poll A, North HM. 2011.** CESA5 is required for the synthesis of cellulose with a role in structuring the adherent mucilage of Arabidopsis seeds. *Plant Physiology* **156**(4): 1725–1739.
- Tarkowská D, Novák O, Floková K, Tarkowski P, Turečková V, Grúz J, Rolčík J, Strnad M. 2014.** Quo vadis plant hormone analysis? *Planta* **240**(1): 55–76.
- Tester M, Davenport R. 2003.** Na⁺ tolerance and Na⁺ transport in higher plants. *Annals of Botany* **91**(5): 503–527.
- Todaka D, Zhao Y, Yoshida T, Kudo M, Kidokoro S, Mizoi J, Kodaira KS, Takebayashi Y, Kojima M, Sakakibara H. 2017.** Temporal and spatial changes in gene expression, metabolite accumulation and phytohormone content in rice seedlings grown under drought stress conditions. *The Plant Journal* **90**(1): 61–78.
- Western TL. 2012a.** The sticky tale of seed coat mucilages: production, genetics, and role in seed germination and dispersal. *Seed Science Research* **22**(01): 1–25.
- Western TL. 2012b.** The sticky tale of seed coat mucilages: production, genetics, and role in seed germination and dispersal. *Seed Science Research* **22**: 1–25.
- Western TL, Burn J, Tan WL, Skinner DJ, Martin-McCaffrey L, Moffatt BA, Haughn GW. 2001.** Isolation and characterization of mutants defective in seed coat mucilage secretory cell development in Arabidopsis. *Plant Physiology* **127**(3): 998–1011.
- Yang X, Zhang W, Dong M, Boubriak I, Huang Z. 2011.** The achene mucilage hydrated in desert dew assists seed cells in maintaining DNA

integrity: adaptive strategy of desert plant *Artemisia sphaerocephala*.
PLoS ONE **6**(9): e24346.

Zohary M. 1937. Die verbreitungsökologischen Verhältnisse der Pflanzen
Palästinas. *Beihefte zum Botanischen Centralblatt* **56**: 1–155.

8. Conclusions

Plants have evolved fascinating mechanisms to cope with the spatial and temporal variability of favourable environmental conditions. The true diaspore heteromorphism in *Ae. arabicum* is best exemplified by the adage “*Don’t put all your eggs in one basket*”, allowing this species to survive in the hostile environments of semi-arid scree slopes. Work in this thesis has shown that elucidating the eco-physiological, biomechanical, and molecular mechanisms of *Ae. arabicum* fruit, seed, and seedling traits has involved a fundamentally novel, interdisciplinary, and comparative approach.

The dispersal mechanisms operating in *Ae. arabicum* (antitelechory and telechory) were shown to differ with respect to biomechanical and ecophysiological properties of its diaspores. These traits confer an interdependence of dormancy and dispersal unlike most heteromorphic systems, in that higher dormancy is combined with high dispersibility (IND fruits) and low dormancy is combined with low dispersibility (M^+ seeds). In the IND fruit, both the seed germination suppressor ABA and the distinct anatomy of the pericarp play crucial roles. In the case of the M^+ seeds, mucilage development, regulated by the key transcription factors *GL2* and *MYB61*, underpins changes in the ovule wall observed soon after flowers are pollinated. Morphological differences arising early in reproductive development were confirmed by high-resolution three-dimensional volumetric investigations using SRXTM.

Seedling establishment is a key stage in the life history of annual plants that is particularly vulnerable to a range of abiotic stresses. Investigation of tissue-specific transcriptional profiles in *Ae. arabicum* suggested why M⁺ and M⁻ seedling morphs had similar growth responses. This was consistent with transcriptional “resetting” having occurred early in seedling pre-emergence growth, in that the number of significant DEGs diminished throughout the completion of germination and transition to seedling. It is for this reason seedlings, and later adult plants, lack phenotypic differences – no matter of their “origin”.

Using *Ae. arabicum* to understand the basis of dimorphism, phenotypic plasticity, and complex persistence in variable environments has therefore revealed remarkable strategies and adaptations in many stages of plant growth. Though the published and unpublished works presented in this thesis have made major contributions in understanding dimorphism as a survival strategy, further studies are, however, needed to obtain a more complete picture of the species, particularly in its natural environment. Questions on morph longevity, seed bank dynamics, and seed coat compositional analyses remain unanswered. A working transgenic approach to enable more mechanistic (functional genomics) insights is also fundamentally required.

Nonetheless, the work and experiments conducted in this thesis provide a solid basis for expanding this area of exciting research, and demonstrate the feasibility of *Ae. arabicum* as an invaluable model species for current and future investigations on bet-hedging diaspore dimorphism.

9. Appendices

In addition to the main body of my independent thesis work presented here, contributions were made as a co-author to other published works. These two papers, though distinct from this thesis, are related through the broader research questions of the SeedAdapt consortium.

9.1 Reference-free (*de novo* assembly) versus reference-dependent (genome-based) approaches for differential expression analysis

This paper compared *de novo* and genome based transcriptome assemblies to evaluate the reference-free versus -dependent approach for identifying differentially expressed genes (DEGs) in *Ae. arabicum* seeds. Comparisons of the strict consensus of three methods (DESeq2, edgeR and NOISeq) and Gene Ontology terms distinguished seed morphs and revealed key genes associated with seed maturation (*e.g.* encoding late embryogenesis abundant proteins and transcription factors regulating seed development and maturation, such as ABI3, FUS3, LEC1 and WRI1 homologs). The work also established a bioinformatics pipeline for future reference-dependent transcriptome analyses. Results indicated M⁺ seeds may desiccate and mature faster than M⁻, thus shedding light on the mechanisms underpinning previously identified differences between morphology and germination behaviour of M⁺ and M⁻ seeds.

The results of the work (Wilhelmsson *et al.*, 2019) were published in *BMC Genomics* under the title “Usability of reference-free transcriptome assemblies for detection of differential expression: a case study on *Aethionema arabicum* dimorphic seeds” (DOI: 10.1186/s12864-019-5452-4), and is presented here in its full form. The contributions W Arshad made to this manuscript were providing the mass and moisture content data, preparation of Figure 1, and drafting of the text.

RESEARCH ARTICLE

Open Access



Usability of reference-free transcriptome assemblies for detection of differential expression: a case study on *Aethionema arabicum* dimorphic seeds

Per K. I. Wilhelmsson¹, Jake O. Chandler², Noe Fernandez-Pozo¹, Kai Graeber², Kristian K. Ullrich^{1,8}, Waheed Arshad², Safina Khan², Johannes A. Hofberger³, Karl Buchta¹, Patrick P. Edger⁴, J. Chris Pires⁵, M. Eric Schranz³, Gerhard Leubner-Metzger^{2,6*} and Stefan A. Rensing^{1,7*}

Abstract

Background: RNA-sequencing analysis is increasingly utilized to study gene expression in non-model organisms without sequenced genomes. *Aethionema arabicum* (Brassicaceae) exhibits seed dimorphism as a bet-hedging strategy – producing both a less dormant mucilaginous (M⁺) seed morph and a more dormant non-mucilaginous (NM) seed morph. Here, we compared de novo and reference-genome based transcriptome assemblies to investigate *Ae. arabicum* seed dimorphism and to evaluate the reference-free versus -dependent approach for identifying differentially expressed genes (DEGs).

Results: A de novo transcriptome assembly was generated using sequences from M⁺ and NM *Ae. arabicum* dry seed morphs. The transcripts of the de novo assembly contained 63.1% complete Benchmarking Universal Single-Copy Orthologs (BUSCO) compared to 90.9% for the transcripts of the reference genome. DEG detection used the strict consensus of three methods (DESeq2, edgeR and NOISeq). Only 37% of 1533 differentially expressed de novo assembled transcripts paired with 1876 genome-derived DEGs. Gene Ontology (GO) terms distinguished the seed morphs: the terms translation and nucleosome assembly were overrepresented in DEGs higher in abundance in M⁺ dry seeds, whereas terms related to mRNA processing and transcription were overrepresented in DEGs higher in abundance in NM dry seeds. DEGs amongst these GO terms included ribosomal proteins and histones (higher in M⁺), RNA polymerase II subunits and related transcription and elongation factors (higher in NM). Expression of the inferred DEGs and other genes associated with seed maturation (e.g. those encoding late embryogenesis abundant proteins and transcription factors regulating seed development and maturation such as ABI3, FUS3, LEC1 and WRI1 homologs) were put in context with *Arabidopsis thaliana* seed maturation and indicated that M⁺ seeds may desiccate and mature faster than NM. The 1901 transcriptomic DEG set GO-terms had almost 90% overlap with the 2191 genome-derived DEG GO-terms.

Conclusions: Whilst there was only modest overlap of DEGs identified in reference-free versus -dependent approaches, the resulting GO analysis was concordant in both approaches. The identified differences in dry seed transcriptomes suggest mechanisms underpinning previously identified contrasts between morphology and germination behaviour of M⁺ and NM seeds.

Keywords: *Aethionema arabicum*, Dimorphic seeds, Reference and reference-free, RNA-seq, Transcriptome,

* Correspondence: gerhard.leubner@rhul.ac.uk; stefan.rensing@biologie.uni-marburg.de

²School of Biological Sciences, Royal Holloway University of London, Egham, Surrey TW20 0EX, UK

¹Plant Cell Biology, Faculty of Biology, University of Marburg, 35043 Marburg, Germany

Full list of author information is available at the end of the article



Background

RNA-sequencing (RNA-seq) technology is a valuable tool to investigate gene expression [1], especially in species where no reference genome is available. Without any prior molecular data about a particular species, de novo transcriptome assembly of RNA-seq data offers a unique opportunity to study gene expression on a transcriptome-wide scale of any trait of interest. Due to drops in library and sequencing costs, it is now widely utilized by many scientists to study traits of particular interest in a wide-range of species. However, there are limitations to using a de novo transcriptome assembly compared to a reference-genome guided approach. Since less sequence information is used in the creation of the transcripts in a de novo transcriptome, in comparison to a reference genome, low expressed genes are more difficult to detect. De novo assembled transcripts are also more likely to be fragmented.

Here, we apply a reference-free and a reference-dependent approach to compare the gene expression in the dry mature dimorphic seeds of *Aethionema arabicum*. This species represents the sister lineage to all other Brassicaceae, and is a herbaceous annual native to parts of Eastern Europe and the Middle East. It exhibits diaspore heteromorphism – i.e. the ability to produce multiple morphologically and physiologically distinct fruit or seed morphs on individual plants [2, 3]. *Ae. arabicum* produces two distinct fruits, a dehiscent (DEH) and an indehiscent (IND) fruit morph. The dehiscent fruit contains typically four seeds, shatters on maturity, and disperses mucilaginous seeds (M^+). Conversely, the indehiscent fruit contains a single non-mucilaginous seed (M^-) encased in a pericarp (fruit coat). Upon maturity, the entire IND fruit detaches, via abscission, from the parent plant leading to the fruit's dispersal [3, 4]. In addition to these morphological differences between the two morphs, the NM seeds appear to be more dormant compared to the M^+ seeds, with NM exhibiting much slower germination at 14°C [3]. The production of two contrasting seed/fruit morphs is proposed to constitute a bet-hedging strategy that increases long-term plant fitness in disturbed and unpredictable extreme environments. However, how this heteromorphism is reflected at the transcriptomic level is unknown. With its recently published genome sequence and its basal phylogenetic position within the Brassicaceae, *Ae. arabicum* has potential as a model species for diaspore heteromorphism [3, 5].

For many other non-model plant species, including other heteromorphic systems, a reference genome is not available. Thus, comparing the effectiveness of reference-free and reference-dependent transcriptome

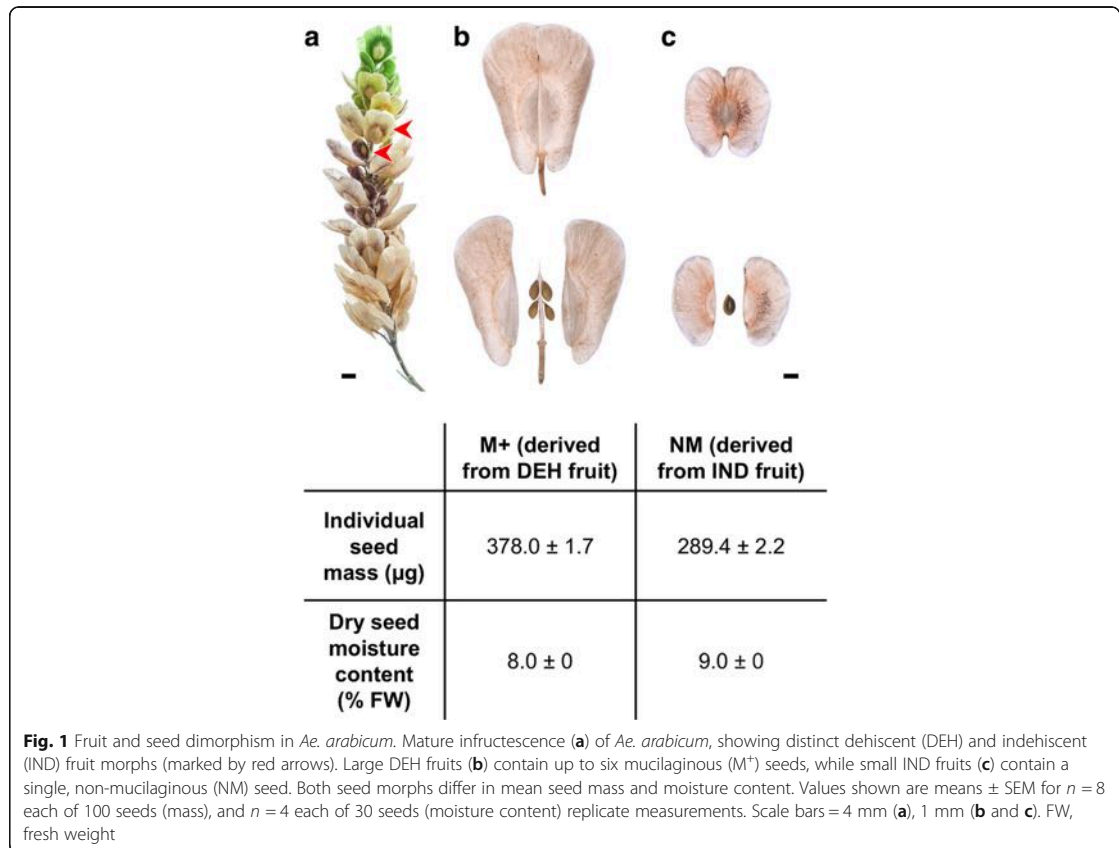
analyses is pertinent to future investigations into such non-model species. Comparison of the transcriptomes of the two *Ae. arabicum* seed morphs represents a realistic and interesting demonstration of both approaches. There are many genomes with accompanying large sets of microarray and qRT-PCR data, and it was early on concluded that de novo assembled transcriptome expression profiles positively correlate with corresponding microarrays and qRT-PCRs [6–8]. Due to the potential of RNA-seq, much work has been done on how to get the best results out of a de novo transcriptome assembly [9–13]. The Trinity suite [14] is one of the most cited de novo transcriptome assemblers exhibiting good performance metrics [13]. In order to generate a representative transcriptome, sequencing depth is important to be able to reconstruct as many genes as possible including those expressed at low levels. The ability to detect weakly expressed sequences can only be improved by increasing the sequencing depth. This highlights the diminishing investment returns (sequencing depth) in relation to yield (sequence resolution) for RNA-seq. Despite the known limiting factors of transcriptome assembly, the knowledge gained per investment makes reference-free gene expression profiling an obvious choice when working with non-model species.

To evaluate the knowledge that can be gained with reference-free gene expression profiling, a reference-dependent expression profiling was carried out using the existing genome assembly of *Ae. arabicum* [5]. To investigate the seed dimorphism of *Ae. arabicum*, we conducted a highly robust differentially expressed genes (DEGs) detection analysis and used it to compare DEGs derived from a transcriptome-based and a genome-based mapping approach. The aim of this study was to find DEGs between *Ae. arabicum* dimorphic seeds, and to compare the RNA-seq analysis performed using two different references, a de novo transcriptome assembly and the *Ae. arabicum* genome sequence V2.5.

Results and discussion

Overview of RNA-seq analysis of *Ae. arabicum* mature dimorphic seeds

The mature dimorphic seeds, M^+ from DEH fruits and NM from IND fruits (designated NM, for “non-mucilaginous”, in our RNA-seq analysis), differed in size and mass but not in seed moisture content (Fig. 1). RNA was extracted from freshly harvested mature M^+ and NM seeds and the resultant RNA samples processed as described in the Methods section. As shown in Fig. 2, RNA-seq raw reads were processed and checked using FastQC

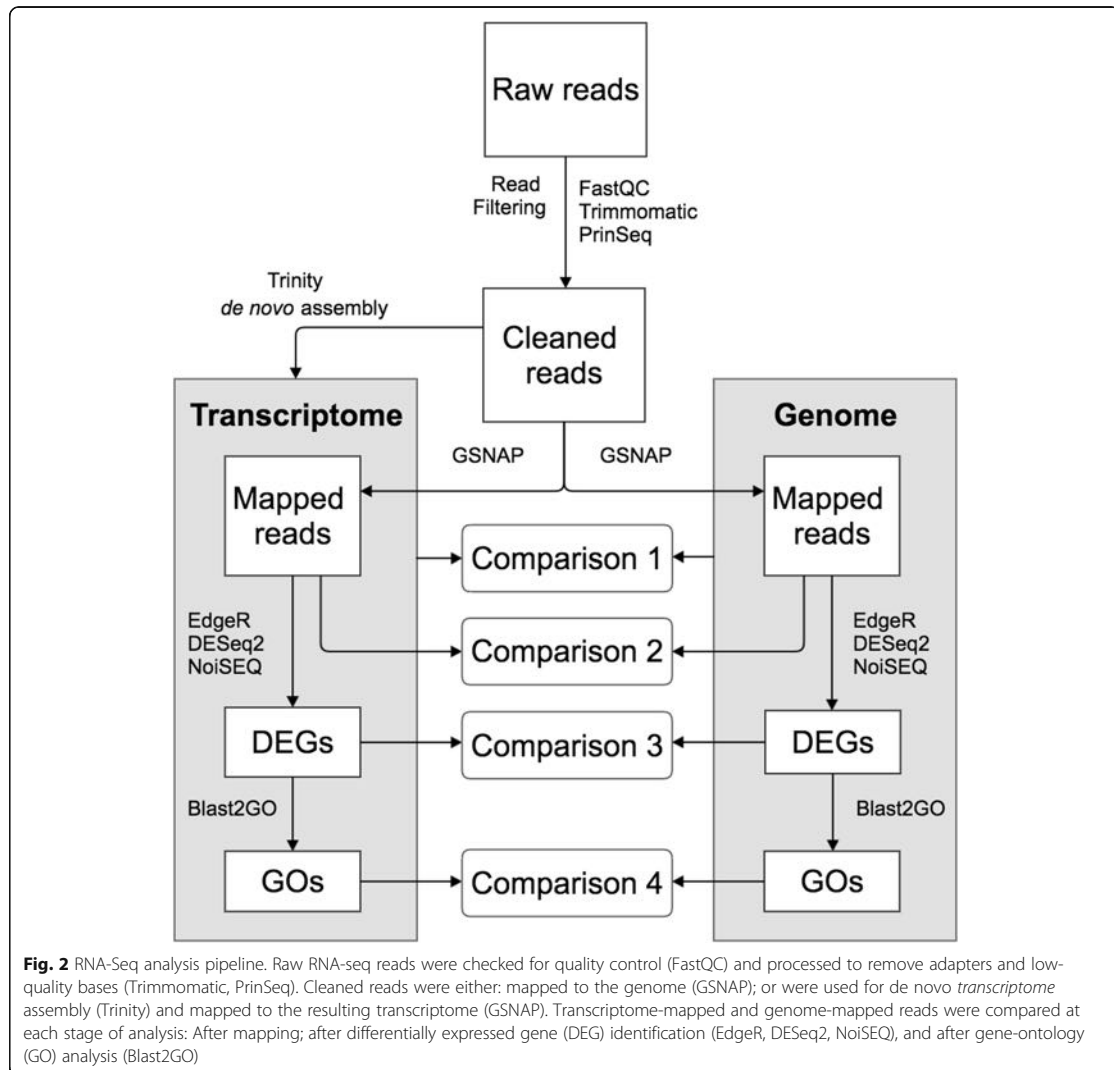


(<https://www.bioinformatics.babraham.ac.uk/projects/fastqc/>), Trimmomatic version 0.32 [15] and PrinSeq [16]. Subsequently, cleaned reads were used for de novo transcriptome assembly for *Ae. arabicum* M^+ and NM seeds using Trinity [14]. The same set of cleaned reads was mapped to the gene models of the reference genome using GSNAP [17]. EdgeR, DESeq2 and NOISeq [18–20] were used to normalize read counts and to detect DEGs in a strict consensus approach, and Blast2GO [21] was used to assign Gene Ontology (GO) terms to the genes. Comparisons were performed between the transcriptome and the genome (Comparison 1, Fig. 2), the reads mapped to both the de novo transcriptome and reference-based genes (Comparison 2, Fig. 2), the DEGs found in both approaches (Comparison 3, Fig. 2), and between their GO terms (Comparison 4, Fig. 2).

Read filtering of RNA-seq raw data

To generate the raw reads, a total of four cDNA libraries were sequenced, with two biological replicates

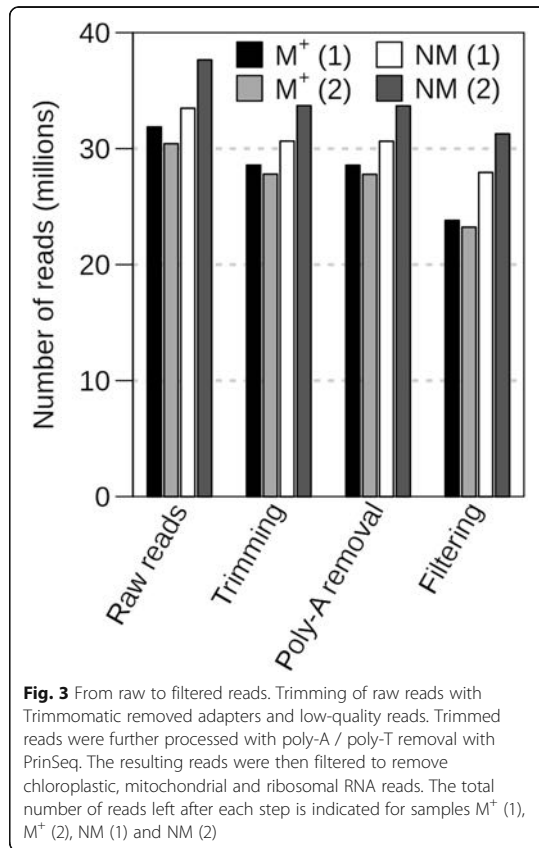
of *Ae. arabicum* dry mature dimorphic seeds, termed $M^+ 1/M^+ 2$ for the M^+ seeds and NM1/NM2 for the NM seeds. Raw reads were processed to remove adapters, organellar, ribosomal RNA (rRNA) and low-quality sequences (Fig. 3). Adapter sequences were removed and low-quality sequences were trimmed using Trimmomatic. Poly-A and poly-T tails were removed using PrinSeq. This process resulted in an average loss of 9.6% of all reads for the four libraries. To reduce the complexity of the assembly/mapping, and to check for correct poly-T selection, all data were filtered to remove reads with plastid, mitochondrial and ribosomal RNA origin resulting in an average loss of 12% of the reads for the four libraries. Visualization of these quality control steps provides a good measure of library quality making possible to see if there are any higher than average read losses in the individual steps. After passing all the filters, the sets of cleaned sequences contained between 20 and 30 million reads (Fig. 3), which is in the range of read numbers commonly used for RNA-seq analysis for DEG detection [22].



De novo transcriptome assembly

Processed reads from all four samples combined were assembled de novo using Trinity to reconstruct the *Ae. arabicum* dry seed transcriptome. From a total of 30,742,186 reads, 27,407,363 reads (89.15%) could be assembled. This resulted in a total of 62,182 transcripts including potential splice variants or fragmentary sequences. The longest gene sequences from each Trinity gene cluster were selected to reduce redundancy, resulting in 34,784 transcripts (Additional file 1). To assess the quality and completeness of the *Ae. arabicum* dry seed de novo transcriptome, and to compare it to

the gene models from the genome (Comparison 1, Fig. 2), it was analyzed using the Benchmarking Universal Single-Copy Orthologs (BUSCO) tool [23] (*embryophyta odb9*) which checks for the presence of Embryophyta “near-universal single-copy orthologs”. For the de novo assembled transcriptome, 908 transcripts out of 1440 of the BUSCO genes were complete (63.1%). Of those, 885 were single copy and 23 duplicated. One hundred sixty-eight transcripts were fragmented and 364 missing (Fig. 4). The corresponding number of BUSCO completeness in the 23,594 gene models of the genome was 1309 (90.9%). Of those, 1274 were single copy and 35



duplicated. Forty-one gene models were fragmented and 90 missing (Fig. 4). To compare these results with a well-annotated model species, *Arabidopsis thaliana* (TAIR10, [24]) was included in the BUSCO analysis. For *A. thaliana*, 1431 complete genes were found (99.3%), 1413 were single copy and 18 duplicated; five genes were fragmented and four missing. The relatively low number of complete genes in *Ae. arabicum* transcriptome is to be expected, since dry seeds represent an atypical tissue that lacks much of the transcription going on in photosynthetically/developmentally active tissue. Also, it is common that some genes are fragmented in de novo assemblies, as shown in Fig. 5a which indicates the length distribution of de novo assembled transcripts is skewed towards shorter lengths compared to the *Ae. arabicum* mRNAs predicted from the genome.

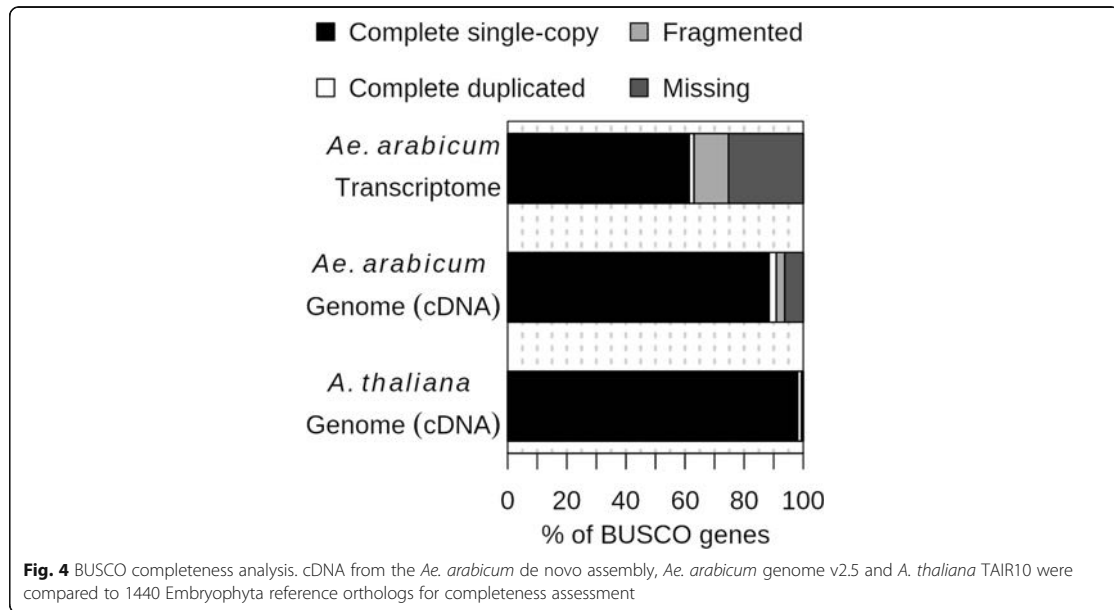
Mapping reads to the transcriptome and the genome

To determine read counts for subsequent DEG analysis, cleaned reads were mapped to the transcriptome and the genome using GSNAP [17] and counted using

HTSeq-count [25] with the respective general feature format (GFF) file. Counted reads for the four samples are shown in Fig. 5b. This analysis showed that on average 84% of reads were mapped to the transcriptome and 94% to the genome. The drop from 89.15% of the reads being used for assembling to 84% mapping is to a large extent explained by the removal of redundancy keeping only the longest isoform of each transcript. On average, the cleaned reads had a read length of 83 bp. Mapping the reads to the 23,594 genomic gene models, 7814 models had a coverage lower than 1 (where 1 corresponds to an average 1-fold coverage of the gene length; see Methods for details) and 11,189 gene models had a coverage lower than 5 (Additional file 2: Table S1). This highlights the challenges to assemble full-length transcripts. Using reciprocal BLASTN with a coverage cut off of 50% for both transcriptomic (virtual transcripts) and genomic coding sequences (CDS), 6745 transcript-gene pairs could be identified (Additional file 2: Table S2). To compare the expression levels between the transcriptome- and the genome-based approach (Comparison 2, Fig. 2), the 6745 gene-transcript pairs were considered. Principal Component Analysis (PCA) using the Reads Per Kilobase per Million mapped reads (RPKM) of the 6745 genes (Additional file 3: Figure S1) showed, as expected [9], that replicates from the same seed morph clustered together and samples from different seed morphs are more distant. This is apparent in both the de novo and reference-genome approach. To assess gene family completeness, the predicted proteins of the reference genome and the de novo transcriptome were screened for Transcription Associated Proteins (TAPs, comprising transcription factors, TF, and transcriptional regulators, TR) using the TAPscan pipeline [26]. 1860 (113 unique families) and 1009 (105 unique families) TAPs were detected in the genome and transcriptome, respectively (Additional file 2: Table S3 and S4). Finding fewer TAPs in the transcriptome is to be expected due to the atypical tissue of the transcriptome in comparison to the whole genome. Genome-wide, 7.6% were multi domain TAPs (defined by more than one domain), while only 4.2% TAPs were multi domain in the transcriptome, due to the fragmented nature of the transcriptome.

Differential gene expression analysis

To learn more about the differences between the mature dimorphic seeds, gene expression was analyzed using both references: the de novo transcriptome assembly and the genome annotation. Since the combination of several methods minimizes false positives [27], DEGs were detected in a robust way using the strict consensus (overlap) of three different DEG analysis programs: edgeR, DESeq2 and NOISeq. This approach combines



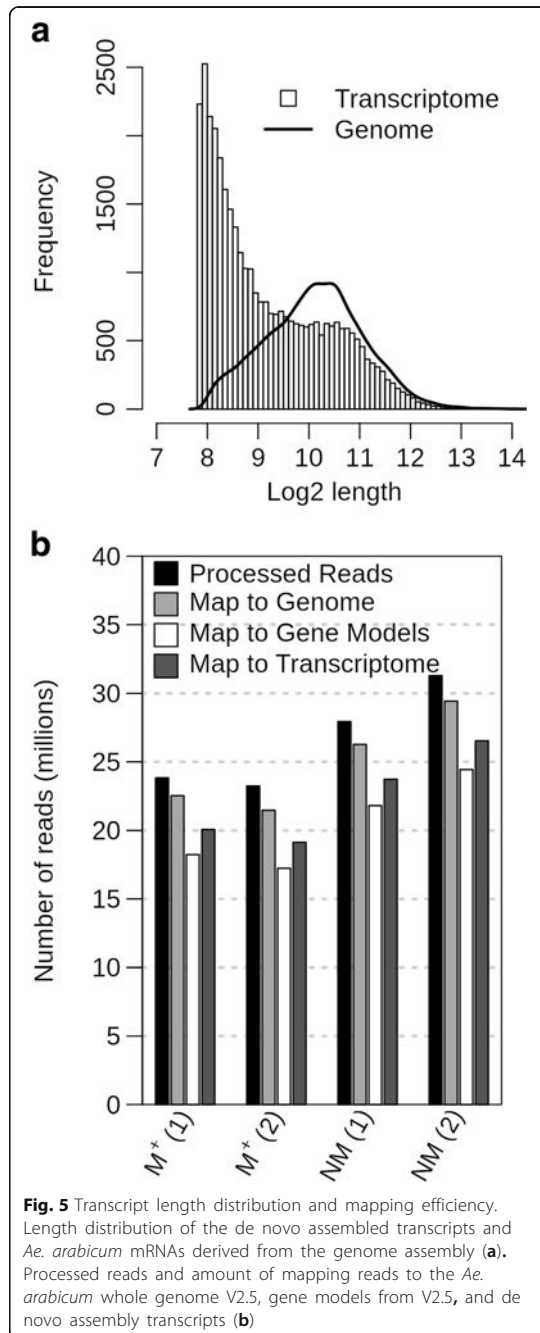
two parametric methods to detect DEGs (edgeR and DESeq2), and a non-parametric method (NOISeq). The intersection of the DEGs obtained by the three methods was considered the resulting DEGs (Fig. 6a, b). In all comparisons edgeR called the most DEGs while NOISeq was the most restrictive (Fig. 6a, b), thus the NOISeq set was representing the consensus DEG set best. This approach resulted in the exclusion of low expressed DEGs (Additional file 3: Figure S2) below RPKM 2, representing genes of low abundance that typically cannot be shown as expressed in a quantitative PCR approach [28].

One thousand five hundred thirty-three and one thousand eight hundred seventy-six DEGs were obtained, respectively, using the de novo transcriptome (Fig. 6a, Additional file 2: Table S4) and the reference genome (Fig. 6b; Additional file 2: Table S3). When comparing common DEGs detected in both approaches (Comparison 3, Fig. 2), 561 gene-transcript pairs were found to be differentially expressed in both. Thus, 561/1533 (37%) of the de novo transcriptome consensus DEGs were also well represented by transcripts identified as DEGs by the genome approach, all of them showing the same direction of expression (Additional file 2: Table S2). PCA for the 561 DEGs identified by both approaches showed that the biological differences between the dimorphic seeds are much greater than the differences deriving from the references used (Fig. 6c). All samples from the same seed morphs clearly clustered together, independently of the sequence reference (transcriptome or genome). The remaining 972 transcripts (63%) of the 1533 transcriptome DEGs did either not pass the 50% coverage cut-off

(405/1533), only had a hit in one direction of the reciprocal BLAST (122/1533), their reciprocal hit was not a DEG in the genome (197/1533) or they did not produce any significant alignment at all (248/1533). Hence, approximately 40% of the DEGs from the de novo transcriptome assembly are equivalent to the DEGs found when a genome reference is available, and 60% of the DEGs were either fragmented or could not be clearly paired up with a gene model. This indicates that data for individual genes might not always be available when working with de novo transcriptome differential expression analysis. In cases like this, it might be important to perform other analyses that study the changes of global functions occurring in the samples, such as Gene Ontology bias. To verify the robustness of the expression pattern between the dimorphic seeds, we performed qRT-PCR on a selection of DEGs with varying levels of RPKM values in an independent biological experiment (Additional file 3: Figure S3). Despite the fact that the qRT-PCR results are derived from a completely independent experiment with different RNA samples, the expression patterns were confirmed for eight of the ten selected DEGs.

Gene ontology analysis

The number of GO terms associated with the genome and the de novo transcriptome, for all transcripts, for the DEGs and for the overlap between both approaches is summarized in Table 1 (and in more detail in Additional file 2: Table S5–S6) and is referred to as a GO-presence list. When comparing



(Comparison 4, Fig. 2) what is shared between the GO-presence list of the reference genome and the de novo transcriptome (All Transcripts Overlapping GO terms from Table 1; using Fisher's exact test with an

fd_r corrected *p* value of 0.05), only 12 out of 5584 GO terms were shown to have significant differences in the number of transcripts associated to them (Additional file 2: Table S5). The GO-presence list of the DEGs (All DEGs Overlapping GO terms from Table 1) showed no significant differences at all between the genome and the transcriptome (Additional file 2: Table S6). Furthermore, having 1663 common GO terms present in the GO-presence lists of both DEG sets (Fig. 7) is a significant over-representation compared to the null hypothesis of selecting 1901 and 2191 GO terms randomly (Chi squared test, *p* = 2.2e-16). This suggests a biological signal, supporting that functional analysis of GO terms by transcriptome de novo assembly resembles the data derived by genomic analysis.

For both the 1256 overlapping GO-terms of the DEGs GO-presence lists with higher abundance in NM (NM) seeds ("NM-high") and 880 overlapping GO-terms of the DEGs GO-presence lists of with lower abundance in NM seeds ("NM-low"), none had significantly different quantities of underlying transcripts. The numbers and overlap of significantly over- and under-represented GO-terms of each class (Biological Process (BP), Molecular Function (MF) and Cellular Component (CC)) for all, NM-high and NM-low DEGs derived from the two approaches are summarized in Additional file 2: Table S7 and in more detail in (Additional file 4: Table S8) and are referred to as GO-bias lists. Overall, the NM-high and NM-low BP GO-bias lists are quite different. In the reference genome approach, NM-high has 340 unique BP terms, NM-low has 137 unique BP terms in the respective GO-bias list, with only 58 BP terms overlapping between both sets. Some of the most significant overlapping BP terms belong to high-level categories, such as 'protein metabolic process' and 'gene expression' (comprehensive lists of GO terms associated with the DEG sets are provided in Fig. 7). In agreement with this, ribonucleoprotein complex is the most significantly over-represented CC term in the genome approach, and structural constituent of ribosome is the most significantly over-represented MF term (Additional file 4: Table S8).

Many of the GO-terms found to be significantly over-represented and under-represented using the transcriptome approach were also found with the genomic approach: Out of the 321 BP terms found to be significantly over (255) and under (66) represented in the transcriptome-derived DEG set (GO-bias lists) (Fig. 7b and Additional file 4: Table S8), 258 (80%) were also found to be the same in the genome-derived DEG set (GO-bias lists) (Fig. 7a and Additional file 4: Table S8). On average, approximately 80% of the significantly over- and under-represented GO terms of the transcriptomic DEG sets (GO-bias lists) were also

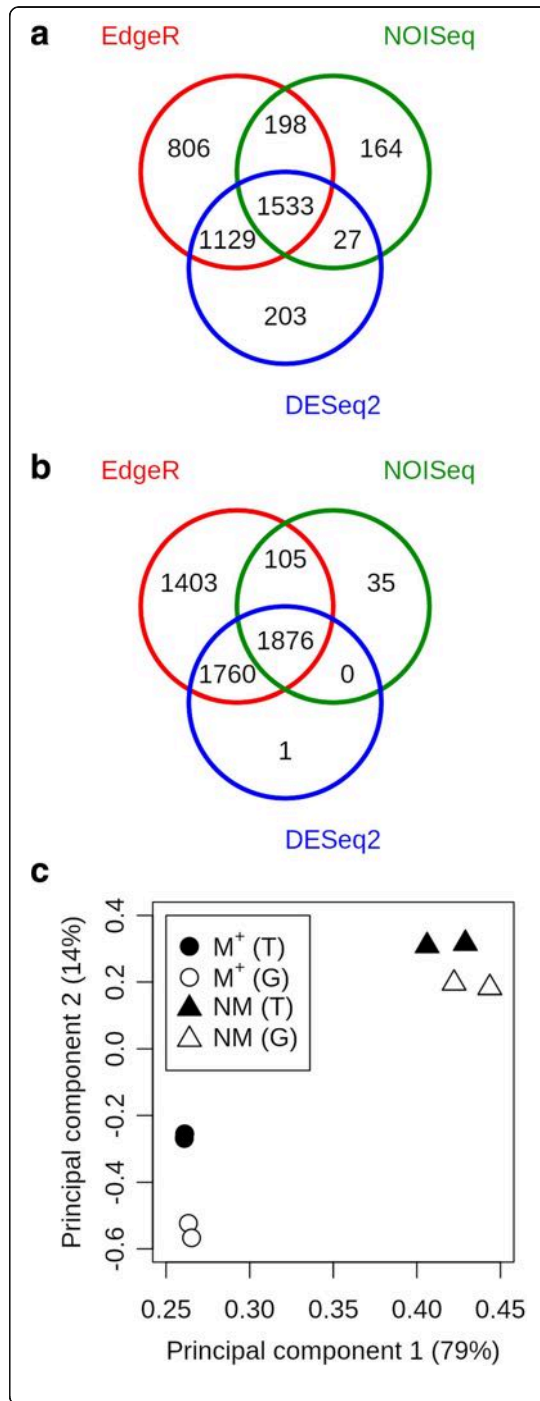


Fig. 6 Consensus of DEG calling and PCA of overlap of common DEGs. Venn diagram of the DEGs called between NM and M⁺ seeds by the three DEG detection programs (edgeR, NOISeq and DESeq2) using the transcriptome (a) and genome (b) approach. Principal Component Analysis of RPKM (Reads Per Kilobase per Million reads) of the 561 DEGs common to the transcriptome, 'T' and genome, 'G' (c). Samples M⁺ (circle) and NM (triangles), in black, show the results for the dehiscent and indehiscent seeds in the transcriptome approach. Samples M⁺ (circle) and NM (triangles), in white, show the corresponding results in the genome approach. The percentage variance explained by each principal component is indicated on the axes

reported using the genomic approach. So, in comparison to the 40% overlap of DEGs on a gene-transcript pair level, we found a much higher overlap of differentially expressed functions between the *Ae. arabicum* M⁺ and NM dimorphic seeds using GO term bias analysis, even though some of the genes involved in these functions are missing in the transcriptome DEG dataset. The genomic approach reports on average 37% more GO-terms to be significantly over- or under-represented, which can be explained by the 22% more DEGs and 10% more GO-terms per gene. Though a transcriptome de novo assembly approach gives less information, the information that is given overlaps very well with a genome-based approach. Taken together, this finding supports the view that analysis of GO terms by transcriptome de novo assembly is a useful tool when no

Table 1 Summary of GO terms associated with both the genome- and transcriptome-derived transcripts and respective DEG sets

		Transcriptome	Genome
All Transcripts	Total number	34,784	23,594
	Number with GO terms	18,845 (54%)	18,320 (78%)
	GO terms per transcript ^a	7.1	7.9
	Amount of GO terms	6091	6080
All DEGs (M ⁺ + NM)	DEGs	1533	1876
	Amount of GO terms	1901	2191
	Overlapping GO terms	1663	
NM-high ^b	DEGs	745	998
	Amount of GO terms	1427	1673
	Overlapping GO terms	1256	
NM-low ^c	DEGs	788	878
	Amount of GO terms	1085	1185
	Overlapping GO terms	880	

^aAverage including only transcripts with at least 1 GO term

^bDEGs where transcript is more abundant in NM dry seed than M⁺ seed

^cDEGs where transcript is less abundant in NM dry seed than M⁺ seed



genome is available, and resembles the data derived by genomic analysis.

DEG analysis of mature dimorphic *Ae. arabicum* seeds

The most significantly over-represented BP terms unique to the NM-high DEGs GO-bias list (transcripts with a higher abundance in NM seed compared to M⁺ seed) include mRNA metabolic process, mRNA processing and response to stimulus. On the other hand, the most significantly over-represented BP terms unique to the NM-low DEGs GO-bias lists (transcripts with a lower abundance in NM seed compared to M⁺ seed) are translation, ribosome biogenesis and nucleosome assembly (Additional file 4: Table S8). This is also reflected in the CC and MF terms, with the nucleus CC term and RNA binding MF term being among the most significantly over-represented terms in the NM-high DEGs (GO-bias list) and the structural constituent of ribosome MF term and ribosome CC term being among the most significantly over-represented terms in the NM-low DEGs (GO-bias lists; Additional file 4: Table S8). Thus, it is generally indicative that the transcriptome of the M⁺ “dry” mature seed morph transcriptome may be relatively more oriented towards translation of RNA and chromatin assembly, whereas the NM “dry” mature seed morph transcriptome may be more oriented to post-transcriptional processing of RNA. It is possible that these differences may reflect the stage which was sampled – the dry seed. Thus, transcriptomic differences may be due to differences in the stage of seed development or maturation the seed morphs have reached before desiccation. For this reason, we put the transcriptomic differences between *Ae. arabicum* NM and M⁺ seed in context of the well-studied seed development and maturation of *A. thaliana*.

The *Ae. arabicum* M⁺ seed morph as well as *A. thaliana* seeds are both dispersed from dehiscent fruits and seem to resemble each other in terms of morphology and physiology [3]. In Fig. 8, we compare the expression of selected *Ae. arabicum* key DEGs (which differ between the dimorphic M⁺ and NM seeds, selected based on the prominent GO terms and genes with importance to seed development and maturation) with the expression of their putative orthologs derived from published transcriptomes of developing and mature *A. thaliana* seeds [29–31]. During the *A. thaliana* seed maturation and late maturation phases desiccation tolerance and dormancy are established in parallel with drying resulting in the low-hydrated dispersed seed state (Fig. 8a) [32, 33].

For the dry mature *Ae. arabicum* dimorphic seeds, we found that the abundance of at least 119 (reference approach) and 113 (de novo approach) ribosomal protein transcripts were 1.5- to 3-fold higher in M⁺ seeds as

compared to NM seeds (Fig. 8d, Additional file 3: Figure S4a). This seems to be a general pattern as there were no ribosomal protein genes with higher transcript abundances in NM seeds. The abundance of the putatively orthologous transcripts of these DEGs decreased during *A. thaliana* seed maturation (Fig. 8b). A genome-wide analysis of ribosomal protein gene expression during *A. thaliana* and *Brassica napus* seed maturation revealed the same temporal pattern [30, 34]. During maturation, ribosomal activity is required for processes such as seed storage compound accumulation which ceases upon late maturation drying. In dry seeds, ribosomes are mainly present in the monosome form [35]. Ribosomal profiles change with polysomes being formed during seed germination and subsequent seedling growth. Interestingly, during these processes, differential expression of ribosomal protein genes occurs and may affect ribosome composition and thereby the selection of translated mRNAs [31, 35–37]. 35–40% (reference approach) and ~30% (de novo approach) of the ribosomal protein genes in M⁺ seeds show approximately 2-fold higher transcript abundances, which suggests that they dry out earlier during late maturation as compared to NM seeds. Considering their overall decrease over time during seed maturation (Fig. 8b), this would explain the higher abundance of transcripts for ribosomal protein genes in dry M⁺ seeds. Alternatively, M⁺ seeds could have a higher translational activity with a higher ribosome per seed content. In the latter case, we would also expect elevated rRNA biosynthesis in the larger M⁺ seeds as compared to the smaller NM seeds. This is however not the case, as evident from the rRNA amounts estimated by filtering during the RNA-seq workflow (Figs. 2 and 3). We therefore conclude that the higher transcript abundance of a large number of ribosomal protein genes in M⁺ seeds seems to be due to faster drying of M⁺ seeds during late maturation. This conclusion is also consistent with the DEG patterns for histones and other genes as discussed later. We propose that the earlier drying out may preserve the mature M⁺ seeds in a state with higher ribosome content and translational activity compared to the mature NM seeds. The distinct states are consistent with the distinct germination and dormancy behavior of the dimorphic *Ae. arabicum* seeds [3].

The NM-low DEGs of the reference approach related to nucleosome assembly include 21 *Ae. arabicum* histone genes, including seven H4, five H3, four H2B, five H2A, but no H1 homolog of *A. thaliana* histone variants. For the dry mature *Ae. arabicum* dimorphic seeds, we found that the abundance of these histone transcripts were 1.5- to 4-fold higher in M⁺ seeds as compared to NM seeds (Fig. 8d, Additional file 3: Figure S4b). The NM-low DEGs of the de novo approach related to nucleosome assembly include nine histone genes, including

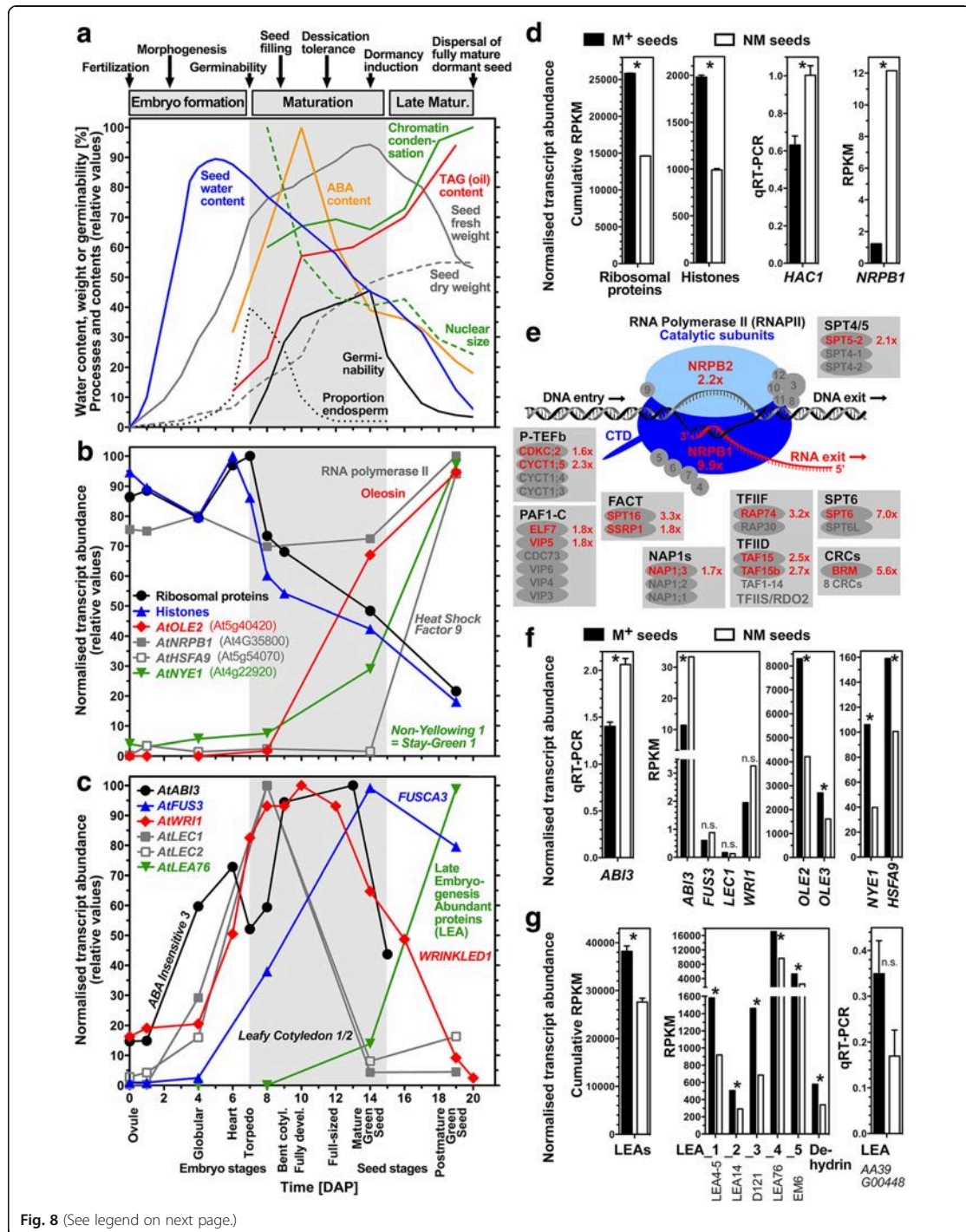


Fig. 8 (See legend on next page.)

(See figure on previous page.)

Fig. 8 Key processes and differentially expressed genes (DEGs) differ between *Ae. arabicum* M⁺ and NM seeds. **a** Timing of key processes during development and maturation of *A. thaliana* seeds. Dormancy and desiccation tolerance coincides with changes in water, abscisic acid (ABA) and triacylglycerol (TAG) contents, seed weight, nuclear size and chromatin condensation, endosperm proportion and germinability; Data from [32, 41, 55]. **b** Selected *Ae. arabicum* DEG putative ortholog expression during *A. thaliana* seed development and maturation. Cumulative transcript abundances for *A. thaliana* putative orthologs of *Ae. arabicum* 21 histone and 119 ribosomal protein genes (Additional file 3: Figure S4); individual abundances for RNA polymerase II large subunit (*AtNRPB1*), oleosin *AtOLE2* (seed storage), heat shock factor *AtHSFA9* (longevity), and *AtNYE1* (chlorophyll degradation); data from Arabidopsis eFP browser [74] and [29–31]. **c** Expression of late embryogenesis abundant (LEA) proteins, seed maturation master regulators (*AtLEC1*, *AtLEC2*, *AtABI3*, *AtFUS3*) and *WRINKLED1* (*AtWR11*), a transcription factor associated with enhanced fatty acid and TAG biosynthesis during *A. thaliana* seed maturation; data from Arabidopsis eFP browser and [29–31, 58]. **d** Expression of selected *Ae. arabicum* DEGs for ribosomal proteins, histones, *NRPB1* (RNAseq) and histone acetyltransferase *HAC1* (qRT-PCR) in M⁺ and NM seeds. Cumulative RPKM values presented for 21 histone and 119 ribosomal protein genes of *Ae. arabicum* (Additional file 3: Figure S4). A * indicates a significant difference between M⁺ and NM seeds based on using a t-test ($p < 0.05$); n.s. means 'not significant'. **e** Expression of RNA polymerase II complex and associated factors [50, 51] that mediate transcription including initiation, elongation and processing of transcripts in *Ae. arabicum* dry seed morphs. Red text indicates factor identified as NM-high DEG with expression ratio (NM / M⁺) indicated. Note core *NRPB1/2* transcript abundance and most factors are several-fold higher in NM seeds. **f** Seed maturation master regulators expression (RNAseq, *ABI3* also by qRT-PCR), oleosins, *NYE1* and *HSFA9* in dry M⁺ and NM *Ae. arabicum* seeds. **g** Selected *Ae. arabicum* LEA expression in dry M⁺ and NM seeds (RNAseq and qRT-PCR). The presented dehydrin is the putative ortholog of At4G39130. Error bars indicate mean \pm SEM for qRT-PCR experiments. For the plotted RPKM values of single genes from the RNAseq data we used the result of the DEG detection pipeline (edgeR + NOISeq + DESeq2) as the indicator of significance

four H3, two H2B, three H2A, with transcript abundance of 1.5- to 4-fold higher in M⁺ seeds as compared to NM seeds. Like the ribosomal protein DEGs, the transcript abundance of the *A. thaliana* histone homologs decreased during seed maturation (Fig. 8b). As with the ribosomal protein DEGs, the approximately 2-fold higher histone transcript abundance in M⁺ seed could be due to faster drying of M⁺ seeds during late maturation. However, as these DEGs represent only ca. 20% of the histones they may serve specific roles which define distinct processes in the dimorphic *Ae. arabicum* seeds. Differential expression of histone variants is linked to DNA replication and transcriptional regulation in response to developmental or environmental cues [38–40]. Histones are major components of chromatin, the protein-DNA complex involved in DNA packaging, chromatin remodeling and heterochromatin formation. *A. thaliana* seed maturation is characterized by nuclear size reduction and increased chromatin condensation (Fig. 8a) [41]. Chromatin condensation and heterochromatin formation involves the expression of specific histone H2B, H2A, and H3 variants [42–44], some of which we found to be *Ae. arabicum* DEGs with higher transcript abundance in M⁺ compared to NM seeds (Fig. 8d). In contrast to those histone transcripts which are NM-low DEGs, genes which modify histones and facilitate transcription and RNA processing were found among the NM-high DEGs. Several genes encoding histone acetyltransferases, deacetylases, and methyltransferases are among the NM-high DEGs, including for example putative orthologs of *A. thaliana* *HAC1* (At1g79000), *HAC12* (At1g16710), *HDA19* (At4g38130), *EFS* (At1g77300) and a SET7/9 family protein (At4g17080) (Fig. 8d, Additional file 3: Figure S4b), with *HAC1*, *HAC12* and *EFS* putative orthologs being

classified as transcriptional regulators by TAPscan (Additional file 2: Table S3). The NM-high DEGs of the de novo approach included *HAC1* (At1g79000), *HAC12* (At1g16710) and *EFS* (At1g77300), with *HAC12* and *EFS* putative orthologs being classified as transcriptional regulators by TAPscan (Additional file 2: Table S4). These histone modifications are involved in regulating seed maturation and dormancy in response to environmental cues [43]. *EFS* for example is known to inhibit seed germination [45], *HDA19* to repress seed maturation genes [46], and *HAC1* to affect seed production and germination [47].

The absence of histone H2B mono-ubiquitination in the *A. thaliana* *hub1* and *hub2* mutants leads to altered chromatin remodeling and reduced seed dormancy [43, 44, 48], but the *HUB1/2* putative orthologs were not among the *Ae. arabicum* NM-high and NM-low DEGs. *HUB1/2* interacts with the Facilitates Chromatin Transcription (FACT) complex, consisting of the SSRP1 and SPT16 proteins, for which mutants exhibit reduced seed production [49, 50]. The FACT complex is a histone chaperone that assists the progression of transcribing RNA polymerase II (RNAPII) on chromatin templates by destabilizing nucleosomes. The transcript abundance of the RNAPII catalytic subunit *NRPB1* increases during the late seed maturation of *A. thaliana* (Fig. 8b). Interestingly, putative *Ae. arabicum* putative orthologs of both RNAPII catalytic subunits were among the NM-high DEGs of the reference approach, with *NRPB1* approximately 10-fold and *NRPB2* 2-fold higher in NM seeds (Fig. 8d, e). *NRPB1* and *NRPB2* were also present with similar expression values in the NM-high DEGs of the de novo approach. Further to this, several key components of the RNAPII elongation complex [50–52] were also among the NM-high DEGs of both

approaches, including transcripts of subunits of almost all known factors known to be involved in regulating RNAPII-mediated transcription initiation, elongation and processing (Fig. 8e, Additional file 3: Figure S4b). In contrast to this, there were no such factors among the NM-low DEGs. Mutants for several of these key components are known for their developmental phenotypes including seed germination and dormancy traits [43, 48, 49, 52, 53]. Moreover, several other transcripts in downstream RNA processing were also among the NM-high DEGs of both approaches. Examples for this include factors with RNA binding, splicing and helicase activity (Additional file 3: Figure S4b). Among them is SMG7 (detected in both approaches) which is involved in nonsense-mediated mRNA decay (NMD) and regulates seed number in *B. napus* [54]. Taken together, these findings support the view that the transcriptome of NM seeds seems to be geared towards transcription which is important for dormancy and persistence. In contrast to this, seed maturation of M⁺ seeds lead to a dry seed transcriptome in which translation is most dominant and is also most important during germination.

Dimorphic *Ae. arabicum* seeds differ in their maturation programmes

Seed-related processes were also amongst the BP terms significantly over-represented in the DEGs (GO-bias list), with the terms embryo development, fruit development, seed development and seed dormancy common to both the NM-high and NM-low DEG list (GO-presence list) (GO terms for each list can be found in Additional file 4: Table S8). However, the BP terms seed maturation, seed germination and seedling development were specific to the NM-high DEG GO-presence list. Additionally, the more specific BP terms positive regulation of seed maturation and negative regulation of seed germination were also identified in the NM-high DEG list. On the other hand, the term seed oil body biogenesis was only identified in the NM-down DEG GO-presence list. Thus, it appears that the M⁺ and NM seed morphs differ in their expression of genes which determine seed traits during maturation. Seed maturation is associated with abscisic acid (ABA) regulated storage reserve accumulation such as oil (triacylglycerol, TAG) which requires gene expression [33, 55–58]. To achieve this fatty acid and TAG biosynthesis genes encoding proteins such as long chain acyl-CoA synthetase (LACS) and acyl-CoA:diacylglycerol acyltransferase (DGAT) are upregulated during *A. thaliana* seed maturation [59]. The TAGs are then transferred and accumulated into oil bodies which are covered on their surface with oleosins. Oleosins are the most abundant proteins found in the seed proteomes of oilseeds [57, 58]. Oleosin gene expression is also upregulated during *A. thaliana*

seed maturation (Fig. 8b), but transcript abundances subsequently decline at the end of late maturation [57]. Their roles include to control oil body dynamics, size, and total oil accumulation during seed maturation. Interestingly, while putative orthologs of *A. thaliana* *LACS7*, *DGAT1*, a fatty acid alcohol dehydrogenase and a lipid transporter are among the NM-high DEGs of the reference approach (Additional file 3: Figure S4b), two oleosin homologs, *OLE2* and *OLE3*, are among the NM-low DEGs (Fig. 8f). In the de novo approach, putative orthologs of *LACS7* and *OLE2* are present among the NM-high and NM-low DEGs respectively, while the *DGAT1* putative ortholog was not detected as DEG and no *OLE3* homolog could be identified. That oleosin and TAG biosynthesis genes are in distinct DEG groups may either be due to distinct regulation during late seed maturation with TAG biosynthesis still up while oleosin expression is declining, or due to more profound differences between the dimorphic seeds in their maturation processes.

Four master regulators of seed maturation have been identified in *A. thaliana*: *ABSCISIC ACID INSENSITIVE3* (*ABI3*, At3g24650), *FUSCA3* (*FUS3*, At3g26790), *LEAFY COTYLEDON2* (*LEC2*, At1g28300), and *LEAFY COTYLEDON1* (*LEC1*, At1g21970) [33, 59, 60]. Whilst *LEC1* encodes the HAB3 subunit of a CCVAAT-box binding TF, *ABI3*, *FUS3*, and *LEC2* are TFs with a B3 DNA binding domain. Corresponding TF classification was detected in the *Ae. arabicum* putative orthologs using TAPscan (Additional file 2: Table S3). In the de novo approach, orthologs of the *ABI3*/VP1 TFs *ABI3* and *FUS3* could be identified, with only *FUS3* being identified by TAPscan, probably because of the shorter length of the transcriptome based protein (577aa) vs. the reference based one (701aa) (Additional file 2: Table S4). These four master regulators control seed maturation including fatty acid and TAG biosynthesis, as well as oleosin expression and oil body formation. Enhancement of fatty acid and TAG biosynthesis by these master regulators is achieved, at least in part, by interaction of the *WRINKLED1* (*WRI1*, At3g54320) TF of the AP2/EREBP family [56, 58–61]. The temporal transcript patterns of these genes during *A. thaliana* seed maturation is depicted in Fig. 8c. Consistent with the *Ae. arabicum* fatty acid and TAG biosynthesis genes being among the NM-high DEGs, the putative *Ae. arabicum* *ABI3* ortholog is among the NM-high DEGs in the reference approach, with a putative *WRI1* ortholog also tending towards higher expression in NM seed (Fig. 8f). It should be noted that the *WRI1* transcript (TR24803|c0_g1_i1) is not represented by a gene model in the current genome version, demonstrating that occasionally the de novo transcriptome approach might out-compete the genomic approach. However, *FUS3* and

LEC1 are expressed roughly equal in dry M^+ and NM seeds (Fig. 8f). Also, if earlier drying of M^+ seeds is the only difference compared to NM seeds, *WRI1* and *ABI3* should be among the NM-low DEGs because their transcript abundances decline in *A. thaliana* during late maturation (Fig. 8c). It therefore seems that M^+ seeds not only dry out earlier, but also mature faster as compared to NM seeds. That M^+ seed maturation is faster is further supported by the finding that the *Ae. arabicum* NM-low DEG list of the reference approach contains the putative orthologs of *NON-YELLOWING1/STAY-GREEN1* (*NYE1/SGR1*, At4g22920), *HEAT SHOCK TRANSCRIPTION FACTOR9* (*HSA9*, At5g54070) and of several Late Embryogenesis Abundant (LEA) protein genes which are upregulated during *A. thaliana* seed maturation (Fig. 8b, c) and are among the NM-low DEGs (Fig. 8f, g). The same findings were made using the de novo approach except that the *HSA9* was not in the NM-low DEG list, but only trended towards lower expression in NM seeds. Efficient chlorophyll degradation during late seed maturation, in part mediated by the *NYE1* protein, is critical for seed quality, longevity (storability), dormancy and germination properties [62]. During seed maturation, *ABI3*, through *HSA9*, induces the accumulation of a subset of heat shock proteins (HSP) that contribute to seed longevity by protecting protein molecules and structures in the dry state [33, 63]. Among the *Ae. arabicum* DEGs, there are indeed *HSA9* and two other HSFs and several HSPs, but different HSPs are expressed in either a NM-low or a NM-high specific manner (Fig. 8f, Additional file 3: Figure S4b). A more distinctive pattern was obtained for the LEA proteins which were primarily found among the *Ae. arabicum* NM-low DEGs (Fig. 8g), supporting the view that M^+ seeds may mature faster and that M^+ and NM seeds may differ in their longevity.

Accumulation of LEA proteins is a landmark of seed maturation and several accumulate only during late maturation drying [33]. The 51 LEA protein encoding genes identified in *A. thaliana* cluster into 9 groups including LEA_1 to LEA_5, Seed Maturation Proteins (SMP) and dehydrins [64]. In the reference approach we found 13 putative LEA orthologs from all these groups in the *Ae. arabicum* NM-low and only two in the NM-high DEGs list (Fig. 8f, Additional file 3: Figure S4b). In the de novo approach, six LEA homologs were amongst the NM-low and only one in the NM-high DEGs list. The cumulative LEA transcript abundances were higher in M^+ compared to NM seeds, and the known most abundant LEA genes followed this pattern (Fig. 8f). Among them are the putative orthologs of *A. thaliana* LEA_1 *LEA76* (At5g06760), LEA_4 (At3g15670), LEA_5 *EM6* (At2g40170), the SMP *RAB28*, and dehydrins which are also most abundant in mature *A. thaliana* seeds [65].

The *A. thaliana* mutant *em6-1* is altered in seed hydration and desiccation tolerance during seed maturation [66]. LEA proteins are highly hydrophilic and intrinsically unstructured, and act by protecting proteins and enzyme activities in the desiccated state which, together with HSPs, may lead to maintaining seed longevity during dry storage [33, 63, 64]. In addition to their higher LEA transcript abundance (Fig. 8g), in both approaches, M^+ seeds also have higher transcript abundances of enzymes involved in detoxifying Reactive Oxygen Species (ROS) such as superoxide dismutase (SOD) and glutathione-S-transferase (GST) (Additional file 3: Figure S4b). ROS are produced during a number of seed related processes: with potentially deleterious effects during seed maturation, desiccation, ageing and germination; but also acting by controlling dormancy and germination [63, 67, 68]. Thus, the two seed morphs may differ in mechanisms by which seed longevity and dormancy are established and regulated. Whilst the GO term 'hormone metabolic process' was amongst 137 BP GO terms significantly under-represented in the reference approach DEGs (GO-bias list), the putative orthologs of genes involved in ABA and gibberellin signaling (*XERICO*), ethylene biosynthesis (*S-adenosylmethionine synthetase*, *SAMS3*) and signaling (*EIN3-binding F-box protein*, *EBF1*), and auxin and brassinosteroid signaling (*Auxin Response Factor 2*, *ARF2*) are amongst the DEGs (Additional file 3: Figure S4b), with all but *XERICO* also being among the de novo approach DEGs. The presence of these genes is consistent with previously observed differences in seed development and dormancy (described further in Additional file 3: Figure S5).

Conclusions

RNA-seq analysis of *Ae. arabicum* M^+ and NM dry seed transcriptomes using either a de novo assembled transcriptome approach or reference genome guided approach showed only a modest overlap in the DEGs identified, but much greater consistency in the GO terms identified. Thus, using global functional annotations such as GO terms, the de novo assembled transcriptome approach would result in similar conclusions being drawn from the data compared to the reference genome approach. Studying seeds, which are a well characterized biological system, allowed us to identify many well studied genes and put them into context using both a de novo assembled transcriptome approach and a reference genome guided approach. This highlights the potential usefulness of de novo transcriptome assembly in the study of species that do not have a reference genome. With the decreasing costs of RNA-seq one should aim for using at least three replicates, potentially bridging the gap between a de novo assembly and reference genome guided approach even further. However, our

results also highlight the limitations of de novo transcriptome analysis. Namely, if the goal is to pinpoint the DEGs underlying a trait, then reference based assemblies perform better.

Major differences in the seed morph transcriptomes were highlighted by GO analysis. In particular, genes associated with translation and histone assembly were more abundant in the less dormant M⁺ dry seed, whereas genes associated with transcription and mRNA processing were more abundant in the more dormant NM dry seed. By putting the M⁺ and NM dry seed transcriptomes in the context of transcriptomes from developing and maturing *A. thaliana* seeds, it was indicated that M⁺ seeds may both desiccate earlier (M⁺ has higher histone and ribosomal protein expression) and mature faster than NM seeds (compared to NM, M⁺ seed have higher expression of genes that increase with maturation, such as homologs of LEAs, *NYE1* and *HSA9*, and lower expression of genes that decrease during maturation such as *AB3* and *WRI1*). The differences identified align with the known development and germination behaviour of the two seed morphs, but hint at other differences such as in longevity mechanisms (LEAs, ROS detoxification). However, the difference in longevity of M⁺ and NM seed are so far unknown. It would also be valuable to study how the differences in dry seed lead to differences in transcription and germination physiology in the imbibed dimorphic seeds.

Methods

Plant material and RNA extraction

Aethionema arabicum (L.) A.DC. accession 0000309 (collected from Turkey and obtained from Kew's Millennium Seed Bank, UK) and ES1020 (collected from Turkey and obtained from Eric Schranz, Wageningen) [3] plants were grown on soil under long-day conditions (16 h light/20°C and 8 h dark/18°C). Freshly matured seeds from dehiscent (harboring M⁺ seeds) and indehiscent (harboring NM seeds) fruits derived from several plants were harvested. Two replicates of 20 mg fresh dry M⁺ and NM seeds, resulting in four samples in total, were pulverized in liquid N₂ using a mortar and pestle. RNA extraction was performed according to [69]. RNA integrity was checked by gel electrophoresis (Additional file 3: Figure S6) followed by quantity and purity determination with a Nanodrop spectrophotometer ND-1000 (Peqlab) showing sufficiently low levels of degradation for RNAseq and OD ratios of at least 2 (260/280 nm) and 1.8 (260/230 nm).

RNA-seq library preparation and sequencing

RNA libraries were prepared following instructions of the TruSeq™ RNA library prep kit (Illumina) using

oligo-dT-based mRNA selection. Libraries were sequenced using a HiSeq-2000 sequencer (Illumina) generating 100 bp single-end reads.

RNA-seq data trimming and filtering

The raw RNA sequences were processed with trimmomatic [15] (ILLUMINACLIP:adaptors:2:20:8, SLIDINGWINDOW:4:15, TRAILING:15, HEADCROP:12, MINLENGTH:20) to remove poor quality stretches and adaptors. Poly-A and Poly-T tails were removed using PrinSeq [16]. To reduce the complexity of the dataset prior to mapping our reads to the genome/transcriptome rRNA, mitochondrial and chloroplast sequences were filtered. Since *Ae. arabicum* sequences for rRNA, mitochondria and chloroplast were not available in public repositories, sequences from closely related and well annotated *A. thaliana* were used. GSNAP version 2016-11-07 [17] with default settings was used to map the reads against the chloroplast (GenBank: AP000423.1), mitochondria (GenBank: Y08501.2) and rRNA (GenBank:X52320.1) sequences from *A. thaliana*.

De novo transcriptome assembly

Prior to the de novo transcriptome assembly, redundant duplicate reads, i.e. reads with the exact same length and sequence, were removed since they might constitute PCR artefacts. The trimmed, filtered and de-duplicated reads were assembled into a transcriptome using Trinity [14] with default settings. For each isoform group, the longest transcript was chosen as representative and its longest open reading frame was translated into protein using a custom python script.

Evaluation of assembly and comparison to genome

Genome scaffolds and accompanying GFF file of *Ae. arabicum* genome version 2.5 [5] was obtained from CoGe (genome id23428, <https://genomevolution.org/coge/OrganismView.pl?gid=23428>). The CDS of each gene was translated into proteins using the R package biostrings version 2.32.0. The completeness of the assembled transcriptome and the available genome of *Ae. arabicum* was evaluated using the Benchmarking Universal Single-Copy Orthologs tool BUSCO v3.0.1 [23] and their accompanying dataset of 1440 plant orthologs (embryophyta odb9). To investigate how well the assembled transcripts represented and paired up with the existing gene models from *Ae. arabicum* genome version 2.5, reciprocal BLAST (version 2.2.29+, [70]) searches were carried out. Reciprocal best hits (RBH) with a minimum query and subject coverage of 50% each were considered as a match and selected for comparison.

Read mapping and feature counting

Processed reads were mapped against the assembled transcriptome and the *Ae. arabicum* genome version 2.5 using GSNAP with default settings. Reads that mapped to multiple positions in the genome were discarded and only uniquely mapped reads were kept. Mapped reads per feature were counted using HTSeq-count (version 0.6.1 [25]) with the options “-s no -t gene -m union”. For the transcriptome a custom GFF was generated with one feature for each transcript, while for the gene models the GFF mentioned above was used. The average coverage was calculated using the genome reference. The total amount of mapped reads (all libraries) for each gene was multiplied by the read length (83) and divided by gene length (Additional file 2: Table S1).

Differential gene expression analysis pipeline

Differentially expressed genes were identified using R [71] and the Bioconductor packages DESeq2 version 1.14.1 [19], edgeR version 3.16.5 [18] and NOISeq version 3.16.5 [20]. It is recommended to discard features with low counts for edgeR DEG analysis, so only genes with at least 10 read counts when summing up all the sample counts were selected for edgeR. Default parameters were used for DESeq2, edgeR (classic approach, “exactTest”) and NOISeq with normalization method relative log expression for DESeq2, trimmed mean of M values for edgeR and RPKM for NOISeq. DESeq2 and edgeR make use of Benjamini-Hochberg [72] adjusted *p*-value (*q*-value) cut offs which were set to 0.001. For NOISeq, which uses probabilities of differential expression, a cutoff value of > 0.9 was used. This is higher than the recommended 0.8 but has been shown to overlap well with experimental array data, representing a conservative (specific) selection of DEGs [28]. The overlap (strict consensus) of the three packages’ outputs was used for further analysis.

Principal component analysis of expression values

To compare the feature counts of the two approaches (de novo transcriptome and reference genome), PCAs were carried out using the built in R package prcomp. RPKM normalized expression values of the 6745 paired de novo transcripts and reference genes were calculated and used as input, as well as the 561 DEGs identified by both approaches.

Annotation and GO-bias

The transcripts of the genome and assembled transcriptome were blasted against the nr database of NCBI (nucleotide release 13-05-2015), UniProtKB/Swiss-Prot (protein release 10–2015) and TAIR 10

(proteins release 20,110,103). GO-terms were retrieved using BLAST2GO version 2.5 [21] in combination with the NCBI nr blast results. GO-bias, i.e. over/under-representation of GO-terms in defined sets of genes as compared to all genes, was calculated as in [73] using Fisher’s exact test with FDR correction [72]. Wordle (www.wordle.net) was used to build word clouds, with word height proportional to $-\log_{10}(q\text{-value})$, significantly over-represented GO-terms colored green ($q \leq 0.0001$ dark green, $q > 0.0001$ light green) and under-represented GO-terms colored red ($q \leq 0.0001$ dark red, $q > 0.0001$ light red). Transcripts of the genome and assembled transcriptome were screened for TAPs using the TAPscan pipeline [26].

qRT-PCR analysis

For technical as well as biological validation of RNA-seq derived gene expression data, RNA was extracted from separate batches of dry fresh mature M⁺ and NM seeds (five biological replicates each) as described above, and quantitative RT-PCR analysis of selected candidate genes was performed as previously described [69]. As normalization factor the geometric mean of three reference genes, *Ae. arabicum* putative orthologs of *ACTIN2* (*ACT2*, AA26G00546), *POLYUBIQUITIN10* (*UBQ10*, AA6G00219) and *ANAPHASE-PROMOTING COMPLEX2* (*APC2*, AA61G00327) was used, which was found to show comparable stable expression in M⁺ and NM seeds (Additional file 3: Figure S7). Primers for qRT-PCR are listed in (Additional file 2: Table S9).

Additional files

Additional file 1: de novo transcriptome assembly. The 34,784 longest gene sequences from each Trinity gene cluster. (FA 28331 kb)

Additional file 2: Gene coverage calculation (Table S1), reciprocal best BLAST paring (Table S2), full annotation and RPKM tables for the genome method (Table S3) and transcriptome method (Table S4). Comparison of abundance of transcripts (genome method vs. transcriptome method) belonging to: the 5584 GO terms shared between both methods (Table S5); or the 1663 overlapping GO terms of the DEG sets (Table S6). Table S7 shows a summary of significantly under- and over-represented GO terms associated with DEG lists. Table S9 contains a list of primers used for qRT-PCR. (XLSX 10033 kb)

Additional file 3: Figure S1. PCA of RPKM values for 6745 paired transcripts (identified in both genome and transcriptome methods) by method and morphotype. Figure S2. RPKM levels (reference genome approach) of the overlapping DEGs as well as of the non-overlapping DEGs called by NOISeq, edgeR and DESeq2. Figure S3. Expression of selected DEGs measured by qRT-PCR. Figure S4. showing abundances of *Ae. arabicum* ribonucleoprotein transcripts (a) and transcripts from selected gene categories (b) and Figure S5. showing the pattern of expression of select hormonal signaling related genes during *A. thaliana* seed maturation. Assessment of RNA integrity and purity (Figure S6.) and validation of reference genes used for qRT-PCR normalization (Figure S7.) (DOCX 2738 kb)

Additional file 4: Table S8. Excel document containing GO term analysis output for BP, CC and MF classes and all DEG lists. (XLSX 347 kb)

Abbreviations

ABA: Abscisic acid; ABI3: ABSCISIC ACID INSENSITIVE3; BP: Biological Process; BUSCO: Benchmarking Universal Single-Copy Orthologs; CC: Cellular Component; CDS: Coding sequence; DEGs: Differentially expressed genes; DEH: Dehiscent; DGAT: Acyl-CoA:diacylglycerol acyltransferase; FACT: Facilitates Chromatin Transcription; FDR: False Discovery Rate; GFF: General feature format; GO: Gene ontology; HSF9: HEAT SHOCK TRANSCRIPTION FACTOR9; HSP: Heat shock proteins; IND: Indehiscent; LACS: Long chain acyl-CoA synthetase; LEA: Late Embryogenesis Abundant; LEC1: LEAFY COTYLEDON1; LEC2: LEAFY COTYLEDON2; M⁺: Mucilaginous; MF: Molecular function; NM: Non-mucilaginous; NYE1/SGR1: NON-YELLOWING1/STAY-GREEN1; PCA: Principal component analysis; RNAPII: RNA Polymerase II; RNA-seq: RNA-sequencing; ROS: Reactive Oxygen Species; RPKM: Reads Per Kilobase per Million mapped reads; rRNA: ribosomal RNA; SMP: Seed Maturation Proteins; TAG: Triacylglycerol; TAPs: Transcription Associated Proteins; WRI1: WRINKLED1

Acknowledgements

We thank the members of the SeedAdapt consortium for useful discussions on the biology of *Ae. arabicum*.

Funding

This work is part of the ERA-CAPS SeedAdapt consortium project (www.seedadapt-leu) and was supported by the Deutsche Forschungsgemeinschaft (grant no. RE 1697/8-1 to S.A.R.) and by the Netherlands Organization for Scientific Research (grant no. 849.13.004 to M.E.S.); by the Biotechnology and Biological Sciences Research Council (grant nos. BB/M00192X/1 and BB/M000583/1 to G.L.-M.); and by a Natural Environment Research Council (NERC) Doctoral Training Partnership studentship to W.A. (grant no. NE/L002485/1).

Availability of data and materials

Single-ended Illumina raw reads from this study were uploaded to the NCBI Sequence Read Archive (SRA) and can be found under BioProject PRJNA413671 (<https://www.ncbi.nlm.nih.gov/bioproject/?term=PRJNA413671>). The following accession numbers correspond to each one of the samples: SRR6157646 (Indehiscent: NM seed rep 1, NM1), SRR6157647 (Indehiscent: NM seed rep 2, NM2), SRR6157648 (dehiscent: M⁺ seed rep 1, M⁺ 1), SRR6157649 (dehiscent: M⁺ seed rep 2, M⁺ 2).

Authors' contributions

KG, MES, JAH and SK prepared *Ae. arabicum* material and RNA. KG and SK performed qRT-PCR. JCP and PPE synthesized sequencing libraries. JOC, PKIW, NF-P, GL-M, SAR, WA and KG prepared figures and wrote the manuscript. KG and WA provided plant and seed images, mass and moisture content data. PKIW, NF-P, KJU, KB, KG and SAR assembled RNA-seq data and analyzed data. GL-M and JOC provided biological interpretation of RNA-seq analysis. All authors read and approved the manuscript.

Ethics approval and consent to participate

The source of the *Ae. arabicum* seeds were accessions 0000309 (obtained from Kew's Millennium Seed Bank) and ES1020 (obtained from Eric Schranz, Wageningen) [3]. This study complies with institutional, national, and international guidelines.

Consent for publication

Not applicable

Competing interests

The authors declare that they have no competing interests.

Publisher's Note

Springer Nature remains neutral with regard to jurisdictional claims in published maps and institutional affiliations.

Author details

¹Plant Cell Biology, Faculty of Biology, University of Marburg, 35043 Marburg, Germany. ²School of Biological Sciences, Royal Holloway University of London, Egham, Surrey TW20 0EX, UK. ³Biosystematics Group, Wageningen University, Wageningen 6708 PB, The Netherlands. ⁴Department of Horticulture, Michigan State University, East Lansing, MI 48864, USA. ⁵Division of Biological Sciences, University of Missouri, Columbia, MO 65211, USA. ⁶Laboratory of Growth Regulators, Centre of the Region Haná for

Biotechnological and Agricultural Research, Palacký University and Institute of Experimental Botany, Academy of Sciences of the Czech Republic, 78371 Olomouc, Czech Republic. ⁷BIOSS Centre for Biological Signalling Studies, University of Freiburg, Freiburg, Germany. ⁸Present Address: Max Planck Institute for Evolutionary Biology, August-Thienemann-Straße 2, 24306 Ploen, Germany.

Received: 16 May 2018 Accepted: 14 January 2019

Published online: 30 January 2019

References

- Brautigam A, Gowik U. What can next generation sequencing do for you? Next generation sequencing as a valuable tool in plant research. *Plant Biol (Stuttg)*. 2010;12(6):831–41.
- Mohammadin S, Peterse K, van de Kerke SJ, Chatrou LW, Donmez AA, Mummenhoff K, Pires JC, Edger PP, Al-Shehbaz IA, Schranz ME. Anatolian origins and diversification of *Aethionema*, the sister lineage of the core Brassicaceae. *Am J Bot*. 2017;104(7):1042–54.
- Lenser T, Graeber K, Cevik OS, Adiguzel N, Donmez AA, Grosche C, Kettermann M, Mayland-Quellhorst S, Merai Z, Mohammadin S, et al. Developmental control and plasticity of fruit and seed dimorphism in *Aethionema arabicum*. *Plant Physiol*. 2016;172(3):1691–707.
- Arshad W, Sperber K, Steinbrecher T, Nichols B, Jansen VAA, Leubner-Metzger G, Mummenhoff K. Dispersal biophysics and adaptive significance of dimorphic diaspores in the annual *Aethionema arabicum* (Brassicaceae). *New Phytol*. 2019;221(3):1434–46. <https://doi.org/10.1111/nph.15490>. Epub 2018 Oct 25.
- Haudry A, Platts AE, Vello E, Hoen DR, Leclercq M, Williamson RJ, Forczek E, Joly-Lopez Z, Steffen JG, Hazzouri KM, et al. An atlas of over 90,000 conserved noncoding sequences provides insight into crucifer regulatory regions. *Nat Genet*. 2013;45(8):891–U228.
- t Hoen PA, Ariyurek Y, Thygesen HH, Vreugdenhil E, Vossen RH, de Menezes RX, Boer JM, van Ommen GJ, den Dunnen JT. Deep sequencing-based expression analysis shows major advances in robustness, resolution and inter-lab portability over five microarray platforms. *Nucleic Acids Res*. 2008;36(21):e141.
- Wilhelm BT, Marguerat S, Watt S, Schubert F, Wood V, Goodhead I, Penkett CJ, Rogers J, Bahler J. Dynamic repertoire of a eukaryotic transcriptome surveyed at single-nucleotide resolution. *Nature*. 2008;453(7199):1239–43.
- Gibbons JG, Janson EM, Hittinger CT, Johnston M, Abbot P, Rokas A. Benchmarking next-generation transcriptome sequencing for functional and evolutionary genomics. *Mol Biol Evol*. 2009;26(12):2731–44.
- Conesa A, Madrigal P, Tarazona S, Gomez-Cabrero D, Cervera A, McPherson A, Szczesniak MW, Gaffney DJ, Elo LL, Zhang X, et al. A survey of best practices for RNA-seq data analysis. *Genome Biol*. 2016;17(1):13.
- Gongora-Castillo E, Buell CR. Bioinformatics challenges in de novo transcriptome assembly using short read sequences in the absence of a reference genome sequence. *Nat Prod Rep*. 2013;30(4):490–500.
- Li B, Fillmore N, Bai Y, Collins M, Thomson JA, Stewart R, Dewey CN. Evaluation of de novo transcriptome assemblies from RNA-Seq data. *Genome Biol*. 2014;15(12):553.
- Surget-Groba Y, Montoya-Burgos JI. Optimization of de novo transcriptome assembly from next-generation sequencing data. *Genome Res*. 2010;20(10):1432–40.
- Zhao QY, Wang Y, Kong YM, Luo D, Li X, Hao P. Optimizing de novo transcriptome assembly from short-read RNA-Seq data: a comparative study. *BMC Bioinformatics*. 2011;12(Suppl 14):S2.
- Grabherr MG, Haas BJ, Yassour M, Levin JZ, Thompson DA, Amit I, Adiconis X, Fan L, Raychowdhury R, Zeng Q, et al. Full-length transcriptome assembly from RNA-Seq data without a reference genome. *Nat Biotechnol*. 2011;29(7):644–52.
- Bolger AM, Lohse M, Usadel B. Trimmomatic: a flexible trimmer for Illumina sequence data. *Bioinformatics*. 2014;30(15):2114–20.
- Schmieder R, Edwards R. Quality control and preprocessing of metagenomic datasets. *Bioinformatics*. 2011;27(6):863–4.
- Wu TD, Nacu S. Fast and SNP-tolerant detection of complex variants and splicing in short reads. *Bioinformatics*. 2010;26(7):873–81.
- Robinson MD, McCarthy DJ, Smyth GK. edgeR: a Bioconductor package for differential expression analysis of digital gene expression data. *Bioinformatics*. 2010;26(1):139–40.
- Love MI, Huber W, Anders S. Moderated estimation of fold change and dispersion for RNA-seq data with DESeq2. *Genome Biol*. 2014;15(12):550.
- Tarazona S, Garcia-Alcalde F, Dopazo J, Ferrer A, Conesa A. Differential expression in RNA-seq: a matter of depth. *Genome Res*. 2011;21(12):2213–23.

21. Conesa A, Gotz S, Garcia-Gomez JM, Terol J, Talon M, Robles M. Blast2GO: a universal tool for annotation, visualization and analysis in functional genomics research. *Bioinformatics*. 2005;21(18):3674–6.
22. Liu Y, Zhou J, White KP. RNA-seq differential expression studies: more sequence or more replication? *Bioinformatics*. 2014;30(3):301–4.
23. Simao FA, Waterhouse RM, Ioannidis P, Kriventseva EV, Zdobnov EM. BUSCO: assessing genome assembly and annotation completeness with single-copy orthologs. *Bioinformatics*. 2015;31(19):3210–2.
24. Berardini TZ, Reiser L, Li D, Mezheritsky Y, Muller R, Strait E, Huala E. The Arabidopsis information resource: making and mining the “gold standard” annotated reference plant genome. *Genesis*. 2015;53(8):474–85.
25. Anders S, Pyl PT, Huber W. HTSeq—a Python framework to work with high-throughput sequencing data. *Bioinformatics*. 2015;31(2):166–9.
26. Wilhelmsson PK, Muhlich C, Ullrich KK, Rensing SA. Comprehensive genome-wide classification reveals that many plant-specific transcription factors evolved in streptophyte algae. *Genome Biol Evol*. 2017;9(12):3384–97.
27. Zhang ZH, Jhaveri DJ, Marshall VM, Bauer DC, Edson J, Narayanan RK, Robinson GJ, Lundberg AE, Bartlett PF, Wray NR, et al. A comparative study of techniques for differential expression analysis on RNA-Seq data. *PLoS One*. 2014;9(8):e103207.
28. Perroud PF, Haas FB, Hiss M, Ullrich KK, Alboresi A, Amirebrahimi M, Barry K, Bassi R, Bonhomme S, Chen H, et al. The *Physcomitrella patens* gene atlas project: large scale RNA-seq based expression data. *Plant J*. 2018;95:168.
29. Le BH, Cheng C, Bui AQ, Wagmaister JA, Henry KF, Pelletier J, Kwong L, Belmonte M, Kirkbride R, Horvath S, et al. Global analysis of gene activity during Arabidopsis seed development and identification of seed-specific transcription factors. *Proc Natl Acad Sci U S A*. 2010;107(18):8063–70.
30. Xiang D, Venglat P, Tibiche C, Yang H, Risseuw E, Cao Y, Babic V, Cloutier M, Keller W, Wang E, et al. Genome-wide analysis reveals gene expression and metabolic network dynamics during embryo development in Arabidopsis. *Plant Physiol*. 2011;156(1):346–56.
31. Nakabayashi K, Okamoto M, Koshiba T, Kamiya Y, Nambara E. Genome-wide profiling of stored mRNA in Arabidopsis thaliana seed germination: epigenetic and genetic regulation of transcription in seed. *Plant J*. 2005;41(5):697–709.
32. Graeber K, Nakabayashi K, Leubner-Metzger G. Seed development and germination. In: Thomas B, Murray BG, Murphy DJ, editors. *Encyclopedia of applied plant sciences*, vol. 1. Waltham: Academic Press; 2017. p. 483–9.
33. Leprince O, Pellizzaro A, Berriri S, Buitink J. Late seed maturation: drying without dying. *J Exp Bot*. 2017;68(4):827–41.
34. Fei H, Tsang E, Cutler AJ. Gene expression during seed maturation in *Brassica napus* in relation to the induction of secondary dormancy. *Genomics*. 2007;89(3):419–28.
35. Bai B, Peviani A, van der Horst S, Gamm M, Snel B, Bentsink L, Hanson J. Extensive translational regulation during seed germination revealed by polysomal profiling. *New Phytol*. 2017;214(1):233–44.
36. Galland M, Rajjou L. Regulation of mRNA translation controls seed germination and is critical for seedling vigor. *Front Plant Sci*. 2015;6:284.
37. Tatematsu K, Kamiya Y, Nambara E. Co-regulation of ribosomal protein genes as an indicator of growth status: comparative transcriptome analysis on axillary shoots and seeds in Arabidopsis. *Plant Signal Behav*. 2008;3(7):450–2.
38. Xiao J, Jin R, Wagner D. Developmental transitions: integrating environmental cues with hormonal signaling in the chromatin landscape in plants. *Genome Biol*. 2017;18:88.
39. Bonisch C, Hake SB. Histone H2A variants in nucleosomes and chromatin: more or less stable? *Nucleic Acids Res*. 2012;40(21):10719–41.
40. Boissard-Lorig C, Colon-Carmona A, Bauch M, Hodge S, Doerner P, Bancharel E, Dumas C, Haseloff J, Berger F. Dynamic analyses of the expression of the HISTONE:YFP fusion protein in Arabidopsis show that syncytial endosperm is divided in mitotic domains. *Plant Cell*. 2001;13(3):495–509.
41. van Zanten M, Koini MA, Geyer R, Liu Y, Brambilla V, Bartels D, Koornneef M, Fransz P, Soppe WJ. Seed maturation in Arabidopsis thaliana is characterized by nuclear size reduction and increased chromatin condensation. *Proc Natl Acad Sci U S A*. 2011;108(50):20219–24.
42. Yelagandula R, Stroud H, Holec S, Zhou K, Feng S, Zhong X, Muthurajan UM, Nie X, Kawashima T, Groth M, et al. The histone variant H2A.W defines heterochromatin and promotes chromatin condensation in Arabidopsis. *Cell*. 2014;158(1):98–109.
43. Footitt S, Muller K, Kermode AR, Finch-Savage WE. Seed dormancy cycling in Arabidopsis: chromatin remodelling and regulation of DOG1 in response to seasonal environmental signals. *Plant J*. 2015;81(3):413–25.
44. Liu Y, Koornneef M, Soppe WJJ. The absence of histone H2B monoubiquitination in the *Arabidopsis hub1 (rod4)* mutant reveals a role for chromatin remodeling in seed dormancy. *Plant Cell*. 2007;19:433–44.
45. Lee N, Kang H, Lee D, Choi G. A histone methyltransferase inhibits seed germination by increasing PIF1 mRNA expression in imbibed seeds. *Plant J*. 2014;78(2):282–93.
46. Zhou Y, Tan B, Luo M, Li Y, Liu C, Chen C, Yu CW, Yang S, Dong S, Ruan J, et al. HISTONE DEACETYLASE1 interacts with HSL1 and participates in the repression of seed maturation genes in Arabidopsis seedlings. *Plant Cell*. 2013;25(1):134–48.
47. Heisel TJ, Li CY, Grey KM, Gibson SI. Mutations in HISTONE ACETYLTRANSFERASE1 affect sugar response and gene expression in Arabidopsis. *Front Plant Sci*. 2013;4:245.
48. Graeber K, Nakabayashi K, Miatton E, Leubner-Metzger G, Soppe WJ. Molecular mechanisms of seed dormancy. *Plant Cell Environ*. 2012;35:1769–86.
49. Lolas IB, Himanen K, Gronlund JT, Lynggaard C, Houben A, Melzer M, Van Lijsebettens M, Grasser KD. The transcription elongation factor FACT affects Arabidopsis vegetative and reproductive development and genetically interacts with HUB1/2. *Plant J*. 2010;61(4):686–97.
50. Antosz W, Pfab A, Ehrnsberger HF, Holzinger P, Kollen K, Mortensen SA, Bruckmann A, Schubert T, Langst G, Griesenbeck J, et al. The composition of the Arabidopsis RNA polymerase II transcript elongation complex reveals the interplay between elongation and mRNA processing factors. *Plant Cell*. 2017;29(4):854–70.
51. Wang Y, Ma H. Step-wise and lineage-specific diversification of plant RNA polymerase genes and origin of the largest plant-specific subunits. *New Phytol*. 2015;207(4):1198–212.
52. Eom H, Park SJ, Kim MK, Kim H, Kang H, Lee I. TAF15b, involved in the autonomous pathway for flowering, represses transcription of FLOWERING LOCUS C. *Plant J*. 2018;93(1):79–91.
53. Liu Y, Geyer R, van Zanten M, Carles A, Li Y, Horold A, van Nocker S, Soppe WJ. Identification of the Arabidopsis REDUCED DORMANCY 2 gene uncovers a role for the polymerase associated factor 1 complex in seed dormancy. *PLoS One*. 2011;6(7):e22241.
54. Li S, Chen L, Zhang L, Li X, Liu Y, Wu Z, Dong F, Wan L, Liu K, Hong D, et al. BnaC9.SMG7b functions as a positive regulator of the number of seeds per silique in Brassica napus by regulating the formation of functional female gametophytes. *Plant Physiol*. 2015;169(4):2744–60.
55. Baud S, Boutin J-P, Miquel M, Lepiniec L, Rochat C. An integrated overview of seed development in Arabidopsis thaliana ecotype WS. *Plant Physiol Biochem*. 2002;40:151–60.
56. Baud S, Wullemme S, To A, Rochat C, Lepiniec L. Role of WRINKLED1 in the transcriptional regulation of glycolytic and fatty acid biosynthetic genes in Arabidopsis. *Plant J*. 2009;60(6):933–47.
57. Miquel M, Trigui G, d'Andrea S, Kelemen Z, Baud S, Berger A, Deruyffelaere C, Trubuil A, Lepiniec L, Dubreucq B. Specialization of oleosins in oil body dynamics during seed development in Arabidopsis seeds. *Plant Physiol*. 2014;164(4):1866–78.
58. Ruska SA, Girke T, Benning C, Ohlrogge JB. Contrapuntal networks of gene expression during Arabidopsis seed filling. *Plant Cell*. 2002;14(6):1191–206.
59. Baud S, Lepiniec L. Physiological and developmental regulation of seed oil production. *Prog Lipid Res*. 2010;49(3):235–49.
60. Devic M, Roscoe T. Seed maturation: simplification of control networks in plants. *Plant Sci*. 2016;252:335–46.
61. Cernac A, Andre C, Hoffmann-Benning S, Benning C. WR1 is required for seed germination and seedling establishment. *Plant Physiol*. 2006;141(2):745–57.
62. Li Z, Wu S, Chen J, Wang X, Gao J, Ren G, Kuai B. NYEs/SGRs-mediated chlorophyll degradation is critical for detoxification during seed maturation in Arabidopsis. *Plant J*. 2017;92(4):650–61.
63. Sano N, Rajjou L, North HM, Debeaujon I, Marion-Poll A, Seo M. Staying alive: molecular aspects of seed longevity. *Plant Cell Physiol*. 2016;57(4):660–74.
64. Hundertmark M, Hincha DK. LEA (late embryogenesis abundant) proteins and their encoding genes in Arabidopsis thaliana. *BMC Genomics*. 2008;9:118.
65. Kimura M, Nambara E. Stored and neosynthesized mRNA in Arabidopsis seeds: effects of cycloheximide and controlled deterioration treatment on the resumption of transcription during imbibition. *Plant Mol Biol*. 2010;73(1–2):119–29.
66. Manfre AJ, LaHatte GA, Climer CR, Marcotte WR Jr. Seed dehydration and the establishment of desiccation tolerance during seed maturation is altered in the Arabidopsis thaliana mutant atem6-1. *Plant Cell Physiol*. 2009;50(2):243–53.
67. Bailly C. Active oxygen species and antioxidants in seed biology. *Seed Sci Res*. 2004;14:93–107.

68. Linkies A, Leubner-Metzger G. Beyond gibberellins and abscisic acid: how ethylene and jasmonates control seed germination. *Plant Cell Rep.* 2012; 31(2):253–70.
69. Graeber K, Linkies A, Wood AT, Leubner-Metzger G. A guideline to family-wide comparative state-of-the-art quantitative RT-PCR analysis exemplified with a Brassicaceae cross-species seed germination case study. *Plant Cell.* 2011;23(6):2045–63.
70. Altschul SF, Madden TL, Schaffer AA, Zhang J, Zhang Z, Miller W, Lipman DJ. Gapped BLAST and PSI-BLAST: a new generation of protein database search programs. *Nucleic Acids Res.* 1997;25(17):3389–402.
71. R: A language and environment for statistical computing. <https://www.r-project.org/>.
72. Benjamini Y, Hochberg Y. Controlling the false discovery rate - a practical and powerful approach to multiple testing. *J R Stat Soc Ser B Methodol.* 1995;57(1):289–300.
73. Widiez T, Symeonidi A, Luo C, Lam E, Lawton M, Rensing SA. The chromatin landscape of the moss *Physcomitrella patens* and its dynamics during development and drought stress. *Plant J.* 2014;79(1):67–81.
74. Winter D, Vinegar B, Nahal H, Ammar R, Wilson GV, Provart NJ. An “electronic fluorescent pictograph” browser for exploring and analyzing large-scale biological data sets. *PLoS One.* 2007;2(8):e718.

Ready to submit your research? Choose BMC and benefit from:

- fast, convenient online submission
- thorough peer review by experienced researchers in your field
- rapid publication on acceptance
- support for research data, including large and complex data types
- gold Open Access which fosters wider collaboration and increased citations
- maximum visibility for your research: over 100M website views per year

At BMC, research is always in progress.

Learn more biomedcentral.com/submissions



9.2 The light control of seed germination: accessions with natural variation between light-sensitive and light-neutral responses

This paper describes *Ae. arabicum* accessions for use in investigations of the mechanism of germination inhibition by light. Seeds of one *Aethionema* accession from Turkey germinate well in light, while the seeds of another accession from Cyprus are quantitatively inhibited by the entire spectrum of visible light. After light perception by phytochrome B, a cascade including several transcription factors and repressors leads to GA synthesis and ABA degradation in light-requiring seeds, thus enabling successful completion of germination. However, transcriptome comparisons of light- and dark-exposed *Ae. arabicum* seeds reveals antipodal hormone regulation upon light exposure, and that the inhibition of Cyprus seed germination in light is associated with a decreased GA:ABA ratio.

The results of the work (Mérai *et al.*, 2019) were published in *Journal of Experimental Botany* under the title “*Aethionema arabicum*: a novel model plant to study the light control of seed germination” (DOI: 10.1093/jxb/erz146), and is presented here in its full form. The contributions W Arshad made to this manuscript were in performing physiological experiments (germination testing) and in the analysis/interpretation of the data.



RESEARCH PAPER

Aethionema arabicum: a novel model plant to study the light control of seed germination

Zsuzsanna Mérai^{1,*}, Kai Graeber², Per Wilhelmsson³, Kristian K. Ullrich^{3,†}, Waheed Arshad², Christopher Grosche³, Danuše Tarkowská⁴, Veronika Turečková⁴, Miroslav Strnad⁴, Stefan A. Rensing³, Gerhard Leubner-Metzger^{2,4}, and Ortrun Mittelsten Scheid^{1,*}

¹ Gregor Mendel Institute of Molecular Plant Biology, Austrian Academy of Sciences, Vienna BioCenter (VBC), Dr. Bohr-Gasse 3, 1030 Vienna, Austria

² School of Biological Sciences, Plant Molecular Science and Centre for Systems and Synthetic Biology, Royal Holloway University of London, Egham, Surrey TW20 0EX, UK

³ Plant Cell Biology, Faculty of Biology, University of Marburg, Karl-von-Frisch-Str. 8, 35043 Marburg, Germany

⁴ Laboratory of Growth Regulators, The Czech Academy of Sciences, Institute of Experimental Botany & Palacký University, Šlechtitelů 27, 78371 Olomouc, Czech Republic

[†] Current address: Department of Evolutionary Genetics, Max Planck Institute for Evolutionary Biology, 24306 Plön, Germany

* Correspondence: zsuzsanna.merai@gmi.oeaw.ac.at or ortrun.mittelsten_scheid@gmi.oeaw.ac.at

Received 19 November 2018; Editorial decision 8 March 2019; Accepted 8 March 2019

Editor: Steve Penfield, John Innes Centre, UK

Abstract

The timing of seed germination is crucial for seed plants and is coordinated by internal and external cues, reflecting adaptations to different habitats. Physiological and molecular studies with lettuce and *Arabidopsis thaliana* have documented a strict requirement for light to initiate germination and identified many receptors, signaling cascades, and hormonal control elements. In contrast, seed germination in several other plants is inhibited by light, but the molecular basis of this alternative response is unknown. We describe *Aethionema arabicum* (Brassicaceae) as a suitable model plant to investigate the mechanism of germination inhibition by light, as this species has accessions with natural variation between light-sensitive and light-neutral responses. Inhibition of germination occurs in red, blue, or far-red light and increases with light intensity and duration. Gibberellins and abscisic acid are involved in the control of germination, as in *Arabidopsis*, but transcriptome comparisons of light- and dark-exposed *A. arabicum* seeds revealed that, upon light exposure, the expression of genes for key regulators undergo converse changes, resulting in antipodal hormone regulation. These findings illustrate that similar modular components of a pathway in light-inhibited, light-neutral, and light-requiring germination among the Brassicaceae have been assembled in the course of evolution to produce divergent pathways, likely as adaptive traits.

Keywords: *Aethionema arabicum*, light inhibition, model plant, natural variation, seed germination, transcriptional regulation.

Introduction

Proper timing of germination is a critical step for the survival and propagation of seed plants. Light is a major environmental factor regulating seed germination, which provides information

about the position in the soil, the presence of competitors, day length, and the season. Plants living in various habitats have different optima for light conditions at the time of germination.

© The Author(s) 2019. Published by Oxford University Press on behalf of the Society for Experimental Biology.

This is an Open Access article distributed under the terms of the Creative Commons Attribution Non-Commercial License (<http://creativecommons.org/licenses/by-nc/4.0/>), which permits non-commercial re-use, distribution, and reproduction in any medium, provided the original work is properly cited. For commercial re-use, please contact journals.permissions@oup.com

Seeds can be categorized based on their response to white light during germination (Takaki, 2001). Light-requiring (positive photoblastic) seeds germinate only after a minimal exposure to light, while light-inhibited (negative photoblastic) seeds germinate only in the dark. A third category, light-neutral seeds, germinate in both light and darkness. The categories are not mutually exclusive: germination of the ricegrass species *Oryzopsis miliacea* and the salt cress (*Theellungiella halophila*) is promoted by a short period of illumination but inhibited by continuous light (Koller and Negbi, 1959; Negbi and Koller, 1964; Li *et al.*, 2015). The photoblastic classification considers only responses to the whole spectrum of white light, regardless of wavelength-specific effects. For example, germination of *Brachypodium* seeds and those of other monocotyledonous species is inhibited by blue light via cryptochrome receptors (Barrero *et al.*, 2014) but induced by red light. In white light, the seeds germinate and therefore belong to the light-requiring seed category (Barrero *et al.*, 2012). Seeds of many accessions of *Arabidopsis thaliana* and lettuce (*Lactuca sativa*), the model plants for research in this field, require a minimal light exposure for complete germination. Therefore, most insight into the role of light for seed germination originates from these light-requiring seed types (Shropshire *et al.*, 1961; Shinomura *et al.*, 1994; Casal and Sanchez, 1998). Only a limited number of plant species with light-inhibited seeds have been described, for example, *Phacelia tanacetifolia* (Chen, 1968; Chen, 1970) or *Citrus lanatus*, for which seed germination is inhibited by the whole spectrum, including white, blue, red, and far-red light (Botha and Small, 1988; Thanos *et al.*, 1991). The different photoblastic responses are likely an adaptive trait to harsh or quickly changing habitats: species with light-inhibited seeds often grow on sea coasts or in deserts where germination on the surface might be risky or deleterious. Light-inhibited germination might be advantageous to avoid direct sunlight, so that germination occurs when the seeds are buried at various depths under shifting sand dunes (Koller, 1956; Thanos *et al.*, 1991; Lai *et al.*, 2016), although this germination strategy is not strictly correlated with specific habitats (Vandelook *et al.*, 2018).

In seeds of all photoblastic categories, light-regulated molecular changes during germination are associated with the perception of light through phytochromes, which regulates hormonal levels (Casal *et al.*, 1998; Takaki, 2001). Gibberellic acid (GA) and abscisic acid (ABA) play a central role: GA induces germination and helps to break seed dormancy, while ABA is involved in the establishment and maintenance of dormancy. The balance of these two hormones determines seed fate (Finch-Savage and Leubner-Metzger, 2006). After light perception by phytochrome B (phyB), a cascade including several transcription factors and repressors leads to GA synthesis and ABA degradation in light-requiring seeds (Seo *et al.*, 2009). A dual role for light has been shown in salt cress, where weak light promotes GA accumulation, but strong light inhibits it (Li *et al.*, 2015). In *Arabidopsis*, in red light, the expression of the GA biosynthesis genes *GA3 OXIDASE 1* (*AtGA3ox1*) and *GA3 OXIDASE 2* (*AtGA3ox2*) as well as the ABA-degrading *CYTOCHROME P450* gene family member *AtCYP707A2* are enhanced, whereas the ABA biosynthesis gene *NCED6*

and the GA-degrading *GA2 OXIDASE 2* (*AtGA2ox2*) are repressed (reviewed in Seo *et al.*, 2009; Shu *et al.*, 2016). In contrast, knowledge about the molecular mechanisms of light-inhibited and light-insensitive germination is lacking, as no species with this seed trait has so far been established as a model for molecular and genetic approaches.

Aethionema arabicum (L.) Andr. ex DC. (Brassicaceae) is an annual spring plant with a relatively small (203–240 Mbp), diploid genome that was recently sequenced (Franzke *et al.*, 2011; Haudry *et al.*, 2013). The Aethionemeae tribe, with approximately 57 species, is the earliest-diverged tribe within the Brassicaceae and shares 70–80% genetic information with *Arabidopsis*. *Aethionema arabicum* (hereafter Aethionema) is distributed in the Middle East and eastern Mediterranean regions.

In this study, we show that the seeds of one Aethionema accession from Turkey (TUR) germinate well in light, while the seeds of another accession from Cyprus (CYP) are strongly inhibited by the entire spectrum of visible light, in a quantitative manner. We characterize the physiological and molecular properties of seed germination in these two accessions and demonstrate that inhibition of germination in light is associated with a decreased GA:ABA ratio, in contrast to the situation in light-requiring *Arabidopsis*. Transcriptome analysis revealed the involvement of similar regulatory components as in *Arabidopsis* but with opposite responses to light. In addition, we identified large natural variation of the photoblastic phenotype within the Aethionemeae tribe. This makes Aethionema a very suitable model to investigate the variation in seed germination responses to light that exist in closely related species.

Materials and methods

Plant material

Experiments were conducted with *Aethionema arabicum* (L.) Andr. ex DC. accessions TUR ES1020 and CYP (obtained from Eric Schranz, Wageningen), Iran8456-1, Iran8456-2, and Iran8458 (obtained from Setareh Mohammadin, Wageningen), *Aethionema carneum* (Banks & Sol.) B.Fedtsch. accession KM2496, and *Aethionema heterocarpum* Trev. accessions KM2491 and KM2614 (obtained from Klaus Mummenhoff, Osnabrück). All seed material was produced by plants grown under 16 h light/19 °C and 8 h dark/16 °C diurnal cycles, under ~50 $\mu\text{mol m}^{-2} \text{s}^{-1}$ light intensity. Indehiscent and dehiscent fruits encompassing non-mucilaginous and mucilaginous seeds, respectively, were manually separated and sieved. After seed harvesting, seed stocks were kept dry at 24 °C for a minimum of 2 months.

Germination test

All germination tests were conducted at the optimal temperature of 14 °C in Petri dishes on four-layer filter paper wetted with distilled H₂O and supplemented with 0.1% plant preservative PPM (Plant Cell Technology). Germination assays shown in Fig. 6 were carried out with the addition of 10 μM GA₄₊₇ (Duchefa), 10 μM fluridone, 10 μM norflurazon (Sigma Aldrich and Duchefa), or ABA (Cayman Chemical) as indicated. All assays were done in triplicate with a minimum of 15–20 seeds each. Except for the experiments reported in Fig. 1C and D and Fig. 2, white, red, and blue light exposure was uniformly set to 100 $\mu\text{mol m}^{-2} \text{s}^{-1}$ light intensity, and far-red exposure was set to 15 $\mu\text{mol m}^{-2} \text{s}^{-1}$ for all experiments. For dark treatments, seeds were placed on wet filter paper in complete darkness. Diurnal and high-light tests were carried out under an LED NS1 lamp with a wide sun-like spectrum (Valoya). Light spectra and intensity were measured by using an LED Meter MK350S (UPRtek). Except for

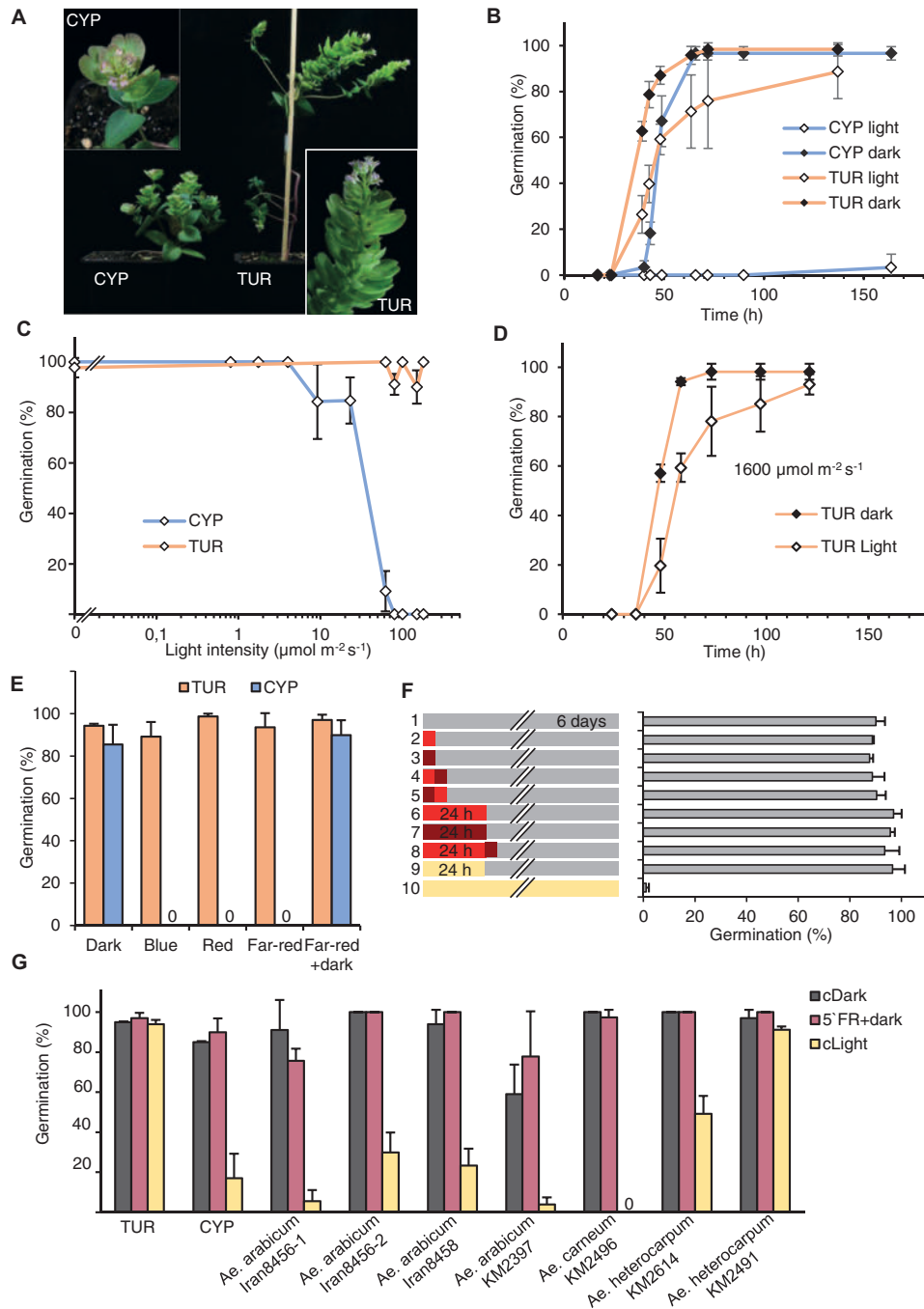


Fig. 1. Light inhibition of seed germination in *Aethionema arabicum* accession CYP. (A) Eight-week-old *A. arabicum* TUR (Turkey) and CYP (Cyprus) plants grown in a growth chamber. (B) Percentage of germinating seeds kept in darkness or under $100 \mu\text{mol m}^{-2} \text{s}^{-1}$ white light, scored over time. (C) Percentage of germinating seeds kept at various light intensities: (0.8, 1.74, 4, 9.2, 23, 62, 80, 100, 150 and $180 \mu\text{mol m}^{-2} \text{s}^{-1}$ white light) or in darkness (indicated as $0 \mu\text{mol m}^{-2} \text{s}^{-1}$), scored after 6 d. (D) Percentage of germinating TUR seeds kept in darkness or under $1600 \mu\text{mol m}^{-2} \text{s}^{-1}$ white light, scored over time. (E) Percentage of germinating seeds in continuous white, red, blue, or far-red light, dark, or exposed to 5 min far-red light followed by darkness, scored after 6 d. (F) Percentage of germinating CYP seeds after various light treatments. The left panel indicates the treatment; the right panel indicates the percentage of germinating seeds, scored after 6 d. Red, dark red, and cream rectangles indicate red, far-red, and white light exposure, respectively. Grey bars indicate dark periods. Short and long red/far-red rectangles indicate 5 min and 24 h exposure, respectively. (G) Percentage of germinating seeds from different *A. arabicum* accessions and closely related species, kept in the dark (black columns), light (yellow columns), or in the dark after a 5 min far-red pulse at imbibition (red columns), scored after 6 d. Error bars represent SD (three independent replicates).

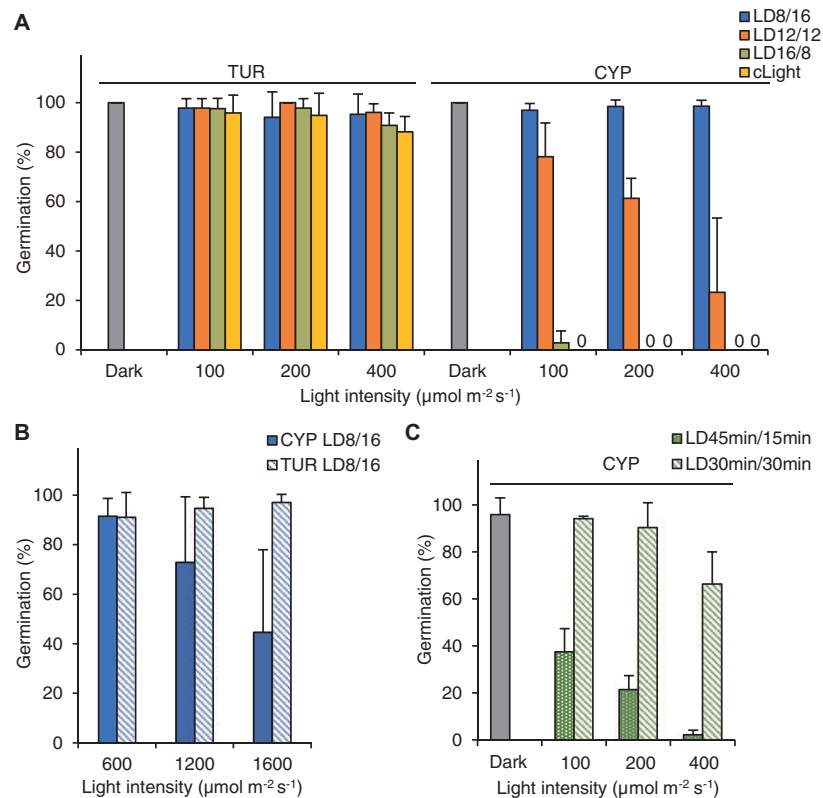


Fig. 2. Diurnal regulation of CYP seed germination. (A) Percentage of germinating CYP and TUR seeds kept under different diurnal regimes, scored after 6 d. LD8/16, 8 h light/16 h dark; LD12/12, 12 h light/12 h dark, LD16/8, 16 h light/8 h dark. In addition, seeds were kept under continuous dark (Dark) or light (cLight). (B) Percentage of germinating CYP and TUR seeds kept under different light intensities with a LD8/16 regime. 0 indicates no germination. (C) Percentage of germinating CYP seeds under continuously repeated 30 min light/30 min dark cycles (LD30min/30min) or 45 min light and 15 min dark cycles (LD45min/45min), scored after 6 d. Error bars represent SD (three independent replicates).

the seeds shown in [Supplementary Fig. S1 at JXB online](#), only mucilaginous seeds were used for all germination assays.

Quantitative RT-PCR

Before imbibition, seeds were sterilized with chlorine gas for 10 minutes. After 23 h incubation in darkness or light, seeds with intact seed coats were collected for RNA extraction (three biological replicates for each sample). RNA was extracted as described by [Oñate-Sánchez and Vicente-Carbajosa \(2008\)](#). Total RNA (3 μ g) was treated with DNase I (Thermo Scientific) and precipitated with 1/10 volume of 3 M sodium acetate (pH 5.2) and 2.5 volumes of ethanol. DNase I-treated RNA (1 μ g) was used for cDNA synthesis with random hexamer primers using the RevertAid H Minus First Strand cDNA Synthesis kit (Thermo Scientific). Quantitative reverse transcription-PCR (qRT-PCR) reactions were performed in a Lightcycler® 96 System (Roche) in duplicate, using FastStart Essential DNA Green Master mix (Roche) and primer pairs listed in [Supplementary Table S2](#), with the following parameters: 95 °C for 10 min, 45 cycles of 95 °C for 10 s and 60 °C for 30 s, and one cycle of 95 °C for 10 s, 60 °C for 30 s, and 97 °C for 1 s to obtain the melting curve for each reaction. Cycle threshold values were calculated using Lightcycler® 96 Software (Roche). The geometric mean of *Aethionema* orthologs of ACTIN2 (*AearACT2*, AA26G00546), POLYUBIQUITIN10 (*AearUBQ10*, AA6G00219), and ANAPHASE-PROMOTING COMPLEX2 (*AearAPC2*, AA61G00327) was used for normalization. For each gene, the expression level under white light is

presented as fold change relative to the level of the dark-treated samples where the mean expression was set to a value of 1.

Aethionema arabicum genome and annotations

Genome scaffolds and the accompanying gene feature format file of the *A. arabicum* genome version 2.5 was obtained from [Haudry et al. \(2013\)](#). The gene models were searched against the non-redundant database of NCBI (release 13-05-2015) using BLAST ([Altschul et al., 1990](#)). Gene ontology (GO) terms were retrieved using BLAST2GO version 2.5 ([Conesa et al., 2005](#)) along with the best hit and its description. The coding DNA sequence of each gene model was translated into amino acid sequence using the R package biostings version 2.32.0 (<https://www.bioconductor.org/packages/release/bioc/html/Biostings.html>) and then searched against the uniprot database (release 2015_10) and The Arabidopsis Information Resource (TAIR, TAIR10_pep_20110103_representative_gene_model_updated) using BLAST for extracting the best hit and its description. Results were filtered for having at least 80% query coverage, according to [Rost \(1999\)](#), to unambiguously detect homologous sequences. Sequence data from *A. arabicum* can be found in the CoGe database (<https://genomeevolution.org/coge/>) under the following genome ID: v2.5, id33968. Accession numbers used in this study are listed in [Supplementary Table S3](#). RNA-Seq information and files are deposited on GEO with accession number GSE125854 (<https://www.ncbi.nlm.nih.gov/geo/query/acc.cgi?acc=GSE125854>).

RNA extraction for RNA-Seq

Light incubation of seed material was done as for the qRT-PCR. Total RNA was isolated as described by Chang *et al.* (1993). Genomic DNA was removed by DNase-I (Qiagen) digestion in solution, followed by additional purification using columns (Qiagen RNeasy Kit). RNA quantity and purity were determined using a NanoDrop™ spectrophotometer (ND-1000, Thermo Scientific™, Wilmington, DE, USA) and an Agilent 2100 Bioanalyzer with the RNA 6000 Nano Kit (Agilent Technologies, CA, USA) using 2100 Expert Software to calculate RNA Integrity Number values. At least three biological replicate RNA samples were used for downstream applications. Sequencing was performed at the Vienna BioCenter Core Facilities GmbH Next Generation Sequencing Unit, Vienna, Austria (www.vbcf.ac.at). Libraries were sequenced in 50 bp single-end mode on Illumina HiSeq 2000 Analyzers using the manufacturer's standard cluster generation and sequencing protocols.

RNA-Seq data trimming and filtering

The cDNA sequence libraries were processed using Trimmomatic (Bolger *et al.*, 2014) with the options 'ILLUMINACLIP:adaptors:2:20:8,SLIDINGWINDOW:4:15, TRAILING:15, HEADCROP:12, MINLENGTH:20' to remove poor quality, adapters, and other technical sequences. Chloroplast, mitochondrial, and ribosomal RNA sequences were filtered out using Bowtie 2 version 2.2.3 (Langmead and Salzberg, 2012) and by mapping the reads against the chloroplast (GenBank: AP000423.1), mitochondrial (GenBank: Y08501.2), and rRNA (GenBank: X52320.1) sequences of *A. thaliana*.

Read mapping and feature counting

Trimmed and filtered reads were mapped against the Aethionema genome version 2.5 using Bowtie2. Uniquely mapped reads were retained. Mapped reads per feature were counted using HTSeq-count version 0.6.1 (Anders *et al.*, 2015).

Differentially expressed genes

R (<http://www.R-project.org>) and the Bioconductor packages Deseq2 version 1.14.1 (Love *et al.*, 2014), edgeR version 2.18 (Robinson *et al.*, 2010), and NOISeq version 3.16.5 (Tarazona *et al.*, 2011) were used in combination with the feature counts to identify differentially expressed genes. For Deseq2, edgeR (classic approach, 'exactTest') and NOISeq default parameters were used. Adjusted *p*-value (*q*-value) cut-offs were set to 0.001 for Deseq2 and edgeR. For NOISeq, which uses probabilities of differential expression, a cut off value of >0.9 was used. The overlap (strict consensus) of the output from the three packages was used for further analysis.

Heatmap and GO term enrichment

Heatmaps were created using Morpheus visualization software (<https://software.broadinstitute.org/morpheus>). GO term enrichment was analyzed using AGI gene identifiers of the Arabidopsis orthologs of Aethionema genes in ThaleMine (<https://apps.araport.org/thalemine/begin.do>). *P* values indicate Benjamini-Hochberg test correction.

Phylogenetic analysis

To verify the ortholog status of phytochromes and gibberellin-2-oxidases in Aethionema, Arabidopsis query protein sequences were searched with BLASTP (Altschul *et al.*, 1990) against a plant-specific, custom-made protein database that included genomes of the species listed in Supplementary Dataset S7. Results were filtered for having at least 80% query coverage according to Rost (1999). Resulting sequences were aligned using MAFFT version 7.037b (Katoh and Standley, 2013) in automatic mode, and resulting alignments were inspected manually and trimmed using Jalview version 2.8 (Clamp *et al.*, 2004). Based on these alignments, neighbor-joining guide trees were built using quicktree_sd

(<http://hdl.handle.net/10013/epic.33164.d001>) with 1000 bootstrap samples. Sequences with very long branches, potentially representing flawed gene models, were removed upon inspection of initial trees. Afterwards, the appropriate models were selected based on AIC/BIC using ProtTest 3.4 (Guindon and Gascuel, 2003; Darriba *et al.*, 2011). Final phylogenies were constructed by Bayesian inference using Mr. Bayes 3.2.5 (Ronquist *et al.*, 2012). Bayesian inference analysis was run with two hot and two cold chains, discarding 25% of trees as burn-in, for 1 688 500 generations (standard deviation of split frequencies 0.009992) and 2 000 000 generations (standard deviation of split frequencies 0.063371) for phytochrome and gibberellin-2-oxidase family trees, respectively. Trees were displayed, colored, and midpoint-rooted with FigTree version 1.4.2 (<http://tree.bio.ed.ac.uk/software/figtree/>).

Measurement of hormone levels

For ABA and GA analysis, seed samples were collected as described for RNA extraction, except that five biological replicates were prepared per sample. For ABA analysis, 13 mg of seed material was homogenized and extracted for 1 h in 1 ml ice-cold methanol/water/acetic acid (10/89/1, v/v). Deuterium-labelled standard (20 pmol of (+)-3',5',5',7',7',7'-²H₆-ABA) was added to each of the samples. The homogenates were centrifuged at 30 000 × *g* for 5 min at 4 °C, and the pellets were then re-extracted in 0.5 ml extraction solvent for 30 min. The combined extracts were purified by solid-phase extraction on Oasis® HLB cartridges (60 mg, 3 ml, Waters, Milford, MA, USA) and then evaporated to dryness in a Speed-Vac (UniEquip). Subsequently, the evaporated samples were methylated, purified by ABA-specific immunoaffinity extraction (Hradecka *et al.*, 2007), and analyzed by UPLC-ESI(+)-MS/MS (Tureckova *et al.*, 2009).

The sample preparation and analysis of GAs was performed as described by Urbanová *et al.* (2013), with some modifications. Briefly, 13 mg of seed material per sample was homogenized in 1 ml ice-cold 80% acetonitrile containing 5% formic acid. After adding 17 internal GA standards ([²H₂]GA₁, [²H₂]GA₃, [²H₂]GA₄, [²H₂]GA₅, [²H₂]GA₆, [²H₂]GA₇, [²H₂]GA₈, [²H₂]GA₉, [²H₂]GA₁₅, [²H₂]GA₁₉, [²H₂]GA₂₀, [²H₂]GA₂₄, [²H₂]GA₂₉, [²H₂]GA₃₄, [²H₂]GA₄₄, [²H₂]GA₅₁ and [²H₂]GA₅₃; purchased from Lewis Mander, Australia), the samples were extracted overnight at 4 °C. The homogenates were centrifuged at 36 670 × *g* for 10 min at 4 °C. Supernatants were further purified using reversed-phase and mixed-mode solid phase extraction cartridges (Waters, Milford, MA, USA) and analyzed by ultra-high-performance chromatography-tandem mass spectrometry (UHPLC-MS/MS; Micromass, Manchester, UK). GAs were detected using multiple-reaction monitoring mode of the transition of the ion [M-H]⁻ to the appropriate product ion. MassLynx 4.1 software (Waters, Milford, MA, USA) was used to analyze the data, and the standard isotope dilution method (Rittenberg and Foster, 1940) was used to quantify the levels of GAs.

Results

Light inhibits seed germination in Aethionema arabicum

The Aethionema accession TUR originates from Konya, Turkey (accession ES1020) and was used to generate the reference genome (Haudry *et al.*, 2013) and to characterize its interesting seed and fruit dimorphism (Lenser *et al.*, 2016). The Aethionema accession CYP comes from the Kato-Moni region of Cyprus (Mohammadin *et al.*, 2018). Both accessions were propagated for several generations under the same conditions in a growth chamber (Fig. 1A). Seeds of both accessions germinate optimally at 14 °C, and all experiments were performed at that temperature. Testing the light dependence, we found that TUR seeds germinated under white light or

in darkness. CYP seeds germinated well in darkness but were strongly inhibited under white light (Fig. 1B). Comparing the dimorphic seed types, we did not find any difference between mucilaginous and non-mucilaginous seeds in response to light, therefore we used mucilaginous seeds for further experiments (see Supplementary Fig. S1). Species with light-requiring seeds need various periods of illumination for germination induction, ranging from seconds to days (Bewley *et al.*, 2013). Conversely, in light-inhibited seeds, light inhibition of germination can be exerted with a wide range of photon irradiance, from a relatively weak $\sim 17 \mu\text{mol m}^{-2} \text{s}^{-1}$ light intensity in *Citrullus lanatus* (Botha and Small, 1988) to strong irradiance with $1000 \mu\text{mol m}^{-2} \text{s}^{-1}$ in some desert plants (Botha and Small, 1988; Lai *et al.*, 2016). Therefore, we tested the germination of TUR and CYP seeds with different light intensities ranging from 0.8 to $180 \mu\text{mol m}^{-2} \text{s}^{-1}$ (Fig. 1C). Increased light intensity gradually decreased the proportion of CYP seeds that germinated: at $62 \mu\text{mol m}^{-2} \text{s}^{-1}$ only $\sim 10\%$ of the seeds germinated, and at $80 \mu\text{mol m}^{-2} \text{s}^{-1}$ the inhibition was complete. Germination of TUR seeds was light-neutral in this range (Fig. 1C). As the irradiance can be much stronger at the geographic origin of the species, we further tested the germination of TUR seeds under $1600 \mu\text{mol m}^{-2} \text{s}^{-1}$ white light with a wide, sun-like spectrum. Although the germination of TUR seeds was slower, almost all seeds germinated under this strong light, therefore we categorized TUR seeds as neutral to light (Fig. 1D).

Light-dependent germination often requires exposure to a specific part of the light spectrum. Therefore, we tested whether the inhibition of CYP seed germination was wavelength-dependent. Continuous monochromatic blue, red, and far-red light were equally effective at inhibiting the germination of CYP seeds (Fig. 1E), while TUR seeds could germinate under any light condition, including continuous far-red light, which inhibits phytochrome-mediated light-induced germination in Arabidopsis and lettuce (Borthwick *et al.*, 1952; Shropshire *et al.*, 1961). A short (5 min) far-red pulse also effectively inhibits germination in Arabidopsis and lettuce, as it converts phyB to the inactive form, while a following red pulse allows germination again by converting phyB to the active form (Borthwick *et al.*, 1952; Shropshire *et al.*, 1961). Importantly, a short (5 min) or longer (24 h) exposure to either far-red or red light at the time of imbibition, followed by 6 days in darkness, allowed CYP seeds to germinate equally well (Fig. 1F). This indicates that (i) the induction of germination is independent of the active form of phyB and (ii) the light inhibition is not established in this time scale (Fig. 1E, F).

TUR and CYP accessions cluster closely together in a network analysis of several *A. arabicum* accessions (Mohammadin *et al.*, 2018). To determine whether the inhibition of CYP seed germination by light is a unique trait in the genus *Aethionema*, we investigated the germination phenotype of other available accessions, including the closest relatives, *Aethionema heterocarpum* and *Aethionema carneum* (Lenser *et al.*, 2016; Mohammadin *et al.*, 2018; Supplementary Table S1), after propagating the seeds under the same controlled conditions as for TUR and CYP. None of the tested accessions required light, as all of them germinated similarly well in constant darkness or after a 5 min far-red pulse followed by darkness (Fig. 1G). We

observed variations in the response to white light: germination of *A. carneum* and two *A. arabicum* (Iran 8456-1 and KM2397) accessions was clearly light-inhibited, one *A. heterocarpum* accession (KM2491) had light-neutral seeds, while the germination of three accessions (*A. arabicum* Iran 8458 and Iran 8456-2, and *A. heterocarpum* KM2614) was partially inhibited by light (Fig. 1G). These findings reveal the presence of natural variation for the negative or neutral photoblastic phenotype, suggesting that light-inhibited or light-neutral seed germination may be an adaptive trait in the Aethionemeae tribe, and provides interesting material for genetic analysis of the phenomenon.

Diurnal regulation of CYP seed germination

To better understand the ecological relevance of light-inhibited germination of CYP seeds, we also tested germination under different diurnal conditions. Again, TUR seeds were unaffected and germinated well under any day length. Interestingly, at a lower range of light intensity, the CYP seeds germinated well under short-day conditions (cycles of 8 h light/16 h darkness, LD8/16), compared to 12 h light/12 h dark cycles (LD12/12), which produced partial inhibition, or long-day conditions (16 h light/8 h dark cycles, LD16/8), which resulted in complete inhibition (Fig. 2A). Remarkably, at higher light intensity, similar to conditions in the plant's natural habitat ($1600 \mu\text{mol m}^{-2} \text{s}^{-1}$), $\sim 40\%$ of the CYP seeds still germinated under short-day conditions (Fig. 2B). Gradual inhibition was also observed with hourly alternating light exposure (Fig. 2C). However, longer uninterrupted light periods resulted in stronger inhibition than more frequent alternations between light and dark, despite equal daily fluence in LD12/12 compared with 30 min light/30 min dark cycles (Fig. 2A and Fig. 2C). These data indicate that CYP seeds integrate the regime, duration, and intensity of illumination into their germination regulation.

Light-neutral and light-inhibited seeds differ in their transcriptomes

To better understand the light-inhibited seed germination phenotype in *Aethionema*, we performed transcriptome analysis of the TUR and CYP accessions. Seeds were imbibed and kept in darkness (D) or under $100 \mu\text{mol m}^{-2} \text{s}^{-1}$ white light (WL) for 23 h, which was determined as the start point for the completion of germination ($\sim 1\%$ seeds in the responsive populations with emerged radicles). It is important to note that CYP seeds are fully able to germinate if transferred to darkness after 23 h of light exposure (Fig. 1F). Only seeds with intact seed coats were sampled and used for the preparation of RNA libraries. Comparison of dark- and light-exposed samples revealed 168 differentially expressed genes in the TUR accession, comprising 51 up-regulated and 117 down-regulated genes in seeds kept in darkness compared with those kept in light (Fig. 3A; Supplementary Dataset S1). In the CYP accession, we found 214 differentially expressed genes, comprising 105 up-regulated and 109 down-regulated genes in seeds kept in darkness (Fig. 3A; Supplementary Dataset S2). Considering the close relation between the accessions, the overlap of 93 genes

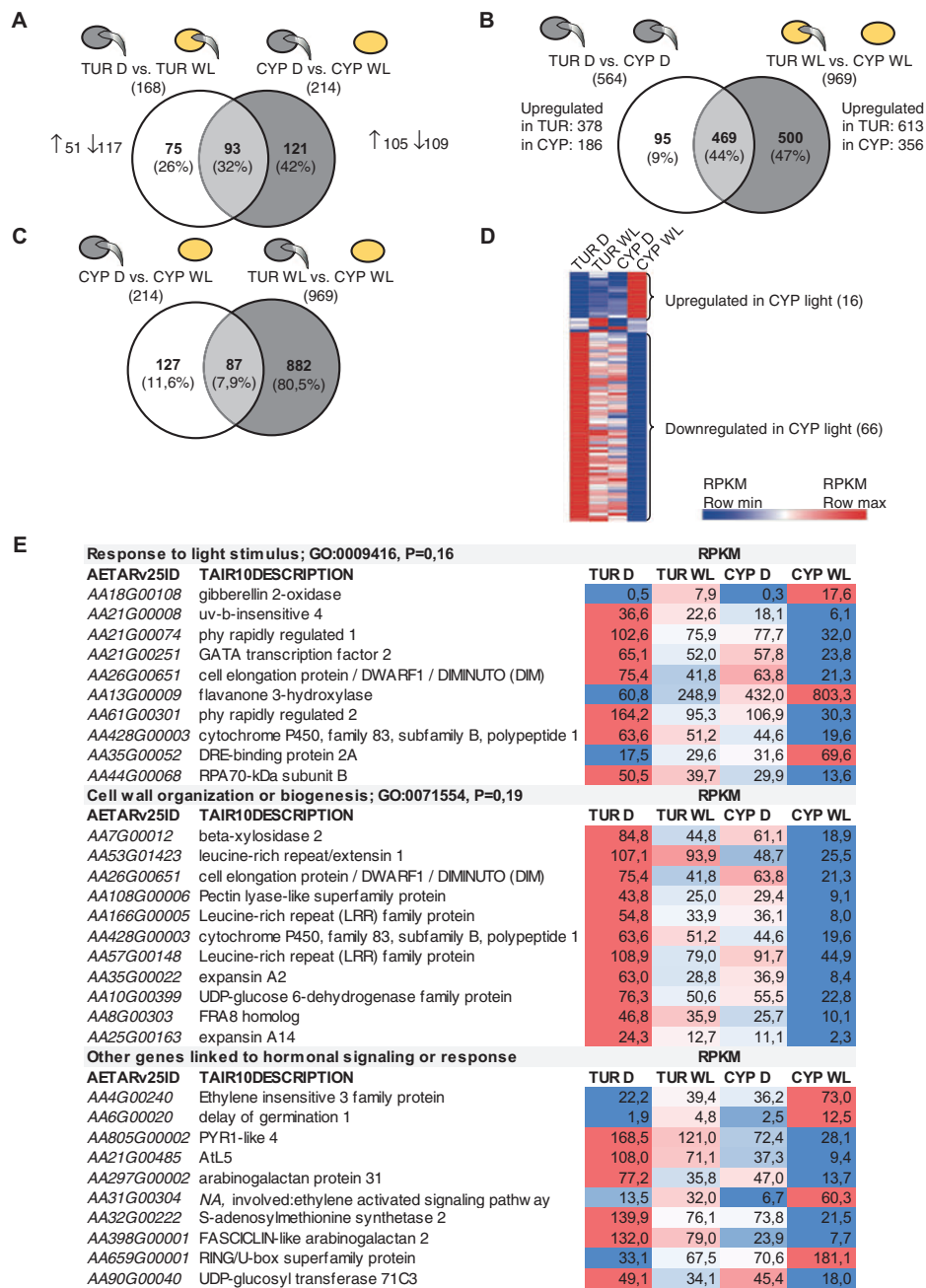


Fig. 3. Transcriptome analysis of *Aethionema* TUR and CYP seeds by RNA-Seq. (A–C) Number of differentially expressed genes and Venn diagrams showing the proportion of overlapping genes in pairwise comparisons between TUR and CYP, and between exposure to darkness (D, grey seed icon), or white light (WL, yellow icon). Icons showing germinating seeds indicate the capability of samples for germination; note that the seeds had not yet germinated at the point of sampling. (D) Heatmap indicating the relative expression of the overlapping 87 genes in the four treatments. Coloring is based on reads per kilobase of transcript per million mapped reads (RPKM) values. A detailed list is provided in [Supplementary Fig. S1](#). (E) Gene list of three selected GO terms with average RPKM values and relative expression differences, indicated by shades of blue (lowest RPKM value) or red (highest RPKM value).

commonly differentially regulated in TUR and CYP was surprisingly small, while 75 genes were light-dependent only in TUR, and 121 only in CYP (Fig. 3A). This comparison, however, did not consider the genetic differences between the two accessions. We therefore compared the transcriptome of each condition between the TUR and CYP samples. In seeds kept in darkness, 564 genes were differentially expressed between the two accessions (Fig. 3B; Supplementary Dataset S3). The number of differentially expressed genes between light-exposed TUR and CYP samples was much higher (969), matching the expectation of a larger difference upon light exposure and a different physiological state regarding the capability for germination. Among the 969 genes, 613 were expressed at higher levels in TUR and 356 were expressed at higher levels in CYP (Fig. 3B; Supplementary Dataset S4). Nearly half of the genes (469) were found in the overlap between the two genotypes, indicating transcriptional differences independent of the light conditions. However, these genes might undergo further light regulation that could contribute to the phenotypes.

To distinguish these possibilities, we hypothesized that the light-inhibited germination in CYP should be associated with genes that are (i) light-regulated in CYP seeds and (ii) differentially expressed in light-exposed TUR and CYP seeds. This selection would include genes that are possibly also light-regulated in TUR seeds, to a lesser extent than in CYP seeds, or genes whose induction/repression would be similar in both accessions but their absolute level results in different expression upon light induction. Both criteria were fulfilled for 87 genes (Fig. 3C, D; Supplementary Dataset S5, Supplementary Fig. S2). Of the 87 genes, 16 were up-regulated and 66 were down-regulated in light-exposed CYP seeds (Fig. 3D). Interestingly, 15 of the 87 genes were also significantly up- or down-regulated in light-exposed TUR seeds, and the direction of the changes in transcript levels was the same in both accessions (Fig. 3D; Supplementary Dataset S5, Supplementary Fig. S2). For 85 of the 87 genes we could identify the Arabidopsis orthologs (Supplementary Dataset S5). Based on the TAIR10 database description, 10 of these genes are linked to light stimuli and 11 to cell wall organization or biogenesis (Fig. 3E). Additionally, 10 genes are involved in hormonal signaling or response (Fig. 3E). Genes associated with ABA biosynthesis or degradation were not present among these genes (Fig. 3E; Supplementary Dataset S5). However, the most strongly up-regulated transcript [>50 -fold induction in CYP seeds exposed to white light (CYP WL in Fig. 3)] was *AA18G00108*, encoding a gibberellin-2-oxidase. Phylogenetic analysis and synteny (Supplementary Fig. S3) of the genomic position confirmed that Aethionema *AA18G00108* is the ortholog of Arabidopsis *AtGA2ox3* (*AT2G34555*), which encodes a protein with C-19 gibberellin 2- β -dioxygenase activity that is involved in the degradation of GA, and therefore expected to negatively influence germination.

Transcriptome analysis reveals differences in light-mediated hormonal responses

In most species, the balance of the hormones GA and ABA is an important component of light-regulated germination.

We therefore tested individual changes in the transcript levels of genes involved in GA and ABA biosynthesis in dark- and white light-germinated TUR and CYP seeds. Overall, upon light exposure of seeds, we found slightly increased transcript levels of the genes encoding ABA biosynthetic enzymes and a decrease of the main GA biosynthetic enzymes (Fig. 4A, B). Expression of the Aethionema orthologs of *ABA1*, *ABA2*, and *ABA3* was slightly but significantly up-regulated upon light exposure, in both the light-neutral TUR and the light-inhibited CYP seeds (Fig. 4A). *NCED6* and *NCED9*, which encode the 9-cis epoxy-carotenoid dioxygenase gating the catalysis of 9'-cis neoxanthin, the rate-limiting step of ABA synthesis, are known to be transcriptionally down-regulated in Arabidopsis upon red light induction (Seo *et al.*, 2006, 2009; Oh *et al.*, 2007). *AearNCED5* was significantly up-regulated in both TUR and CYP accessions, and *AearNCED6* only in CYP seeds kept in light. The level of *AearNCED9* was similar in dark and light (Fig. 4A). In contrast, expression of the gene for the ABA-deactivating enzyme *AearCYP7072A* was also elevated, in this case matching the observations in Arabidopsis seeds (Fig. 4A) (Seo *et al.*, 2006; Oh *et al.*, 2007).

Light-induced GA accumulation in Arabidopsis seeds is mediated by the enhanced expression of GA biosynthetic enzymes, encoded by *AtGA3ox1* and *AtGA3ox2*, and the decrease of the GA-deactivating gibberellin-2-oxidase encoded by *AtGA2ox2* (Yamaguchi *et al.*, 1998; Seo *et al.*, 2006). We found a reciprocal situation in Aethionema seeds: the expression of both *AearGA3ox1* and *AearGA3ox2* was decreased on exposure to white light (Fig. 4B). In good agreement with the RNA-Seq results, the expression of *AearGA2ox3* was increased upon illumination with white light in both accessions (Fig. 4B). Remarkably, the repression of *AearGA3ox1* was considerably more pronounced in the light-inhibited CYP seeds than in TUR seeds (Fig. 4B). This also suggests that the TUR and CYP accessions might differ in the regulatory network upstream of GA-related genes. Therefore, we further investigated the transcriptome for regulation by factors known to be involved in light-mediated hormonal responses in seeds.

In Arabidopsis, upon light reception, the active P_{if} form of phyB interacts with PIL5, a basic helix-loop-helix (bHLH) protein, facilitating its degradation by the 26S proteasome (Oh *et al.*, 2004, 2007; Shen *et al.*, 2008). Under conditions of darkness or far-red light, PIL5 mediates the stable expression of *GAI* and *RGA*, two genes encoding DELLA proteins, which are negative components of GA signaling (Oh *et al.*, 2007; Piskurewicz *et al.*, 2009). In parallel, PIL5 directly stimulates the expression of *SOM* (*SOMNUS*), a negative regulator of light-dependent germination that controls the expression of ABA and GA metabolic genes (Kim *et al.*, 2008). Both *pil5* and *som* mutants of Arabidopsis germinate in a light-insensitive manner (Oh *et al.*, 2004; Kim *et al.*, 2008). The link between *SOM* and the *GA3ox1/2* genes is formed by the two jumonji-domain proteins JM120 and JM122 that are directly repressed by *SOM* and support germination by removing the repressing histone H4 arginine 3 methylation from *GA3ox1/2*, allowing their expression (Cho *et al.*, 2012). Another negative regulator of seed germination is *DAG1* (*DOF AFFECTING GERMINATION1*), which is under indirect positive control downstream of PIL5

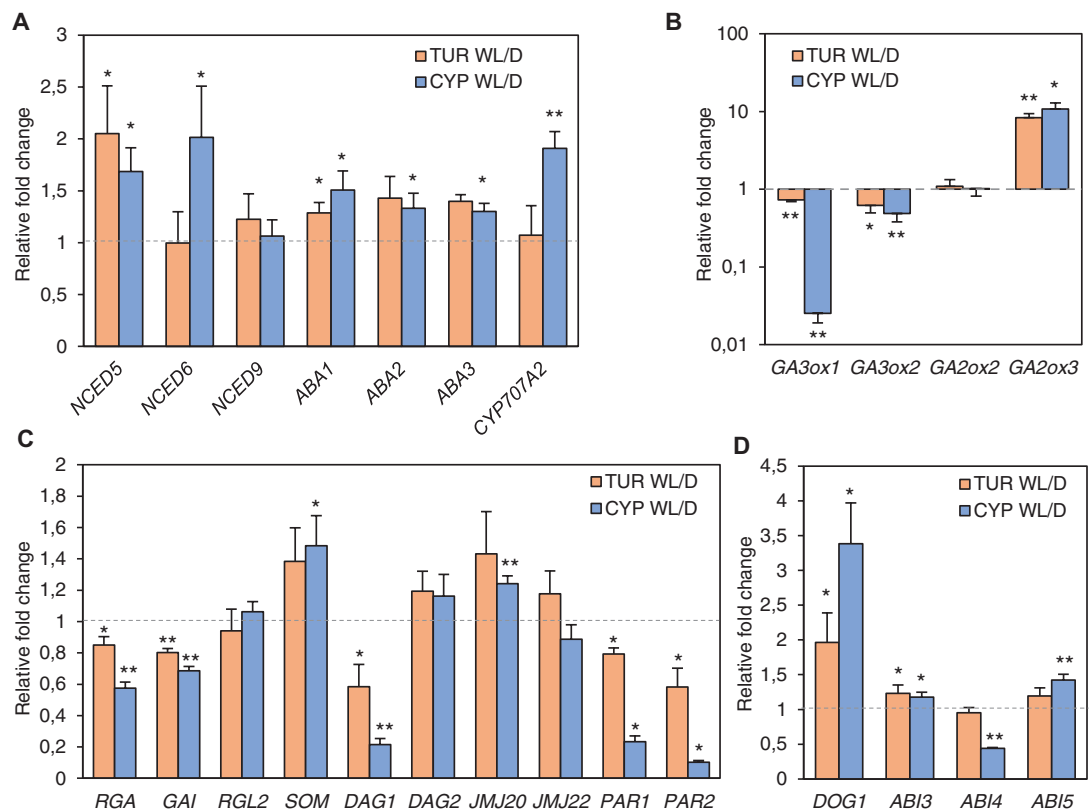


Fig. 4. Analysis of the Aethionema light-regulated transcriptome network in the TUR and CYP accessions. (A–D) Quantitative RT–PCR for selected genes. The expression level under white light (WL) is presented as fold change relative to the average expression level in darkness (D), which is set to a value of 1 (indicated by the grey dashed line). Asterisks indicate significant differences between the WL and D expression level of a gene, based on the Welch test: * $P < 0.05$, ** $P < 0.01$. Error bars represent SD (three independent biological replicates).

and directly represses the transcription of *GA3ox1* and *DAG2*, which was recently identified as a positive regulator of light-induced germination (Gabriele *et al.*, 2010; Boccaccini *et al.*, 2014; Santopolo *et al.*, 2015). We found significant changes in the transcript levels of the Aethionema orthologs of *RGA*, *GAI*, *SOM*, *DAG1*, and *JMJ20* in light-exposed seeds compared with those in the dark, either in both TUR and CYP accessions or only in CYP (Fig. 4C). The expression of *DAG1* was decreased in light-exposed seeds of both accessions, similar to its response in Arabidopsis (Fig. 4C). *PHYTOCHROME RAPIDLY REGULATED 1* and *2* (*PAR1* and *PAR2*) were both down-regulated in seeds exposed to white light (Fig. 3E; Supplementary Dataset S5). In Arabidopsis, *PAR1* and *PAR2* are negative factors in shade avoidance (Roig-Villanova *et al.*, 2007) and promote seedling de-etiolation under different light conditions, likely through interaction with PIF proteins (Zhou *et al.*, 2014). Their role during seed germination has not been elucidated, although available transcriptome data suggest that *PAR2* is repressed by *PIL5* and up-regulated in seeds exposed to red light (Shi *et al.*, 2013). Importantly, we also confirmed the RNA-Seq results that *AearPAR1* and *AearPAR2* are down-regulated in seeds exposed to white light (Figs 3E and 4C; *AA21G00074* and *AA61G00301*).

Germination under unfavorable conditions can be avoided by the establishment of seed dormancy, which is strongly correlated with the key dormancy protein *DOG1* (DELAY OF GERMINATION 1) (Bentsink *et al.*, 2006, 2010; Footitt *et al.*, 2011; Graeber *et al.*, 2014; Kerdaffrec *et al.*, 2016). The expression of the *DOG1* gene is regulated by environmental signals and highly variable among Arabidopsis accessions (Chiang *et al.*, 2011; Kendall *et al.*, 2011; Finch-Savage and Footitt, 2017). Therefore, we tested whether the exposure of TUR or CYP seeds to light enhances *DOG1* expression. *AearDOG1* was indeed among the light-responsive genes up-regulated in CYP (Fig. 3E, *AA6G00020*). qRT-PCR data confirmed that *DOG1* expression was significantly enhanced in both accessions in light-exposed seeds, but the increase was more pronounced in the light-inhibited CYP seeds (Fig. 4D). These results indicate that light can indeed influence the level of dormancy of light-responsive seeds. The expression of Aethionema orthologs of ABA-responsive transcription factors linked to dormancy, including *ABI3*, *ABI4*, and *ABI5* (*ABA INSENSITIVE 3, 4, 5*) (Shu *et al.*, 2013; Dekkers *et al.*, 2016) showed significant, but only moderate, differences in light-exposed CYP seeds (Fig. 3D). Taking these findings together, (i) Aethionema uses similar key regulatory components to control germination as

Arabidopsis, but (ii) the direction of change of transcript levels for several genes in light-exposed seeds are opposite in seeds of both *Aethionema* accessions compared with Arabidopsis, and (iii) at least two genes related to GA biosynthesis or degradation (*GA3ox1* and *GA2ox3*) show a much more pronounced response in the light-inhibited CYP seeds compared with the light-neutral TUR seeds and might be responsible for the observed contrasting effect of light on germination.

The GA:ABA ratio decreases during light inhibition of *Aethionema* seed germination

To test whether the differential expression of the GA- or ABA-related genes would indeed affect the levels of the respective bioactive hormones, we compared GA and ABA levels in TUR and CYP seeds during the different germination regimes. For induction of germination of Arabidopsis seeds, the most active form of GA is GA₄, among other GAs studied (Derkx et al., 1994). The absolute GA₄ hormone level was similar in both *Aethionema* accessions in seeds kept in darkness and in light-exposed TUR seeds (Fig. 5A). In contrast, and in good correlation with the light-induced repression of *GA3ox1* expression (Fig. 4B), we observed the lowest level of the bioactive GA₄ in

CYP seeds exposed to light for 23 h (Fig. 5A; Supplementary Fig. S4). Moreover, the level of GA₉, the biosynthetic precursor of GA₄, was also significantly higher in light-exposed CYP seeds compared with TUR seeds, indicating that the GA₉ → GA₄ conversion might be less efficient in CYP seeds exposed to light (Fig. 5A). Given the enhanced expression of the catabolic *GA2ox3* in light-exposed CYP seeds, we expected an increased level of the catabolic GA₃₄ in CYP seeds. We did not observe this tendency during the 23 h period, but this might have been due to the slower turnover of GA (Fig. 5A). Absolute ABA levels were higher in CYP than TUR seeds under both regimes, in agreement with the later onset of CYP germination in the dark compared with TUR and significantly higher ABA levels in light-exposed CYP seeds compared with light-exposed TUR (Fig. 5B).

As seed germination is determined by the balance of the two antagonistically acting hormones, we calculated the ratio of average GA and ABA levels. Interestingly, the GA:ABA ratio decreased in both accessions under light (Fig. 5C), but to a much larger extent in light-exposed CYP seeds, which had the lowest GA:ABA ratio of all. This indicates a threshold for the hormonal control below which germination of CYP seeds under continuous light exposure is not possible.

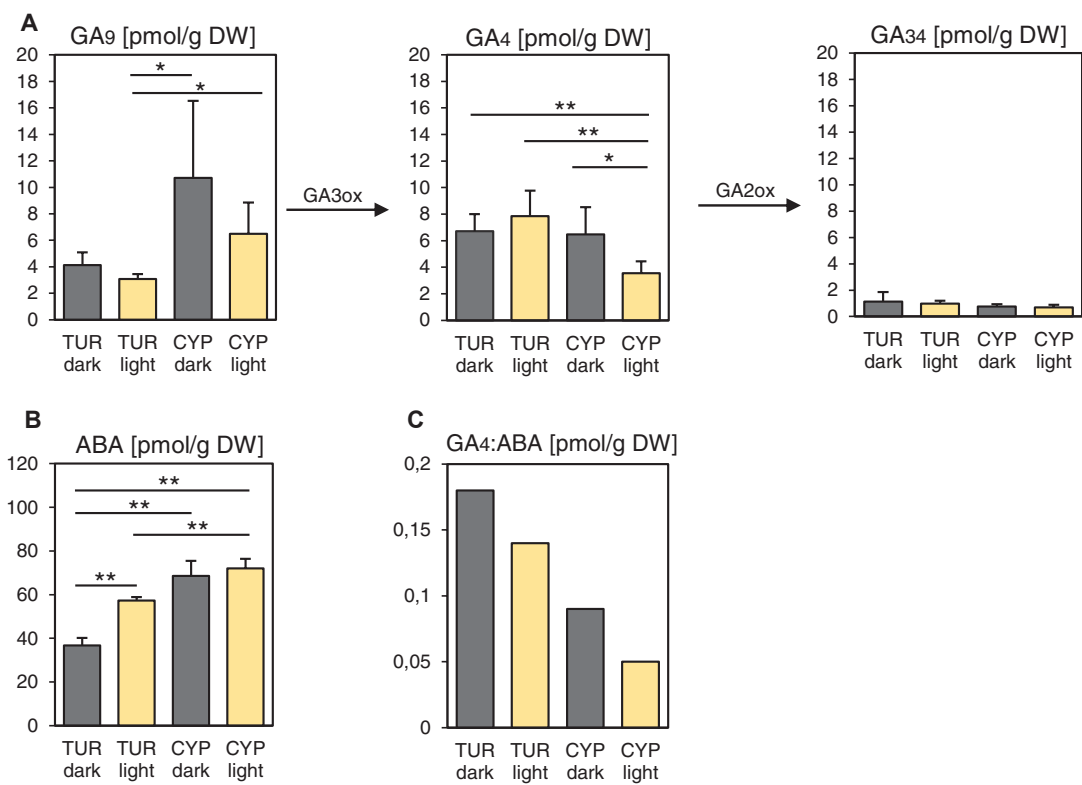


Fig. 5. Decreased GA:ABA hormone ratio in light-exposed *Aethionema* CYP seeds. Hormone concentrations [in pmol g⁻¹ dry weight (DW)] of GA₉ precursor, bioactive GA₄, and GA₃₄ catabolite (A) and ABA (B) are shown for dark-exposed (grey columns) and light-exposed (cream columns) TUR and CYP seeds. (C) Ratio of the averages from GA₄ and ABA measurements. Significance was tested using the Welch test in pairwise comparisons; asterisks indicate significant differences: **P*<0.05, **<0.01. Error bars represent SD (five independent replicates). Values for other GA metabolites are presented in Supplementary Fig. S4.

GA and ABA are involved in light inhibition of CYP seed germination

In *Arabidopsis*, germination of far-red-exposed seeds can be rescued by removal of the seed coat and the endosperm layer, as these extraembryonal tissues release ABA in response to far-red light, thereby inhibiting germination (Lee *et al.*, 2012; Yan *et al.*, 2014). Therefore, we tested whether the light inhibition of germination in *Aethionema* CYP seeds was also mediated by the seed coat and endosperm. Indeed, after mechanical removal of the extraembryonal tissue 24 h after imbibition under light exposure, development of CYP and TUR seedlings was similar, and 100% of the seedlings grew normally, even under continuous light (Fig. 6A). These data indicate that although *Arabidopsis* and *Aethionema* CYP seeds respond differently to

light, the role of the seed coat and endosperm, and likely the involvement of ABA, appear similar.

Germination of light-requiring lettuce seeds in the dark or under far-red light could also be rescued by the addition of norflurazon [4-chloro-5-methylamino-2-(3-trifluoromethylphenyl)pyridazin-3-one] (Widell *et al.*, 1981). Fluridone [1-methyl-3-phenyl-5-(3-trifluoromethyl-phenyl)-4-(1H)-pyridinone] restored the germination of lettuce and other seeds at suboptimal temperatures (Yoshioka *et al.*, 1998; Debeaujon and Koornneef, 2000; Argyris *et al.*, 2008). Both chemicals are inhibitors of carotenoid biosynthesis, which is required for *de novo* ABA synthesis (Bartels and Watson, 1978). We applied fluridone and norflurazon to both *Aethionema* accessions under continuous light exposure. CYP seed germination

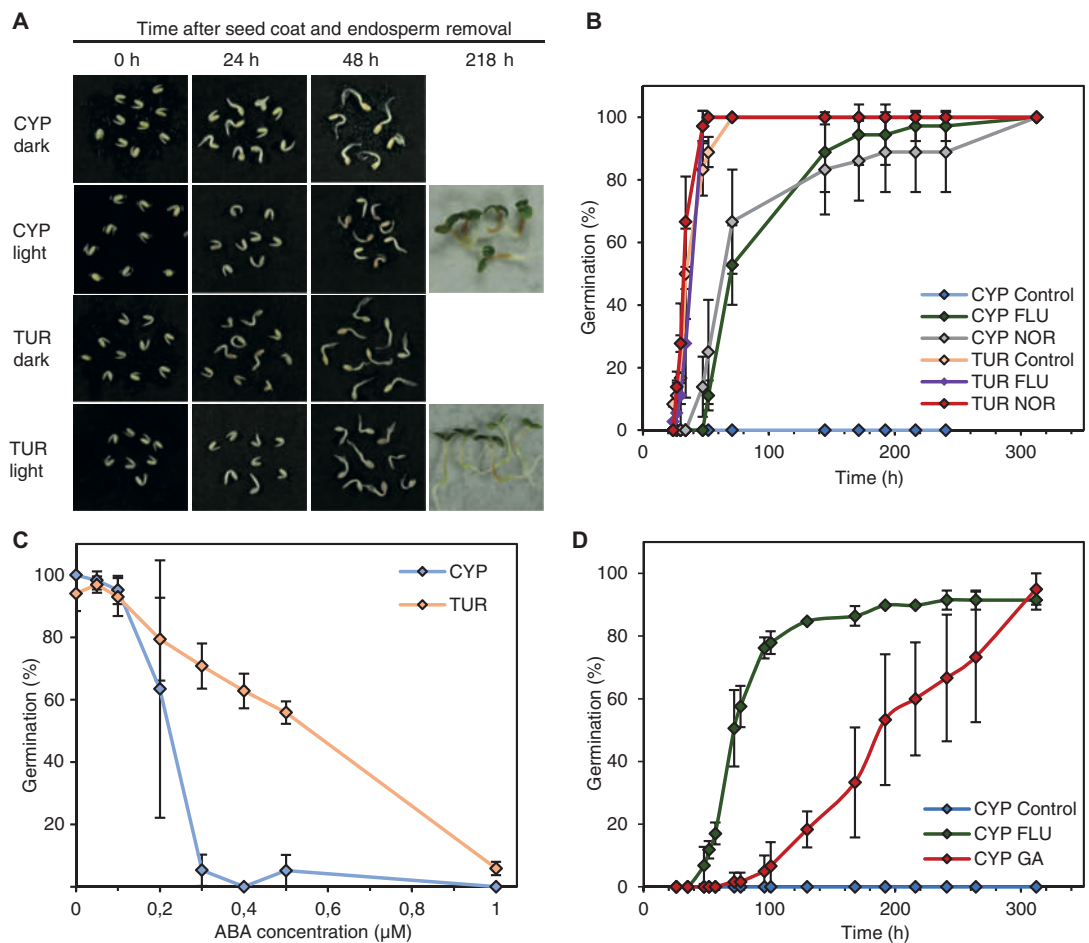


Fig. 6. Rescue of CYP seed germination in light by interference with ABA and GA signaling. (A) Development of CYP and TUR seedlings in darkness or $100 \mu\text{mol m}^{-2} \text{s}^{-1}$ light after removal of the ABA-producing seed coat and endosperm. 0 h represents the status directly after seedling isolation. (B) Percentage of germination over time when seeds were kept on plates supplemented with the ABA inhibitors $10 \mu\text{M}$ fluridone (FLU) or $10 \mu\text{M}$ norflurazon (NOR), or 0.01% DMSO as a control, under continuous $100 \mu\text{mol m}^{-2} \text{s}^{-1}$ light. (C) Percentage of germination scored after 6 days for seeds kept in the dark on plates with external application of ABA at concentrations of 0.05, 0.1, 0.2, 0.3, 0.4, 0.5, or $1 \mu\text{M}$, or 0.01% DMSO as a control. (D) Percentage of germination over time for seeds kept under continuous $100 \mu\text{mol m}^{-2} \text{s}^{-1}$ light on plates with external application of $10 \mu\text{M}$ GA_{4+7} (GA) or 0.01% DMSO as a control. Error bars represent SD (three independent replicates).

was completely rescued (Fig. 6B), indicating that *de novo* ABA synthesis induced by light is an important component of the negative control of germination in light-exposed CYP seeds.

The difference in the GA:ABA ratio between TUR and CYP seeds exposed to the dark (Fig. 5C) suggested that exogenously applied ABA might inhibit the germination of CYP seeds in darkness, which is otherwise optimal for the germination of both accessions. When this was tested by applying increasing concentrations of ABA, germination of CYP seeds was inhibited by 0.3 μM ABA while for TUR seeds 1 μM ABA was needed to produce the same level of inhibition (Fig. 6C).

Finally, we tested whether externally applied GA could overcome the inhibitory effect of light on germination. The addition of 10 μM GA₄₊₇ allowed CYP seeds to germinate under continuous light, although the germination was slower than that of seeds treated with fluridone (Fig. 6D). These data suggest that GA and ABA are indeed involved in the control of germination, as in other plants. However, the signaling pathways downstream of light reception to the transcriptional control of these two key hormones must be antipodal to those in *Arabidopsis*.

Discussion

Ecological significance of light-regulated germination

The first observations on photoblastic differences were reported more than a century ago (Kinzel, 1913), and since then, several species have been described to have a light-inhibited or light-neutral germination phenotype (Grime *et al.*, 1981). Despite this, research in the past decades about the molecular control of seed germination focused nearly exclusively on the light-requiring germination of *Arabidopsis*. Here, we present an initial physiological and molecular characterization of light-neutral and light-inhibited germination in two accessions of *Aethionema*, another Brassicaceae species.

The light requirement for seed germination is often considered to be a depth-sensing strategy associated with small seed size (Grime *et al.*, 1981; Fenner and Thompson, 2005). As light penetrates only a few millimeters into the soil, light dependence of small seeds ensures that the elongating hypocotyl will reach the surface before its resources are exhausted (Woolley and Stoller, 1978; Fenner and Thompson, 2005). Additionally, the light quality, sensed by the phytochrome photoreceptors as the ratio of red:far-red wavelengths, provides information about the leaf canopy, as leaves absorb more red than far-red light. Therefore, the minimum red:far-red ratio required for seed germination of a certain species may determine the optimal season when competition is reduced, as was shown for *Cirsium palustre* (Pons, 1984).

In contrast, light-inhibited germination is plausible in species originating from open, arid, or semi-arid habitats where high light intensity is likely coupled with drought conditions, which could be unfavorable for young seedlings (Thanos *et al.*, 1991; Lai *et al.*, 2016). These conditions occur at many original habitats of *A. arabicum*. Our data indicate that the light-inhibitable germination of the CYP accession might be a photoperiod-sensing mechanism, as the seeds germinate well

under short-day but not long-day conditions. Short-day conditions correspond to the day length of early spring days, when *Aethionema* germinates in its natural habitat. As the average lifespan of *Aethionema* is around 4 months, germination in early spring is necessary in order to complete the life cycle and seed production before the dry and warm season. Similar to the CYP accession of *Aethionema*, seeds of the light-inhibited garden variant of *Nemophila insignis* germinate preferentially in short-day conditions (Black and Wareing, 1960; Chen, 1968). Seasonal adaptation of germination via opposite photoperiod sensitivity was described for arctic tundra species, which are inhibited by short days and prefer to germinate under long days, corresponding to the short summer season in Alaska (Densmore, 1997). Although only these few examples are known, photoperiod dependence of seed germination is likely more common for plants in habitats where optimal timing of germination is crucial.

Germination in most of the examined *Aethionema* species was at least partially inhibited by light, whereas the Turkish accession of *Aethionema* (TUR) and one *A. heterocarpum* accession germinated independently of light. The occurrence of both phenotypes among close relatives in the *Aethionemeae* indicates that it is likely an adaptive trait that appeared more than once during evolution, although the exact environmental cues that favor light-neutral germination is unknown. Given the limited number of *Aethionema* accessions available that have been propagated under controlled conditions, it is too early to conclude which of the phenotypes is ancestral. Based on the habitats of most *Aethionema* species and the identified transcriptome changes of key regulatory genes, in the same direction but to different degrees, in TUR and CYP, it is tempting to speculate that light-inhibited germination is the ancestral mechanism that has been desensitized in some instances. Collection and amplification of seed material and analysis of further *Aethionema* species and accessions for which detailed phylogenetic data are available (Mohammadin *et al.*, 2017) are expected to provide an answer to this question.

Light-dependent versus light-inhibited germination control

The species for which light inhibition of seed germination have been previously described (Chen, 1968, 1970; Botha and Small, 1988; Thanos *et al.*, 1991) are phylogenetically distant from the model plants lettuce and *Arabidopsis*, which show light-dependent germination. Some molecular aspects of light-inhibited germination have been investigated for monocotyledonous plants (Barrero *et al.*, 2012; Hoang *et al.*, 2014), and in both cases were clearly restricted to blue light. The comparisons within the triangle of closely related species with different germination phenotypes—light-requiring *Arabidopsis*, light-neutral *Aethionema* TUR, and *Aethionema* CYP that is inhibited by the full spectrum of visible light—may allow us to understand the mechanistic and evolutionary divergence of the light-controlled signaling network that induces germination. Previous studies in numerous species (Finch-Savage and Leubner-Metzger, 2006) together with the data presented here leave no doubt about the central role of ABA and GA in the

inhibition and stimulation, respectively, of germination. The positive, essential stimulus of light in Arabidopsis and its negative, blocking role in Aethionema CYP are expected to reflect a fundamental and qualitative difference between light reception and hormonal control. Although many other factors, including other hormones, are known to modulate germination (Argyris *et al.*, 2008; Linkies and Leubner-Metzger, 2012; Meng *et al.*, 2016), the antipodal changes in transcript levels in Aethionema upon light exposure for some of the same ABA/GA key regulatory components as in Arabidopsis indicate a major source of the difference in this signaling pathway (Fig. 7). Among these components are *AearSOM*, *AearABI3*, *AearABI5*, *AearABA1*, *AearNCED6*, *AearGA3ox1*, *AearGA3ox2*, and *AearGA2ox3*. However, the expression of many other genes responds to light in a similar fashion in Aethionema and Arabidopsis (e.g. *RGA*, *GAI*, *DAG1*, *CYP707A2*, and *JMJ20*), indicating that the light response is partially conserved (Fig. 7). In Arabidopsis, PIL5/PIF1, a key regulator in the light-induced transcriptional cascade, undergoes rapid protein degradation (Shen *et al.*, 2008). As the antibody to Arabidopsis PIL5/PIF1 did not recognize the Aethionema protein from the orthologous gene (*AA33G00286*) (our unpublished results), we were unable to test its light-responsive protein degradation in Aethionema seeds. However, it is remarkable that the direct downstream target genes (*DAG1*, *SOM*, *DELLAs*, and *ABI5*) are either up- or down-regulated in Aethionema, whereas their transcriptional repression by light is rather uniform in Arabidopsis (Fig. 7). A study based on chromatin immunoprecipitation in Arabidopsis with the PIL5/PIF1 antibody and microarray data revealed 166 genes that are under the direct control of PIL5/PIF1 (Oh *et al.*, 2009). The Aethionema orthologs of the direct PIL5 target genes that could be identified (132 out of the 166) were found to have relatively stable and light-independent expression in Aethionema seeds; only eight genes in TUR and seven genes in CYP showed more than 2-fold changes in either

direction (Supplementary Dataset S6). Therefore, one possible divergence between Arabidopsis and Aethionema might be in the regulation of PIL5/PIF1 protein activity or stabilization. The germination of Arabidopsis *pil5* mutant seeds in darkness and far-red light further indicates that PIL5/PIF1 is the most upstream element in the network that is possibly associated with germination in the dark.

Light-independent versus light-inhibited germination control

Remarkably, among the 87 genes that were light-responsive in CYP and differentially regulated between the TUR and CYP accessions, 15 nevertheless showed the same direction of change in transcript levels in both accessions. One possible explanation for this observation might be a reduced sensitivity of germination of TUR seeds to light. In Arabidopsis, screens for light-hyposensitive mutants have often identified *PHYB* or *PHYA* mutations, indicating that the primary reason for the hyposensitive response may be variations within the phytochrome protein. As in Arabidopsis, there are five phytochromes in Aethionema, which are highly conserved (Supplementary Fig. S5A). The protein sequences of *PHYB*, *PHYC*, and *PHYD* are identical in the CYP and TUR accessions, while the *PHYA* and *PHYE* proteins harbor a few missense single nucleotide polymorphisms (SNPs) (Supplementary Fig. S5B–F). However, the second, light-inhibited accession from Turkey (KM2397) shares most of the same SNPs with the light-neutral TUR accession. It is therefore unlikely that allelic variations of phytochromes are responsible for the different responses (Supplementary Fig. S5B–F). Similarly, there are no SNPs in the PIL5/PIF1 coding sequences that would cause non-synonymous amino acid changes and that diverge between the light-neutral TUR and the two light-inhibited accessions (Supplementary Fig. S6). A detailed analysis of phytochrome

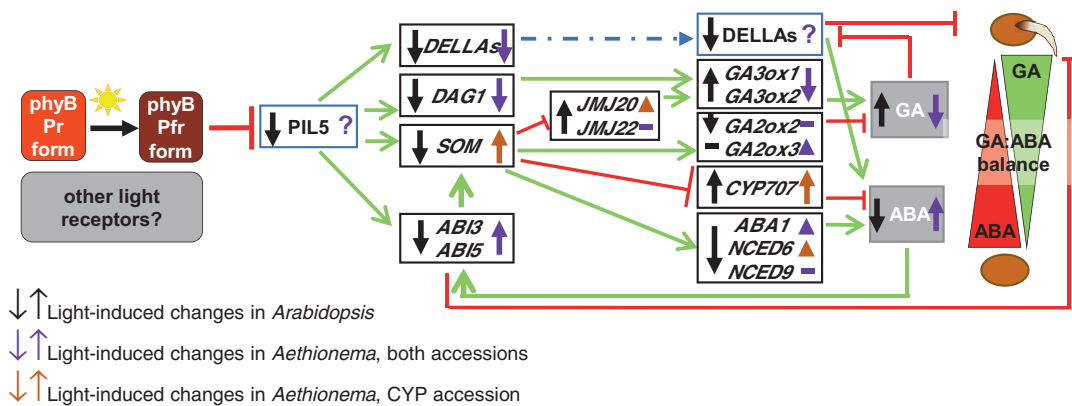


Fig. 7. Antipodal transcriptional changes in Arabidopsis and Aethionema of key hormone regulatory genes. Summary of light-regulated changes in transcript levels in seeds, based on published data for Arabidopsis (after Stawska and Oracz 2015) and with the data for Aethionema presented in this study. Blue boxes indicate proteins whose stability is regulated by light. Black boxes indicate genes whose expression is light-regulated. Changes in expression upon light exposure are indicated by black (Arabidopsis), purple (Aethionema, both accessions), and orange (Aethionema, CYP accession only) arrows. The role of other photoreceptors in Aethionema seed germination is not yet known. As indicated by question marks, the stability of PIL5 and DELLA proteins is unknown in Aethionema.

actions may help to understand and identify the photoreceptors involved in light-inhibited germination.

As the qRT-PCR data indicated, many genes of the light-regulated network are differentially expressed either slightly or strongly in TUR and CYP seeds under dark and light conditions, resulting in substantial differences in *AearGA3ox1* and *AearGA2ox2* expression and lower levels of GA₄ in CYP seeds under light. The differential GA:ABA ratio is likely determined by more than one upstream event early in the transcriptional cascade. Our data show that the *PAR1* and *PAR2* genes are significantly differentially expressed in TUR and CYP seeds under dark and light conditions. *PAR1* and *PAR2* both encode bHLH proteins, but do not possess DNA binding activity and are involved in the shade avoidance response (Wray *et al.*, 2003; Roig-Villanova *et al.*, 2007). Although their precise mechanism of action and role in seed germination is still unknown, it has been speculated that they form heterodimers with other bHLH proteins, such as PIFs, and modulate their activity as transcriptional cofactors (Roig-Villanova *et al.*, 2007). Therefore, the differential expression of *AearPAR1* and *AearPAR2* in TUR and CYP seeds might play a role in the regulation of PIL5/PIF1 activity, influencing the network downstream of PIL5/PIF1.

While our data did not identify a unique point of divergence in the molecular control of light over seed germination between the investigated *Aethionema* accessions, the identified natural variation within the genus, and the phylogenetic relationship with the conversely responding *Arabidopsis*, provide great opportunities to elucidate the mechanism of an ecologically important but underinvestigated trait. Based on the current evidence, the basic components seem to be conserved but connected in a different cascade of events. Growth conditions, genome size, and generation time of *Aethionema* are similar to those of *Arabidopsis*, allowing for future forward mutant screens and genetic association studies.

Supplementary data

Supplementary data are available at *JXB* online.

Fig. S1. Germination of dimorphic seed types in response to light.

Fig. S2. Heatmap of all 87 genes light-regulated in *Aethionema arabicum* CYP seeds and differentially expressed in light-exposed TUR and CYP seeds based on RPKM values.

Fig. S3. Identification of the *Arabidopsis* orthologue of *Aethionema AA18G00108* as *GA2ox3*.

Fig. S4. Accumulation of GA forms in *Aethionema arabicum* TUR and CYP seeds under dark and light conditions.

Fig. S5. Identification and alignments of phytochromes in *Aethionema arabicum*.

Fig. S6. Alignment of the PIL5/PIF1 protein sequence of three *Aethionema arabicum* accessions.

Table S1. Information about the geographic origin of *Aethionema arabicum* accessions.

Table S2. List of primers used for quantitative RT-PCR analysis.

Table S3. List of *Aethionema* accession numbers used for this study.

Dataset S1. List of differentially expressed *Aethionema arabicum* genes in TUR Dark versus TUR Light.

Dataset S2. List of differentially expressed *Aethionema arabicum* genes in CYP Dark versus CYP Light.

Dataset S3. List of differentially expressed *Aethionema arabicum* genes in CYP Dark versus TUR Dark.

Dataset S4. List of differentially expressed *Aethionema arabicum* genes in CYP Light versus TUR Light.

Dataset S5. List of common differentially expressed *Aethionema arabicum* genes in CYP Light versus TUR Light and TUR Dark versus TUR Light.

Dataset S6. List of target genes of *Arabidopsis* PIL5/PIF1 and transcriptional changes of orthologues in the *Aethionema* experiments.

Dataset S7: List of plant species for which protein sequences were considered for phylogenetic tree constructions.

Acknowledgements

This work is part of the European Research Area Network for Coordinating Action in Plant Sciences (ERA-CAPS) ‘SeedAdapt’ consortium project (<https://www.seedadapt.eu/>). We thank all members for fruitful cooperation and discussion. We are especially grateful to Eric M. Schranz, Klaus Mummenhof, and Setareh Mohammadin for providing various *Aethionema* seed stocks. We also thank the staff of the Vienna BioCenter Core Facilities GmbH (VBCF), a member of Vienna BioCenter (VBC), Austria, especially the Plant Sciences Facility for growth of the plants and the wavelength-specific light experiments, and the Next Generation Sequencing Facility for generating the RNA-Seq data. We thank Nicole Lettner and Sarhan Khalil for technical support. We further acknowledge critical reading of the manuscript by J. Matthew Watson, Frederic Berger, Peter Hedden, and the anonymous reviewers. The work was funded by the Austrian Science Fund (FWF) to OMS (FWF I1477) and to ZM (FWF I3979), the Deutsche Forschungsgemeinschaft (DFG) to SAR (RE1697/8-1), the Biotechnology and Biological Sciences Research Council (BBSRC) to GLM (BB/M00192X/1), a Natural Environment Research Council (NERC) Doctoral Training Grant to WA (NE/L002485/1), the Czech Grant Agency to DT (18-10349S), and the European Regional Development Fund Project ‘Centre for Experimental Plant Biology’ (CZ.02.1.01/0.0/0.0/16_019/0000738) to DT and MS.

Author contributions

ZM, KG, MS, SAR, GLM, and OMS planned and designed the research; ZM, KG, WA, DT, and VT performed the experiments; ZM, KG, PW, KKU, WA, CG, DT, VT, MS, SAR, GLM, and OMS analyzed and interpreted the data; ZM, GLM, and OMS wrote the paper. All authors approved the submitted version.

References

- Altschul SF, Gish W, Miller W, Myers EW, Lipman DJ. 1990. Basic local alignment search tool. *Journal of Molecular Biology* **215**, 403–410.
- Anders S, Pyl PT, Huber W. 2015. HTSeq—a Python framework to work with high-throughput sequencing data. *Bioinformatics* **31**, 166–169.

- Argyris J, Dahal P, Hayashi E, Still DW, Bradford KJ. 2008. Genetic variation for lettuce seed thermoinhibition is associated with temperature-sensitive expression of abscisic acid, gibberellin, and ethylene biosynthesis, metabolism, and response genes. *Plant Physiology* **148**, 926–947.
- Barrero JM, Downie AB, Xu Q, Gubler F. 2014. A role for barley CRYPTOCHROME1 in light regulation of grain dormancy and germination. *The Plant Cell* **26**, 1094–1104.
- Barrero JM, Jacobsen JV, Talbot MJ, White RG, Swain SM, Garvin DF, Gubler F. 2012. Grain dormancy and light quality effects on germination in the model grass *Brachypodium distachyon*. *New Phytologist* **193**, 376–386.
- Bartels PG, Watson CW. 1978. Inhibition of carotenoid synthesis by fluridone and norflurazon. *Weed Science* **26**, 198–203.
- Bentsink L, Hanson J, Hanhart CJ, et al. 2010. Natural variation for seed dormancy in *Arabidopsis* is regulated by additive genetic and molecular pathways. *Proceedings of the National Academy of Sciences, USA* **107**, 4264–4269.
- Bentsink L, Jowett J, Hanhart CJ, Koornneef M. 2006. Cloning of DOG1, a quantitative trait locus controlling seed dormancy in *Arabidopsis*. *Proceedings of the National Academy of Sciences, USA* **103**, 17042–17047.
- Bewley JD, Bradford K, Hilhorst H, Nonogaki H. 2013. *Seeds. Physiology of development, germination and dormancy*, 3rd edn. New York: Springer.
- Black M, Wareing PF. 1960. Photoperiodism in the light-inhibited seed of *Nemophila insignis*. *Journal of Experimental Botany* **11**, 28–39.
- Boccaccini A, Santopolo S, Capauto D, Lorrari R, Minutello E, Belcram K, Palaquini JC, Costantino P, Vittorioso P. 2014. Independent and interactive effects of DOF affecting germination 1 (DAG1) and the DELLA proteins GA insensitive (GAI) and Repressor of ga1-3 (RGA) in embryo development and seed germination. *BMC Plant Biology* **14**, 200.
- Bolger AM, Lohse M, Usadel B. 2014. Trimmomatic: a flexible trimmer for Illumina sequence data. *Bioinformatics* **30**, 2114–2120.
- Borthwick HA, Hendricks SB, Parker MW, Toole EH, Toole VK. 1952. A reversible photoreaction controlling seed germination. *Proceedings of the National Academy of Sciences, USA* **38**, 662–666.
- Botha FC, Small JGC. 1988. The germination response of the negatively photoblastic seeds of *Citrullus lanatus* to light of different spectral compositions. *Journal of Plant Physiology* **132**, 750–753.
- Casal JJ, Sanchez RA. 1998. Phytochromes and seed germination. *Seed Science Research* **8**, 3.
- Casal JJ, Sanchez RA, Botto JF. 1998. Modes of action of phytochromes. *Journal of Experimental Botany* **49**, 127–138.
- Chang S, Puryear J, Cairney J. 1993. A simple and efficient method for isolating RNA from pine trees. *Plant Molecular Biology Reporter* **11**, 113–116.
- Chen SSC. 1968. Germination of light-inhibited seed of *Nemophila insignis*. *American Journal of Botany* **55**, 1177–1183.
- Chen SS. 1970. Influence of factors affecting germination on respiration of *Phacelia tanacetifolia* seeds. *Planta* **95**, 330–335.
- Chiang GC, Bartsch M, Barua D, Nakabayashi K, Debieu M, Kronholm I, Koornneef M, Soppe WJ, Donohue K, De Meaux J. 2011. *DOG1* expression is predicted by the seed-maturation environment and contributes to geographical variation in germination in *Arabidopsis thaliana*. *Molecular Ecology* **20**, 3336–3349.
- Cho JN, Ryu JY, Jeong YM, Park J, Song JJ, Amasino RM, Noh B, Noh YS. 2012. Control of seed germination by light-induced histone arginine demethylation activity. *Developmental Cell* **22**, 736–748.
- Clamp M, Cuff J, Searle SM, Barton GJ. 2004. The Jalview Java alignment editor. *Bioinformatics* **20**, 426–427.
- Conesa A, Götz S, García-Gómez JM, Terol J, Talón M, Robles M. 2005. Blast2GO: a universal tool for annotation, visualization and analysis in functional genomics research. *Bioinformatics* **21**, 3674–3676.
- Darriba D, Taboada GL, Doallo R, Posada D. 2011. ProtTest 3: fast selection of best-fit models of protein evolution. *Bioinformatics* **27**, 1164–1165.
- Debeaujon I, Koornneef M. 2000. Gibberellin requirement for *Arabidopsis* seed germination is determined both by testa characteristics and embryonic abscisic acid. *Plant Physiology* **122**, 415–424.
- Dekkers BJ, He H, Hanson J, Willems LA, Jamar DC, Cuff G, Rajjou L, Hilhorst HW, Bentsink L. 2016. The *Arabidopsis* *DELAY OF GERMINATION 1* gene affects *ABSCISIC ACID INSENSITIVE 5* (*ABI5*) expression and genetically interacts with *ABI3* during *Arabidopsis* seed development. *The Plant Journal* **85**, 451–465.
- Densmore R. 1997. Effect of day length on germination of seeds collected in Alaska. *American Journal of Botany* **84**, 274.
- Derx MPM, Vermeer E, Karssen CM. 1994. Gibberellins in seeds of *Arabidopsis thaliana*: biological activities, identification and effects of light and chilling on endogenous levels. *Plant Growth Regulation* **15**, 223–234.
- Fenner M, Thompson K. 2005. *The ecology of seeds*. *Annals of Botany* **97**, 151–152.
- Finch-Savage WE, Footitt S. 2017. Seed dormancy cycling and the regulation of dormancy mechanisms to time germination in variable field environments. *Journal of Experimental Botany* **68**, 843–856.
- Finch-Savage WE, Leubner-Metzger G. 2006. Seed dormancy and the control of germination. *New Phytologist* **171**, 501–523.
- Footitt S, Douterelo-Soler I, Clay H, Finch-Savage WE. 2011. Dormancy cycling in *Arabidopsis* seeds is controlled by seasonally distinct hormone-signaling pathways. *Proceedings of the National Academy of Sciences, USA* **108**, 20236–20241.
- Franzke A, Lysak MA, Al-Shehbaz IA, Koch MA, Mummenhoff K. 2011. Cabbage family affairs: the evolutionary history of Brassicaceae. *Trends in Plant Science* **16**, 108–116.
- Gabriele S, Rizza A, Martone J, Circelli P, Costantino P, Vittorioso P. 2010. The Dof protein DAG1 mediates PIL5 activity on seed germination by negatively regulating GA biosynthetic gene *AtGA3ox1*. *The Plant Journal* **61**, 312–323.
- Graeber K, Linkies A, Steinbrecher T, et al. 2014. *DELAY OF GERMINATION 1* mediates a conserved coat-dormancy mechanism for the temperature- and gibberellin-dependent control of seed germination. *Proceedings of the National Academy of Sciences, USA* **111**, E3571–E3580.
- Grime JP, Mason G, Curtis AV, Rodman J, Band SR. 1981. A comparative study of germination characteristics in a local flora. *Journal of Ecology* **69**, 1017–1059.
- Guindon S, Gascuel O. 2003. A simple, fast, and accurate algorithm to estimate large phylogenies by maximum likelihood. *Systematic Biology* **52**, 696–704.
- Haudry A, Platts AE, Vello E, et al. 2013. An atlas of over 90,000 conserved noncoding sequences provides insight into crucifer regulatory regions. *Nature Genetics* **45**, 891–898.
- Hoang HH, Sechet J, Bailly C, Leymarie J, Corbineau F. 2014. Inhibition of germination of dormant barley (*Hordeum vulgare* L.) grains by blue light as related to oxygen and hormonal regulation. *Plant, Cell & Environment* **37**, 1393–1403.
- Hradecká V, Novák O, Havlíček L, Strnad M. 2007. Immunoaffinity chromatography of abscisic acid combined with electrospray liquid chromatography-mass spectrometry. *Journal of Chromatography* **847**, 162–173.
- Katoh K, Standley DM. 2013. MAFFT multiple sequence alignment software version 7: improvements in performance and usability. *Molecular Biology and Evolution* **30**, 772–780.
- Kendall SL, Hellwege A, Marriot P, Whalley C, Graham IA, Penfield S. 2011. Induction of dormancy in *Arabidopsis* summer annuals requires parallel regulation of *DOG1* and hormone metabolism by low temperature and CBF transcription factors. *The Plant Cell* **23**, 2568–2580.
- Kerdaffrec E, Filiault DL, Korte A, Sasaki E, Nizhynska V, Seren U, Nordborg M. 2016. Multiple alleles at a single locus control seed dormancy in Swedish *Arabidopsis*. *eLife* **5**, e22502.
- Kim DH, Yamaguchi S, Lim S, Oh E, Park J, Hanada A, Kamiya Y, Choi G. 2008. SOMNUS, a CCH-type zinc finger protein in *Arabidopsis*, negatively regulates light-dependent seed germination downstream of PIL5. *The Plant Cell* **20**, 1260–1277.
- Kinzel W. 1913. Frost und Licht als beeinflussende Kräfte bei der Samenkeimung. Stuttgart: Ulmer.
- Koller D. 1956. Germination-regulating mechanisms in some desert seeds. *Ecology* **37**, 430–433.
- Koller D, Negbi M. 1959. The regulation of germination in *Oryzopsis miliacea*. *Ecology* **40**, 20–36.
- Lai LM, Chen LJ, Jiang LH, Zhou JH, Zheng YR, Shimizu H. 2016. Seed germination of seven desert plants and implications for vegetation restoration. *AoB Plants* **8**, plw031.

- Langmead B, Salzberg SL. 2012. Fast gapped-read alignment with Bowtie 2. *Nature Methods* **9**, 357–359.
- Lee KP, Piskurewicz U, Tureckova V, Carat S, Chappuis R, Strnad M, Fankhauser C, Lopez-Molina L. 2012. Spatially and genetically distinct control of seed germination by phytochromes A and B. *Genes and Development* **26**, 1984–1996.
- Lenser T, Graeber K, Cevik ÖS, *et al.* 2016. Developmental control and plasticity of fruit and seed dimorphism in *Aethionema arabicum*. *Plant Physiology* **172**, 1691–1707.
- Li WQ, Khan MA, Yamaguchi S, Liu XJ. 2015. Hormonal and environmental regulation of seed germination in salt cress (*Thellungiella halophila*). *Plant Growth Regulation* **76**, 41–49.
- Linkies A, Leubner-Metzger G. 2012. Beyond gibberellins and abscisic acid: how ethylene and jasmonates control seed germination. *Plant Cell Reports* **31**, 253–270.
- Love MI, Huber W, Anders S. 2014. Moderated estimation of fold change and dispersion for RNA-seq data with DESeq2. *Genome Biology* **15**, 550.
- Meng YJ, Chen F, Shuai HW, *et al.* 2016. Karrikins delay soybean seed germination by mediating abscisic acid and gibberellin biogenesis under shaded conditions. *Scientific Reports* **6**, 22073.
- Mohammad S, Peterse K, van de Kerke SJ, Chatrou LW, Dönmez AA, Mummenhoff K, Pires JC, Edger PP, Al-Shehbaz IA, Schranz ME. 2017. Anatolian origins and diversification of *Aethionema*, the sister lineage of the core Brassicaceae. *American Journal of Botany* **104**, 1042–1054.
- Mohammad S, Wang W, Liu T, *et al.* 2018. Genome-wide nucleotide diversity and associations with geography, ploidy level and glucosinolate profiles in *Aethionema arabicum* (Brassicaceae). *Plant Systematics and Evolution* **304**, 619–630.
- Negbi M, Koller D. 1964. Dual action of white light in the photocontrol of germination of *Oryzopsis miliacea*. *Plant Physiology* **39**, 247–253.
- Oh E, Kang H, Yamaguchi S, Park J, Lee D, Kamiya Y, Choi G. 2009. Genome-wide analysis of genes targeted by PHYTOCHROME INTERACTING FACTOR 3-LIKE5 during seed germination in *Arabidopsis*. *The Plant Cell* **21**, 403–419.
- Oh E, Kim J, Park E, Kim JI, Kang C, Choi G. 2004. PIL5, a phytochrome-interacting basic helix-loop-helix protein, is a key negative regulator of seed germination in *Arabidopsis thaliana*. *The Plant Cell* **16**, 3045–3058.
- Oh E, Yamaguchi S, Hu J, Yusuke J, Jung B, Paik I, Lee HS, Sun TP, Kamiya Y, Choi G. 2007. PIL5, a phytochrome-interacting bHLH protein, regulates gibberellin responsiveness by binding directly to the *GAI* and *AGA* promoters in *Arabidopsis* seeds. *The Plant Cell* **19**, 1192–1208.
- Oñate-Sánchez L, Vicente-Carbajosa J. 2008. DNA-free RNA isolation protocols for *Arabidopsis thaliana*, including seeds and siliques. *BMC Research Notes* **1**, 93.
- Piskurewicz U, Turecková V, Lacombe E, Lopez-Molina L. 2009. Far-red light inhibits germination through DELLA-dependent stimulation of ABA synthesis and ABI3 activity. *The EMBO Journal* **28**, 2259–2271.
- Pons TL. 1984. Possible significance of the light requirement of *Cirsium palustre* seeds after dispersal in ash coppice. *Plant, Cell & Environment* **7**, 263–268.
- Rittenberg D, Foster GL. 1940. A new procedure for quantitative analysis by isotope dilution, with application to the determination of amino acids and fatty acids. *Journal of Biological Chemistry* **133**, 737–744.
- Robinson MD, McCarthy DJ, Smyth GK. 2010. edgeR: a Bioconductor package for differential expression analysis of digital gene expression data. *Bioinformatics* **26**, 139–140.
- Roig-Villanova I, Bou-Torrent J, Galstyan A, Carretero-Paulet L, Portolés S, Rodríguez-Concepción M, Martínez-García JF. 2007. Interaction of shade avoidance and auxin responses: a role for two novel atypical bHLH proteins. *The EMBO Journal* **26**, 4756–4767.
- Ronquist F, Teslenko M, van der Mark P, Ayres DL, Darling A, Höhna S, Larget B, Liu L, Suchard MA, Huelsenbeck JP. 2012. MrBayes 3.2: efficient Bayesian phylogenetic inference and model choice across a large model space. *Systematic Biology* **61**, 539–542.
- Rost B. 1999. Twilight zone of protein sequence alignments. *Protein Engineering* **12**, 85–94.
- Santopolo S, Boccaccini A, Lorrain R, Ruta V, Caputo D, Minutello E, Serino G, Costantino P, Vittorioso P. 2015. DOF AFFECTING GERMINATION 2 is a positive regulator of light-mediated seed germination and is repressed by DOF AFFECTING GERMINATION 1. *BMC Plant Biology* **15**, 72.
- Seo M, Hanada A, Kuwahara A, *et al.* 2006. Regulation of hormone metabolism in *Arabidopsis* seeds: phytochrome regulation of abscisic acid metabolism and abscisic acid regulation of gibberellin metabolism. *The Plant Journal* **48**, 354–366.
- Seo M, Nambara E, Choi G, Yamaguchi S. 2009. Interaction of light and hormone signals in germinating seeds. *Plant Molecular Biology* **69**, 463–472.
- Shen H, Zhu L, Castillon A, Majee M, Downie B, Huq E. 2008. Light-induced phosphorylation and degradation of the negative regulator PHYTOCHROME-INTERACTING FACTOR1 from *Arabidopsis* depend upon its direct physical interactions with photoactivated phytochromes. *The Plant Cell* **20**, 1586–1602.
- Shi H, Zhong S, Mo X, Liu N, Nezames CD, Deng XW. 2013. HFR1 sequesters PIF1 to govern the transcriptional network underlying light-initiated seed germination in *Arabidopsis*. *The Plant Cell* **25**, 3770–3784.
- Shinomura T, Nagatani A, Chory J, Furuya M. 1994. The induction of seed germination in *Arabidopsis thaliana* is regulated principally by phytochrome B and secondarily by phytochrome A. *Plant Physiology* **104**, 363–371.
- Shropshire W, Klein WH, Elstad VB. 1961. Action spectra of photomorphogenic induction and photoinactivation of germination in *Arabidopsis thaliana*. *Plant & Cell Physiology* **2**, 63–69.
- Shu K, Liu XD, Xie Q, He ZH. 2016. Two faces of one seed: hormonal regulation of dormancy and germination. *Molecular Plant* **9**, 34–45.
- Shu K, Zhang H, Wang S, Chen M, Wu Y, Tang S, Liu C, Feng Y, Cao X, Xie Q. 2013. ABI4 regulates primary seed dormancy by regulating the biogenesis of abscisic acid and gibberellins in *Arabidopsis*. *PLoS Genetics* **9**, e1003577.
- Stawska M, Oracz K. 2015. Network of signal transduction pathways mediated by phytochromes, cryptochromes and regulators of growth and development in seed biology. *Postepy Biologii Komorki* **42**, 687–706.
- Takaki M. 2001. New proposal of classification of seeds based on forms of phytochrome instead of photoblastism. *Revista Brasileira de Fisiologia Vegetal* **13**, 104–108.
- Tarazona S, García-Alcalde F, Dopazo J, Ferrer A, Conesa A. 2011. Differential expression in RNA-seq: a matter of depth. *Genome Research* **21**, 2213–2223.
- Thanos CA, Georghiou K, Douma DJ, Marangaki CJ. 1991. Photoinhibition of seed germination in Mediterranean maritime plants. *Annals of Botany* **68**, 469–475.
- Turecková V, Novák O, Strnad M. 2009. Profiling ABA metabolites in *Nicotiana tabacum* L. leaves by ultra-performance liquid chromatography-electrospray tandem mass spectrometry. *Talanta* **80**, 390–399.
- Urbanová T, Tarkowská D, Novák O, Hedden P, Strnad M. 2013. Analysis of gibberellins as free acids by ultra performance liquid chromatography-tandem mass spectrometry. *Talanta* **112**, 85–94.
- Vandeloos F, Newton RJ, Carta A. 2018. Photophobia in Lilioid monocots: photoinhibition of seed germination explained by seed traits, habitat adaptation and phylogenetic inertia. *Annals of Botany* **121**, 405–413.
- Woolley JT, Stoller EW. 1978. Light penetration and light-induced seed germination in soil. *Plant Physiology* **61**, 597–600.
- Wray GA, Hahn MW, Abouheif E, Balhoff JP, Pizer M, Rockman MV, Romano LA. 2003. The evolution of transcriptional regulation in eukaryotes. *Molecular Biology and Evolution* **20**, 1377–1419.
- Yamaguchi S, Smith MW, Brown RG, Kamiya Y, Sun T. 1998. Phytochrome regulation and differential expression of gibberellin 3 β -hydroxylase genes in germinating *Arabidopsis* seeds. *The Plant Cell* **10**, 2115–2126.
- Yan DW, Duermeier L, Leoveanu C, Nambara E. 2014. The functions of the endosperm during seed germination. *Plant and Cell Physiology* **55**, 1521–1533.
- Yoshioka T, Endo T, Satoh S. 1998. Restoration of seed germination at supraoptimal temperatures by fluridone, an inhibitor of abscisic acid biosynthesis. *Plant and Cell Physiology* **39**, 307–312.
- Zhou P, Song M, Yang Q, *et al.* 2014. Both PHYTOCHROME RAPIDLY REGULATED1 (PAR1) and PAR2 promote seedling photomorphogenesis in multiple light signaling pathways. *Plant Physiology* **164**, 841–852.

9.3 Successful proposal to conduct Synchrotron-based X-ray Tomographic Microscopy (SRXTM)

Beamtime for research at the Swiss Light Source is obtained by competitive application, that also covers the cost of beamtime.

A research proposal (ID: 20180809) for beamtime at the TOMCAT beamline was submitted in March 2018, entitled “*A tale of two morphs: bet-hedging survival strategies in the Brassicaceae as adaptations in unpredictable environments*”, and is presented here in its full form. Work resulting from this proposal provided the most accurate morph-specific volumetric investigations of *Ae. arabicum* to date and were major contributions to two manuscripts (Chapter 4 and Chapter 5).

W Arshad conceived and designed the experiment within the proposal, prepared the text and figures, and requested 5 shifts (each of 8 hours) of beamtime. The proposal was accepted in May 2018 and all requested shifts were successfully allocated. The proposal ranked 4.17 (compared to maximum: 4.87, average: 3.76), with a total cost in the order of 42500 CHF (~36,000 GBP).

Proposal 20180809

Title
A tale of two morphs: bet-hedging survival strategies in the Brassicaceae as adaptations in unpredictable environments

Abstract
Plants are the backbone of all life on earth and seed germination is the crucial first step in a plant's life cycle. To maintain agricultural productivity and plant diversity, we need to understand the complex mechanisms of germination. Seeds have an amazing diversity of strategies to cope with harsh, unpredictable and changing environments. Some species, including <i>Aethionema arabicum</i> , produce and disperse two morphologically distinct fruits and seeds. This has been proposed to be a bet-hedging strategy to survive in variable environments. Our goal is to use this model system to understand the basis of dimorphism and phenotypic plasticity and its implication for plant dispersal/germination success. How are internal structures (ovules, cell walls, tissue distribution) connected to size, shape and dispersal success? New SRXTM data on the developmental morphology of this fascinating and highly adaptive dispersal system will be linked to a large-scale molecular data set and physical properties already obtained in the ERA-CAPS SeedAdapt project (www.seedadapt.eu).

Proposer / Spokesperson	
Dr. Tina LH Steinbrecher	Department of Earth Sciences, Royal Holloway University of London tina.steinbrecher@rhul.ac.uk

Principal investigator	
Dr. Tina LH Steinbrecher	Department of Earth Sciences, Royal Holloway University of London

Co-Proposer	
Mr. Waheed Arshad	Department of Earth Sciences, Royal Holloway University of London
Prof. Dr. Margaret E Collinson	Department of Earth Sciences, Royal Holloway University of London
Prof. Dr. Gerhard Leubner	Department of Earth Sciences, Royal Holloway University of London

Experiment Category	
Experiment Type	Normal
Research Area	Environmental and Earth Science

Experiment Requirements	
Eligible for EU Support	Yes
Number of Shifts Required	5
Schedule Preferences	Not available 01-08.July, 12-14.July, 04-26.Aug, 11-15. Sept, 10-14.Nov, 14-26.Dec
Beamline/Station	TOMCAT

Links to related proposals of relevance to the current proposal		
Proposal	Title/Proposer/Infos given by the proposer about the relation	Report
20161437	<p>Title: Controls on seed germination and dormancy: is variation in seed coat flavonoids linked to physical changes in seed coat structure?</p> <p>Proposer: Prof. Dr. Margaret E Collinson</p> <p>Infos: Related work on Brassicacea fruit structures. Proposal 20161437 showed proof of concept that work on Aethionema arabicum is feasible and revealed key differences in the internal structure of mature Aethionema seeds.</p>	Available

A) Goal of the experiment

Our goal is to study diaspore heteromorphism – the production of two or more different morphologies (morphs) of seeds or fruits by a single individual plant – using a model species *Aethionema arabicum* (“stone-cress”, Brassicaceae). A plant’s ability to adapt to changing environments is crucial, particularly in light of climate change as a global reality and one of the biggest threats to our biodiversity. Various mechanisms have evolved as adaptations to harsh and variable environments, and heteromorphism is thought to be one of them [1]. Its underpinning mechanisms, however, are largely unknown. Through the work of the Leubner-Steinbrecher laboratory in the ERACAPS SeedAdapt project (www.seedadapt.eu), we have established *Ae. arabicum* as an excellent model system [2]. The advantages of this species are its fruit and seed dimorphism. Two morphologically distinct fruit types (large DEHiscent, splitting at maturity to release seeds / small INDehiscent, not splitting) are produced on the same fruiting head and they contain two very different seed types (mucilaginous “M+”, and non-mucilaginous “M–”) (Fig 1A). Further to this, its genome sequence is available [3], and we have already established molecular and biomechanical tools in SeedAdapt [4]. The goal of this experiment is to create a unique data set to complement our molecular and biomechanical findings by a comparative developmental analysis of the two (dimorphic) fruit and seed types using SRXTM. We aim to discover if and when developmental differences between the two fruit/seed types occur. We will link changes in the internal structures e.g. the differentiation of ovule integuments that give rise to the mucilage in the “M+” seed coat (proposed SRXTM work), to the gene expression of specific mucilage-related genes (e.g. *MUCILAGE-MODIFIED 4 (MUM4)*) during fruit and seed development (current PhD work of W. Arshad). Biomechanical experiments have revealed distinct fracture mechanics of the two different fruit types (how they split open and how much force is needed to do so). We will link fracture mechanics to the development of thickening of cell walls in fruit tissues such that separation layers do not develop and dehiscence does not occur in IND fruits. To gain a complete picture of the dispersal unit, the fruit pedicel (stalk structure attaching fruit to the plant stem) will be included in the analyses. As the fruit pedicel has an impact on the fruit dispersal strategy, we propose there are huge differences in internal structures between the two fruit morphs. Combining previous data sets with new understanding of development of physical structure, gained from SRXTM work, will create new insight into the underpinning mechanisms of a fascinating and highly adaptive plant dispersal system.

B) Background

Plants have developed an incredible range of fruit and seed (“diaspores”) shapes, sizes, and colours to maximise their success and to fill every available niche. Although diaspores are cornerstones for food quality and safety, the biodiversity of mechanisms underlying the adaptation to abiotic stresses and climate change are only poorly understood. Most plant species produce seeds and fruits of a single type that is optimally adapted to a suitable habitat [1]. Some plant species exhibit diaspore dimorphism, where two distinctly different types of seeds or fruits are produced by a single individual [2, 5]. *Aethionema arabicum*, an annual belonging to the most basal lineage of the Brassicaceae family [6], exhibits true diaspore dimorphism with no intermediate morphs (Fig. 1A). Its unique ability to produce two distinct fruits (DEHiscent and INDehiscent) containing two different seed types (mucilaginous “M+” and nonmucilaginous “M–”), presents an excellent model system with which to study aspects of

diaspore dimorphism. The fruit ratios (DEH:IND) change in response to environmental conditions [2]. Furthermore, *Ae. arabicum* shows a moisture-dependent movement of its fruit pedicels; exposure to moisture results in an outward bending of the pedicel. All these features aid distinct dispersal mechanisms. As details of the development which brings about the final products of the dimorphic syndrome (Fig. 1B–D) are completely unknown we aim to utilise the distinct diaspores to explore the key, early morphological and developmental processes associated with fruit and seed morph differentiation. Other aspects of this model system were studied by the SeedAdapt project, including ourselves. A comparative approach was used to understand the physiological, genetic and biophysical adaptations of the dimorphic diaspore syndrome. This knowledge and team of investigators, therefore provides a unique opportunity to use SRTXM in a fundamentally novel and comparative approach, to investigate the linkage between seed and fruit development in heteromorphic systems. The SRTXM work will create a unique data set gaining new insights into the morphological and developmental basis of fruit and seed trait diversity, contributing to a field of major importance in physiology, seed industry, food security, and crop breeding.

C) Experimental method; specific requirements

During the embedding, sectioning, and mounting processes associated with traditional histological sections folding, tearing, or loss of tissues can occur [7] (Fig. 1E and 1F). Especially in developing seeds, naturally occurring cavities are hard to distinguish from tears or holes that are one of the most common artefacts. The non-invasive and non-destructive method of SRXTM to visualise both internal and external morphology and anatomy, provides a technique well-established for fossil and extant plants [7-10]. Crucially for this study, digital sections from the TOMCAT beamline reveal morphology and anatomy in multiple planes without artefacts, providing a methodology to study *Aethionema* fruit and seed development at high resolution. Digital sections of the mature seed types (Fig. 1G and 1H) obtained at TOMCAT using the 20X magnification objective and reconstructed using phase contrast (coupled with an LSO:Tb 5.9 μm scintillator, resulting in a voxel size of 0.1625 μm), demonstrate feasibility for high-resolution cell and tissue details with good contrast between cell wall and cell layer edges and spaces. This approach also proved extremely successful for the study of *Lepidium* seeds (Collinson *et al.*, beamtime report 20161437) and for the reproductive structures of the fossil *Azolla* (Collinson *et al.*, beamtime report 20131224) [11]. We will study the physical structure of developmental stages in the DEH and IND fruits of *Aethionema*, focussing on (i) the differentiation of ovule integuments that give rise to the mucilage in the “M+” seed coat (within DEH fruits), and (ii) the thickening of cell walls of parenchymatous tissue in fruits such that separation layers do not develop and dehiscence does not occur (within IND fruits). We aim to scan three replicates of each of the two fruit morphs, at three different stages of development (18 samples). Additionally, the fruit pedicels will be analysed separately in the dry (straight pedicel) and wet (bent pedicel) stage (12 samples) relevant to dispersal.

- DEH fruits: 3, 7, and 35 days after pollination (DAP) (Fig. 1B–1D)
- IND fruits: 3, 7, and 35 DAP (Fig. 1B–1D)
- DEH/IND fruit pedicels from a dry specimen (straight pedicel)
- DEH/IND fruit pedicels from a wet specimen (bent pedicel)

We will employ critical-point drying, a commonly used method for drying specimens for electron microscopy, as a preparative procedure for our fresh (hydrated) fruits. Fruits will then be glued to a standard brass pin using epoxy

adhesive. After phase retrieval (Paganin), datasets will then be reconstructed with an efficient Fourier based algorithm (gridrec) and analysed using Avizo 9.1.

D) Results expected

We will determine the physical changes in the two fruit morphs at each stage of development that give rise to the huge differences in seed coat morphology (mucilage layer), as demonstrated in our X20 proof of concept scans of mature seeds (Fig. 1G and 1H). This will elucidate a key internal structural change at the point at which the DEH and IND developmental pathways diverge (Fig. 1B). We expect the following results that will lead to project goals of linking internal structures to dispersal mode:

- Identification of the developmental stage at which the “fate” of a fruit (either IND or DEH morph) is determined
- Timing of physical changes (after 3, 7 and 35 days after pollination) in the differentiation of ovule integuments (seed coat morphology/mucilage layer). Do these structural changes relate to changes in expression of specific mucilage-related genes?
- Determination of the stage at which the development of a separation layer is detectable in the parenchymatous fruit wall that would lead to a “dehiscent” zone in the DEH fruits (and respectively does not develop in IND fruits). How do these developmental stages correlate with fruit fracture mechanics?
- Does the pedicel differ between the two fruit morphs, and is its internal structure linked to a specific dispersal mechanism (e.g. dehiscence vs. abscission)?

Contrasting differences in the internal structures between IND and DEH will be contextualised within our existing knowledge base of seed physiology and dormancy behaviour, linked to molecular aspects and dispersal biomechanics. Together, these SRXTM datasets will document key structural events associated with dimorphic fruit and seed development.

E) Estimate and justification of the beamtime

Two fruit categories, at three developmental stages, with three replicates of each (18 fruits). Two fruit categories with two “stages” of the pedicel, with three replicates (12 samples). Total 30 samples. Based on the proof of concept beamtime and discussions with Dr Federica Marone, fruits will take up to approx. one hour to scan using the X20 objective with three vertical stacks (akin to the mature seeds). Larger, more mature fruits (Fig. 1D) may require additional time to set up. We therefore request five shifts. We will need the assistance of Dr Marone for experimental setup and phase contrast (Paganin) reconstruction.

F) References relevant to the experiment description

1. Imbert, E., 2002. *PPEES*, **5**(1): p. 13-36.
2. Lenser, T., *et al.*, 2016. *Plant Physiol*, **172**(3): p. 1691-1707.
3. Haudry, A., *et al.*, 2013. *Nature Genetics*, **45**(8): p. 891-U228.
4. Steinbrecher, T. and G. Leubner-Metzger, 2016. *JXB*, **68**(4): p. 765-783.
5. Baskin, C.C. and J.M. Baskin, 2014. *Seeds*. Elsevier.
6. Couvreur, T.L.P., *et al.*, 2009. *Molec Biol Evol*, **27**(1): p. 55-71.
7. Smith, S.Y., *et al.*, 2009. *PNAS*, **106**(29): p. 12013-12018.
8. Collinson, M.E., *et al.*, 2012. *Palaeobiodiversity and Palaeoenvironments*, **92**(4): p. 403-416.
9. Friis, E.M., *et al.*, 2015. *Nature*, **528**(7583): p. 551-554.
10. Benedict, J.C., *et al.*, 2015. *Am J Bot*, **102**(11): p.1814-1841.
11. Collinson, M.E., *et al.*, 2013. *IJPS*, **174**(3): p. 350-363.

SLS related publications of the proposers (within the last 18 months)
Collinson Margaret E, van Konijnenburgvan Cittert Johanna HA, Marone F, Brain Anthony PR Reinterpretation of <i>Azolla primaeva</i> (Azollaceae, Eocene, Canada) using electron microscopy and X-ray tomographic microscopy REVIEW OF PALAEOBOTANY AND PALYNOLOGY 240 33 (2017) Beamline: TOMCAT
Benedict John C, Smith Selena Y, Specht Chelsea D, Collinson Margaret E, Leong-Skornickova Jana, Parkinson Dilworth Y, Marone Federica Species diversity driven by morphological and ecological disparity: a case study of comparative seed morphology and anatomy across a large monocot order AoB Plants 8 plw063 (2016) Beamline: TOMCAT

Other publications of the proposers (within the last 18 months)
Pearce, S., King, J., Steinbrecher, T., Leubner, G., Everitt, N. & Holdsworth, M. 24 Jan 2018, Finite indentation of highly curved elastic shells. In : Proceedings of the Royal Society A: Mathematical, Physical & Engineering Sciences. 474, 20170482
Sperber, K., Steinbrecher, T., Graeber, K., Scherer, G., Clausing, S., Wiegand, N., Hourston, J., Kurre, R., Leubner, G. & Mummenhoff, K. 30 Nov 2017, Fruit fracture biomechanics and the release of <i>Lepidium didymum</i> pericarp-imposed mechanical dormancy by fungi. In : Nature Communications. 8, 1868
Inglis, G. N., Collinson, M. E., Riegel, W., Wilde, V., Farnsworth, A., Lunt, D. J., Valdes, P., Robson, B. E., Scott, A. C., Lenz, O. K., Naafs, B. D. A. & Pancost, R. D. 15 Feb 2017, Mid-latitude continental temperatures through the early Eocene in western Europe. In : Earth and Planetary Science Letters. 460, p. 86-96
Leubner, G. Sep 2017, Improving Crop Seed Quality and Seedling Performance. In : IMPACT. 7, p. 81-83
Steinbrecher, T. & Leubner, G. 1 Feb 2017, The biomechanics of seed germination. In : Journal of Experimental Botany. 68, p. 765-783
Hourston, J., Ignatz, M., Reith, M., Leubner, G. & Steinbrecher, T. 18 Jan 2017, Biomechanical Properties of Wheat Grains: the implications on Milling. In : Journal of the Royal Society. Interface. 14, 126
Graeber, K., Nakabayashi, K. & Leubner-Metzger, G. 2017, Seed dormancy: Development of Dormancy. Encyclopedia of Applied Plant Sciences. Thomas, B., Murray, B. & Murphy, D. (eds.). 2nd ed. Waltham, MA: Elsevier, Vol. 1, p. 483-489 209
Nakabayashi, K., Graeber, K. & Leubner-Metzger, G. 2017, Seed Dormancy: Genetics of Dormancy. Encyclopedia of Applied Plant Sciences. Thomas, B., Murray, B. & Murphy, D. (eds.). 2nd ed. Waltham, MA: Elsevier, Vol. 1, p. 504-508 210
Graeber, K., Schulze, C., Steinbrecher, T., Leubner-Metzger, G. & 19 others 4 Oct 2016, Developmental control and plasticity of fruit and seed dimorphism in <i>Aethionema arabicum</i> . In : Plant Physiology. 172, November, p. 1691-1707, PP2016-00838R1
Adams, N., Collinson, M., Smith, S. Y., Bamford, M. K., Forest, F., Malakasi, P., Marone, F. & Sykes, D. 19 Sep 2016, X-rays and virtual taphonomy resolve the first <i>Cissus</i> (Vitaceae) macrofossils from Africa as early diverging members of the genus. In : American Journal of Botany. 103, 9, p. 1657-1677
Stull, G. W. & Collinson, M. 7 Sep 2016, Revision of Icacinaceae from the Early Eocene London Clay flora based on X-ray micro-CT. In : Botany. 94, p. 713-745
Benedict, J., Smith, S. Y., Specht, C. & Collinson, M. 4 Sep 2016, Species diversity driven by morphological and ecological disparity: a case study of comparative seed morphology and anatomy across a large monocot order. In : AoB Plants.

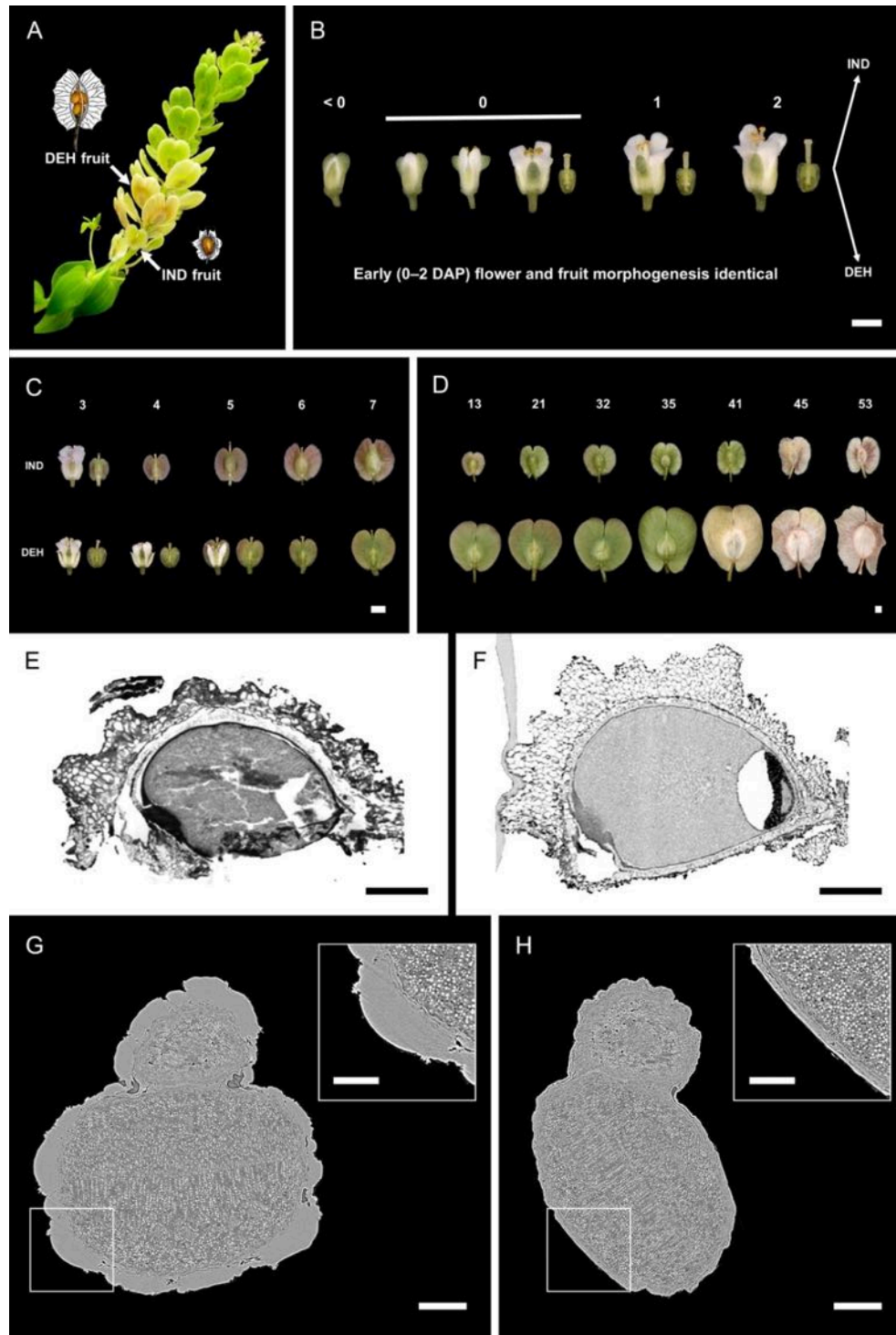


Figure 1: A) Mature *Aethionema arabicum* (Brassicaceae) infructescence, with schematic drawings of dehiscent (DEH) and indehiscent (IND) fruit morphs. B–D) Floral and fruit morphogenesis appears phenotypically identical in early (0–3 days after pollination [DAP]) growth, after which fruits become morphologically distinct (3–7 DAP), without any deviance in development during fruit maturation (13–53 DAP). E–F) Modern fruit of *Saururus chinensis* (Saururaceae) showing (E) longitudinal section by traditional sectioning, with various spaces, tears, tissue loss and tissue folding, uncertain what is real and what is sectioning artefact; (F) Longitudinal section by SRXTM showing undamaged fruit wall and seed coat, and the presence of a genuine space between embryo and food storage tissue [E–F from Smith, Collinson, Marone *et al.* 2009, PNAS **106**: 12013–12018]. G–H) SRXTM digital transverse section of mature “M+” (G) and “M–” (H) seeds, showing differences in embryo positioning and seed shape between the two morphs. Of particular interest is the abundance of mucilage in the “M+” (G, inset) seed morph, produced as large papillae by the outermost layer of the seed coat. In contrast, the “M–” seed coat (H, inset) lacks the thickness of this outermost layer, but still possesses a thin layer of mucilage. Scale bars = 1 mm (B–D), 200 μm (E–F), 100 μm (G–H) and 50 μm (G inset and H inset).

Sample

Sample #1	Sample and chemical substance to be used in this experiment	
	Substance	Modern Seeds
	Chemical formula	Organic Plant Material
	Structure	Biological material
	Size X	1
	Size Y	1
	Size Z	1
	Mass	2
	Container	brass pin
	High purity	No
	After the experiment the sample will be	Removed by user
	No ethical issues or safety aspects declared on this sample.	
	Sample environment	
	Hotair blower	No
High voltage	No	
High pressure	No	
High temperature	No	
Magnetic field	No	
Cryogenic liquid	No	
Be window	No	



SLS Management

c/o Stefan Mueller
PRC Coordinator

Telephone direct +41 (56) 310 5427
secretary +41 (56) 310 3178

E-mail stefan.mueller@psi.ch

Dr.
Dr. Tina LH Steinbrecher
Royal Holloway University of London
Department of Earth Sciences
Egham
Surrey
TW20 0EX
United Kingdom

May 07, 2018

Decision of the SLS Program Review Committees

Proposal ID: 20180809

A tale of two morphs: bet-hedging survival strategies in the Brassicaceae as adaptations in unpredictable environments

<i>Beamline</i>	<i>Period</i>	<i>Type</i>	<i>Status</i>	<i>Beamtime allocated (8h shifts)</i>	
				<i>Total</i>	<i>This period</i>
TOMCAT	Jul 2018 - Dec 2018	Normal	Accepted	5	5

Ranking: 4.17 (compared to maximum: 4.87, average: 3.76) *Proposal ranking*

For shift allocations and arranging the details of your experiment please contact the beamline manager Prof. Dr. Marco Stampanoni (marco.stampanoni@psi.ch). Please visit the SLS Website (<https://www.psi.ch/sls>) for up-to-date information about the SLS operation.